PROCESSING, STRUCTURE, AND PROPERTIES OF RECYCLED TEXTILES INTO INSULATION MATERIALS

by

SHAFIQUL ISLAM

(Under the Direction of Gajanan S. Bhat)

ABSTRACT

The goal of this study was to understand the potentiality for recycled textiles to be used as environmental-friendly insulation materials and to understand the structure-property relationship of such insulation materials. A systematic study was conducted to evaluate the recycling of used apparel to produce commercially feasible sustainable insulation products using nonwoven fabrication techniques with a biodegradable thermoplastic binder fiber (Sorona® or PLA). Produced materials showed very good insulation properties with maximum transmission loss of about 24 dB at around 1000 Hz and minimum thermal conductivity value of 0.049 W/mK, which are much better than those of commercially available insulation materials.

Another study conducted to understand the effect of processing parameters on the properties of insulation materials, showed that with the increase of bonding time and temperature, thickness decrease, whereas density increases, air permeability initially slightly increases, then decreases, and acoustic insulation property increases, but thermal insulation property decreases.

Insulation materials were also prepared utilizing 3D printing technology to check the effect of structural parameters on insulation properties with the assumption that precise structural parameters produced by 3D printing technology would show accurate relation compared to

nonwoven composites, which are irregular by nature. Results showed a similar effect of structural parameters on insulation properties that was observed in nonwoven composites.

An analytical model is proposed by combining and modifying Maxwell-Eucken model to predict thermal insulation properties. Tested results showed that experimental data agree with the predicted data with a percentage of difference less than 8.5%.

A cradle to gate life cycle assessment (LCA) was conducted to check the environmental impacts of produced insulation materials. The result showed that produced insulation materials have overall very low environmental impacts compared to stone wool and natural flax.

This systematic study revealed that produced insulation materials have very good potentiality to be used as environmentally friendly building insulation materials that can replace the commercially available ones. Waste textiles have the potential to give another useful life before safely disposing of them in composting environments.

INDEX WORDS: Textile waste, insulation materials, nonwoven composites, structure-property relationship, LCA, analytical modeling.

PROCESSING, STRUCTURE, AND PROPERTIES OF RECYCLED TEXTILES INTO INSULATION MATERIALS

by

SHAFIQUL ISLAM

B.Sc., Bangladesh University of Textiles, Bangladesh, 2011

M.Sc., Bangladesh University of Textiles, Bangladesh, 2015

A Dissertation Submitted to the Graduate Faculty of The University of Georgia in Partial Fulfillment of the Requirements for the Degree

DOCTOR OF PHILOSOPHY

ATHENS, GEORGIA

2021

PROCESSING, STRUCTURE, AND PROPERTIES OF RECYCLED TEXTILES INTO INSULATION MATERIALS

by

SHAFIQUL ISLAM

Major Professor:	Gajanan S. Bhat
Committee:	Sergiy Minko
	Vladimir Reukov
	Sudhagar Mani
	Crystal Leach

Electronic Version Approved:

Ron Walcott
Vice Provost for Graduate Education and Dean of the Graduate School
The University of Georgia
August 2021

DEDICATION

Dedicated to my father - in a loving memory. I always feel his presence beside me and guiding me.

ACKNOWLEDGEMENTS

There are so many people who lay the foundation and help me to make this dissertation successful. I would like to convey my humble and sincere appreciation to those people.

My foremost thanks to my major professor, Dr. Gajanan S. Bhat, for his support, guidance, encouragement, and kindness during my study. Without his advisement and effort, this research would not be fruitful.

Special thanks go to my committee members: Sergiy Minko, Vladimir Reukov, Sudhagar Mani, and Crystal Leach, who provided their expert guidance and helped my research. I am also grateful to the faculty and staff of the TMI department for their support and for making the UGA life memorable.

I am also thankful to Cotton Incorporated for funding part of this project and Edward Schut from GeoPellet for valuable discussions. Also, support by providing samples from DuPont Polymers, Wilmington, DE, FIT Fibers, Johnson city, TN, and Phoenix Fibers, Chandler, AZ is acknowledged.

I would always be indebted to my mother, who encouraged and supported my education in every possible way. I would like to thank my younger brother, Al-jamil Suvo, for giving me good support and take care of my mother during my absence from home. Special thanks go to my wife, Farjana Mahmud, for her understanding, patience, encouragement, and support.

Table of Contents

Page

LIST OF TABLES

Page

LIST OF FIGURES

Page

CHAPTER 1

Introduction

One of the biggest challenges of the 21st century is to maintain sustainability in all levels of energy resources and environmental context [1]. There is a steadily increasing concern in the energy and environmental sectors [2]. In the energy sector, concern is mainly due to the imbalance between the consumption and limited resources of energy [3]. In the environmental sector, concern is due to the rapid increase of world population with their consumption rate, and gradual increase in tendency to discard materials to landfill as waste before the end of lifetime of the products [4]. Building and automobile sectors are considered as main consuming sectors of global energy. At the global level, it is estimated that buildings consume about 40% of the global energy, 25% of global water, and 40% of the global resources [5]. Buildings are responsible for one-third of CO_2 productions [6], approximately two-thirds of halocarbon, and 25–33% of black carbon emissions [7]. In Europe, buildings are accountable for the consumption of 40% energy [8] and for the emission of 36% of the total CO_2 [9]. Therefore, reducing energy consumption in buildings is becoming a major concern and is challenging policies in the present world [10].

Thermal insulation in building materials can play a vital role in reducing energy consumption. Using efficient insulation materials can help save energy by minimizing the losses and gains of heat during heating and cooling of buildings [11]. Based on literature, a good insulation could save about 65% of energy consumption in domestic buildings [12] and could save over one hundred times of the impacts of carbon footprint from material usage and disposal, irrespective of the type of materials used [13].

Of the several ways to reduce CO_2 emission during construction and renovation of buildings, some of the efficient techniques are improving building design to save energy, increasing use of sustainable building materials such as reuse or recycling [14], increasing use of renewable energy (solar, wind, hydropower, bioenergy), integrating solar system with building to supply energy to building [15]–[17], reducing electricity consumption (as a result of indirect emission) by using more efficient instruments, utensils and lighting, and capturing and storing of CO_2. Carbon capture and storage methods have the potential to reduce CO_2 emissions by more than 80% [18]. However, this technology is not fully commercially proven yet [18]. CO_2 is captured by combustion process followed by transport and storage. However, combustion is a very costly process. According to the US National Energy Technology Laboratory, post-combustion capture of CO_2 would increase the cost of electricity production by 70% [19]. However, widely used technique is to use building insulation materials that reduce CO_2 emission by reducing energy consumption [20]. It was observed that solid wall insulation is the most cost-effective approach to reduce CO_2 emission when applied to large electrically heated buildings and used in conjunction with building construction or renovation [20].

On the other hand, the gradual increase of noise pollution due to urbanization, industrialization, increased use of vehicles, electrical and mechanical appliances in home and industry, become a major health and environmental concern [21]. Noise pollutions are responsible for several health effects, including sensorial, stress, high blood pressure, coronary heart disease, and stroke [22]. In most cases, the diagnosis is not immediate, which leads to further worse situations. A study estimated that about 65% of European citizens are exposed to noise levels which may lead to several adverse effects on health [23]. Besides health problems, noise pollution also disturbs work and reduces work efficiency of humans [24]. Sound insulation is certainly one of the techniques

that can be used to reduce the harmful effects of noise. Several countries in Europe have regulations that buildings must install soundproof materials to reduce the adverse effect of noise pollution [25]. These regulations have further increased the demand for efficient and low-cost sound insulation materials.

Thus, by using effective insulation material, it is possible to minimize energy consumption and adverse effect of noise pollution. At present, commonly used building insulation materials are polyurethane foam, glass wool, mineral wool, fiberglass, expanded polystyrene (EPS), extruded polystyrene (XPS), polyurethane, and others [26].

1.1. Problem

The problem with currently used building insulation materials is that these materials are produced from synthetic sources, which have adverse environmental and health effects [27]. It was estimated that around 60% of manufactured thermal insulation materials in buildings come from mineral or inorganic fibrous materials (glass and stone wool), 30% are from foam materials (expanded polystyrene, extruded polystyrene, less widespread polyurethane), and the remaining 10% are from other non-traditional or composite materials (wool-wood insulations, gypsum-foam, etc.) [28]. In 2011, mineral wool and plastic shared 52% and 41% of the world thermal insulating materials market [5]. These types of materials can have adverse effects on the environment due to their non-renewable and non-disposable properties [5]. Glass fiber-based materials are obtained from silica sources [27] which have carcinogenic effects on human body [29]. Similarly, sound insulation materials are also composed of porous synthetic materials, including rock wool, glass wool, polyurethane, or polyester, which are generally based on petrochemicals [27] and have an adverse effect on human health and environment. Due to these adverse effects of insulation materials, the demand for environmentally-friendly insulation materials is increasing [30].

1.2. Approaches to Solve the Problem

Several researchers have been proposed to solve and reduce the adverse effect of synthetic insulation materials on human health and environment. Some authors proposed natural materials and fibers to develop thermal and acoustic insulation panels [31]–[35] due to their positive environmental effect, low carbon footprint [36], and low hazardous effect on health. However, some researchers have expressed doubt on the actual sustainability of natural materials as some of the natural materials (fibers, flax, sunflower stalk, and others) are produced using toxic chemicals [30]. Again, these products are not compatible to replace the presently used synthetic insulation materials due to their low mechanical and insulation properties [37].

In this research, we try to come up with a new idea to solve these critical problems. We plan to produce and evaluate insulation materials by blending waste textiles (cotton/nylon fibers) with biodegradable thermoplastic fibers (PLA/Sorona®) using nonwoven techniques. Using waste textiles, which otherwise go into landfill, for acoustic and thermal insulations can help the development of energy performance, reduction in consumption of non-renewable resources, reduction of strain on the environment, and improvement of the health of humans and other living beings [38].

1.3. Rationale

Every year millions of tons of clothing and textile wastes are discarded in landfills which cause serious environmental pollution. In 2017, 16.9 million tons of textile wastes were produced in the USA, which was about 6.3% of total municipal solid waste (MSW). Among these huge amounts of textile wastes, only 2.57 million tons were recycled, and 11.15 million tons were discarded to landfills [39]. These huge amounts of landfilled textile wastes cause series of environmental pollution by contaminating groundwater and forming greenhouse gases upon decomposition [40].

Decomposed biodegradable textile waste produces methane, a powerful greenhouse gas that contributes to global warming [41]. On the other hand, due to non-biodegradable and toxic nature, harmful effects of the landfilled synthetic materials on environment are immeasurable.

These huge amounts of textile waste have great potentiality for reuse or recycling into value-added products. It is estimated that up to 95% of textile waste could be recycled into different valuable products [40]. Waste textiles could be recycled into fibers which can be utilized to produce yarn and fabrics. However, fabric production process from waste textiles is costly, and the quality of recycled fiber is lower (very short fiber length and respinning into yarn is hard) than the virgin fibers [42]. Thus, fabric production by recycling is not economically viable. Recycled waste textiles could be applied in many fields such as automotive, furnishing, sailing and/or insulation. Among several application fields, recycled textiles have excellent potential to be used as insulation materials [43].

Producing acoustic and thermal insulation materials by textile waste is one of the effective, sustainable recycling processes. Recently researchers also found that the physical properties of textile waste are very much comparable to that of the conventional building insulation materials [21]. For this reason, textile wastes are recommended as feedstock to building insulation materials by several researchers with multiple benefits [44]. It will help to get rid of adverse environmental effects due to landfilling of textiles waste, help to reduce the fiber production by extraction or agricultural methods which contribute the highest amount of carbon footprint in apparel sector [40], and help minimize the deleterious effect of using synthetic insulation materials. Waste for one sector would be a prospective reusable resource for another segment.

Again, textile fibers have excellent insulation properties. Materials produced from textile fibers are porous in structure that have the ability to absorb energy and are suitable to produce good

insulation materials [26]. Insulation properties of cotton waste are comparable to those of synthetic EPS, and cotton has very good potential to be used as an alternative to EPS and other cushioned insulations [45].

Successful recycling of textiles also has socio-economic benefits. New jobs will be created in the collection, sorting, and recycling of clothing and will provide opportunities for establishing small or family businesses [46]. A circular economic system will be developed, which will boost the national economy [47]. A report published by European Union estimated that the transition to a circular system could generate a net economic benefit of €1.8 trillion by 2030 [48].

However, there is an obstacle to using recycled fibers due to their shorter fiber length. To overcome this problem, in this research, nonwoven techniques were utilized to produce insulation panels because these techniques are not only cheap and suitable to process short recycled fibers, but also produce a porous and bulky structure of materials that further enhance the thermal insulation properties.

Some other researchers studied natural and recycled fibers to produce building insulation materials due to their positive environmental effect, low carbon footprint, and less harmful effect on health [5], [31], [33]–[35]. Ricciardi et al. used recycled polypropylene fiber and paper to produce acoustic insulation materials. [49]. Some other researchers like Binici et al. mixed textile waste, sunflower stalk, and stubble fibers [31], Tiuc et al. mixed polyurethane foam with textile waste [50], and Trajković et al. used polyester apparel cutting waste to produce acoustic insulation materials [51].

However, these researches are in very initial stages, and most of them fail to produce sustainable insulation materials. For example, produced insulation materials by Ricciardi et al. are not environmentally friendly as their products involve relatively large energy consumptions (267.7

MJ) and a high global warming potential (14.68 kg CO_2eq) in comparison to similar synthetic insulation materials like EPS [49]. This may be from the use of glue for binding fibers. Therefore, for producing sustainable insulation materials from recycled textiles, researchers may need to avoid external chemicals for binding. In this research, instead of using just any chemical resin/binder, thermoplastic fibers (PLA or Sorona®) were used as binding agents. Most of the other researchers did not conduct life cycle assessment (LCA) to check the sustainability of insulation materials. However, insulation products based on natural resources did not necessarily warrant more environmentally friendly products [11]. A quantitative environmental assessment is necessary to define a product as environmentally friendly. Therefore, in this research, LCA was conducted to check the true sustainability of insulation materials.

Hence, it is clearly evident that although some research has been conducted to produce sustainable insulation materials, these researches are in very initial stages, and present market is completely occupied by conventional synthetic insulation materials. More research is needed to help make sustainable insulation materials that are lightweight, cost-effective, and have very good insulation properties [52]–[54].

1.4. Hypothesis

It is hypothesized that produced insulation panels from waste textiles will be environmentally friendly and will give good insulation and physical properties.

1.5. Objectives

The objective of this paper is to identify the realistic picture of the present status and the potential for recycled textiles to be used as environmentally friendly insulation materials and to understand the structure-property relationship of such materials. To achieve these goals, a systematic study

has been conducted to evaluate the recycling of used apparel to produce commercially feasible sustainable insulation products.

In this study, nonwoven fabrication process has been utilized to produce insulation materials that can process short recycled fibers. Low melting thermoplastic biodegradable fibers (PLA/Sorona®) have been utilized as binder fibers which have potentiality to replace the glue and toxic binding chemical and reduce the environmental impacts. After producing materials, their insulation properties have been determined and compared with commercially used insulation materials. A thorough structure-property relationship was also determined in order to understand which factors have significant influences on insulation property and the strategies to improve insulation properties. Another study was conducted to understand the effect of processing parameters (thermal bonding conditions) on thickness, density, air permeability, and porosity and subsequently on thermal and acoustic insulation properties of produced composite materials. Insulation materials were also prepared utilizing 3D printing technology to recheck the effect of structural parameters on insulation properties as it is assumed that precise structural parameters produced by 3D printing technology would show accurate relation compared to nonwoven composites, which are irregular by nature. An analytical model was proposed by combining and modifying Maxwell-Eucken model to predict thermal insulation properties of porous fibrous materials. This study also investigates the applicability of existing models (series, parallel, ME1, ME2, and EMT) for predicting thermal insulation properties of such materials. Finally, A cradle to gate life cycle assessment (LCA) was conducted to analyze the environmental impacts, to analyze the environmental impacts at different manufacturing stages, and to compare the impacts of several thermal insulation materials.

1.6. References

[1] J. A. Palmer, *Environmental education in the 21st century: Theory, practice, progress and promise*. London: Routledge, 2002.

[2] M. EL Wazna, A. Gounni, A. EL Bouari, M. EL Alami, and O. Cherkaoui, "Development, characterization and thermal performance of insulating nonwoven fabrics made from textile waste," *J. Ind. Text.*, vol. 48, no. 7, pp. 1167–1183, 2019, doi: 10.1177/1528083718757526.

[3] L. Rüttinger and M. Feil, *Sustainable Prevention of Resource Conflicts: New Risks from Raw Materials for the Future? Case Study and Scenarios for China and Rare Earths*, First ed. Berlin: Adelphi, 2010.

[4] J. C. Bergstrom and A. Randall, *Resource economics: an economic approach to natural resource and environmental policy*, Fourth ed. Northampton, MA: Edward Elgar Publishing, 2016.

[5] F. Asdrubali, F. D'Alessandro, and S. Schiavoni, "A review of unconventional sustainable building insulation materials," *Sustain. Mater. Technol.*, vol. 4, pp. 1–17, 2015, doi: 10.1016/j.susmat.2015.05.002.

[6] L. Pérez-Lombard, J. Ortiz, and C. Pout, "A review on buildings energy consumption information," *Energy Build.*, vol. 40, no. 3, pp. 394–398, 2008, doi: 10.1016/j.enbuild.2007.03.007.

[7] D. Ürge-Vorsatz, L. F. Cabeza, S. Serrano, C. Barreneche, and K. Petrichenko, "Heating and cooling energy trends and drivers in buildings," *Renew. Rev. Sustain. Energy*, vol. 41, pp. 85–98, 2015.

[8] Directive, "Directive 2010/75/EU of the European Parliament and of the Council," *Official Journal of the European Union*, 2010. https://eur-lex.europa.eu/LexUriServ/LexUriServ.do?uri=OJ%3AL%3A2010%3A334%3A0017%3A0119%3Aen%3APDF (accessed Apr. 11, 2021).

[9] M. del Mar Barbero-Barrera, O. Pombo, and M. de los Angeles Navacerrada, "Textile fibre waste bindered with natural hydraulic lime," *Compos. Part B Eng.*, vol. 94, pp. 26–33, 2016.

[10] J. Iwaro and A. Mwasha, "A review of building energy regulation and policy for energy conservation in developing countries," *Energy Policy*, vol. 38, no. 12, pp. 7744–7755, 2010, doi: 10.1016/j.enpol.2010.08.027.

[11] M. S. Al-Homoud, "Performance characteristics and practical applications of common building thermal insulation materials," *Build. Environ.*, vol. 40, no. 3, pp. 353–366, 2005.

[12] A. Hadded, S. Benltoufa, F. Fayala, and A. Jemni, “Thermo physical characterisation of recycled textile materials used for building insulating,” *J. Build. Eng.*, vol. 5, pp. 34–40, 2016.

[13] A. C. Schmidt, A. A. Jensen, A. U. Clausen, O. Kamstrup, and D. Postlethwaite, “A comparative life cycle assessment of building insulation products made of stone wool, paper wool and flax,” *Int. J. Life Cycle Assess.*, vol. 9, no. 1, pp. 53–66, 2004, doi: 10.1007/BF02978536.

[14] F. Meggers *et al.*, “Reduce CO2 from buildings with technology to zero emissions,” *Sustain. Cities Soc.*, vol. 2, no. 1, pp. 29–36, 2012, doi: 10.1016/j.scs.2011.10.001.

[15] D. Mills, “Advances in solar thermal electricity technology,” *Sol. Energy*, vol. 76, no. 1–3, pp. 19–31, 2004, doi: 10.1016/S0038-092X(03)00102-6.

[16] J. Schlaich, *The solar chimney: electricity from the sun*. Fellbach, Germany: Edition Axel Menges, 1995.

[17] S. Kennedy, “Going SOFT: Design strategies for a new materiality of energy,” in *Re-inventing construction*, I. Ruby and A. Ruby, Eds. Berlin: Ruby Press, 2011.

[18] D. Y. C. Leung, G. Caramanna, and M. M. Maroto-Valer, “An overview of current status of carbon dioxide capture and storage technologies,” *Renew. Sustain. Energy Rev.*, vol. 39, pp. 426–443, 2014, doi: 10.1016/j.rser.2014.07.093.

[19] L. C. Elwell and W. S. Grant, “https://www.osti.gov/biblio/20823938,” *Power*, vol. 150, no. 8, pp. 60–65, 2006, [Online]. Available: https://www.osti.gov/biblio/20823938.

[20] J. Gummer *et al.*, “Fourth carbon budget review–technical report: sectoral analysis of the cost-effective path to the 2050 target,” 2013. https://www.theccc.org.uk/wp-content/uploads/2013/12/1785b-CCC_TechRep_Singles_Book_1.pdf (accessed Apr. 11, 2021).

[21] J. Zach, A. Korjenic, V. Petránek, J. Hroudová, and T. Bednar, “Performance evaluation and research of alternative thermal insulations based on sheep wool,” *Energy Build.*, vol. 49, pp. 246–253, 2012.

[22] W. Passchier-Vermeer and W. F. Passchier, “Noise exposure and public health,” *Environ. Health Perspect.*, vol. 108, no. suppl 1, pp. 123–131, 2000, doi: 10.1289/ehp.00108s1123.

[23] H. Wallace, M. A. Pollack, C. Roederer-Rynning, and A. R. Young, *Policy-making in the European Union*. Oxford, UK: Oxford University Press, USA, 2020.

[24] D. Chen, J. Li, and J. Ren, “Study on sound absorption property of ramie fiber reinforced poly (l-lactic acid) composites: Morphology and properties,” *Compos. Part A Appl. Sci. Manuf.*, vol. 41, no. 8, pp. 1012–1018, 2010, doi: 10.1016/j.compositesa.2010.04.007.

[25] R. Reixach, R. Del Rey, J. Alba, G. Arbat, F. X. Espinach, and P. Mutjé, “Acoustic properties of agroforestry waste orange pruning fibers reinforced polypropylene composites as an alternative to laminated gypsum boards,” *Constr. Build. Mater.*, vol. 77, pp. 124–129, 2015.

[26] S. Islam and G. Bhat, “Environmentally-friendly thermal and acoustic insulation materials from recycled textiles,” *J. Environ. Manage.*, vol. 251, p. 109536, 2019.

[27] A. Patnaik, M. Mvubu, S. Muniyasamy, A. Botha, and R. D. Anandjiwala, “Thermal and sound insulation materials from waste wool and recycled polyester fibers and their biodegradation studies,” *Energy Build.*, vol. 92, pp. 161–169, 2015, doi: 10.1016/j.enbuild.2015.01.056.

[28] F. Ardente, M. Beccali, M. Cellura, and M. Mistretta, “Building energy performance: a LCA case study of kenaf-fibres insulation board,” *Energy Build.*, vol. 40, no. 1, pp. 1–10, 2008, doi: 10.1016/j.enbuild.2006.12.009.

[29] A. M. Papadopoulos, “State of the art in thermal insulation materials and aims for future developments,” *Energy Build.*, vol. 37, no. 1, pp. 77–86, 2005.

[30] U. Berardi and G. Iannace, “Acoustic characterization of natural fibers for sound absorption applications,” *Build. Environ.*, vol. 94, pp. 840–852, 2015.

[31] H. Binici, M. Eken, M. Dolaz, O. Aksogan, and M. Kara, “An environmentally friendly thermal insulation material from sunflower stalk, textile waste and stubble fibres,” *Constr. Build. Mater.*, vol. 51, pp. 24-33., 2014.

[32] V. Desarnaulds, E. Costanzo, A. Carvalho, and B. Arlaud, “Sustainability of acoustic materials and acoustic characterization of sustainable materials,” 2005, [Online]. Available: https://paginas.fe.up.pt/~carvalho/icsv12.pdf.

[33] S. Fatima and A. R. Mohanty, “Acoustical and fire-retardant properties of jute composite materials,” *Appl. Acoust.*, vol. 72, no. 2–3, pp. 108–114, 2011.

[34] M. H. Fouladi, Md.Ayub, and M. J. M. Nor, “Analysis of coir fiber acoustical characteristics,” *Appl. Acoust.*, vol. 72, no. 1, pp. 35–42, 2011.

[35] X. Zhou, F. Zheng, H. Li, and C. Lu, “An environment-friendly thermal insulation material from cotton stalk fibers,” *Energy Build.*, vol. 42, no. 7, pp. 1070–1074, 2010, doi: 10.1016/j.enbuild.2010.01.020.

[36] M. Pervaiz and M. M. Sain, “Carbon storage potential in natural fiber composites,” *Resour. Conserv. Recycl.*, vol. 39, no. 4, pp. 325–340, 2003, doi: 10.1016/S0921-3449(02)00173-8.

[37] S. Ahmadzadeh, A. Nasirpour, J. Keramat, N. Hamdami, T. Behzad, and S. Desobry, "Nanoporous cellulose nanocomposite foams as high insulated food packaging materials," *Colloids Surfaces A Physicochem. Eng. Asp.*, vol. 468, pp. 201–210, 2015.

[38] J. Zach, J. Hroudová, and A. Korjenic, "Environmentally efficient thermal and acoustic insulation based on natural and waste fibers," *J. Chem. Technol. Biotechnol.*, vol. 91, no. 8., pp. 2156–2161, 2016, doi: 10.1002/jctb.4940.

[39] "EPA," *Facts and Figures about Materials, Waste and Recycling*, 2020. https://www.epa.gov/facts-and-figures-about-materials-waste-and-recycling/textiles-material-specific-data (accessed Jun. 04, 2020).

[40] D. G. K. Dissanayake, D. U. Weerasinghe, K. A. P. Wijesinghe, and K. M. D. M. P. Kalpage, "Developing a compression moulded thermal insulation panel using postindustrial textile waste," *Waste Manag.*, vol. 79, pp. 356–361, 2018, doi: 10.1016/j.wasman.2018.08.001.

[41] Y. Wang, "Fiber and textile waste utilization," *Waste and Biomass Valorization*, vol. 1, no. 1, pp. 135–143, 2010.

[42] A. Palme, A. Idström, L. Nordstierna, and H. Brelid, "Chemical and ultrastructural changes in cotton cellulose induced by laundering and textile use," *Cellulose*, vol. 21, no. 6, pp. 4681–4691, 2014, doi: 10.1007/s10570-014-0434-9.

[43] "WRAP," *Evaluation of the end markets for textile rag and fibre within the UK*, 2014. https://wrap.org.uk/sites/default/files/2021-03/WRAP-evaluation-of-end-markets-final.pdf (accessed May 25, 2021).

[44] M. El Wazna, M. El Fatihi, A. El Bouari, and O. Cherkaoui, "Thermo physical characterization of sustainable insulation materials made from textile waste," *J. Build. Eng.*, vol. 12, pp. 196–201, 2017.

[45] I. Montgomery, "Could These Materials be the Future of Packaging?," 2019. https://www.lumi.com/blog/sustainable-alternative-packaging-materials (accessed Jun. 04, 2020).

[46] W. Leal Filho *et al.*, "A review of the socio-economic advantages of textile recycling," *J. Clean. Prod.*, vol. 218, pp. 10–20, 2019, doi: 10.1016/j.jclepro.2019.01.210.

[47] S. Cuc and M. Vidovic, "Environmental sustainability through clothing recycling," *Oper. Supply Chain Manag.*, vol. 4, no. 2, pp. 108–115, 2014, doi: 10.31387/oscm0100064.

[48] "McKinsey Sustainability," *Europe's circular-economy opportunity*, 2015. https://www.mckinsey.com/business-functions/sustainability/our-insights/europes-circular-economy-opportunity (accessed May 25, 2021).

[49] P. Ricciardi, E. Belloni, and F. Cotana, “Innovative panels with recycled materials: thermal and acoustic performance and life cycle assessment,” *Appl. Energy*, vol. 134, pp. 150–162, 2014, doi: 10.1016/j.apenergy.2014.07.112.

[50] A.-E. Tiuc, H. Vermeşan, T. Gabor, and O. Vasile, “Improved sound absorption properties of polyurethane foam mixed with textile waste,” *Energy Procedia*, vol. 85, pp. 559–565, 2016, doi: 10.1016/j.egypro.2015.12.245.

[51] D. Trajković, S. Jordeva, E. Tomovska, and K. Zafirova, “Polyester apparel cutting waste as insulation material,” *J. Text. Inst.*, vol. 108, no. 7, pp. 1238–1245, 2017.

[52] R. Maderuelo-Sanz, A. V Nadal-Gisbert, J. E. Crespo-Amorós, and F. Parres-García, “A novel sound absorber with recycled fibers coming from end of life tires (ELTs),” *Appl. Acoust.*, vol. 73, no. 4, pp. 402–408, 2012.

[53] J. Ramis Soriano, J. Alba Fernández, R. M. del Rey Tormos, E. M. Escuder Silla, S. RICO, and V. JORGE, “Nuevos materiales absorbentes acústicos basados en fibra de kenaf,” *Constr. Mater.*, vol. 60, no. 299, pp. 133–143, 2010.

[54] S. Huda and Y. Yang, “Composites from ground chicken quill and polypropylene,” *Compos. Sci. Technol.*, vol. 68, no. 3–4, pp. 790–798, 2008.

CHAPTER 2

Literature Review

2.1. Acoustic Insulation

2.1.1. Sound absorption of porous materials

In order to achieve good acoustic insulation properties, the materials should be porous in structure. Porous materials allow sound to enter their matrix and dissipate. When sound waves enter into porous materials, air molecules within the pores vibrate that transform sound energy into thermal and viscous heat [1]. At low frequencies, this energy is dissipated by the isothermal process (limited amount), but at high frequencies, energy is lost by the adiabatic process [1], [2]. As a result, a low amount of sound is absorbed in low frequency, but absorption is higher at high frequency, resulting in low sound absorption coefficient at low frequencies.

Textile fibrous products which are porous in structure can absorb sound energy and can be used as good sound-absorbing materials [3]. Some of the useful parameters that can influence sound absorptions are the diameter, length, and regularity of the fibers. Textile fibers with high density can increases the sound absorption value in the mid to high-frequency ranges [4]. Thicker materials comparatively have lower air permeability but higher sound absorption properties [5]. The nonwoven structure has good sound absorption properties at the mid and higher frequency range but low sound absorption properties at lower frequencies (100–400 Hz) [6].

Several researchers have studied the relationship between noise reduction coefficient and various macro/micro-structural parameters of fibers [7], [8]. Both empirical and theoretical models

have been developed to describe the acoustic absorption properties [9]. These models have been mainly developed based on fiber length, fiber diameter, porosity, bulk density, and thickness.

Empirical models were built applying regression analysis or curve fitting procedures by measuring the characteristics of wave impedance and propagation constants [10]–[12]. Delany and Bazley developed acoustic model using a non-acoustical parameter of airflow resistivity for predicting the acoustical characteristics [13]. Delany and Bazley's models were developed over a specified frequency range $(10 < f/\sigma < 1000)$ and with a porosity of the material close to 1. Therefore, this model can be applied with materials that have a high fraction of pores. Furthermore, this model was developed by measuring fibers whose diameters were between 1 and 10 μm, but some natural fibers' diameters are around 20 to 50 μm [1]. Hence, Delany and Bazley's model has limitations for use with structures produced from thicker fibers [12], [14], [15]. Garai and Pompoli modified the Delany–Bazley model by experimenting with thicker polyester fibers (20 to 50 μm diameter) [12]. Garai–Pompoli model gives more accurate results when using natural fibers with larger diameters [1]. Several other authors, including Dunn-Davern [16], Miki [17], [18], Ramis [19], and Yoon [20], also proposed models to predict noise reduction coefficient. But the reliability of these models is limited for the interpretation of the behavior of natural materials due to high irregularity of fibers' diameters, pores, and structures [2].

2.1.2. Measurement of sound absorption

According to literature, researchers use several parameters (transmission loss, absorption coefficient, scattering coefficient, and sound reduction index) to describe acoustic properties of insulation materials. The sound reduction index (R) is used to measure the acoustic properties of the real sized sample, including windows, door, wall, and ventilator. It can be measured in decibels following the international standard (ISO 10140) by using the following equation [21].

$$R = L_1 - L_2 + 10\log\frac{S}{A} \quad (2.1)$$

where, L_1, L_2 are the energy average sound pressures in the source and receiving room respectively (dB), S is the area of the free test opening in which the test element is installed (m^2), and A is the equivalent sound absorption area in the receiving room (m^2)

But impedance tube is used to measure the acoustic properties of small size samples. By using impedance tube, several parameters of sound can be calculated, including absorption coefficient (α) [22] and transmission loss (TL), by applying the following equations [23].

$$\alpha = 1 - |r|^2 \quad (2.2)$$

$$TL = -20\log|\tau| \quad (2.3)$$

where, r is the reflection coefficient, and τ is the transmission coefficient.

There are several international standards to measure these acoustic properties, including ISO 10534- 2 [24], ISO 354 [25], and ASTM C423-17 [26]. Sound absorption properties could also be measured using a single rating system, including noise reduction coefficient (NRC) and sound absorption average (SAA) [27]. NRC is the arithmetic average of sound absorption coefficients at four 1/3 octave frequencies (250, 500, 1000, and 2000 Hz) to the nearest multiple of 0.05. SAA is also the arithmetic average of sound absorption coefficients at twelve one-third octave bands from 200 to 2500 Hz to the nearest multiple of 0.01.

2.2. Thermal Insulation

Heat transfers from higher temperature to lower temperature by conduction, convection, and radiation processes. Thermal insulation is the property of a material to reduce heat flow or transfer. Heat transfer by radiation can be reduced by using absorbing or reflecting surfaces [28]. Heat

transfer by conduction can be controlled by using less conductive materials and breaking the continuous structure [29].

Transfer of heat through fibrous materials depends on the number of fibers, packing geometry, contact between fibers, and temperature differences [30]. Heat transfer through conduction and radiation can be reduced by increasing the thickness of fibrous assemblies [31]. Thicker webs for the same areal density entrap a higher amount of air that reduces conduction [32]. Thicker webs also create a tortuous path that increases the absorption or scattering of radiation and reduce heat transfer [28], [32].

As thermal insulation properties of materials depend on porosity (Smith et al., 2013) and tortuosity (ratio of the open pores length and the thickness) of that material [33], textile fabrics that have a huge fraction of interconnected voids [34] have become good choice to produce thermal insulation materials.

Fibrous insulation materials produced by nonwoven techniques possess adequate small void spaces with entrapped air layers which are ideal for preventing convective heat transfer [35]. The layering of several fibrous webs increases air layers and thickness without adding proportional weight that increases the thermal insulation properties of those materials [36].

Thermal insulation property of a material is normally measured by thermal conductivity (k) or thermal transmittance (U-Value). Thermal conductivity can be defined as the rate at which heat is transferred at unit length of a material in a direction perpendicular to the surface of a unit cross-sectional area as a result of the temperature gradient. It is quantified by using the units of W/mK. Thermal transmittance is the rate at which heat is transferred through one square meter of a material with a 1K temperature difference. It is denoted by W/m^2K.

If heat flow, Q, (W) passed through an area (A) of m^2 of the fabric with a thickness of L (m) at a temperature difference (T_1-T_2) of K, then conductivity factor k (W/mK) can be expressed by following equation [37].

$$k = QL / A\left(T_1 - T_2\right) \tag{2.4}$$

Specific heat resistance (r) is the characteristic inverse of k and is expressed by the following equation [38].

$$r = 1/k = A\left(T_1 - T_2\right)/QL \tag{2.5}$$

Thermal resistance, R_{th} (m^2K/W) of textile fabrics, is the ratio of actual thickness (L) of sample in meter to the thermal conductivity (k).

$$R_{th} = L/k \tag{2.6}$$

Thermal conductivity is considered the most important parameter to evaluate thermal insulation material. A material with a thermal conductivity lower than 0.07 W/mK can be regarded as a thermal insulator [27]. Thermal conductivity can be measured by following international standard ASTM C518 [39], and thermal transmittance can be estimated by following ISO 6946 [40]. Thermal insulation value of textile materials can be determined by three common methods, Disc or plate methods (The lee's disc method), constant temperature method, and the cooling method. The lee's disc method is commonly practiced in laboratories [41].

2.3. Textile Waste Context

2.3.1. Present condition of textile waste

Clothing is one of the five basic needs requires for the survival of human beings. However, presently, in many parts of the world, clothing is subject to fashion, and style results in overconsumption of clothing [42]. Consumption of apparel and textile products has been increasing rapidly due to the increase of world population, consumer's buying power, and

changing consumption and fashion patterns [43], [44]. Fast fashion textile industries are responsible for high production and consumption of apparel and textiles. About 20% of global wastewater is produced by fashion industry. Fashion brand Burberry had burned about $40m of unsold clothes, accessories, and perfume instead of selling it off cheaply, in order to protect the brand's value [45]. Within 15 years, from 2000 to 2014, global clothing production has increased by 100%. At present, on average, a person buys 60 percent more clothing items and uses half of the time compared to 15 years ago. These changing consumption behaviors are generating a huge amount of textile waste [46]. In the US, from 2000 to 2014, the amount of textile waste has increased by 71.1%, while overall other solid waste has increased by 6.17%. Only 16.2% of this textile waste has been recycled [47], and most of the wastes are disposed into landfills. It is estimated that around 92 million metric tons (mt) of textile waste is produced annually, and this waste is likely to increase by about 60% from the year 2015 to 2030 [48]. In 2017, 16.9 million tons of textile wastes were produced in the USA, which were about 6.3% of total municipal solid wastes (MSW). Among these huge amounts of textile wastes, 11.15 million tons were discarded in landfills [49]. Similarly, in Europe, among 5.8 million mt of waste textile, only 1.5 million mt were recycled, and rest of the 4.3 million mt were sent to landfills [27], [33], [50]. A recent report estimated that the present waste of textiles in Europe has increased to about 16 million mt per year [51]. In addition to these, a huge amount of waste is produced in the textile industry during the manufacturing process. These wastes are composed of short fibers, yarns, threads, cutting waste, fabric scraps, and rejected fabric in quality control sections [52]. Figure 2.1 shows a summary of textile waste around the world.

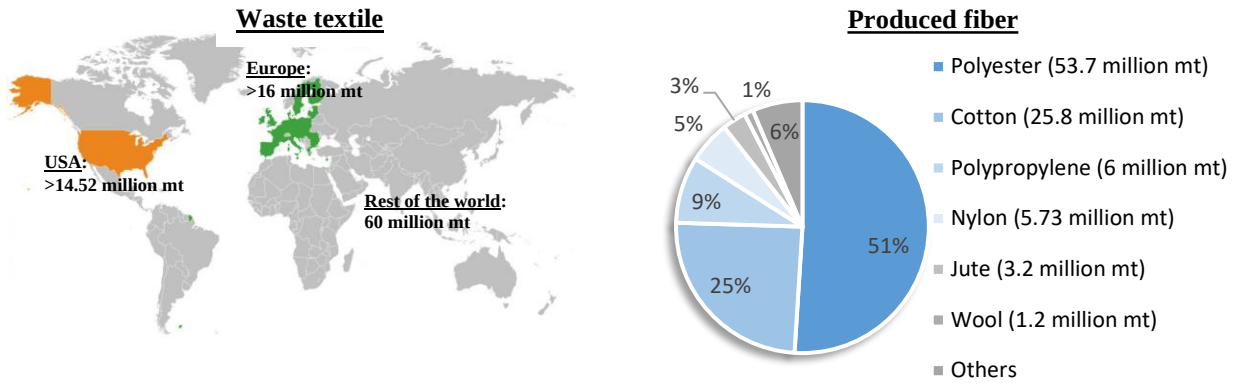

(a) (b)

Figure 2.1. Worldwide production of (a) textile waste and (b) textile fibers, based on the data from various sources cited.

It seems that post-consumer textile wastes are landfilled as it is the most convenient method. But things are changing in the developed and densely populated cities where it is difficult to find an open space to discard waste. In USA, it is estimated that the average landfilling cost of waste per ton (0.907 mt) was USD 50.3 in 2017, and present increase in rate of landfilling cost is about 6 percent which will be much higher in the future [53]. The condition is worse in the northeastern states of the US, where landfilling cost was 74.75 USD per ton (0.907 mt) in 2017 [53].

2.3.2. Environmental effects

Rapid increase in generation of textile waste has been creating a serious problem on the environment and on public health. It is estimated that the annual environmental effect of a family's clothing is equivalent to the amount of water needed to fill 1,000 bathtubs and the amount of carbon dioxide that is emitted due to run a modern car for about 6,000 miles [46]. The emission of CO_2 is predicted to increase by more than 60% to nearly 2.8 billion mt by the year 2030 [48]. Studies have estimated that if half of the people in UK use their clothes nine months longer than their present use time, then the carbon footprint and water footprint will decrease by about 8% and

10%, respectively [54]. Based on these results, one can easily understand that textile waste has huge adverse effect on the environment.

Both natural and synthetic fibers are responsible for this harmful effect. Textile waste from natural cellulosic fibers produces methane gas after degradation, which is a powerful greenhouse gas and is responsible for global warming [55]. Formation of greenhouse gases may also pollute groundwater. In 2017, 30 people died in Srilanka due to exposure to high concentration of methane gas which was produced by careless landfilling of waste [56]. Textile waste from organic animal fibers like wool produces ammonia, which is responsible for creating toxicity in land and water [57]. Synthetic textile waste, which comes from petroleum-based resources, has a more adverse effect on the environment due to its non-biodegradable and toxic characteristics. Textile waste that is discarded in landfills also produces leachate after decomposition, which has the potential to pollute both surface and groundwater sources [58]. Therefore, just by discarding textile waste, we are polluting our environment in various ways, at the same time contributing to depleting our valuable natural resources.

2.3.3. Sources of textile waste

Textile waste comes from a variety of sources, starting from fiber producers to end-users. Although most of the textile waste comes from household sources, wastes from production lines are also increasing. Based on sources, textile waste can be classified as pre-consumer or post-industrial, and post-consumer [59].

Pre-consumer waste or post-industrial waste is generated during the manufacturing process of apparel and textiles. These types of wastes include short fibers, combers noils, yarn waste, rejected fabrics due to manufacturing or dyeing faults, garments cutting waste, rejected garments, trimming, and end lots from surplus production [60]. It is estimated that a total of 10-20% textiles

are wasted during the manufacturing process [61]. Post-industrial textile wastes are considered virgin or clean waste as the materials are discarded without being used [56].

Post-consumer textile waste is referred to any types of clothing or textiles that are no longer used by the consumer due to damage, wear, out of fashion, or any other problems in the materials that end the willingness to use the products by the consumer. These post-consumer textile waste can be used for different purposes. It is estimated that more than 70% of useful life remains at the time of discarding the clothes [62].

2.3.4. Reuse or recycling of textile waste

Textile waste can be utilized in different applications by reuse or recycling the waste [63]. Reuse of textile waste means extending the serviceability of textiles with or without some preceding modification and transferring to a new consumer [64]. Recycling means converting the textile waste into new (textile or non-textile) products with or without damaging the previous one [65].

Recycling routes of textile waste can be mechanical, chemical, thermal, or combination of mechanical, chemical, and thermal processes. Based on the disassembling process, recycling can be referred to as fabric recycling (also referred to as reuse), fiber recycling (fabric dissembled up to fiber), and polymer recycling (break it down to polymer) [65]. Based on end products, recycling can be classified into two categories. One is recycling within the production process which is related to the production of new items that are similar to the textiles. Another approach is recycling out of the production process, which refers to producing a different item like developing a composite material for building insulation [60], [66].

Cost of recycling also varies with recycling routes, dissembling process, and categories of recycling. Again, industrial data of recycling cost is hardly found in the literature. However, we can indirectly get an idea about recycling cost to produce insulation materials, and it is very cheap.

For example, at present, average price of 1 kg cotton fiber is $1.39 [67], and average price of 1 kg cotton yarn is $2.80 [68]. Therefore, production cost of 1 kg cotton yarn should be less than $1.40 (as yarn price $2.80 includes fiber price, profit, and other costs). General production process of yarn from fibers includes blow-room, carding, drawing, roving, and spinning. On the other hand, most insulation materials from waste textiles are produced by nonwoven techniques, which required only carding process. Hence recycling waste textiles required one step out of five steps of yarn production. Therefore, it is possible to get an idea about recycling cost, which would be around one-fifth of the production cost of yarns.

Although recycling cost of textile waste is low, and it is estimated that up to 95% of textile waste could be recycled into different valuable products [56] but still, the rate of recycling is relatively low. This may be due to the diversity of fibrous waste and structure [59]. Textile waste varies with colors, types, compositions, and properties make it difficult to find an appropriate recycling technique [63]. In order to promote the recycling rate, Directive [69] has been passed in European parliament. Integrated knowledge and effort are required to increase the rate of recycling [52], [70] and for producing economically feasible products.

Producing acoustic and thermal insulation materials by textile waste is one of the effective, sustainable recycling processes. Recently researchers also found that the physical properties of textile waste are very much comparable to the conventional building insulation materials [71]. For this reason, textile wastes are recommended as feedstock to building insulation materials by several researchers [72].

The recycling of textile waste into building insulation materials has potential benefits in environmental, health, social, and economic sectors. The use of high quality thermal and acoustic insulation materials can reduce strain on the environment, energy consumption, space required for

landfill, virgin fibrous materials, greenhouse gases, pollution (noise, air, water, land); can save petroleum, fuel, and natural resources; and can improve the healthiness of human habitat [52], [73], [74]. The recycling of textile waste as an insulation material could also develop a new model of the circular economy [60]. By producing acoustic and thermal insulation materials, it is possible to get rid of the harmful effect of discarded textile waste, a new market or economy can grow for selling and buying these discarded textiles. On the other side, by producing low-cost thermal insulation materials, energy required for heating and cooling of our buildings and automobiles can be reduced.

2.4. Conversion of Waste to Acoustic and Thermal Insulation

Conversion of textile waste to thermal and acoustic insulation materials is not a straightforward process. As the type of textile waste is different, including industrial or post-consumer, synthetic and natural, therefore the conversion process is also varied.

In general, at first, pre-consumer textiles or post-consumer garments are accumulated from various textile industries and consumers. After that, the wastes are preciously categorized according to their fiber type, quality, and color. Then these wastes are cut into small pieces, shredded, and carefully opened back into fibers without breaking the length of the fibers. The obtained fibers are sorted again based on the characteristics of fibers, including length, strength, and count [75]. But for synthetic fibers, the process can go back up to polymer formation. Then these fibers or polymers may be used to produce thermal or acoustic insulation materials by a nonwoven processing technique, including web formation, web bonding, and finishing. According to desired end properties, different fibers can be blended together. In some cases, nonwoven materials may undergo high heat and pressure to produce hard composite materials.

However, all researchers do not follow the same steps. Researchers are continuously developing novel methods to optimize processes for maximum benefits. Some researchers directly used scrap fabric, then join them together and produce insulation materials [76], [77]. Several others used nonwoven techniques and prepared composites by applying heat and pressure [78]–[80]. Some researchers used waste textile fibers and mixed them with building materials, including lime, cement [81]–[84].

2.4.1. Direct method

In this method, fabrics are directly used to produce insulation materials without converting fabrics into fibers. In some cases, the opening of fabrics into fibers may lead to loss of structure and mechanical strength of fibers. Synthetic fabrics like polyester may get melted due to the heat generated from the applied mechanical force during the conversion of fabrics into fibers. On top of that sometimes fiber recycling may not be economically beneficial due to higher time and energy. In these cases, fabrics are directly used for the manufacture of insulation materials [77].

Several researchers investigated the use of waste fabrics directly to produce insulation materials [76] by cutting textile wastes and then stabilizing the wastes by stitching. Trajković et al. directly used polyester apparel cutting to construct the insulation structures [77]. In this research, three different types of polyester woven clothes were collected, then cut into small species (both irregular and exactly small species) by using rotary blades and vertical knife, and marked them A, C, and D (Figure 2. 2). Trajković et al. also collected polyester knitted (70/25/5 PES/cotton / Lycra®), converted them into partials fibrous form (for comparison), and marked them as B (Figure 2.2).

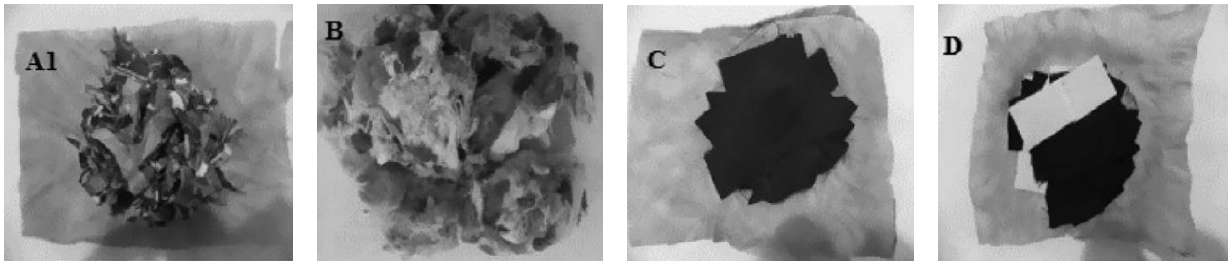

(a) (b) (c) (d)

Figure 2.2. Wasted polyester (a) Woven cut pieces at different size (b) Knitted fabric with fibrous form (c) Woven cut pieces at average dimension 6 × 4 inches (d) Woven cut pieces at average dimension 8 × 4 inches (reprinted with permission) (Adapted from [77]).

Trajković et al. encased the cutting waste by using 100% polypropylene nonwoven fabric and prepared insulation materials. By applying this method, very good thermal and acoustic properties were achieved with the thermal conductivity ranging from 0.0520 to 0.0603 W/mK and NRC ranging from 54.71 to 74.77%, and no significant difference with sample B to others [77].

2.4.2. Nonwoven technique

Nonwoven is the most commonly used technique for preparing insulation materials [77]. Several researchers have tried to produce acoustic and thermal insulation materials from waste textiles by the nonwoven technique [78]–[80]. Nonwovens are ideal methods for producing insulation materials due to their unique fiber orientation and porous structure [85].

General steps in nonwovens techniques start from the fiber or polymer that is recycled from textile waste. The recycled fibers are then transformed into webs with different areal densities. Web formation is a process where loose fibers are arranged in a sheet structure by laying down of fibers in a number of ways, including dry-laid webs, wet-laid webs, spunbonding, and film casting. Both staple and filament fibers can be used to produce a fiber web depending on the technique used [86]. After web formation, there needs to be some kind of bonding between the fibers to increase the strength and stability of the materials. There are mainly three different bonding processes, chemical (latex or chemical reagents), thermal or heat, and mechanical bonding (needle

punching or hydroentanglement) [86]. Selection of web formation and bonding process depends on several factors, including fiber type, required strength, density, thickness, and the desired end-use properties of the produced nonwovens. General steps of dry-laid webs (carding) and needle punched bonds are presented in the following (Figure 2.3).

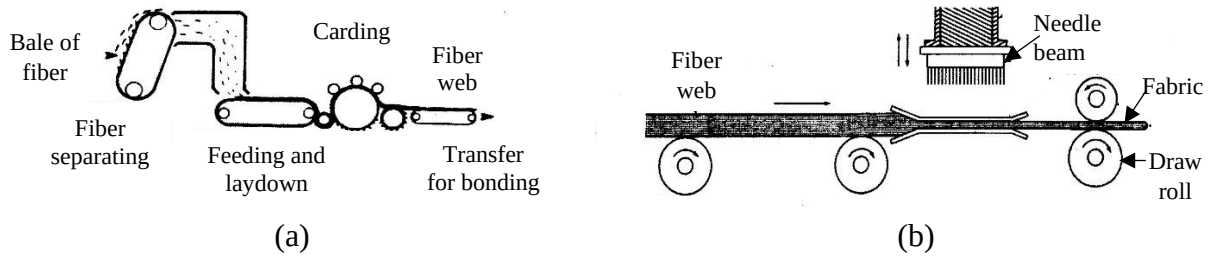

Figure 2.3. Schematic diagram of (a) web formation (dry-laid) and (b) bonding (needle punch) (Adapted from [86]).

Wazna et al. used the nonwoven technique to produce insulation materials from acrylic and wool wastes [85]. After collecting textile wastes and shredded into fibers, these fibers are opened and cleaned into short-staple fibers. Then, fiber webs with controlled thickness were produced by a dry-laid process where fibers were introduced into the card stage and folded ten times per meter. Wazna et al. used needle punching technique for bonding [85] which is the oldest method of making nonwoven fabrics. A barbed needle is used, which is driven upward and downward through fiber webs. These actions of needles interlock the fibers and hold the structure together by frictional forces. In this method, bonding is done without using any toxic binders [60]. Wazna et al. produced four different nonwoven thermal insulation materials by varying waste materials and got excellent insulation performance, with thermal conductivity values in the range of 0.03476–0.04877 W/mK [85].

Patnaik et al. also used a similar nonwoven technique to produce thermal and acoustic insulation materials from waste wool and recycled polyester fibers (RPET) [87]. In this research, a bale opener was used to convert the waste textile into individual fibers, followed by cross lapper to

produce a cross-lapped web and a needle punching machine to make a bond of the fiber web. In addition, the authors included a mixture of diammonium phosphate and sodium tetraborate as a fire retardant (5% by weight) and silicon (1% by weight) with the fiber web to increase the fire retardancy and moisture resistance properties of the insulation materials. The average thermal conductivity and sound absorption coefficients of their materials were 0.032 to 0.035 W/mK and 0.42 to 0.58 (at 1000 to 2000Hz), respectively [87].

Zach et al. produced thermal and acoustic insulation materials using recycled cotton, polyester, and flax fiber [74]. In this research, a nonwoven technique was also used, but instead of using the carding process, airlay method was used for web formation. In airlay method, fibers can be separated by suspending them in an airstream then blowing the fibers onto a moving belt to form a uniform layer of fiber web [86]. The production capacity in airlaying method is higher than that of the carding process [74]. After forming layers of fiber webs, bonding was done by the hot-air or mechanical bonding process. Zach et al. designed five different mixtures of the sample by combining polyester, flax, cotton, and bicomponent fibers of polyester with lower sheath melting temperature. The average thermal conductivity and absorption coefficients of their materials were 0.037 to 0.049 W/mK and 0.7 to 0.9 (at around1000 Hz) respectively [74].

2.4.3. Preparing composites with heat and pressure/compression molding

Insulation materials from textile waste can also be produced as composites by applying heat and pressure. In most cases, fiber webs are initially produced by a nonwoven technique. After that, heat and pressure are applied to different layers or mixture of fibers to form the composite. When the cellulosic fibers are used in the mixer or layer of composite, extra care should be taken so that the high temperature does not degrade the cellulosic fiber. If the melting temperature of synthetic

binder fiber is higher than that of the cellulosic fiber, then the plasticization and hydrolysis process are done to reduce the melting temperature of the synthetic fiber.

Palakurthi developed a composite material from recycled PET and cotton [88]. As the melting temperature of PET (260°C) is higher than the degradation temperature of cotton (146°C), she treated PET with plasticizers (2 Phenyl phenol, Benzyl Butyl Phthalate, Diallyl Phthalate, Benzoic Acid) and alkali (Dimethyl Sulfoxide, Tetramethyl ammonium hydroxide) to reduce the melting temperature of PET [88]. Ramamoorthy et al. also investigated reusing of discarded cotton/PET blend fabrics as reinforcement in composites [89]. Three compression-molded concepts were discussed and evaluated. In the first method, the melting temperature was used higher than that of polyester fabric with or without using plasticizer. The drawback of this method was that cotton fiber degrades due to high temperatures. In the second method, a bio-based resin from soybean oil was used as a matrix. And in the third method, a thermoplastic core-sheath type bi-component fiber was used that is carded and needle punched to form a nonwoven fabric. Ramamoorthy et al. placed this nonwoven between layers of recycled cotton/PET fabrics and subjected it to compression molding to form composites. Compression molding temperatures were used in such a way so that the sheath of the bicomponent fiber melts and acts as a matrix. Ramamoorthy et al. were able to produce a composite successfully by using methods two and three without degrading cotton fiber. It was observed that the composite produced by the third method showed four times improved mechanical properties, and 2.2 times higher tensile strength from composite types 1 and 2, respectively [89].

Lin et al. produced composite materials for acoustic and thermal insulation by using recycled Kevlar/Nylon/low-melting polyester nonwoven, which is reinforced with recycled polypropylene selvages [90]. Similar to the previously discussed methods, Lin et al. also produced

Kevlar/Nylon/low-melting PET nonwoven fabrics through the opening, blending, carding, lapping, and needle-punching processes. Then these nonwoven fabrics were passed through 1-mm-gap Twin-Roller Hot-presser at 160°C at a speed of 0.5 m/min. After that, 10 wt% of two-layer PP nonwoven selvages were kept between Kevlar/Nylon/low-melting PET nonwoven fabrics and did needle punching again. Finally, the composite layers were hot-pressed at different temperatures. Lin et al. found the best puncture resistance of their hot-pressed composite layer at a temperature of 180°C. It was also observed low thermal conductivity and good sound absorption coefficient for their five layers composite materials, which were 0.047 W/mK and above 0.9 at 1000 Hz, respectively [90].

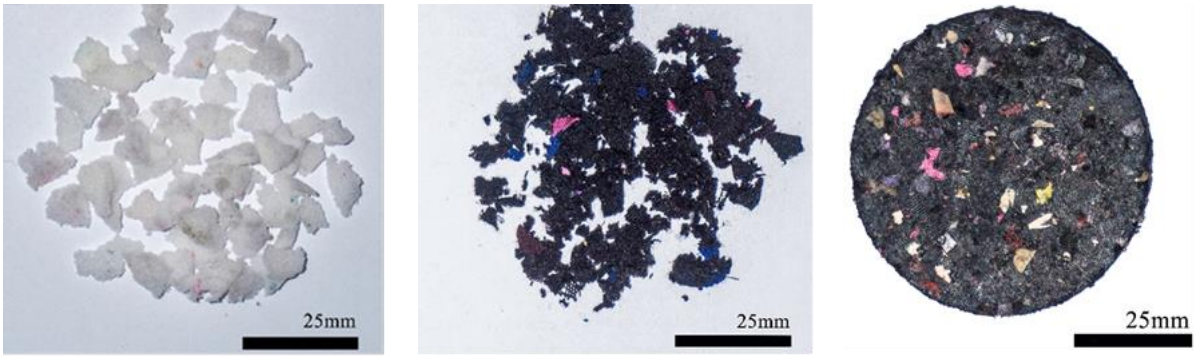

Figure 2.4. (a) Shredded PU, (b) Shredded NS, and (c) molded sample (reprinted with permission) (Adapted from [56]).

Dissanayake et al. used nylon/spandex (NS) and polyurethane (PU) to produce insulation materials by using a compression molding technique [56]. At first, NS and PU fabric wastes were collected and shredded into very small pieces (2 mm × 2 mm) (Figure 2.4a and Figure 2.4b) by using a commercial shredding machine. Then NS and PU were mixed at different ratios.

After that, circular insulation materials were produced (Figure 2.4c) with varying thickness using a compression molding method where the shredded samples were pre-heated and

compressed by high pressure. It was observed the best thermal conductivity at the composition (%W/W) 60:40, NS: PU with a thermal conductivity value of about 0.0953 W/mK [56].

2.4.4. Mixing with building materials

Textile waste has been used with building materials (lime, cement, and others.) for decades. Textile fiber shows a higher homogeneity in its performance than agro-based fibers [91]. Fabric weight is about 1/30 to the brick, steel, or concrete which can be used as a low-cost reinforcement material [92]. Recently researchers observed that textile waste used in mud-brick structures [83], [93], [94], or other ways to produce buildings has several other advantages, including earthquake resistance [93], low thermal conductivity [94], and good sound insulation properties [83]. Along with these properties, textile fiber can increase strength, performance, and durability of the building materials [52], [95].

The conversion of textile waste to thermal and acoustic insulation materials is very simple when used with building materials. Here conversion method is completely different from nonwoven and composite techniques. In this case, there is a need to mix the textile waste with appropriate ratio with the cement, lime, water, bricks, and other building materials.

(a) (b)

Figure 2.5. Textile waste fiber and produced board (reprinted with permission) (Adapted from [52]).

Several research articles investigating the use of textile waste with building materials [81]–[84] have already been published. Del Mar Barbero-Barrera et al. used textile fiber waste with natural hydraulic lime to produce boards with higher acoustic and thermal insulation properties [52]. Initially, textile wastes (mainly cotton) were collected from industry (Figure 2.5a), and without any further processing, these wastes were mixed with natural hydraulic lime and water with three different ratios. After several days of curing and drying, the samples were tested (Figure 2.5b). Del Mar Barbero-Barrera et al. got the best thermal conductivity of 0.14 (W/mK), which is much lower than the similar board made with wood–gypsum (0.189 to 0.277 W/mK) [96] (Bekhta and Dobrowolska, 2006) and newspaper sandwiched aerated lightweight concrete panel (0.300 – 0.600 W/mK) [97]. But the acoustic absorption coefficient was about 0.2 at 2000 Hz which is comparatively low. Higher compression strength was also observed after using textile waste fiber [52].

Binici et al. used textile waste (cotton), sunflower stalk, and stubble fibers to produce sound and thermal insulation materials for building applications. In this research, insulation boards were produced by two approaches: one is by using plaster and another by using epoxy as a binder [98]. In the first method, the mixture of textile wastes and sunflower stalks was grounded. Then these materials were applied to the wall (mud bricks, concrete bricks, and red bricks) along with plaster binder. In the second method, sunflower stalks, cotton waste, and textile waste fiber were mixed with an epoxy binder at different ratios and produced layers. After that, high pressure was applied to these layers to produce insulation boards. Binici et al. found lower thermal conductivity of the wall (0.0728 W/mK) and high sound insulation properties compared to the wall without these insulation materials [98].

2.5. Life Cycle Assessment

Life Cycle Assessment (LCA) is a systematic way to assess or estimate the environmental impact of a product in its complete lifetime from production to disposal [99]. It covers every phase from raw materials to disposal [100]. Normally, design and development of a product are not included in calculating LCA as it is considered that design and development do not significantly impact the environment. But some researchers have disagreed with this and showed that design and development of a product could enormously affect other stages of life cycle [101]. For estimation of LCA of a product, the emissions to air, water, and land are assessed during production, use, and disposal of the product. After that, the assessed amount is related to the possible environmental effects, including resource depletion, ozone depletion, and global warming [99]. A complete LCA analysis can be accomplished by following the international standards of ISO 14040 [102] and ISO 14044 [103].

LCA analysis is normally done by some consultancy companies or research institutes [75]. Several researchers have evaluated the effect of cotton cultivation on environment both by conventional and organic agriculture methods [104], [105] and the effect of different dyeing and finishing processes on the environment [106], [107] using LCA. Van der Velden et al. have studied LCA of different textile fibers, polyester, nylon, acrylic, and cotton, and determined the comparative effects of these fibers on the environment [108]. But in the case of recycled textile fibers, only a limited number of researchers did some LCA study [99], [109].

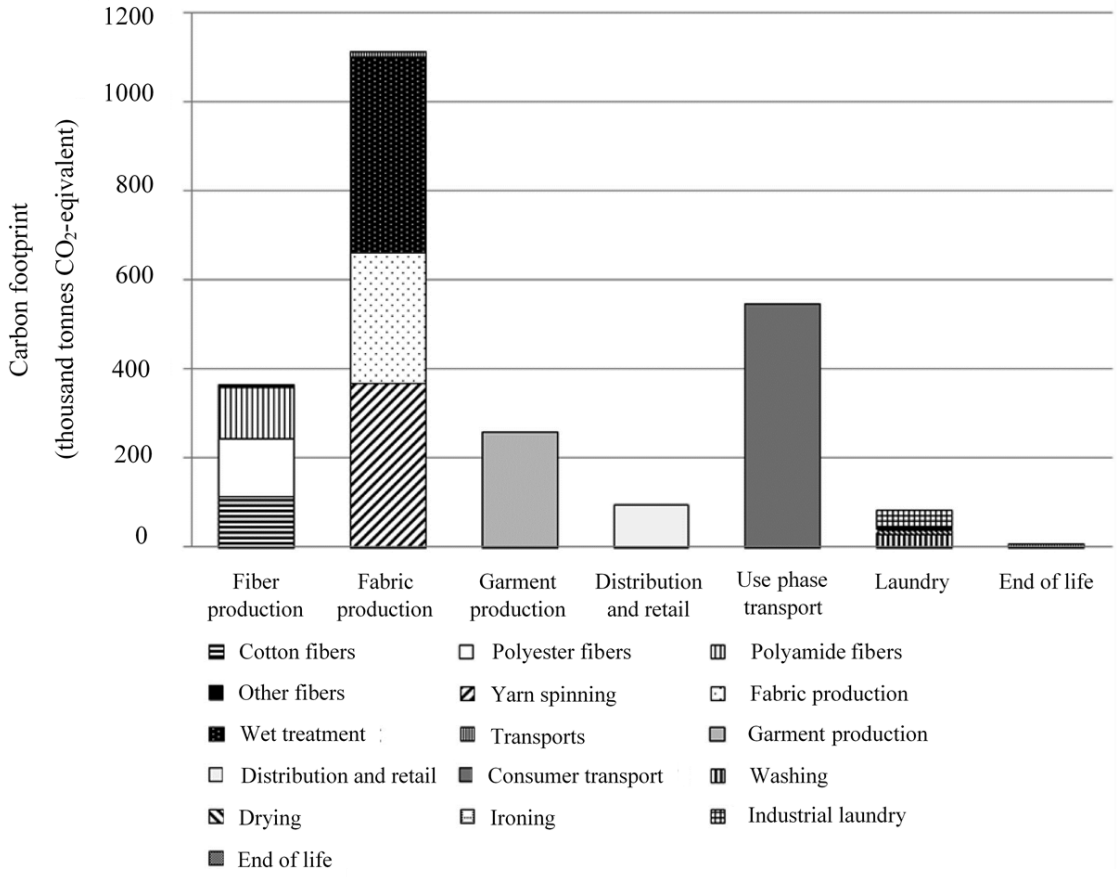

Figure 2.6. The carbon footprint of the Swedish apparel sector over one year (reprinted with permission) (Adapted from [110]).

Roos et al. studied the LCA of Swedish apparel sector to investigate the contribution of carbon footprint (Figure 2.6) at different stages of clothing and textiles from fiber production to end of life [110]. Here carbon footprint of cotton, polyester, and polyamide was determined at different production stages [110]. Some other researchers also estimated carbon footprint and water footprint of textiles. Cotton consumption is accountable for 2.6% use of global water [111]. Worldwide water consumption for the production of cotton fiber from 1997 to 2001 was 256 GM^3 (256×10^{30} liters) [111].

One of the ways to reduce water consumption is to replace cotton fibers with recycled cotton. Roos et al. found that in Swedish factory by using recycled cotton fiber over one year, carbon

footprint and water consumption can be reduced by around 2.4×10^6 tons equivalent CO_2 and above 900 billion liters of water, respectively. Similarly, by using recycled polyester, carbon footprint and water consumption can be reduced by around 2.3×10^6 tons equivalent CO_2 and above 1000 billion liters of water, respectively [110].

van der Velden et al. did LCA analysis of textiles made of cotton, polyester, nylon, acryl, or elastane. It was observed that acrylic and polyester have least effect on environment, and cotton has the highest effect [108]. Woolridge et al. conducted life cycle assessment at different stages of textile manufacturing of cotton and polyester fibers, including fiber, spinning, knitting, dyeing, and garments sections. It was found that by using one tonne of cotton and reused polyester garments, the net energy of 64 951 kWh and 89 811 kWh can be saved [99]. After considering several factors, including extraction of resources, manufacture of materials, electricity generation, clothing collection, processing, distribution, and final disposal of wastes, it was found that by replacing 1kg of virgin cotton with 1kg of second-hand clothing, approximately 65 kWh energy could be saved. And for one kg of polyester, the energy-saving amount is about 90 kWh [99]. Production of 1ton recycled polyester garments required only 1.8% energy in comparison to the production of 1ton polyester garments from virgin materials. Similarly, producing 1ton cotton cloths needed only 2.6% energy compared to the production of 1ton cotton cloths from virgin materials [99].

2.6. Thermal and Acoustic Insulation from Different Textile Wastes

2.6.1. Polyester

Polyester is the most widely used fiber in apparel and textiles. In 1990 global polyester fiber production was 8.67 million mt [112], and present production has increased more than 5 times compared to 1990. In 2017, the annual production of polyester fiber was around 53.7 million mt,

which is about 51 percent of the global fiber production [113]. Although Polyester waste is the leading element of the clothing industry waste, its recycling rate is very low. In 2017, only 14% of waste had been recycled (Figure 2.7), and a huge amount of this synthetic fiber has been discarded to landfills as waste [113]. Several researchers are studying approaches to minimize the environmental effects by recycling polyester waste into different materials, including acoustic and thermal insulation materials.

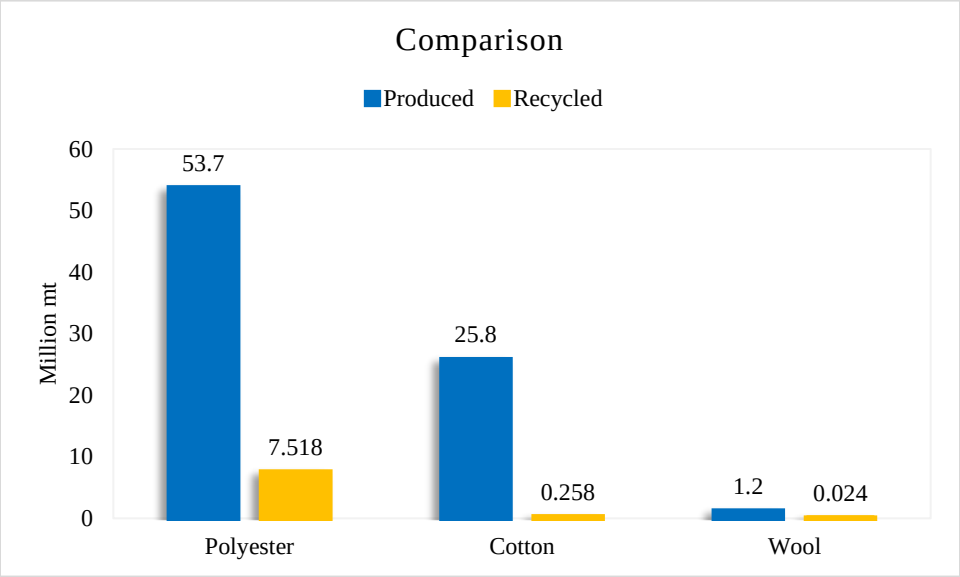

Figure 2.7. Comparison of produced and recycled fibers.

Trajković et al. used polyester cutting waste during apparel manufacturing to produce thermal and acoustic insulation materials [77]. Here polyester cutting waste was directly used as an insulation blanket for roofing and buildings' internal walls. A good insulation property was observed with the thermal conductivity was between 0.0520 and 0.0603 W/mK, and the noise reduction coefficient was ranging from 54.71 to 74.77%. Trajković et al. also found that their insulation materials had good resistance against fire and were less degradable in moist conditions [77].

Lee et al. developed sound-absorbing nonwoven materials using recycled polyester fibers [115]. Here, the influences of fiber diameter and fiber orientation angles on sound absorption coefficient were also investigated. Although significant influence of fiber orientation on the absorption coefficient was not found, it was noticed that with the increase in fiber diameter, the absorption coefficient of nonwoven mats had increased [115]. Drochytka et al. also investigated polyester waste and found that bulk density (Figure 2.8) had influences on both sound absorption and thermal conductivity [114]. It was observed that with the increase of bulk density, sound absorption coefficient increases, and thermal conductivity decrease. But the influence of bulk density is more prominent for thermal insulation. Drochytka et al. also studied the effect of temperature on thermal insulation properties. It was observed that the thermal conductivity of polyester mat significantly decreases with decrease in temperature (Figure 2.8) [114]. Alcaraz et al. analyzed the effect of microfiber layers on sound absorption properties by adding microfiber layers with the polyester nonwoven mats [22]. It was observed that the sound absorption coefficient had significantly increased with the addition of microfiber layers [22]. Valverde et al. developed insulation from textile industry scraps, constituted of polyester and polyurethane. It was noticed that the insulation panel showed the lowest thermal conductivity, 0.041 W/mK, at a density of 396 kg/m^3 [116].

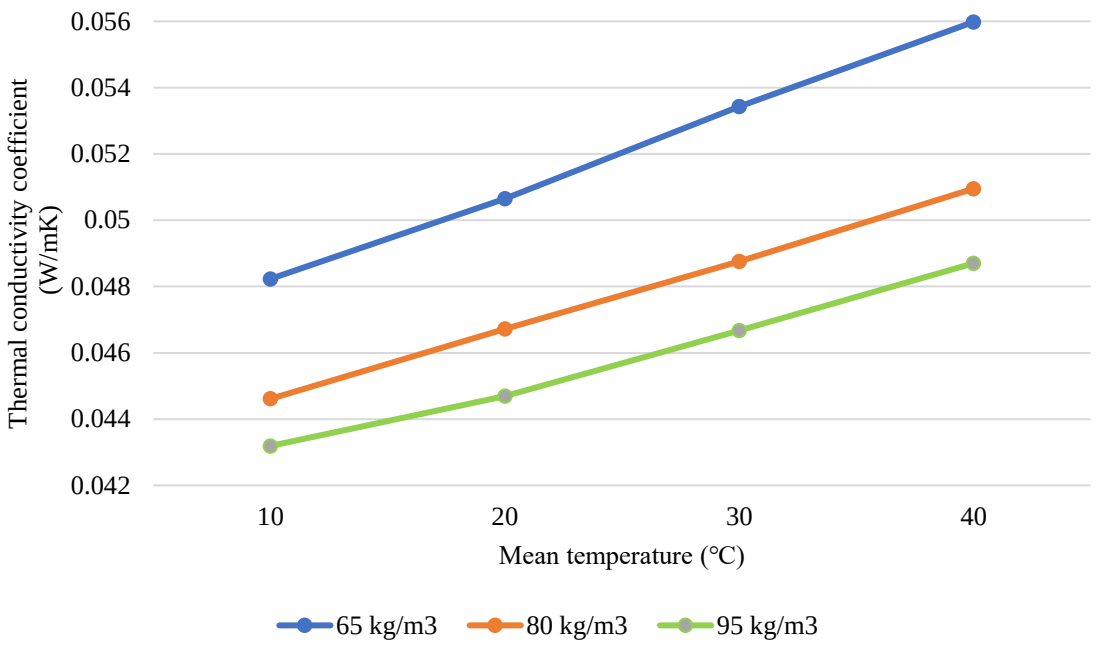

Figure 2.8. Influence of temperature and bulk density on thermal conductivity of polyester mat (reprinted with permission) (Adapted from [114]).

2.6.2. Cotton

Cotton fiber is the natural vegetable fiber collected from cotton plant seeds. It is one of the most cultivated non-agricultural products mainly used in apparel production [27]. At present cotton is the second largest produced fiber after polyester, and in the case of natural fibers, it is the largest produced fiber [113]. In 2017, the average production of cotton around the world was 25.8 million mt (Fig2.7), which was about 24.5% of the global textile fiber market [113]. According to the Ellen MacArthur Foundation, less than one percent of all clothing is recycled back into clothing [113]. Therefore, a huge amount of cotton fiber is landfilled as discarded apparel. In addition to this, a massive amount of virgin cotton fiber is discarded as waste during cotton yarn production. Several researchers proposed the use of cotton waste for the production of thermal and acoustic insulation materials.

Some companies have started commercial production of insulation materials from cotton waste. Bonded Logic incorporated commercially produced Echo Eliminator™ Acoustic Panels from recycled cotton fibers. The noise reduction coefficient of their products was 0.8 to 1.15 measured according to ASTM C 423 standard test method [117].

Küçük and Korkmaz produced nonwoven composites by mixing cotton and polyester fibers at different ratios. It was observed that a mixture of 70% cotton and 30% polyester had an excellent sound absorption coefficient in the mid-to-high frequency ranges [5]. Del Rey et al. also observed similar results of sound absorption properties for recycled cotton and polyester composites [118]. It was also noticed that the absorption coefficient and airflow resistivity values of recycled cotton polyester composites are very similar to those of commercially available sound absorptive materials in the market [118].

Sedlmajer et al. studied the thermal conductivity of insulation mats produced from recycled polyester, cotton, and bicomponent fibers at different ratios. It was found that mats with higher cotton fiber ratio showed better insulation properties [119]. Binici et al. also observed similar properties for the cotton fiber. In their research, lightweight composite materials from cotton waste and fly ash were produced, and it was found that the composites with higher amount of cotton waste showed better thermal conductivity [92].

Some researchers examined the effect of mixing cotton waste with building materials to improve the insulation properties. Aghaee et al. focused on increasing the thermal insulation of building materials with cotton waste. In this research, lightweight perlite and concrete panels were produced for building a partition. Aghaee et al. embedded the waste textile fibers consisting of cotton fibers and woven meshes of glass fibers, then confined with textile meshes embedded in the central part of perlite lightweight concrete. The perlite porosity and the textile fiber core reduced

the thermal conductivity to 0.3 W/mK [120], [121]. Binici et al. also used textile waste (cotton), sunflower stalk, and stubble fibers to produce sound and thermal insulation material for building applications [98]. Forty-four samples were produced by mixing these materials at different ratios. Among 44 samples, some noticeable desirable thermal conductivity values were 0.0871 and 0.0893 produced by a combination of sunflower stem/cotton waste/epoxy (36.36/36.36/27.27) and sunflower stem/sunflower stalk fiber/cotton waste/epoxy (37.04/7.41/24.69/30.86) respectively [98]. Rajput et al. mixed recycled cotton waste and paper mill waste with cement bricks. Cotton fiber waste increased the porosity of cement bricks from 0.18 to 0.29 and improved the thermal insulation of the building. Thermal conductivity value decreased from 0.32 to 0.25 W/mK [122]. Binici et al. combined cotton waste with fly ash and analyzed the potential use of this combination for manufacturing low-cost and lightweight composites as building materials. Here cotton waste and fly ash were mixed with cement and built a model house. Then compared the thermal insulation properties of this model house with a control sample that was made without using cotton waste and fly ash. Binici et al. determined that the thermal insulation properties of their model house were superior to that of the control one (thermal conductivity was 29.3% lower). The compressive strength, flexural strength, unit weight, and water absorption properties of their developed materials also fulfilled the required standards [84], [123].

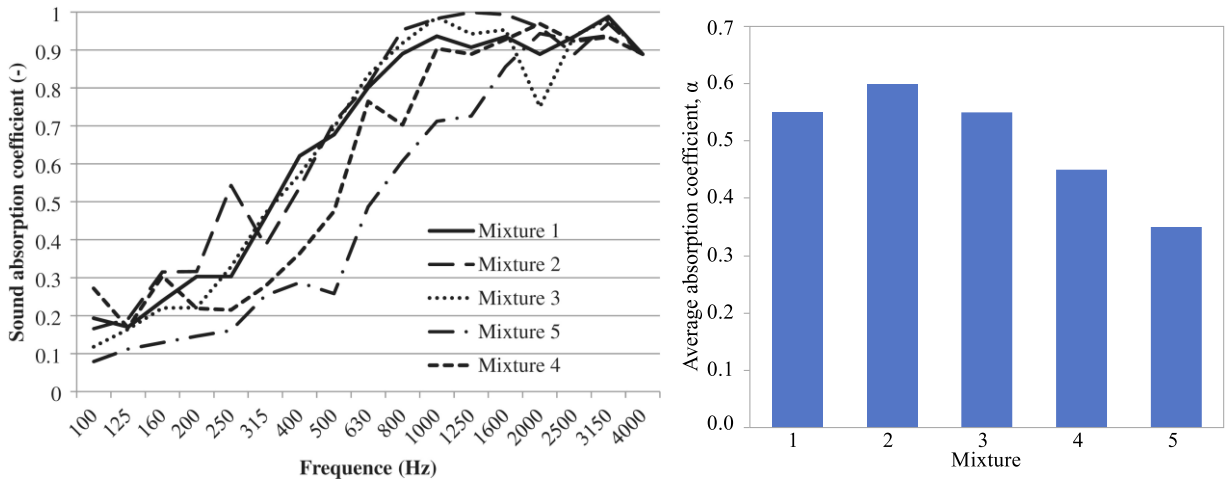

(a) (b)

Figure 2.9. (a) Sound absorption coefficient of polyester, flax, and cotton mixtures at different frequencies (b) Average absorption coefficient of polyester, flax, and cotton mixtures at five different ratios (reprinted with permission) (Adapted from [74]).

Zach et al. produced thermal and acoustic insulation materials by combining recycled cotton, polyester, and flax fibers [74]. In this research, five different mixtures of the samples were designed by combining polyester, flax, cotton, and bicomponent fiber of polyester with lower sheath melting temperature and tested thermal conductivity and sound absorption properties (Figure 2.9). The average thermal conductivity and sound absorption coefficients of their materials were 0.037 to 0.049 W/mK, and Mixture 2 (40% cotton, 40% polyester, and 20% bicomponent) has the highest sound absorption coefficient [74].

2.6.3. Nylon

Synthetic nylon has excellent strength and other mechanical properties. In 2017, 5.73million mt of nylon was produced in the world, which consisted of 5.4 percent of world fiber production market [113]. A huge amount of this synthetic fiber has been discarded as waste both in a landfill as well as in water.

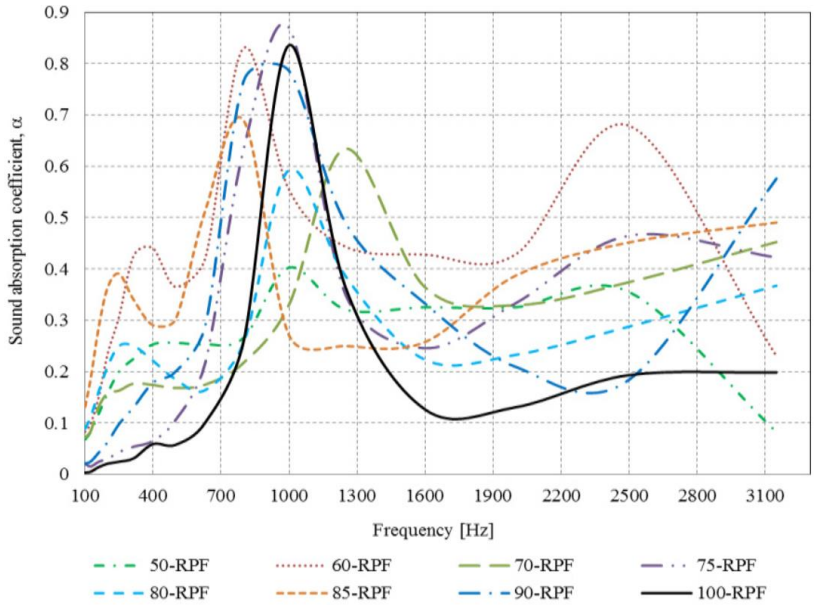

Figure 2.10. The sound absorption coefficient of textile waste, where 100RPF means 100% rigid polyurethane and 60 RPF means 60% rigid polyurethane and 40% textile waste (nylon, modal, and acrylic) and so on (reprinted with permission) (Adapted from [124]).

Dissanayake et al. used the post-industrial textile waste of nylon fiber mixed with spandex (NS) and polyurethane (PU) waste to produce thermal insulation materials. It was observed that the combination of 60% NS and 40% PU gave the best thermal insulation properties [56]. Tiuc et al. did some experimental study by mixing textile waste (nylon, modal and acrylic fiber) with polyurethane foam at different ratios [124]. Polyurethane foam was considered the best thermal insulation material [125], and it is widely used in industry for its mechanical, electrical, thermal, and acoustic properties [126]. Tiuc et al. found that the composite material with 40% textile waste and 60% rigid polyurethane foam had better sound absorption properties than other compositions. The noise reduction coefficient of composite materials is almost twice that of 100% rigid polyurethane foam (Figure 2.10) [124].

2.6.4. Other materials

Wool fiber is one of the most used animal fibers in the world since ancient times due to its excellent thermal insulation properties. In 2017, world wool fiber production was 1.2 million mt, 95% of which are sheep wool. At present, around 22,000 mt wool has been recycled (Figure 2.7), and the rest of the fiber has been discarded as waste [113]. Waste wool can be collected from different sources. Along with discarded textiles, short virgin wool fibers can be obtained during shearing sheep's hairs. As short wool fiber is not suitable for apparel production, it is discarded as waste [87]. Wool is generally composed of many different amino acids, which form long chains. The coiled springs of wool's molecular chains contribute to fiber resilience, which is suitable for sound absorption [127], [128]. The sheep wool has excellent sound-absorbing properties due to its micro-cavities as well [1], [128]. The value of the absorption coefficient at medium frequency 1000 Hz to 2000 Hz is very high as well as uniform. The absorption coefficient of wool is about 0.9 at around 800 Hz to 2000 Hz [127], [128]. Berardi and Iannace used inverse method to predict the acoustical properties of sheep wool and obtained higher sound absorption coefficient (above 0.95) for wool fiber at 1500 Hz to 2000 Hz [2]. Zach et al. studied the thermal conductivity of wool fiber at different thicknesses, temperatures, and moistures. It was found that thermal conductivity of sheep wool fiber decreased with the decrease of temperature, moisture, and density and with the increase of thickness [71]. Hassanin et al. developed insulating panels by mixing of Tetra Pak waste and wool yarn waste at different ratio. Air trapped within the wool fibers improved the thermal insulation properties of Tetra Pak and wool fiber waste composite [129].

There are some other waste fibers that are also used in producing thermal and acoustic insulation materials. Acrylic fiber is considered as artificial wool fiber, and it replaces wool fiber, especially in hand-made knitted and hosiery garments due to their bulkiness and high elastic properties [130].

These fibers have very good insulation properties. Jute is the second largest natural fiber after cotton which is used mainly in industrial applications [131], has very good potential to be used as efficient thermal and acoustic insulation materials [132]. Devireddy and Biswas observed very high insulation properties of jute fiber with the thermal conductivity value of 0.036 W/mK [133]. Polypropylene is the lightest of all fibers. It is 34% and 20% lighter than polyester and nylon fibers. Due to its low specific gravity, this fiber yields the largest volume at a given weight and provides good bulk and cover. This unique property of polypropylene fiber helps it to retain heat for a longer time. The thermal conductivity of polypropylene fiber is lower than other natural and synthetic fibers [134].

Sometimes researchers and manufacturers collect textile wastes from industry which is the combination of different types of fibers, and which is very difficult and time-consuming to separate one type of fibers from another. In this case, researchers used mixed waste materials as textile waste to produce thermal and acoustic insulation materials. Hadded et al. used recycled textile waste materials and developed two samples of waste linter and tablecloth. It was found that the thermal conductivity of waste linter and tablecloth were 0.039 W/mK and 0.033 W/mK, respectively, which means that this material will have the potential to be used in the building insulation materials [33].

2.7. Summary

In this chapter, an extensive overview of thermal and acoustic insulation materials produced from textile waste has complied. The mechanism of thermal and acoustic insulation and measurement process by following the international standards were discussed. The effect of discarded textiles on environment and health, and ways to minimize it by recycling have been summarized. The transformation of textile waste into insulation materials is also discussed. Although the present

market is completely dominated by some conventional synthetic insulation materials, there is a potential to replace these conventional materials with recycled textiles. In some cases, thermal and acoustic insulation materials produced from waste textiles show much better results than the currently available and dominating products in the market. In addition to that, by discussing LCA, it was specifically reported how much environmental effect could be minimized by using recycled textiles.

However, the research of using textile wastes as an insulation material is still in its initial stages. Research has been done only on some of the common fibers. Majority of the investigated materials are not entirely characterized. In every study, researchers mentioned the environmental advantages of using recycled textiles, but very few authors include the LCA analysis.

Based on above discussion, it can be concluded that textile waste has the potential to be used as an environmently friendly insulation material, but still, lots of limitations should be overcome to commercialize the insulation materials. Well-focused research is required to overcome these limitations and answer some questions so that it will be possible to successfully commercialize such products.

2.8. References

[1] U. Berardi and G. Iannace, “Acoustic characterization of natural fibers for sound absorption applications,” *Build. Environ.*, vol. 94, pp. 840–852, 2015.

[2] U. Berardi and G. Iannace, “Predicting the sound absorption of natural materials: Best-fit inverse laws for the acoustic impedance and the propagation constant,” *Appl. Acoust.*, vol. 115, pp. 131–138, 2017, doi: 10.1016/j.apacoust.2016.08.012.

[3] A. Patnaik, “Materials Used for Acoustic Textiles,” in *Acoustic Textiles*, R. Padhye and R. Nayak, Eds. Singapore: Springer, 2016, pp. 73–92.

[4] T. Koizumi, N. Tsujiuchi, and A. Adachi, “The development of sound absorbing materials using natural bamboo fibres,” in *High performance structures and materials IV.*, C. A. Brebbia & De Wilde, WP., Ed. Southampton: WIT Press, 2002, pp. 157–166.

[5] M. Küçük and Y. Korkmaz, “The effect of physical parameters on sound absorption properties of natural fiber mixed nonwoven composites,” *Text. Res. J.*, vol. 82, no. 20, pp. 2043–2053, 2012, doi: 10.1177/0040517512441987.

[6] H. S. Seddeq, N. M. Aly, A. Marwa, and M. Elshakankery, “Investigation on sound absorption properties for recycled fibrous materials,” *J. Ind. Text.*, vol. 4, no. 1, pp. 56–73, 2013, doi: 10.1177/1528083712446956.

[7] M. E. Nute and K. Slater, “A study of some factors affectng sound reduction by carpeting,” *J. Text. Inst.*, vol. 64, no. 11, pp. 645–651, 1973, doi: 10.1080/00405007308630314.

[8] M. E. Nute and K. Slater, “The effect of fabric parameters on sound-transmission loss,” *J. Text. Inst.*, vol. 64, no. 11, pp. 652–658, 1973.

[9] X. Tang and X. Yan, “Acoustic energy absorption properties of fibrous materials: a review,” *Compos. Part A Appl. Sci. Manuf.*, vol. 101, pp. 360–380, 2017, doi: 10.1016/j.compositesa.2017.07.002.

[10] J. P. Arenas, J. Rebolledo, R. del Rey, and J. Alba, “Sound absorption properties of unbleached cellulose loose-fill insulation material,” *BioResources*, vol. 9, no. 4, pp. 6227–6240, 2014.

[11] P. Bonfiglio and F. Pompoli, “Inversion problems for determining physical parameters of porous materials: Overview and comparison between different methods,” *Acta Acust. united with Acust.*, vol. 99, no. 3, pp. 341–351, 2013.

[12] M. Garai and F. Pompoli, “A simple empirical model of polyester fibre materials for acoustical applications,” *Appl. Acoust.*, vol. 66, no. 12, pp. 1383–1398, 2005.

[13] M. E. Delany and E. N. Bazley, “Acoustical properties of fibrous absorbent materials,” *Appl. Acoust.*, vol. 3, no. 2, pp. 105–116, 1970.

[14] K. Attenborough, “Acoustical characteristics of porous materials,” *Phys. Rep.*, vol. 82, no. 3, pp. 179–227, 1982.

[15] K. V Horoshenkov, K. Attenborough, and S. N. Chandler-Wilde, “Padé approximants for the acoustical properties of rigid frame porous media with pore size distributions,” *J. Acoust. Soc. Am.*, vol. 104, no. 3, pp. 1198–1209, 1998.

[16] I. P. Dunn and W. A. Davern, “Calculation of acoustic impedance of multi-layer absorbers,” *Appl. Acoust.*, vol. 19, no. 5, pp. 321–334, 1986, doi: 10.1016/0003-682X(86)90044-7.

[17] Y. Miki, “Acoustical properties of porous materials-generalizations of empirical models,” *J. Acoust. Soc. Japan*, vol. 11, no. 1, pp. 25–28, 1990, doi: 10.1250/ast.11.25.

[18] Y. Miki, “Acoustical properties of porous materials-Modifications of Delany-Bazley models,” *J. Acoust. Soc. Japan*, vol. 11, no. 1, pp. 19–24, 1990.

[19] J. Ramis, J. Alba, R. Del Rey, E. Escuder, and V. J. Sanchís, “New absorbent material acoustic based on kenaf’s fibre,” *Mater. Construcción*, vol. 60, no. 299, pp. 133–143, 2010, doi: 10.3989/mc.2010.50809.

[20] G. H. Yoon, “Acoustic topology optimization of fibrous material with Delany–Bazley empirical material formulation,” *J. Sound Vib.*, vol. 332, no. 5, pp. 1172–1187, 2013.

[21] “ISO 10140-2,” *Acoustics -- Laboratory measurement of sound insulation of building elements -- Part 2: Measurement of airborne sound insulation*, 2010. https://www.iso.org/standard/42088.html.

[22] M. P. S. Alcaraz, M. Bonet-Aracil, J. G. S. Alcaraz, and I. M. Seguí, “Sound absorption of textile material using a microfibres resistive layer,” in *IOP Conference Series: Materials Science and Engineering*, 2017, vol. 254, no. 7, p. 72022, [Online]. Available: https://iopscience.iop.org/article/10.1088/1757-899X/254/7/072022/meta.

[23] S. S. Jung, Y. T. Kim, Y. B. Lee, S. Il Cho, and J. K. Lee, “Measurement of sound transmission loss by using impedance tubes,” *J. Korean Phys. Soc.*, vol. 53, p. 596, 2008.

[24] “ISO 10534-2,” *Acoustics -- Determination of sound absorption coefficient and impedance in impedance tubes -- Part 2: Transfer-function method*, 1998. https://www.iso.org/standard/22851.html.

[25] “ISO 354,” *Acoustics -- Measurement of sound absorption in a reverberation room*, 2003. https://www.iso.org/standard/34545.html.

[26] "ASTM C423," *Standard Test Method for Sound Absorption and Sound Absorption Coefficients by the Reverberation Room Method*, 2017. https://www.astm.org/Standards/C423.htm.

[27] F. Asdrubali, F. D'Alessandro, and S. Schiavoni, "A review of unconventional sustainable building insulation materials," *Sustain. Mater. Technol.*, vol. 4, pp. 1–17, 2015, doi: 10.1016/j.susmat.2015.05.002.

[28] C. M. Pelanne, "Heat flow principles in thermal insulations," *J. Therm. Insul.*, vol. 1, no. 1, pp. 48–80, 1977.

[29] H. Simmler *et al.*, "Vacuum Insulation Panels. Study on VIP-components and panels for service life prediction of VIP in building applications (Subtask A)," 2005. [Online]. Available: https://www.osti.gov/etdeweb/biblio/21131463.

[30] R. Viskanta, "Heat transfer by conduction and radiation in absorbing and scattering materials," *J. Heat Transfer*, vol. 87, no. 1, pp. 143–150, 1965.

[31] M. Zakriya, G. Ramakrishnan, N. Gobi, N. K. Palaniswamy, and J. Srinivasan, "Jute-reinforced non-woven composites as a thermal insulator and sound absorber–A review," *J. Reinf. Plast. Compos.*, vol. 36, no. 3, pp. 206–213, 2017.

[32] M. K. Anjaria, *Thermal insulation properties of low density nonwoven battings*. Raleigh: North Carolina State University, 1988.

[33] A. Hadded, S. Benltoufa, F. Fayala, and A. Jemni, "Thermo physical characterisation of recycled textile materials used for building insulating," *J. Build. Eng.*, vol. 5, pp. 34–40, 2016.

[34] S. B. Stanković, D. Popović, and G. B. Poparić, "Thermal properties of textile fabrics made of natural and regenerated cellulose fibers," *Polym. Test.*, vol. 27, no. 1, pp. 41–48, 2008.

[35] S. S. Woo, I. Shalev, and R. L. Barker, "Heat and moisture transfer through nonwoven fabrics: Part I: Heat transfer," *Text. Res. J.*, vol. 64, no. 3, pp. 149–162, 1994.

[36] R. L. Barker and R. C. Heniford, "Factors affecting the thermal insulation and abrasion resistance of heat resistant hydro-entangled nonwoven batting materials for use in firefighter turnout suit thermal liner systems," *J. Eng. Fiber. Fabr.*, vol. 6, no. 1, pp. 1–10, 2011.

[37] S. Sukigara, H. Yokura, and T. Fujimoto, "Compression and thermal properties of recycled fiber assemblies made from industrial waste of sweater products," *Text. Res. J.*, vol. 73, no. 4, pp. 310–315, 2003, doi: 10.1177/004051750307300406.

[38] Z. S. Abdel-Rehim, M. M. Saad, M. El-Shakankery, and I. Hanafy, “Textile fabrics as thermal insulators,” *AUTEX Res. J.*, vol. 6, no. 3, pp. 148–161, 2006.

[39] “ASTM C518-17,” *Steady-State Thermal Transmission Properties by Means of the Heat Flow Meter Apparatus*, 2017. https://www.astm.org/Standards/C518.

[40] “ISO 6946,” *Building components and building elements -- Thermal resistance and thermal transmittance -- Calculation methods*, 2017. https://www.iso.org/standard/65708.html.

[41] E. A. ElNashar and G. Bashkova, “Comfort of thermal insulatiuon of bulky woven fabrics for clothes,” *ARTTE*, vol. 2, no. 4, pp. 329–344, 2014.

[42] B. Piribauer and A. Bartl, “Textile recycling processes, state of the art and current developments: A mini review,” *Waste Manag. Res.*, vol. 37, no. 2, pp. 112–119, 2019, doi: 10.1177/0734242X18819277.

[43] R. E. Marshall and K. Farahbakhsh, “Systems approaches to integrated solid waste management in developing countries,” *Waste Manag.*, vol. 33, no. 4, pp. 988–1003, 2013.

[44] N. Tojo, *Prevention of textile waste: material flows of textiles in three Nordic countries and suggestions on policy instruments*. Copenhagen: Nordic council of ministers, 2012.

[45] K.-L. Cooper, “Fast fashion: Inside the fight to end the silence on waste,” 2018. https://www.bbc.com/news/world-44968561 (accessed Apr. 12, 2021).

[46] R. Leblance, “The balance small business,” *Textile Recycling Facts and Figures*, 2018. https://www.thebalancesmb.com/textile-recycling-facts-and-figures-2878122.

[47] “EPA,” *Advancing sustainable materials management: 2014 tables and figures*, 2016. https://www.epa.gov/sites/production/files/2016-11/documents/2014_smm_tablesfigures_508.pdf (accessed Apr. 12, 2019).

[48] “GFA,” *Pulse of the fashion industry*, 2017. https://www.globalfashionagenda.com/initiatives/pulse/# (accessed Apr. 12, 2019).

[49] “EPA,” *Facts and Figures about Materials, Waste and Recycling*, 2020. https://www.epa.gov/facts-and-figures-about-materials-waste-and-recycling/textiles-material-specific-data (accessed Jun. 04, 2020).

[50] M. S. Al-Homoud, “Performance characteristics and practical applications of common building thermal insulation materials,” *Build. Environ.*, vol. 40, no. 3, pp. 353–366, 2005.

[51] “European Commission,” *Circular economy in practice - reducing textile waste*, 2017. https://ec.europa.eu/easme/en/news/circular-economy-practice-reducing-textile-waste (accessed Apr. 12, 2019).

[52] M. del Mar Barbero-Barrera, O. Pombo, and M. de los Angeles Navacerrada, “Textile fibre waste bindered with natural hydraulic lime,” *Compos. Part B Eng.*, vol. 94, pp. 26–33, 2016.

[53] J. Thompson, R. Watson, C. Galantino, and C. Weiler, “SWEEP,” *No End in Sight to US Landfill Cost Increases — Pacific Region to Experience Highest Growth*, 2018. https://nrra.net/sweep/no-end-in-sight-to-us-landfill-cost-increases-pacific-region-to-experience-highest-growth/ (accessed Apr. 12, 2019).

[54] S. Creed, Ed., “Valuing Our Clothes: The Cost of UK Fashion,” 2017. http://www.wrap.org.uk/sites/files/wrap/valuing-our-clothes-the-cost-of-uk-fashion_WRAP.pdf.

[55] Y. Wang, “Fiber and textile waste utilization,” *Waste and Biomass Valorization*, vol. 1, no. 1, pp. 135–143, 2010.

[56] D. G. K. Dissanayake, D. U. Weerasinghe, K. A. P. Wijesinghe, and K. M. D. M. P. Kalpage, “Developing a compression moulded thermal insulation panel using postindustrial textile waste,” *Waste Manag.*, vol. 79, pp. 356–361, 2018, doi: 10.1016/j.wasman.2018.08.001.

[57] I. H. Jayasinghe, B. F. A. Basnayake, K. S. P. Amarathunga, and P. B. R. Dissanayake, “Environmental conservation efforts in developing textile waste incorporated cement blocks,” *Trop. Agric. Res.*, vol. 21, no. 2, pp. 126–133, 2010.

[58] M. K. Jha, V. Kumar, L. Maharaj, and R. J. Singh, “Studies on leaching and recycling of zinc from rayon waste sludge,” *Ind. Eng. Chem. Res.*, vol. 43, no. 5, pp. 1284–1295, 2004.

[59] A. Serra, Q. Tarrés, J. Claramunt, P. Mutjé, M. Ardanuy, and F. X. Espinach, “Behavior of the interphase of dyed cotton residue flocks reinforced polypropylene composites,” *Compos. Part B Eng.*, vol. 128, pp. 200–207, 2017.

[60] C. Rubino, S. Liuzzi, F. Martellotta, and P. Stefanizzi, “Textile wastes in building sector: A review,” *Model. Meas. Control B*, vol. 87, no. 3, pp. 172–179, 2018.

[61] J. Domask, “Achieving goals in higher education: An experiential approach to sustainability studies,” *Int. J. Sustain. High. Educ.*, vol. 8, no. 1, pp. 53–68, 2007.

[62] “SATCOL,” *Why reuse and recycle?*, 2019. http://www.satradingco.org/donating/why-reuse-and-recycle (accessed Apr. 12, 2021).

[63] A. Briga-Sa *et al.*, “Textile waste as an alternative thermal insulation building material solution,” *Constr. Build. Mater.*, vol. 38, pp. 155–160, 2013, doi: 10.1016/j.conbuildmat.2012.08.037.

[64] L. M. Fortuna and V. Diyamandoglu, “Optimization of greenhouse gas emissions in second-hand consumer product recovery through reuse platforms,” *Waste Manag.*, vol. 66, pp. 178–189, 2017, doi: 10.1016/j.wasman.2017.04.032.

[65] G. Sandin and G. M. Peters, “Environmental impact of textile reuse and recycling–A review,” *J. Clean. Prod.*, vol. 184, pp. 353–365, 2018, doi: 10.1016/j.jclepro.2018.02.266.

[66] W. F. Zonatti, J. Baruque-Ramos, and W. Duleba, “Brazilian Scope of Management and Recycling of Textile Wastes,” in *Natural Fibres: Advances in Science and Technology Towards Industrial Applications*, R. Fangueiro and S. Rana, Eds. Dordrecht, Netherlands: Springer, 2016, pp. 429–439.

[67] “Markets Insider,” *Cotton Price Commodity*, 2019. https://markets.businessinsider.com/commodities/cotton-price (accessed Apr. 12, 2021).

[68] “TEXTILEBEACON,” *Fibre to Yarn Export Statistics – India*, 2019. http://www.textilebeacon.com/news/cotton-yarn-export-rises-march/ (accessed Apr. 12, 2021).

[69] Directive, “Directive 2010/75/EU of the European Parliament and of the Council,” *Official Journal of the European Union*, 2010. https://eur-lex.europa.eu/LexUriServ/LexUriServ.do?uri=OJ%3AL%3A2010%3A334%3A0017%3A0119%3Aen%3APDF (accessed Apr. 11, 2021).

[70] D. R. Mulinari, H. J. C. Voorwald, M. O. H. Cioffi, C. A. A. Lima, C. Baptista, and G. J. M. Rocha, “Composite materials obtained from textile fiber residue,” *J. Compos. Mater.*, vol. 45, no. 5, pp. 543–547, 2011, doi: 0.1177/0021998310376098.

[71] J. Zach, A. Korjenic, V. Petránek, J. Hroudová, and T. Bednar, “Performance evaluation and research of alternative thermal insulations based on sheep wool,” *Energy Build.*, vol. 49, pp. 246–253, 2012.

[72] M. El Wazna, M. El Fatihi, A. El Bouari, and O. Cherkaoui, “Thermo physical characterization of sustainable insulation materials made from textile waste,” *J. Build. Eng.*, vol. 12, pp. 196–201, 2017.

[73] P. P. Pichardo, G. Martínez-Barrera, M. Martínez-López, F. Ureña-Núñez, and L. I. Ávila-Córdoba, “Waste and Recycled Textiles as Reinforcements of Building Materials,” in *Natural and Artificial Fiber-Reinforced Composites as Renewable Sources*, E. Günay, Ed. London: IntechOpen, 2017, pp. 89–104.

[74] J. Zach, J. Hroudová, and A. Korjenic, “Environmentally efficient thermal and acoustic insulation based on natural and waste fibers,” *J. Chem. Technol. Biotechnol.*, vol. 91, no. 8., pp. 2156–2161, 2016, doi: 10.1002/jctb.4940.

[75] F. A. Esteve-Turrillas and M. de la Guardia, “Environmental impact of Recover cotton in textile industry,” *Resour. Conserv. Recycl.*, vol. 116, pp. 107–115, 2017, doi: 10.1016/j.resconrec.2016.09.034.

[76] S. Jordeva, E. Tomovska, D. Trajković, and K. Zafirova, “Textile waste as a thermal insulation material,” *Tekst. J. Text. Cloth. Technol.*, vol. 63, no. 5–6, pp. 174–178, 2014.

[77] D. Trajković, S. Jordeva, E. Tomovska, and K. Zafirova, “Polyester apparel cutting waste as insulation material,” *J. Text. Inst.*, vol. 108, no. 7, pp. 1238–1245, 2017.

[78] Y. Z. Shoshani and M. A. Wilding, “Effect of pile parameters on the noise absorption capacity of tufted carpets,” *Text. Res. J.*, vol. 61, no. 12, pp. 736–742, 1991.

[79] Y. Shoshani and Y. Yakubov, “A model for calculating the noise absorption capacity of nonwoven fiber webs,” *Text. Res. J.*, vol. 69, no. 7, pp. 519–526, 1999.

[80] Y. Shoshani and Y. Yakubov, “Numerical assessment of maximal absorption coefficients for nonwoven fiberwebs,” *Appl. Acoust.*, vol. 59, no. 1, pp. 77–87, 2000.

[81] H. M. Algin and P. Turgut, “Cotton and limestone powder wastes as brick material,” *Constr. Build. Mater.*, vol. 22, no. 6, pp. 1074–1080, 2008, doi: 10.1016/j.conbuildmat.2007.03.006.

[82] J. Balasubramanian, P. C. Sabumon, J. U. Lazar, and R. Ilangovan, “Reuse of textile effluent treatment plant sludge in building materials,” *Waste Manag.*, vol. 26, no. 1, pp. 22–28, 2006.

[83] H. Binici, O. Aksogan, D. Bakbak, H. Kaplan, and B. Isik, “Sound insulation of fibre reinforced mud brick walls,” *Constr. Build. Mater.*, vol. 23, no. 2, pp. 1035–1041, 2009.

[84] H. Binici, R. Gemci, O. Aksogan, and H. Kaplan, “Insulation properties of bricks made with cotton and textile ash wastes,” *Int. J. Mater. Res.*, vol. 101, no. 7, pp. 894–899, 2010.

[85] M. EL Wazna, A. Gounni, A. EL Bouari, M. EL Alami, and O. Cherkaoui, “Development, characterization and thermal performance of insulating nonwoven fabrics made from textile waste,” *J. Ind. Text.*, vol. 48, no. 7, pp. 1167–1183, 2019, doi: 10.1177/1528083718757526.

[86] S. A. Belal, *Understanding Textiles for a Merchandiser*. Dhaka: BMN foundation, 2009.

[87] A. Patnaik, M. Mvubu, S. Muniyasamy, A. Botha, and R. D. Anandjiwala, “Thermal and sound insulation materials from waste wool and recycled polyester fibers and their biodegradation studies,” *Energy Build.*, vol. 92, pp. 161–169, 2015, doi: 10.1016/j.enbuild.2015.01.056.

[88] M. Palakurthi, “Development of composites from waste PET-cotton textiles,” University of Nebraska - Lincoln, 2016.

[89] S. K. Ramamoorthy, A. Persson, and M. Skrifvars, “Reusing textile waste as reinforcements in composites,” *J. Appl. Polym. Sci.*, vol. 131, no. 17, pp. 1–16, 2014.

[90] J.-H. Lin, T.-T. Li, and C.-W. Lou, “Puncture-resisting, sound-absorbing and thermal-insulating properties of polypropylene-selvages reinforced composite nonwovens,” *J. Ind. Text.*, vol. 45, no. 6, pp. 1477–1489, 2016.

[91] N. Reddy and Y. Yang, “Biofibers from agricultural byproducts for industrial applications,” *TRENDS Biotechnol.*, vol. 23, no. 1, pp. 22–27, 2005.

[92] H. Binici, R. Gemci, A. Kucukonder, and H. H. Solak, “Investigating sound insulation, thermal conductivity and radioactivity of chipboards produced with cotton waste, fly ash and barite,” *Constr. Build. Mater.*, vol. 30, pp. 826–832, 2012.

[93] H. Binici, O. Aksogan, and T. Shah, “Investigation of fibre reinforced mud brick as a building material,” *Constr. Build. Mater.*, vol. 19, no. 4, pp. 313–318, 2005.

[94] H. Binici, O. Aksogan, M. N. Bodur, E. Akca, and S. Kapur, “Thermal isolation and mechanical properties of fibre reinforced mud bricks as wall materials,” *Constr. Build. Mater.*, vol. 21, no. 4, pp. 901–906, 2007.

[95] M. Zakaria, M. Ahmed, M. M. Hoque, and S. Islam, “Scope of using jute fiber for the reinforcement of concrete material,” *Text. Cloth. Sustain.*, vol. 2, no. 1, p. 11, 2017, doi: 10.1186/s40689-016-0022-5.

[96] P. Bekhta and E. Dobrowolska, “Thermal properties of wood-gypsum boards,” *Holz als Roh- und Werkst.*, vol. 64, no. 5, pp. 427–428, 2006, doi: 10.1007/s00107-005-0074-8.

[97] S. C. Ng and K.-S. Low, “Thermal conductivity of newspaper sandwiched aerated lightweight concrete panel,” *Energy Build.*, vol. 42, no. 12, pp. 2452–2456, 2010, doi: 10.1016/j.enbuild.2010.08.026.

[98] H. Binici, M. Eken, M. Dolaz, O. Aksogan, and M. Kara, “An environmentally friendly thermal insulation material from sunflower stalk, textile waste and stubble fibres,” *Constr. Build. Mater.*, vol. 51, pp. 24-33., 2014.

[99] A. C. Woolridge, G. D. Ward, P. S. Phillips, M. Collins, and S. Gandy conservation, “Life cycle assessment for reuse/recycling of donated waste textiles compared to use of virgin material: An UK energy saving perspective,” *Resour. Conserv. Recycl.*, vol. 46, no. 1, pp. 94–103, 2006, doi: 10.1016/j.resconrec.2005.06.006.

[100] G. Bhat, “Processing postconsumer recycled plastics,” in *Envirnmentally conscious materials and chemicals processing*, M. Kutz, Ed. New Jersey: John Wiley & Sons, 2007, pp. 357–383.

[101] G. Rebitzer *et al.*, “Life cycle assessment: Part 1: Framework, goal and scope definition, inventory analysis, and applications,” *Environ. Int.*, vol. 30, no. 5, pp. 701–720, 2004, doi: 10.1016/j.envint.2003.11.005.

[102] “ISO 14040,” *Environmental management — Life cycle assessment — Principles and framework*, 2006. https://www.iso.org/standard/37456.html.

[103] “ISO 14044,” *Environmental management -- Life cycle assessment -- Requirements and guidelines*, 2006. https://www.iso.org/standard/38498.html.

[104] G. Baydar, N. Ciliz, and A. Mammadov, “Life cycle assessment of cotton textile products in Turkey,” *Resour. Conserv. Recycl.*, vol. 104, pp. 213–223, 2015, doi: 10.1016/j.resconrec.2015.08.007.

[105] B. K. Murugesh and M. Selvadass, “Life cycle assessment for cultivation of conventional and organic seed cotton fibres,” *Int. J. Res. Environ. Sci. Technol.*, vol. 3, no. 1, pp. 39–45, 2013.

[106] K. B. Murugesh and M. Selvadass, “Life cycle assessment for the dyeing and finishing process of organic cotton knitted fabrics,” *J. Text. Apparel, Technol. Manag.*, vol. 8, no. 2, pp. 1–16, 2013.

[107] Z.-W. Yuan, Y.-N. Zhu, J.-K. Shi, X. Liu, and L. Huang, “Life-cycle assessment of continuous pad-dyeing technology for cotton fabrics,” *Int. J. Life Cycle Assess.*, vol. 18, no. 3, pp. 659–672, 2013.

[108] N. M. van der Velden, M. K. Patel, and J. G. Vogtländer, “LCA benchmarking study on textiles made of cotton, polyester, nylon, acryl, or elastane,” *Int. J. Life Cycle Assess.*, vol. 19, no. 2, pp. 331–356, 2014.

[109] N. Morley, S. Slater, S. Russell, M. Tipper, and G. D. Ward, “Recycling of Low Grade Clothing Waste. Prepared for Defra Aylesbury, UK: Oakdene Hollins Ltd Salvation Army Trading Company Ltd and Nonwovens Innovation & Research Institute Ltd. Morley, Nick, Caroline Bartlett and Ian McGill. 2009." Maximising Reuse and,” Appendix 1-Technical Report." London: A research report completed for Defra …, 2006. [Online]. Available: http://randd.defra.gov.uk/Default.aspx.

[110] S. Roos, B. Zamani, G. Sandin, G. M. Peters, and M. Svanström, “A life cycle assessment (LCA)-based approach to guiding an industry sector towards sustainability: the case of the Swedish apparel sector,” *J. Clean. Prod.*, vol. 133, pp. 691–700, 2016, doi: 10.1016/j.jclepro.2016.05.146.

[111] A. K. Chapagain, A. Y. Hoekstra, H. H. G. Savenije, and R. Gautam, “The water footprint of cotton consumption: An assessment of the impact of worldwide consumption of cotton products on the water resources in the cotton producing countries,” *Ecol. Econ.*, vol. 60, no. 1, pp. 186–203, 2006, doi: 10.1016/j.ecolecon.2005.11.027.

[112] “statistica,” *Production of polyester fibers worldwide from 1975 to 2017*, 2019. https://www.statista.com/statistics/912301/polyester-fiber-production-worldwide/.

[113] “Textile Exchange,” *Preferred fiber & materials market report 2018*, 2018. https://textileexchange.org/wp-content/uploads/2018/11/2018-Preferred-Fiber-Materials-Market-Report.pdf.

[114] R. Drochytka, M. Dvorakova, and J. Hodna, “Performance Evaluation and Research of Alternative Thermal Insulation Based on Waste Polyester Fibers,” *Procedia Eng.*, vol. 195, pp. 236–243, 2017, doi: 10.1016/j.proeng.2017.04.549.

[115] Y. Lee and C. Joo, “Sound absorption properties of recycled polyester fibrous assembly absorbers,” *AUTEX Res. J.*, vol. 3, no. 2, pp. 78–84, 2003.

[116] I. C. Valverde, L. H. Castilla, D. F. Nuñez, E. Rodriguez-Senín, and R. De la Mano Ferreira, “Development of new insulation panels based on textile recycled fibers,” *Waste and Biomass Valorization*, vol. 4, no. 1, pp. 139–146, 2013, doi: 10.1007/s12649-012-9124-8.

[117] “Bonded Logic,” *Echo Eliminator™ Acoustic Panels*, 2019. http://www.bondedlogic.com/echo-eliminator-acoustic-panels/.

[118] R. del Rey, L. Bertó, J. Alba, and J. P. Arenas, “Acoustic characterization of recycled textile materials used as core elements in noise barriers,” *Noise Control Eng. J.*, vol. 63, no. 5, pp. 439–447, 2015, doi: 10.3397/1/376339.

[119] M. Sedlmajer, J. Zach, and J. Hroudova, “Possibilities of Development of Thermal Insulating Materials based on Waste Textile Fibers,” *Adv. Mater. Res.*, vol. 1124, 2015, doi: 0.4028/www.scientific.net/AMR.1124.183.

[120] K. Aghaee and M. Foroughi, “Construction of lightweight concrete partitions using textile waste,” in *ICSDEC 2012: Developing the Frontier of Sustainable Design, Engineering, and Construction*, W. Chong, J. Gong, J. Chang, and M. Siddiqui, Eds. Reston, VA: American Society of Civil Engineers, 2013, pp. 793–800.

[121] K. Aghaee and M. Foroughi, “Mechanical properties of lightweight concrete partition with a core of textile waste,” *Adv. Civ. Eng.*, vol. 2013, pp. 1–7, 2013, doi: 10.1155/2013/482310.

[122] D. Rajput, S. S. Bhagade, S. P. Raut, R. V Ralegaonkar, and S. A. Mandavgane, “Reuse of cotton and recycle paper mill waste as building material,” *Constr. Build. Mater.*, vol. 34, pp. 470–475, 2012.

[123] H. Binici and O. Aksogan, “Engineering properties of insulation material made with cotton waste and fly ash,” *J. Mater. Cycles Waste Manag.*, vol. 17, no. 1, pp. 157–162, 2015, doi: 10.1007/s10163-013-0218-6.

[124] A.-E. Tiuc, H. Vermeşan, T. Gabor, and O. Vasile, “Improved sound absorption properties of polyurethane foam mixed with textile waste,” *Energy Procedia*, vol. 85, pp. 559–565, 2016, doi: 10.1016/j.egypro.2015.12.245.

[125] M. Kapps and S. Buschkamp, “The production of rigid polyurethane foam,” *Bayer Mater. Sci.*, vol. 20, pp. 3–12, 2004.

[126] R. Verdejo *et al.*, “Enhanced acoustic damping in flexible polyurethane foams filled with carbon nanotubes,” *Compos. Sci. Technol.*, vol. 69, no. 10, pp. 1564–1569, 2009, doi: 10.1016/j.compscitech.2008.07.003.

[127] G. Bhat, *Structure and Properties of High-Performance Fibers*. New York: Woodhead Publishing, 2016.

[128] D. J. Oldham, C. A. Egan, and R. D. Cookson, “Sustainable acoustic absorbers from the biomass,” *Appl. Acoust.*, vol. 72, no. 6, pp. 350–363, 2011.

[129] A. H. Hassanin, Z. Candan, C. Demirkir, and T. Hamouda, “Thermal insulation properties of hybrid textile reinforced biocomposites from food packaging waste,” *J. Ind. Text.*, vol. 47, no. 6, pp. 1024–1037, 2018.

[130] P. Bajaj, D. K. Paliwal, and A. K. Gupta, “Modification of acrylic fibres for specific end uses,” *Indian J. Fibre Text. Res.*, vol. 21, pp. 143–154, 1996.

[131] C. Datta, D. Basu, A. Roy, and A. Banerjee, “Mechanical and dynamic mechanical studies of epoxy/VAc-EHA/HMMM IPN–jute composite systems,” *J. Appl. Polym. Sci.*, vol. 91, no. 2, pp. 958–963, 2004, doi: 10.1002/app.13295.

[132] N. Paul and M. Mukhopadhyay, “Thermal insulation values of jute fabrics and its blends with their fibres,” *Indian J. Fibre Text. Res.*, vol. 2, no. 3, pp. 88–91, 1977.

[133] S. B. R. Devireddy and S. Biswas, “Physical and thermal properties of unidirectional banana–jute hybrid fiber-reinforced epoxy composites,” *J. Reinf. Plast. Compos.*, vol. 35, no. 15, pp. 1157–1172, 2016.

[134] “Syntech Fibers,” *Properties of Polypropylene Fibres*, 2013. http://syntechfibres.com/polypropylene/properties-of-polypropylen-fibres/.

CHAPTER 3

Insulation Materials from Post-Consumer Recycled Denim Fabrics[1]

[1] Islam, S., El Messiry, M., Sikdar, P. P., Seylar, J., & Bhat, G. (2020). *Journal of Industrial Textiles*, https://doi.org/10.1177/1528083720940746. (Some part of this chapter).
Reprinted here with permission of the publisher.

Abstract

The goal of this study was to evaluate the feasibility of recycling used apparel to produce commercially practicable sustainable products using nonwoven fabrication techniques with biodegradable thermoplastic binder fibers for possible use as insulation panels. Recycled denim fibers were used with Sorona® or a PLA binder fiber to successfully produce insulation with good performance properties. Maximum transmission loss of about 23 dB and transmission coefficient close to zero at around 1000 Hz were observed. The data indicated that there is a direct correlation between loss of sound transmission with increase in thickness, areal density, and decrease in air permeability. Lowest thermal conductivity of 0.049 W/mK was obtained from produced insulation panels. When compared with commercially available acoustic insulation material (gypsum board) and thermal insulation panel (mineral wool), these products had better or comparable insulation properties, indicating that recycled textile products can be used to produce such value-added materials, giving them another useful life before safely disposing in composting environments.

Keywords: Textile recycling, insulation materials, composites, nonwovens

3.1. Introduction

Every day there is increasing concern in the environmental sectors regarding rapidly growing energy consumption [1], [2]. Building and automobile sectors are considered as main consuming sectors of global energy (discussed in detail in chapter one). Noise pollution is also continuously increasing due to urbanization, industrialization, increased use of vehicles, electrical and mechanical appliances in home and industry, etc., and becoming a major health and environmental concern (discussed in detail in chapter one) [2], [3]. Using proper thermal and acoustic insulation materials can help minimize these adverse effects. However, presently used synthetic insulation materials are mainly mineral or petrochemical-based materials that have an adverse effect on human health and environment (discussed in detail in chapter one). Thus the goal of this research is to produce insulation materials using waste textiles. Using waste textiles for producing insulation materials will also help minimize the adverse effect due to landfill waste textiles which has been discussed in detail in chapter one and two.

Materials produced from textile fibers are porous in structure that have very good potentiality to be used as thermal and acoustic insulation materials [4]. When sound energy enters the porous structure of materials, the kinetic energy of the sound is converted into heat energy as the sound strikes the surface of the fiber. Sound energy is reduced within the porous fibrous structure due to frictional losses, momentum losses, and generation of heat [5]. Similarly, porous materials have very good thermal insulation properties as conductive property of heat through void medium is very low.

However, there are also some obstacles to use textile fibers especially waste textiles for value-added materials. One of the challenges for using recycled natural fibers in traditional textiles is its shorter fiber length. Nonwoven techniques can use short fibers and overcome this obstacle. Also,

products produced by nonwoven techniques have very good acoustic insulation properties in the mid and high frequency (around 2000 Hz) [6] and excellent thermal insulation properties as bulky material produced by nonwoven techniques.

Some researchers have already taken steps to develop insulation materials by using recycled textiles. Some materials are already present in the markets, and majority of the materials are in research or development stage [7]. Ricciardi et al. used recycled polypropylene fiber and paper to produce insulation materials. Although they produce good insulation materials, their products cause relatively large energy consumptions (267.7 MJ) and a high global warming potential (14.68 kg CO_2eq) in comparison to similar synthetic insulation materials like EPS [8]. This may be due to the use of glue for binding fibers. Therefore, for producing sustainable insulation materials from recycled textiles, researchers may need to avoid external chemicals for binding. In this research, instead of using any chemical resin/binding, thermoplastic fibers (PLA or Sorona®) were used as binding materials. Polylactic acid (PLA) is a biodegradable and bio-based aliphatic polyester that is derived from renewable sources such as corn sugar, potato, and sugar cane [9]. PLA exhibits optical, mechanical, and thermal properties that are comparable with some of the commercially available synthetic materials, including polypropylene and poly (ethylene terephthalate) (PET), and may be able to replace the synthetic materials in a wide range of applications [10], [11]. Sorona® fiber recently commercialized by DuPont is derived from corn-based 1,3-propanediol [12]. Sorona® 3GT has unique stretch-recovery characteristics, excellent physical and chemical properties, dimensional stability, low moisture absorption, easy care, good weather resistance, easy processability, and recyclability. Also, recycling of Sorona® is made much easier by the absence of heavy metals in the product, compared to that of PET and Nylon [12]. Some other researchers like Tiuc et al. mixed polyurethane foam with textile waste [13], and Trajković et al. used polyester

apparel cutting waste to produce insulation materials [14]. However, the research is in very initial stages, and present market is completely occupied by conventional synthetic insulation materials. Additional research is needed to make insulation materials that are lightweight, thin, cost-effective, and have very good acoustic insulation properties [15]–[17].

The goal of this study was to demonstrate that post-consumer textile waste is suitable to produce commercially feasible sustainable products for insulation by using nonwoven fabrication techniques. The plan was to use recycled denim fibers (cotton) and compostable thermoplastic binder fibers to successfully produce insulation materials. The relationship of sound transmission loss and thermal conductivity with several factors, including air permeability, thickness, and density of the fiber-based composites, was developed using a statistical regression model. Also, insulation properties of the developed materials were compared with those of the commercially available materials.

3.2. Materials and Methods

3.2.1. Materials

Composite samples were prepared by mixing recycled denim (cotton fibers) with Sorona® or PLA fibers at different ratios. Post-consumer denim waste fibers (cotton fibers) were obtained from Phoenix Fibers which is a textile-based recycling company [18]. Sorona® fibers were provided by DuPont Chemical Co., Wilmington, DE. PLA staple fibers were provided by Fiber Innovation Technology, Inc., Johnson City, TN. Both PLA and Sorona® staple fibers are derived from corn starch as the source. The properties of used Sorona® and PLA fibers obtained from the manufacturer are listed in table 3.1.

Table 3.1. Properties of PLA and Sorona® staple fibers.

Properties	PLA	Sorona®
Chemical composition	Polylactic acid: > 99% by weight Anti-static finishing agents: 0.18% by weight	Poly (trimethylene terephthalate) based on corn-derived 1,3-propanediol.
Melting point	Around 160 ℃	Around 228 ℃
Glass transition	Around 60 ℃	45 – 55 ℃
Staple length	(38 ± 2.5) mm	--
Density	(1.25 ± 0.5) g/cc	1.32 g/cc
Denier	(1.4 ± 0.15) dpf	--
MR%	0.5 ± 0.1	0.2 – 0.3
Tenacity	(4.00 ± 0.35) gpd	4 – 5 gpd
Elongation	(55 ± 15) %	15 %

3.2.2. Processing

Web formation by nonwoven techniques: Figure 3.1 shows different components of the web formation process. Fiber webs with uniform thickness were produced by the dry-laid process, where the blended fibers were passed through a carding machine. At first, recycled denim fibers (figure 3.1a) is blended with the thermoplastic binding fibers Sorona® (figure 3.1b) or PLA at different ratio by weight. Then the blended fibers were fed into the laboratory carding machine (figure 3.1c), where it was passed through different fine wire mounted rollers. Carding and stripping actions that occur during this process opened and cleaned the fibers and produce uniform fiber webs (figure 3.1d).

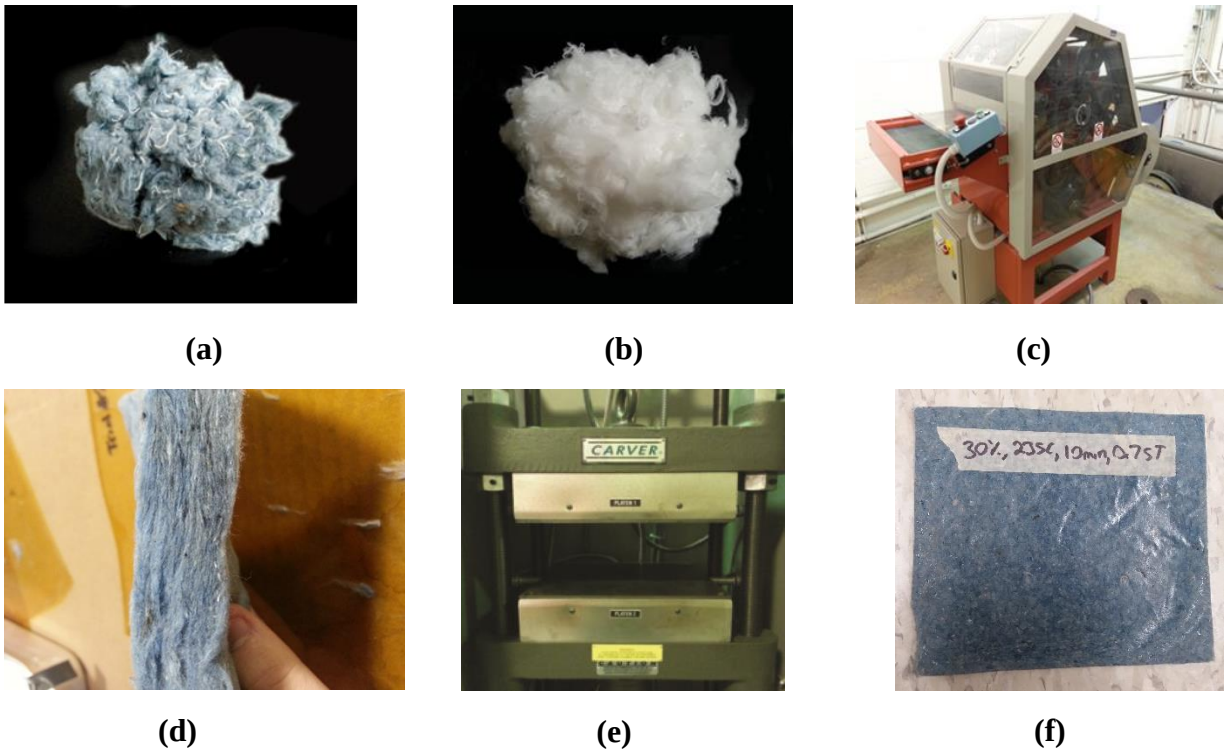

(a) **(b)** **(c)**

(d) **(e)** **(f)**

Figure 3.1. Different components of insulation panel preparation: (a) Recycled denim, (b) biodegradable binder fibers (Sorona®), (c) carding machine, (d) prepared blended fiber web, (e) hot press, (f) Consolidated panel.

Composite preparation: Insulation panels were prepared by blending recycled denim and the binder fibers at different ratios as given in table 3.2. The carded webs were consolidated using a laboratory Carver hot press where the values of heat and pressure applied during the sample preparation could be controlled. Several layers of fiber webs produced from the card web were combined. These layers of fiber webs were placed between the two plates of a carver hot press (figure 3.1e) and then formed into composite panels (figure 3.1f). Based on initial trials and visual examination of samples, the temperature and pressure used in hot press were fixed, and they were different for the two binder fibers used due to differences in their melting temperature. Composite panels were produced by varying fiber compositions, temperature, pressure, number of layers, and the type of binders (table 3.2). Samples one to three were produced with increasing Sorona® fiber

percentage as binder content. The fourth sample had the PLA binder fiber, and correspondingly lower bonding temperature was used. Also, more layers of webs were used in sample 4. PLA binder sample was added in this investigation to show that comparable panels can be produced at a lower temperature, which is probably desirable to reduce the chances of degradation of cotton.

Table 3.2. Different parameters of composite samples.

Sample no.	Sample Id.	Fiber type	Temperature (°C)	Time (m)	Pressure (kPa)	No. of layers
1	A1	70% Denim/30% Sorona®	235	10	275 (40psi)	4
2	A2	60% Denim/40% Sorona®	235	10	275 (40psi)	4
3	A3	50% Denim/50% Sorona®	235	10	275 (40psi)	4
4	A4	60% Denim/40% PLA	180	2	380 (55psi)	12

3.2.3. Characterization

3.2.3.1. Determination of thickness and density

At first, samples were conditioned for 48 hours in a standard atmosphere, i.e., (20 ± 2)°C temperature and (65 ± 2)% relative humidity. Thickness of samples was determined in accordance with the standard testing method of ISO 9073-2 [19]. Thickness was measured using the progage thickness tester.

Samples were weighed using an electronic balance, and area of the samples was measured. After that, areal density, s (g/m^2) was calculated by dividing weight over area. Bulk density, ρ (kg/m^3), was calculated from areal density and thickness by using the following formula.

$$\rho = \frac{s}{t} \tag{3.1}$$

where, s = areal density in kg/m^2 and t = thickness in m.

Multiple measurements were taken for each sample as per the standard, and average values of thickness, areal density, and bulk density were calculated.

3.2.3.2. Determination of air permeability

Air permeability is the rate of airflow passing perpendicularly through a known area of porous material under a certain air pressure difference [20]. Air permeability was measured using a Textest FX 3300 instrument following the standard method of ASTM D737 [21].

3.2.3.3. Determination of porosity

Porosity is the ratio of the voids to the total volume of materials [22]. Porosity (ϕ) of composite panels was calculated by the following relation [23].

$$\phi = 1 - \frac{\rho}{\rho'} \tag{3.2}$$

where, ρ' is the density of fiber and ρ is the density of composite panels. In this experiment, three different types of fibers (cotton, Sorona®, and PLA) were used. The average densities of cotton, Sorona®, and PLA used in the calculation were 1.52 g/cm^3 [24], 1.32 g/cm^3, and 1.25 g/cm^{3,} respectively.

3.2.3.4. Determination of tortuosity

Tortuosity of a porous material is the ratio between the actual flow path length to the straight distance between the ends of the flow path [25]. Tortuosity (τ') was calculated using the following empirical formula [26].

$$\tau' = 1 + \frac{1-\phi}{2\phi} \tag{3.3}$$

where, ϕ is the porosity of composite sample.

3.2.3.5. Determination of mean flow pore pressure, diameter, and pore size distribution

Mean flow pore indicates the size of the pore that allows half of the full airflow through the materials. Porous materials Inc. (PMI), model no. CFP-100AEX, instrument was used to measure

the mean flow pore pressure, pore diameter, and pore size distribution of different composite panels following the standard test method ASTM F316-03 [27].

3.2.3.6. Structure of composite panels

An FEI Teneo field emission scanning electron microscope (FE-SEM) was used to analyze the surface of composite panels. Gold coating was done to each sample before capturing SEM pictures.

3.2.3.7. Determination of fiber diameter and distribution of fiber diameter

Some of the useful parameters that can influence sound absorption are the fiber diameter and distribution of fiber diameter. Average fiber diameter and distribution of fiber diameter of composite panels were determined using ImageJ Software from SEM observations. In this case, cotton fibers were assumed to be round for approximation.

3.2.3.8. Determination of flame retardance properties

Burning tests (vertical and 45° angle) were conducted (figure 3.2) to investigate the flame retardance characteristics of produced composite panels following the international standards of ASTM D1230-17 [28]. The sample of composite panel with a size of 104 × 80 mm was clammed in the testing instrument (figure 3.2), and a flame was applied to the bottom edge of samples for 12 seconds. Then the composite panel was allowed to burn, and after flame time, dripping time, after glow time, and char length were recorded.

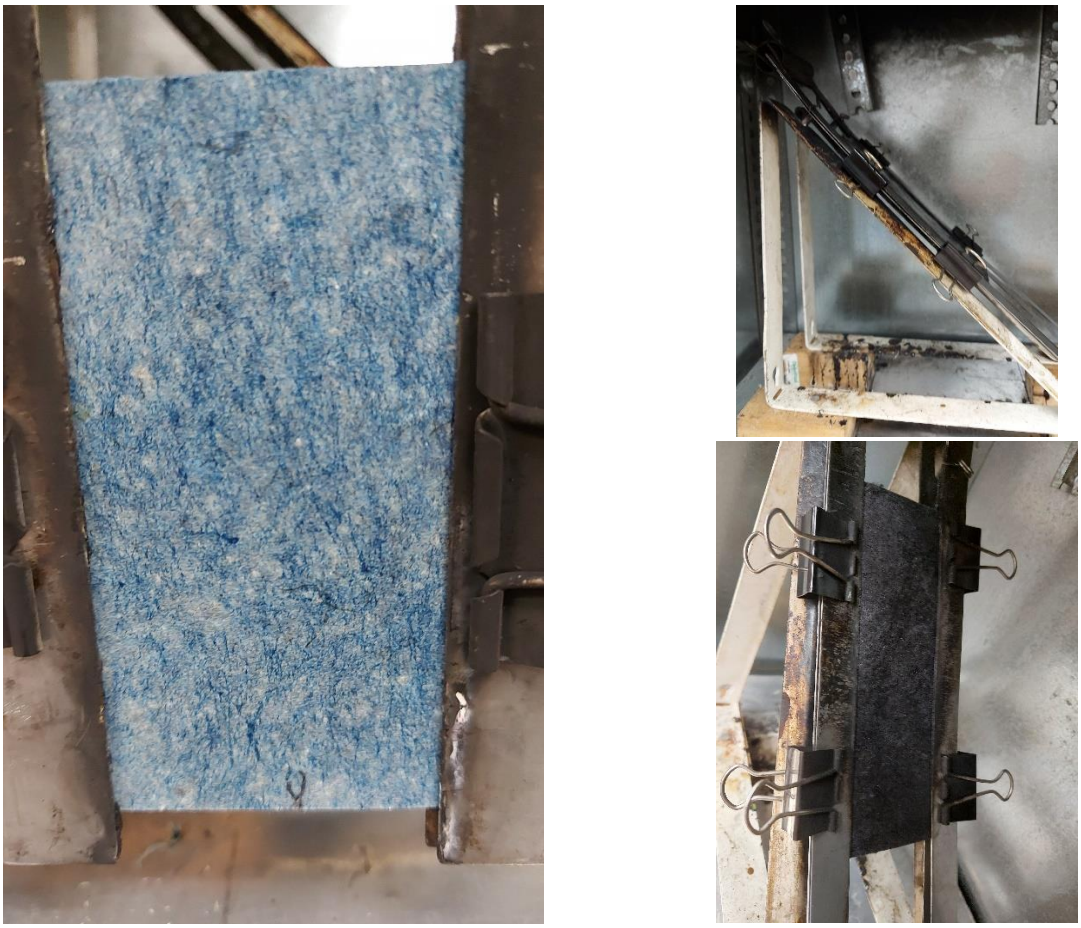

(a) (b)

Figure 3.2. Burning test. (a) vertical (b) 45° angle.

3.2.3.9. Determination of moisture properties

Moisture content (MC) of insulation materials was measured according to ASTMD2495 – 07 [29]. In this process, samples were weighted at atmospheric temperature and relative humidity (RH). After that, samples were dried in an oven at 110±2 ℃ for 1 hour then weighed. Subsequently, samples were dried in an oven at 110±2 ℃ for another 1 hour and weighed, followed by another drying and weighing process. Several drying cycles were carried out in order to get a constant dry mass (W_d) of samples (less than 0.1% of mass differences between successive weighing). After that, samples are placed in CARON climatic chamber at 23±2 ℃ and 65 ± 2% RH followed by 23±2 ℃ and 90 ± 5% RH for 72 hours and weighed (wet mass, W_w). Finally, MCs of composite

samples were calculated at two different atmospheric conditions (23±2 ℃ & 65 ± 2% RH and 23±2 ℃ & 90 ± 5% RH) using following formula.

$$\frac{W_W - W_d}{W_W} \times 100 \qquad (3.4)$$

3.2.3.10. Determination of acoustic properties

Acoustic properties of a material can be determined by measuring several parameters, including transmission coefficient, transmission loss, and absorption coefficient. In this research, transmission coefficient and transmission loss were measured using four-microphone impedance tube.

Principle of measurement: Impedance tube with four microphones was used to measure the acoustic properties of composite panels. By using four microphones impedance tube several parameters, including sound transmission coefficient (τ) and transmission loss (TL) can be calculated [30].

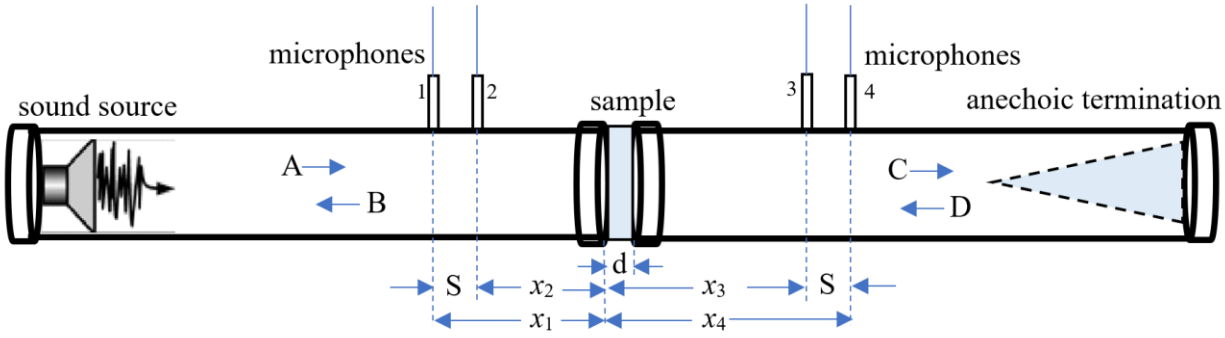

Figure 3.3. Schematic diagram of the impedance tube for measuring the sound transmission loss.

The schematic diagram of four microphone impedance tube is shown in figure 3.3. A sound source and an anechoic termination were mounted on the left and right end of impedance tube, respectively. One set of two microphones (1 and 2) was fixed in the upstream tube, and another set of two microphones (3 and 4) was fixed in the downstream tube. A sample is placed between

the two sets of microphones. Distance of four microphones from the front surface of sample is denoted as x_1, x_2, x_3, and x_4, respectively. A single frequency sound was generated from the sound sources, and it was passed through the sample. A and B indicate the incident and reflected sound component in the upstream tube, and C and D indicate the transmitted and reflected sound component in the downstream tube, respectively. Coefficient of A, B, C, and D can be determined using following equations [30].

$$A = \frac{j\left(p_1 e^{jkx_2} - p_2 e^{jkx_1}\right)}{2\sin ks} \tag{3.5}$$

$$B = \frac{j\left(p_2 e^{-jkx_1} - p_1 e^{-jkx_2}\right)}{2\sin ks} \tag{3.6}$$

$$C = \frac{j\left(p_3 e^{jkx_4} - p_4 e^{jkx_3}\right)}{2\sin ks} \tag{3.7}$$

$$D = \frac{j\left(p_4 e^{-jkx_3} - p_3 e^{-jkx_4}\right)}{2\sin ks} \tag{3.8}$$

where, p_1, p_2, p_3, p_4 are the fourier components of the sound pressure of microphones 1, 2, 3, and 4, respectively, and k is the wavenumber.

The transmission coefficient, τ and transmission loss, TL [30] can be calculated using the following equations:

$$\textit{Transmission coefficient, } \tau = \frac{C}{A} \tag{3.9}$$

$$\textit{Transmission loss, } TL = -20\log|\tau| \tag{3.10}$$

Test procedure: Figure 3.4 shows the actual four microphone impedance tube used to measure the acoustic properties of the composite panels. The instrument was developed and assembled as described in an earlier paper [31].

Figure 3.4. Four microphone impedance tube for measurement of acoustic properties.

A data acquisition (DAQ) instrument was attached with four microphones and a computer. BK precision signal generator was connected to a speaker that delivered different frequency to the sample. Fast Fourier Transform (FFT) spectrum analyzer was used to analyze the signal and measure the sound in decibel at different microphone points. International standard ASTM E2611 – 17 [32] was followed as guidance to complete the test procedure. Transmission coefficient and transmission loss were calculated using equations 3.9 and 3.10.

3.2.3.11. Determination of thermal properties

Thermal resistance, *R*-value, and heat flux (*Q*) of insulation panels were measured using sweating guarded hotplate following the standard ASTM-F18868-C [33]. According to this standard, thermal resistance was measured by total heat loss where plate & guard temperature was kept at 35℃, and ambient temperature was kept at 25℃. Thermal conductivity (*k*) was measured from heat flux, thickness, and temperature differences using following equation:

$$k = \frac{Q \times t}{\Delta T} \tag{3.11}$$

where Q is the heat flow (W/m^2), t is the thickness (m) of the specimen, and ΔT is the temperature difference (K) between hot and cold surfaces.

3.2.3.12. Statistical analysis and modeling of acoustic properties

Statistical analysis of different test results of the samples carried out. A statistical regression model of sound transmission coefficient and transmission loss was carried out using JMP software. Model is helpful to predict sound transmission loss at different frequencies. Comparison of measured and predicted sound transmission loss of composite panels at different frequencies was also carried out (using JMP software) to check whether there is any deviation between predicted value of sound transmission loss with measured value of sound transmission loss. Relation of transmission loss with respect to thickness, areal density, and air permeability are plotted.

A statistical regression model of thermal insulation was also carried out using JMP software. Relation of thermal insulation with respect to thickness, areal density, and air permeability was also plotted.

3.3. Results and Discussions

3.3.1. Physical properties

The acoustical and thermal properties of different samples are presented and discussed in the following sections. Physical properties of composite samples, including air permeability, thickness, areal density, bulk density, porosity, and tortuosity, are shown in table 3.3.

Table 3.3. Properties of tested sample.

Sample Id.	Air permeability ($cm^3/s/cm^2$)	Thickness (mm)	Areal density (g/m^2)	Bulk Density (kg/m^3)	Porosity, ϕ	Tortuosity, τ'	Mean flow pore diameter (μm)	Mean flow pore pressure (N/cm^2)
A1	2.77 ± 0.15	1.97 ± 0.08	830.26 ± 13.65	421.45 ± 6.94	0.71 ± 0.01	1.203 ± 0.01	17.2	0.266
A2	2.60 ± 0.02	1.85 ± 0.05	824.88 ± 16.09	462.10 ± 8.68	0.70 ± 0.01	1.236 ± 0.01	20.5	0.223
A3	2.99 ± 0.12	0.90 ± 0.07	471.25 ± 19.07	520.83 ± 11.08	0.63 ± 0.02	1.289 ± 0.02	18.1	0.253
A4	1.83 ± 0.12	4.30 ± 0.08	1798.3 ± 14.78	418.21 ± 3.89	0.70 ± 0.01	1.210 ± 0.01	18.0	0.254

Mean value ± SD

From data in table 3.3, it is obvious that the bulk density of the composite samples is high. All of the samples have comparable values of porosity and mean flow pore diameter. Density of

sample A3 is comparatively higher, and porosity is comparatively lower. The thickness of sample A3 is much lower than other samples due to better consolidation, but the areal density is lower, which may lead to comparatively higher air permeability of sample A3. Fabric thickness from sample A1 to A3 has been decreasing due to the difference in the structure of samples caused by increasing binder fiber content. Sample A3 has higher percentage of binder fibers that melted at high temperatures. Similarly, thickness of sample A4 is much higher, mainly due to the fact that it had more layers of fibers, and its air permeability is much lower than that of other samples.

3.3.2. Analysis of composite surface

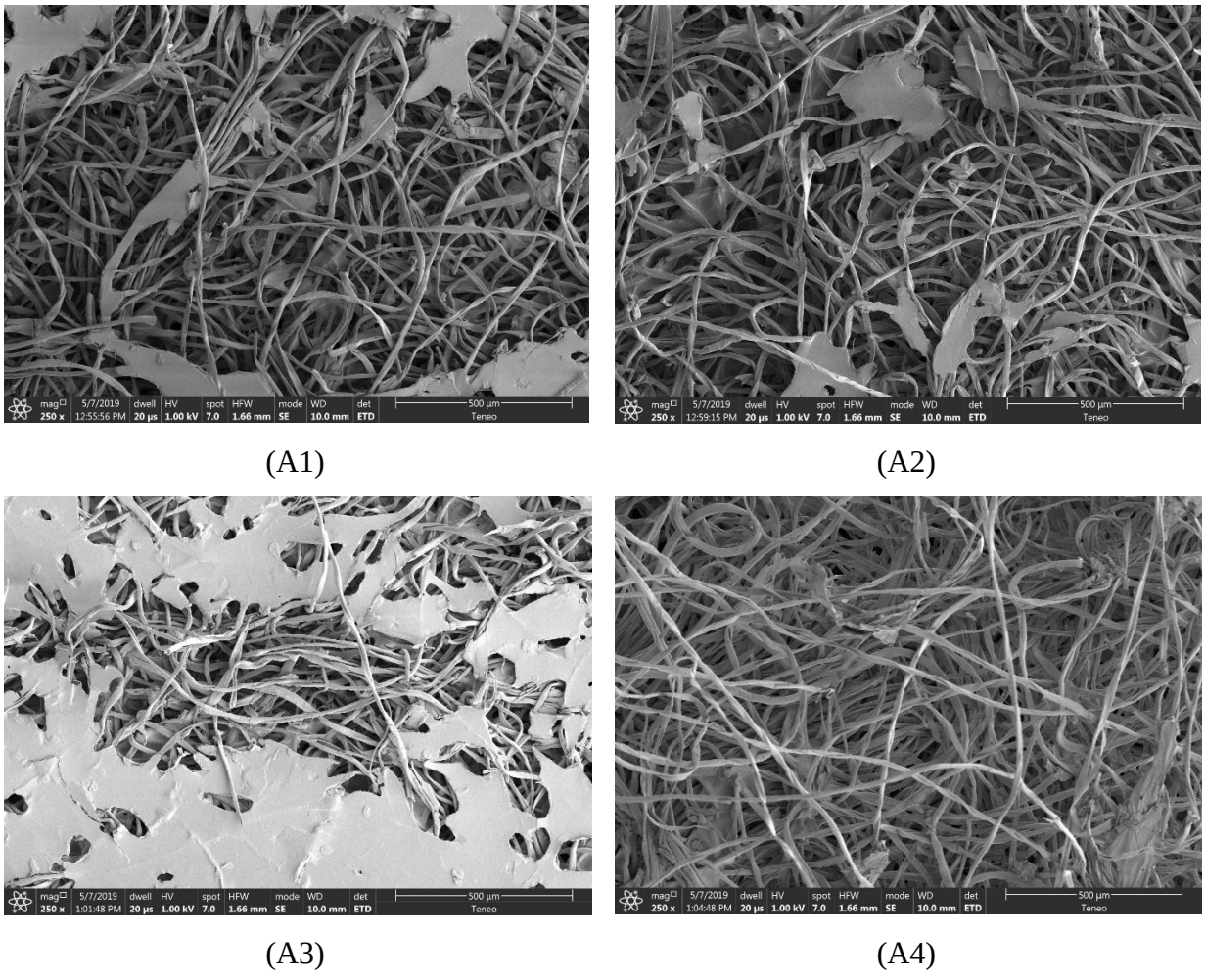

(A1) (A2)

(A3) (A4)

Figure 3.5. SEM image of four different composite samples.

SEM pictures allow us to analyze the surface morphology of the prepared composite samples. The convolutions of cotton fibers are clearly visible in all samples (figure 3.5). It is apparent that most of the binder fibers have melted and fused together at high temperature and pressure. It is also observed that melting and fusing occurred more at the surface than inner part of the composite materials. More amount of fusing and solid surface was observed in sample A3, where higher percentage of binder fiber was used. However, there was still enough porosity in the structure, and thus air permeability was higher.

3.3.3. Fiber diameter and distribution of fiber diameter

The distribution of fiber diameter is presented in figure 3.6. Fiber distribution is unimodal and close to symmetrical. Most of the fiber diameters are within the range of 12 to 22 µm. The average fiber diameter of four different composite samples, A1, A2, A3, and A4, are 16.3 µm, 16.8 µm, 16.2 µm, and 17.4 µm, respectively, which are almost similar to one another.

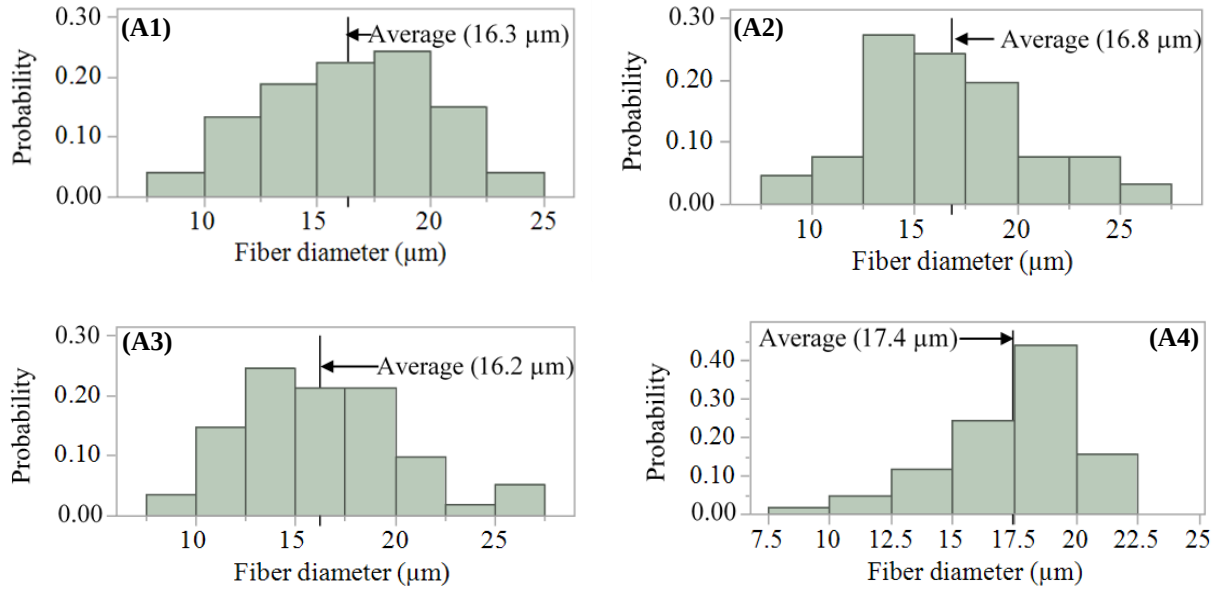

Figure 3.6. Distribution of fiber diameter of four different composite samples.

3.3.4. Pore size distribution

The distribution of pore size is presented in figure 3.7. Pore size distribution of composite samples is unimodal and asymmetrical. Sample A2 shows left-skewed pore distribution, and sample A3 shows a little bit right-skewed pore distribution. All the pore sizes are within micro scale. Most of the pore size values of composite samples are between 10 – 25 micrometers, and medians are located around 15 – 20 micrometers. Sample A3 has higher number of smaller pores within the range of 10 – 15 micrometers. This reduction in pore size is due to higher level of consolidation of the webs as discussed above due to higher amount of binder content used. Sample A4 has higher number of pores within the range of 15 – 20 micrometers, again an indication of overall better consolidation of the webs.

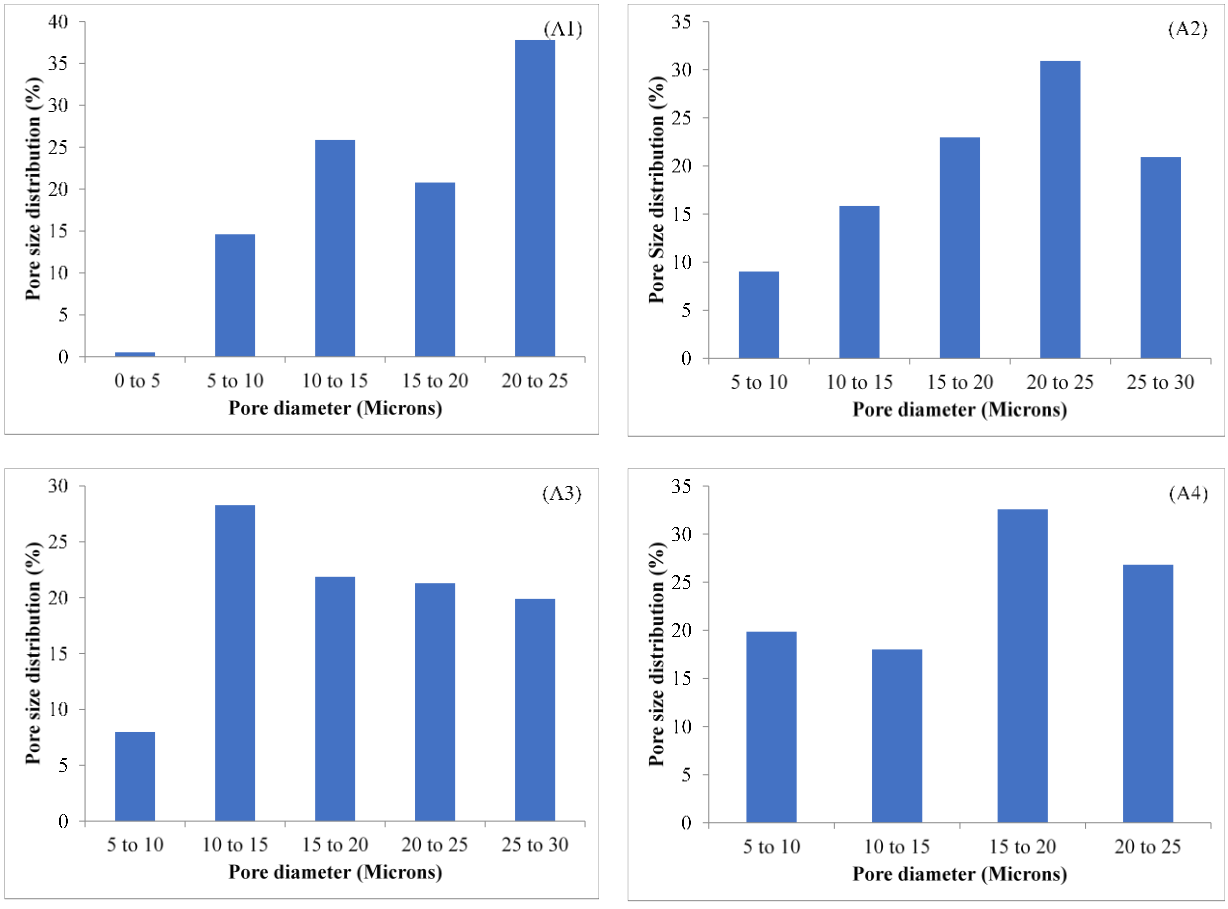

Figure 3.7. Pore size distribution of four different composite samples.

3.3.5. Flammability properties

The vertical and 45° angle burning tests were conducted to assess the flame retardant properties of composite panels. Figure 3.8 shows the burning test of composite panels. The flame had been spread over the entire sample and continue to combustion until the sample was completely burned out. Afterglow was observed (red glow) following the extinction of flame (figure 3.8b). At the end of burning, only ash was remained (figure 3.8c).

Data obtained from burning test are listed in table 3.4. It was found that after flame and after glow time of all composite panels is higher. The burning rate of composite panelsA1, A2, A3, and A4 are 96.0 mm/min, 116.5 mm/min, 166.7 mm/min and 58.9 mm/min respectively. The residue percentage of composite panel A4 (8.3%) is a little bit higher than the residue % of other composite panels. For a material to be certified as automotive interior (based on US Federal Regulations), the burning rate of the material should be less than 102 mm per minute [34]. The burning rate of sample A4 is about 59 mm per minute, which is much less than 102. For the use of aircraft interior, dripping time should be less than 3s [35]. The dripping time of all composite panels is zero seconds. Testing results suggest that sample A4 has required flame retardance properties to be used as interior material in case of burning rate and dripping time. However, for a standard flame resistance interior material, the flame extinguishing time should be less than 15s (US aircraft interior standard) [35] or 30s (Chinese automotive interior standard) [36]. But produced insulation materials continue to burn until fully damaged of material. Using some flame resistant finish will be helpful to obtain this property.

(a) (b) (c)

Figure 3.8. Photos of flame test, (a) during burning, (b) after glow, (c) remaining char.

Table 3.4. Flammability data acquired from burning test of composite panels.

Sample	After flame time (s)	After glow time (s)	Burning rate (mm/minute)	Drip	Residue %
A1	82	205	96.0	No	5.8
A2	88	245	116.5	No	4.3
A3	60	195	166.7	No	3.7
A4	215	160	58.9	No	8.3

3.3.6. Moisture properties

The moisture content (MC) of all composite panels at different conditions (65 ± 2% RH & 23±2°C and 90 ± 5% RH & 23 ± 2 °C) are shown in table 3.5. It was found that at standard atmospheric condition (65 ± 2% RH and 23 ± 2 °C), MCs are in the range of 1.7 to 2.2%, and at high humid

condition (90 ± 5% RH and 23 ± 2 °C), MCs are in the range of 2.1 to 3.2% which is well below the allowable range of MC for building insulation materials. According to the ASTM C208 – 12, the MC of cellulosic building insulation materials should be less than 10% [37].

The low MCs are due to the compactness of produced insulation materials. Although cotton fibers have high moisture regain (MR) (7-8%) and MC 6.5-7.4% at 65% RH [38], the thermoplastic fibers Sorona® and PLA has very low moisture absorption, which is 0.2-0.3% [12] and 0.4-0.6 [38] respectively at 65% RH. Melting of thermoplastic fibers sealed the surface of composite panels (figure 3.5) that causes small pore diameter, and fewer open places for water molecules to enter into the composite panels result in smaller overall MC value. Therefore, with the increase of Sorona® fiber percentage, moisture content decreases (table 3.5).

Table 3.5. Moisture content of various composite panels.

Sample Id.	Dry weight, W_d (g)	Wet weight, W_W (g) at (65±2)% RH	Wet weight, W_W (g) at (90 ± 5) % RH	MC (%) at (65±2)% RH	MC (%) at (90 ± 5) % RH
A1	4.56	4.66	4.71	2.16 ± 0.46	3.00 ± 0.15
A2	4.98	5.07	5.12	1.82 ± 0.25	2.59 ± 0.12
A3	1.89	1.92	1.94	1.72 ± 0.49	2.11 ± 0.09
A4	12.25	12.53	12.68	2.32 ± 0.40	3.20 ± 0.10

3.3.7. Acoustical measurement

Transmission coefficient: Transmission coefficient is the fraction of incident airborne sound power that is transmitted through the material. Transmission coefficients of the four different samples at different frequencies are shown in table 3.6.

Table 3.6. Transmission coefficient (τ) at different frequencies.

	Transmission coefficient (τ) at different frequencies													
Sample Id.	125 Hz	160 Hz	200 Hz	250 Hz	315 Hz	400 Hz	500 Hz	630 Hz	1000 Hz	1250 Hz	1600 Hz	2000 Hz	2500 Hz	Average
A1	1.00	0.86	0.53	0.53	0.21	0.20	0.14	0.14	0.14	0.13	0.12	0.23	1.00	0.402
A2	0.69	0.77	0.63	0.44	0.54	0.35	0.13	0.12	0.18	0.12	0.11	0.17	1.00	0.404
A3	1.00	0.98	0.68	0.48	0.60	0.38	0.39	0.27	0.23	0.22	0.21	0.33	1.00	0.521
A4	0.61	0.02	0.33	0.10	0.45	0.17	0.07	0.10	0.08	0.07	0.07	0.14	0.71	0.238

All of the samples showed similar trends. Transmission coefficient is very high at low frequencies and low at medium frequency, from 600 Hz to 1800 Hz. After 2000 Hz, transmission coefficient increases again. These observations are similar to those observed by other researchers for porous fiber-based insulation materials [39], and the phenomena were discussed in the following sections. Sample A3 showed higher transmission coefficient, whereas sample A4 showed lower transmission coefficient.

The transmission coefficient observed seems to relate well to the differences in thickness and permeability of the samples. Sample that showed lowest transmission coefficient was the thickest and had the lowest permeability.

A regression analysis of transmission coefficient (figure 3.9) was done to develop models which may be helpful to predict transmission coefficient at different frequencies.

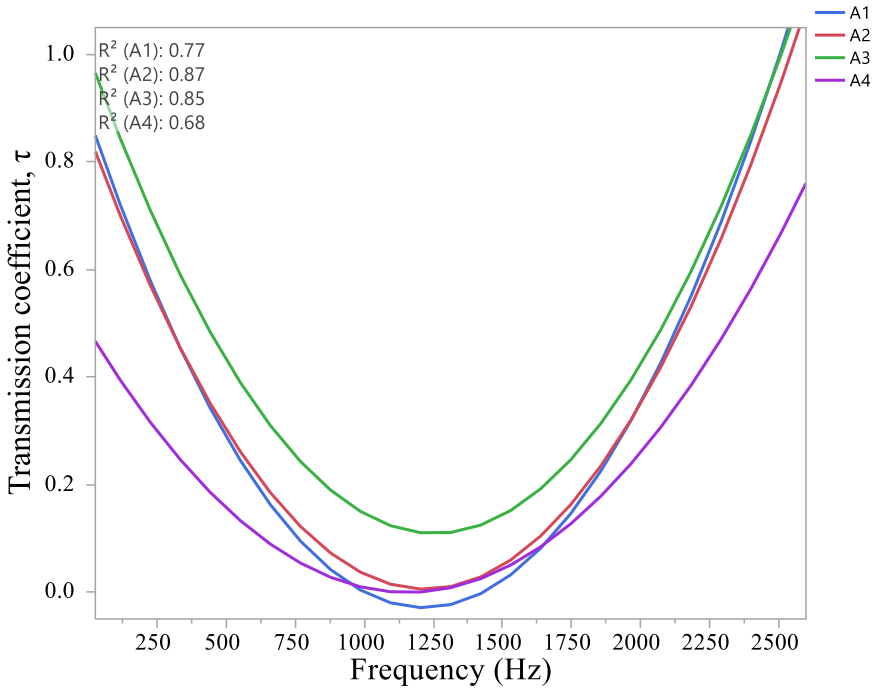

Figure 3.9. Statistical model of sound transmission coefficient of four composite panels at different frequencies.

Transmission loss: Transmission loss is the loss of sound while passing through a material. Transmission loss of the four samples at different frequencies is presented in table 3.7.

Table 3.7. Transmission loss in dB of four composite panels at different frequencies.

Sample Id.	Transmission loss, *TL* (dB), at different frequencies													Average
	125 Hz	160 Hz	200 Hz	250 Hz	315 Hz	400 Hz	500 Hz	630 Hz	1000 Hz	1250 Hz	1600 Hz	2000 Hz	2500 Hz	
A1	0	1.30	5.51	5.44	13.55	13.89	16.93	16.96	16.90	17.55	18.33	12.67	0	10.70
A2	3.22	2.27	4.02	7.20	5.30	9.09	18.06	18.62	14.92	18.24	19.36	15.56	0	10.45
A3	0	0.17	3.39	6.34	4.47	8.32	8.20	11.39	12.91	13.15	13.57	9.54	0	7.03
A4	4.29	13.98	9.63	14.02	6.94	15.39	22.54	20.23	22.28	23.01	23.08	17.31	2.92	15.05

Transmission loss of sound of four different samples also showed similar trends at different frequencies. This trend is exactly opposite to that of the transmission coefficient, as expected, i.e., higher the transmission coefficient, lower the transmission loss, and vice versa. Transmission loss is very low at low and high frequencies, and transmission loss is very high at medium frequency

range from 600 to 1800 Hz. Sample A3 exhibited comparatively lower transmission loss, whereas sample A4 exhibited higher transmission loss. This may be due to the difference in the thickness, microstructure, and lower air permeability of sample A4 compared to other samples. A regression model of transmission loss (figure 3.10) was developed that may be helpful in predicting transmission loss at different frequencies.

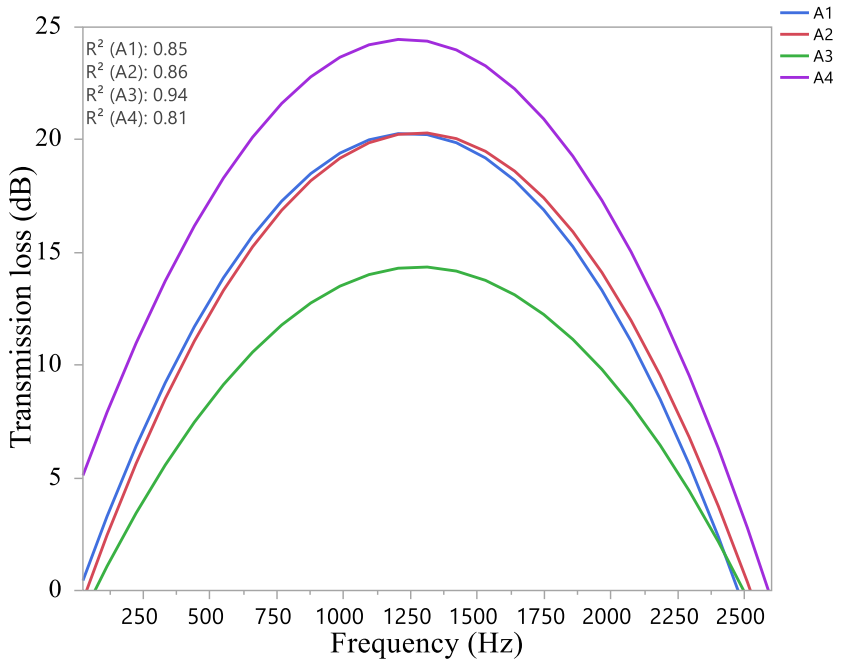

Figure 3.10. Statistical model of sound transmission loss (dB) of four composite panels at different frequencies.

Model was also compared with actual measured data of four composite panels (figure 3.11). It was observed that the measured value of sound transmission loss is almost similar to the prediction line. There are some deviations at the lower frequency, but the deviation is very small.

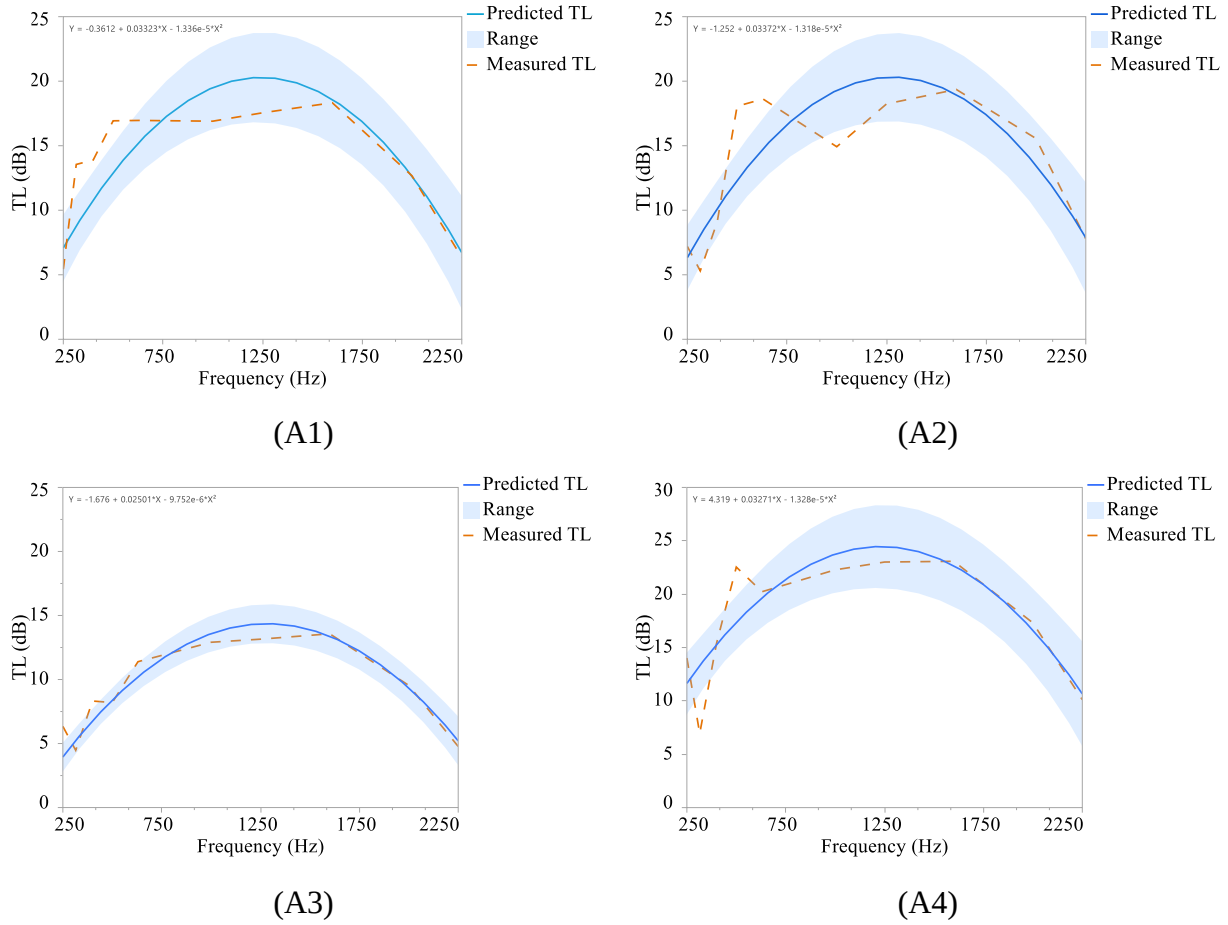

Figure 3.11. Comparison of measured and predicted sound transmission loss (*TL*) in dB of four composite panels at different frequencies.

Several other researchers also observed similar trends of lower acoustic insulation properties for porous materials at low frequencies and higher acoustic insulation properties at medium frequency range [39]. When sound waves enter into porous materials, air molecules within the pores vibrate that transform sound energy into thermal and viscous heat [31], [40]. At low frequencies, this energy is dissipated by the isothermal process (limited amount), but at high-frequency range, energy is lost by the adiabatic process [41]. As a result, a low amount of sound is absorbed in low-frequency range, but absorption is higher at higher frequencies (resulting in low sound absorption coefficient at low frequencies). That's why porous materials show good acoustic insulation properties at medium frequency range. On the other hand, energy of wave decreases

with the increases of frequency. At very high frequency, sound energy is not strong enough to vibrate the air molecule. Therefore, transformation of sound energy to thermal and viscous heat is less and as a result transmission loss of sound is also less.

3.3.8. Effect of air permeability, thickness, and density on sound transmission

Influence of air permeability on sound transmission can be seen in figure 3.12. It is found that air permeability has significant effect on sound transmission loss (F = 21.75, P = 0.043). Air permeability is inversely related to sound transmission loss, i.e., with the increase in air permeability, sound transmission loss decreases. Due to high air permeability, more sound energy passes through the materials. Less internal reflection of sound energy occurs within the porous structure, and as a result, less sound energy is converted and dissipated into thermal and viscous heat. In this study, sample A4 has low air permeability and higher sound transmission loss.

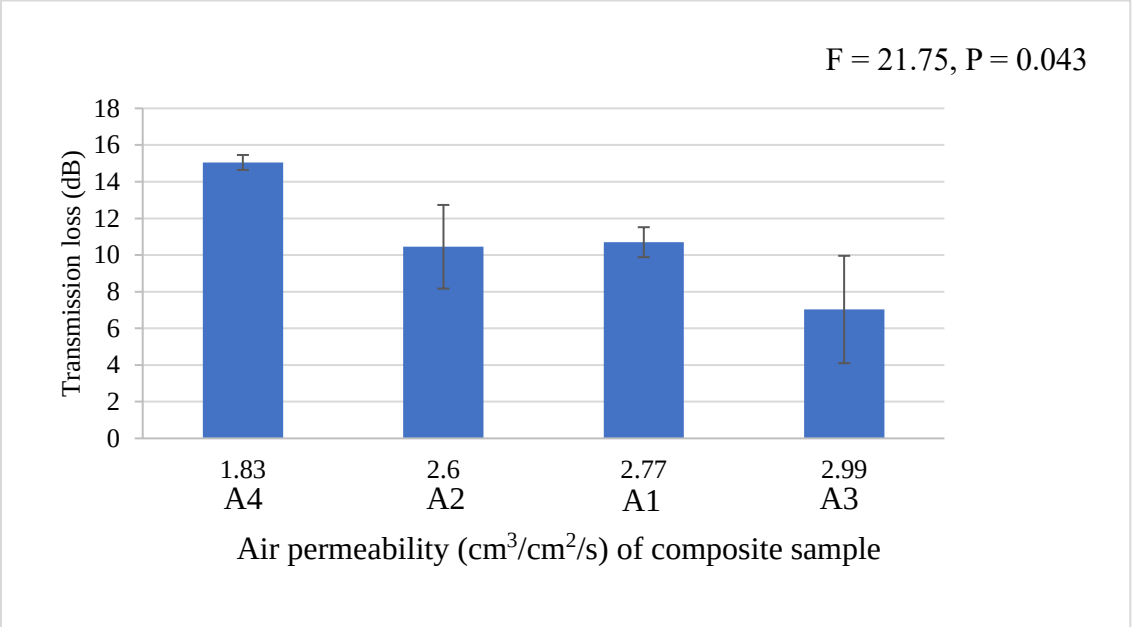

Figure 3.12. Relation of air permeability with sound transmission loss of four composite panels.

Thickness is one of the most important factors that also have significant influence on sound transmission loss (F = 49.9, P = 0.0195). Changes in sound transmission loss with thickness are

plotted in figure 3.13. Sound transmission loss increases with increases in thickness. Sound energy has to travel through a comparatively longer path when it passes through thicker materials. As a result, more sound energy is entrapped within the porous structure and converted into thermal and viscous heat.

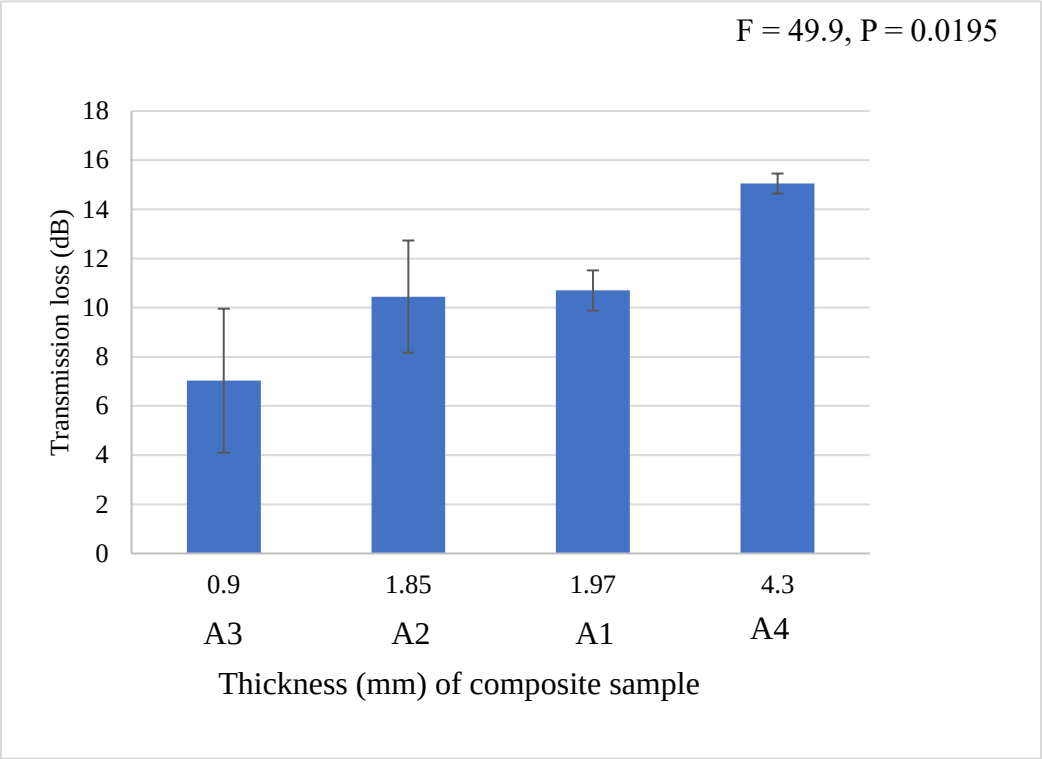

Figure 3.13. Relation of thickness with sound transmission loss of four composite panels.

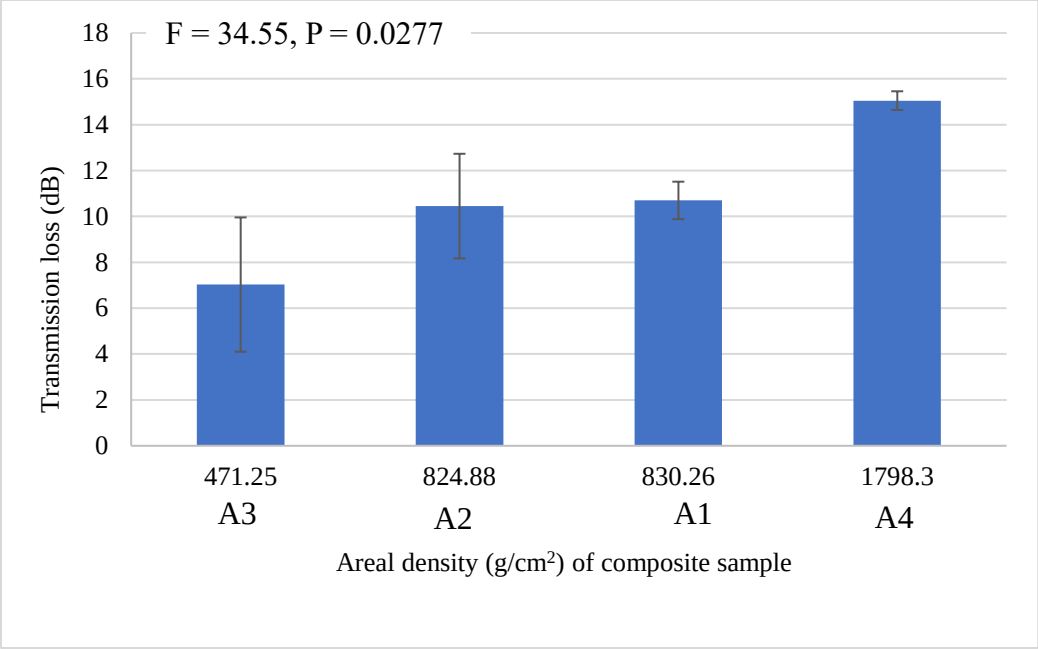

Figure 3.14. Relation of areal density with sound transmission loss of composite panels.

Similar to thickness, areal density also has a significant impact on sound transmission loss (F = 34.55, P = 0.0277). Sound transmission loss increases with increase in areal density of the composite panels (figure 3.14) due to the larger distance the sound has to travel through longer path to pass the material successfully.

A similar relationship has been observed by some other authors. Koizumi et al. found that textile fibers with high density and thickness can increase the sound absorption properties at medium frequency ranges [42]. Liu et al. also observed that insulation properties of composite materials increased with the increase of no. of layers and thickness [43]. Küçük and Korkmaz explained that thicker materials have comparatively lower air permeability that increases the acoustic insulation properties of the materials [44]. This research also shows an identical pattern for the composite materials produced from recycled fibers. Thickness of sample A4 is comparatively higher and results in lower air permeability and higher sound transmission loss.

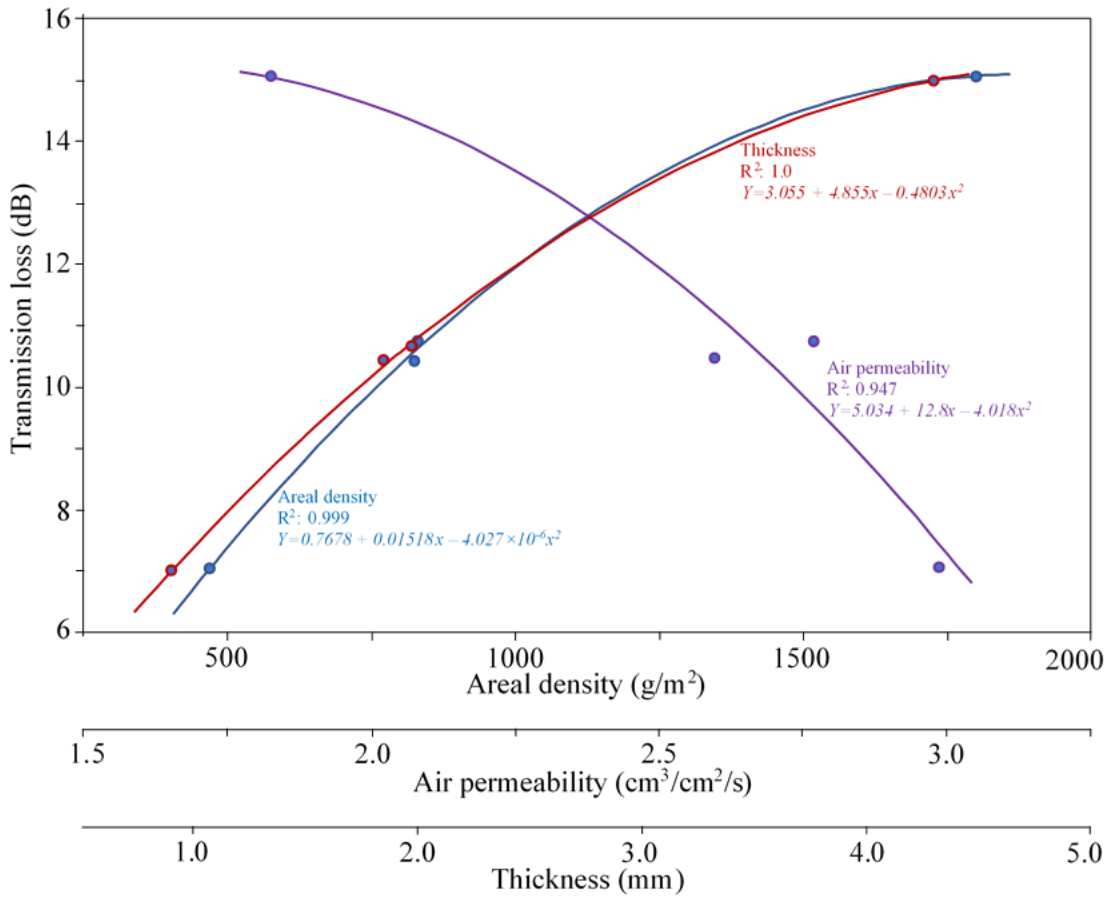

Figure 3.15. Statistical model of transmission loss (dB) with variation of areal density, air permeability, and thickness.

A regression analysis was done to develop statistical model that is helpful to predict sound transmission loss with the variation of areal density, thickness, and air permeability. All three models are combined in figure 3.15 to compare and predict the effect of areal density, thickness, and air permeability on sound transmission loss. It is shown from figure 3.15 that r^2 value of all three models is very high (close to 1), which indicates that almost all of the variation of sound transmission loss can be explained by the relation between transmission loss with areal density, thickness, and air permeability.

From the statistical model (figure 3.15), it is clearly observed that the transmission loss of sound can be increased by increasing thickness and density and with the decreasing of air

permeability of materials. But at the same time, air permeability decreases with the increases in thickness and density. For successful commercialization of a product, it is necessary to optimize all the properties. Based on this model (figure 3.15), it may be concluded that in case of acoustic insulation panels produced from recycled textile fibers, the optimum acoustic insulation properties may be found at the areal density of around 1125 (g/m^2) and at the thickness of around 2.7 mm.

3.3.9. Comparison with commercially available acoustic insulation materials

One of the most commonly used building insulation materials is gypsum board. The sound transmission loss of 15 mm thick gypsum board is 26.3 dB [39]. The thickness was normalized to unit mm, and the sound transmission loss of gypsum board with our insulation materials was compared (table 3.8). It is observed that the sound transmission loss of these insulation materials A1, A2, A3, and A4 are 5.43 dB, 5.64 dB, 7.81 dB, and 3.5 dB, respectively, which is higher than the sound transmission loss (1.76 dB) of gypsum board of comparable thickness, assuming the normalization holds good. This indicates that the recycled composite panels have great potential to be used as acoustic insulating materials.

Table 3.8**.** Comparison of sound transmission loss of prepared composite panels with the sound transmission loss of commercially available insulation panels, gypsum board.

Sample	Thickness (mm)	TL (dB)	Normalized TL (dB) per mm	Comparison (dB)
A1	1.97	10.70	5.43	+3.67
A2	1.85	10.45	5.64	+3.88
A3	0.90	7.03	7.81	+6.05
A4	4.30	15.05	3.50	+1.74
Gypsum	15.00	26.3	1.76	0.00

3.3.10. Thermal measurement

The thermal properties four different composite panels are shown in table 3.9 and figure 3.16 and figure 3.17.

Table 3.9. Thermal properties of four different composite panels.

Sample	Composition	Heat flow, Q (W/m^2)	Density (kg/m3)	Porosity	Thermal resistance, (m^2K/W)	Thermal Conductivity, k (W/mK)
A1	70% Denim/30% Sorona®	56.57	460.05	0.68	0.25	0.050
A2	60% Denim/40% Sorona®	66.03	503.46	0.65	0.19	0.059
A3	50% Denim/50% Sorona®	82.29	544.95	0.62	0.16	0.065
A4	60% Denim/40% PLA	42.21	434.21	0.69	0.31	0.049

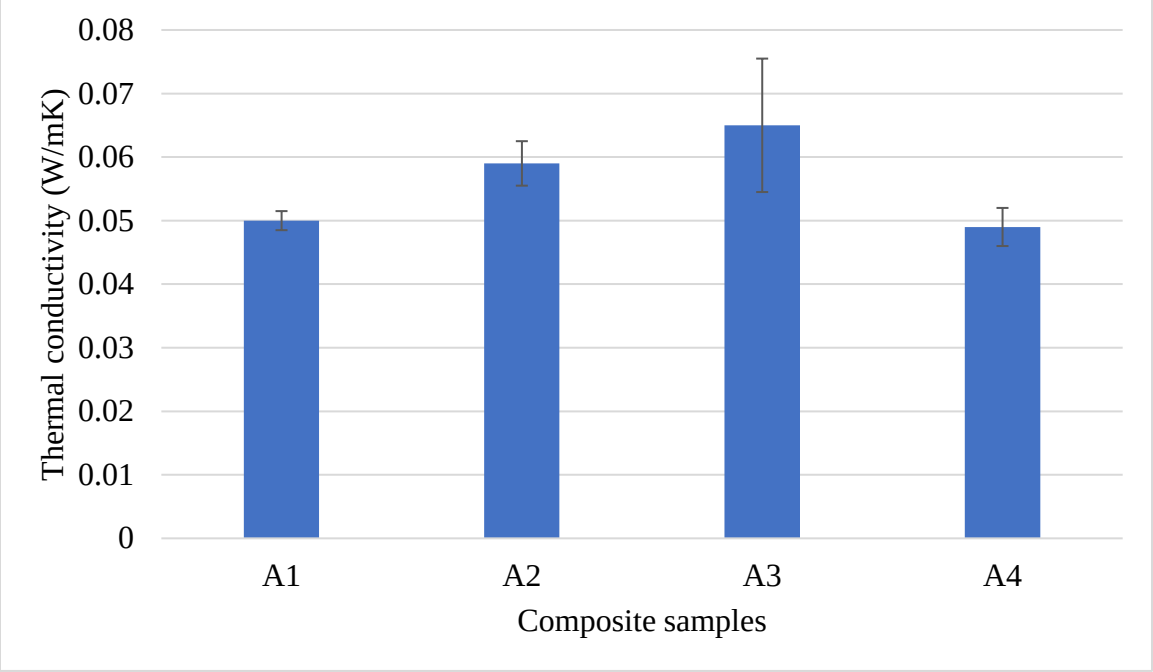

Figure 3.16. Thermal conductivity of four different composite panels.

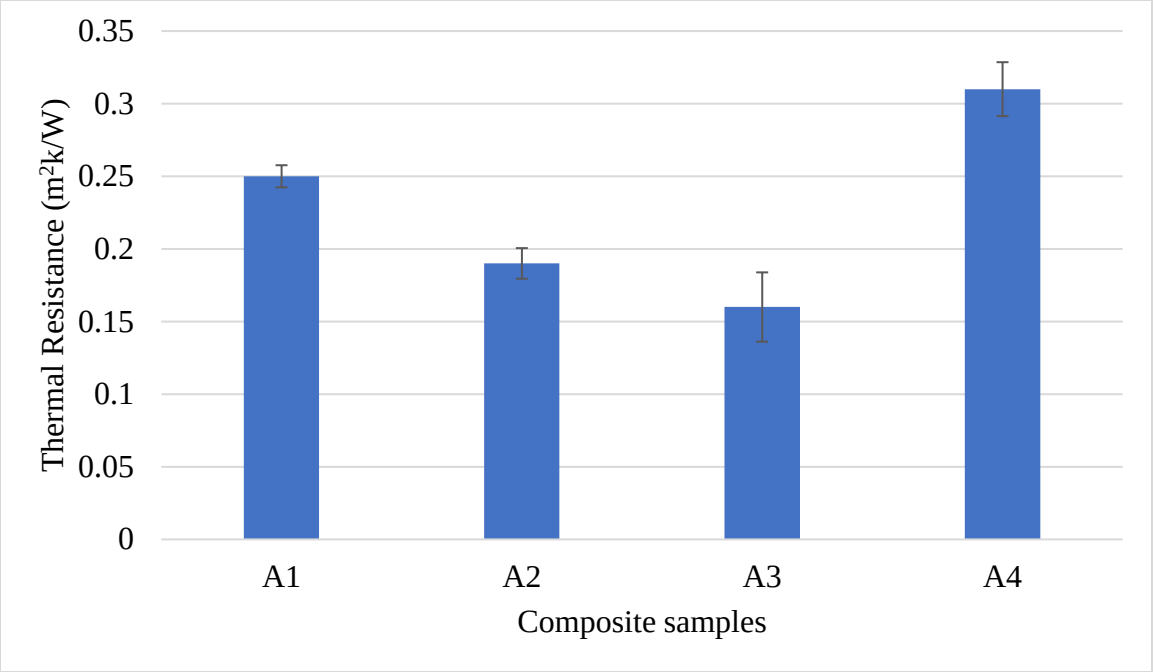

Figure 3.17. Thermal resistance of four different composite panels.

From the results, it can be found that all the composite panels have very good thermal insulation properties. According to TS 805 EN 60155, if a material has thermal conductivity lower than 0.1 W/mK, then the material is considered as building insulation material [45]. According to the literature, a material with a thermal conductivity lower than 0.07 W/mK can be regarded as a good thermal insulator [7]. As all four insulation panels have thermal conductivity lower than 0.07 W/mK, therefore produced materials can be successfully used as thermal insulation building materials. Among four insulation panels, sample A4 has the best thermal insulation properties with thermal conductivity of 0.049 W/mK. Thus, it can be said that combination of cotton and PLA fiber is more suitable for producing thermal insulation panels.

3.3.11. Effect of air permeability, density, and porosity on thermal conductivity

Effect of air permeability on thermal conductivity has been shown in figure 3.18. It was found that there is a little bit of increase in thermal conductivity with the increase of air permeability. However, the increase is not statistically significant ($F = 1.71$, $P = 0.3215$). Thus, we can say that

contrary to acoustic insulation properties, air permeability does not have significant influence on thermal insulation properties. This may be due to very low heat-flowing properties of air.

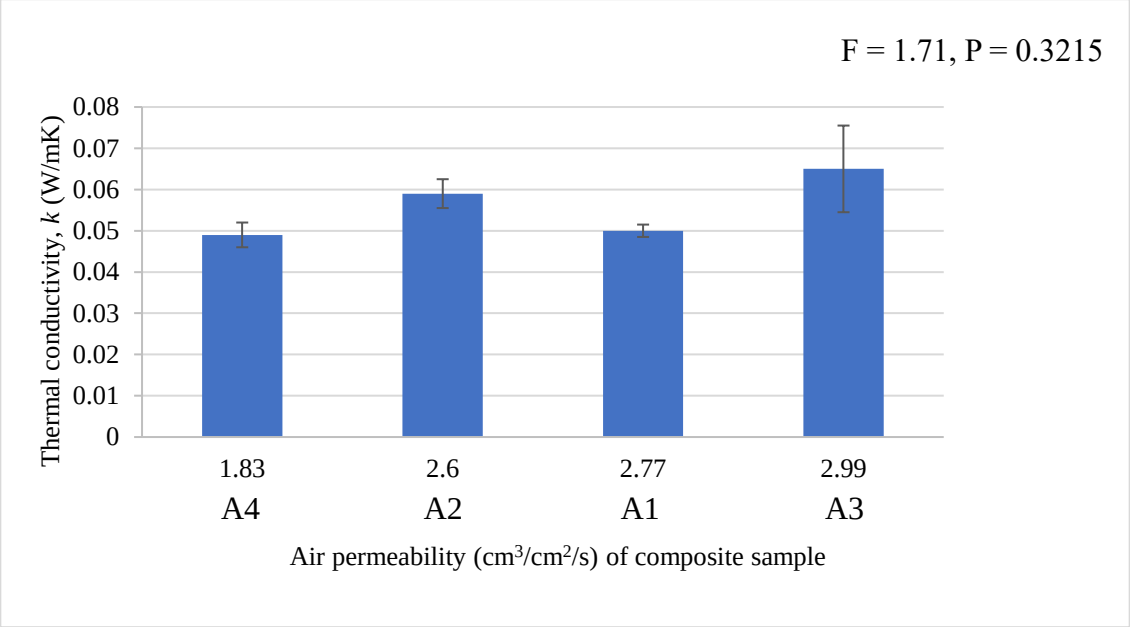

Figure 3.18. Relation of air permeability with thermal conductivity of composite panels.

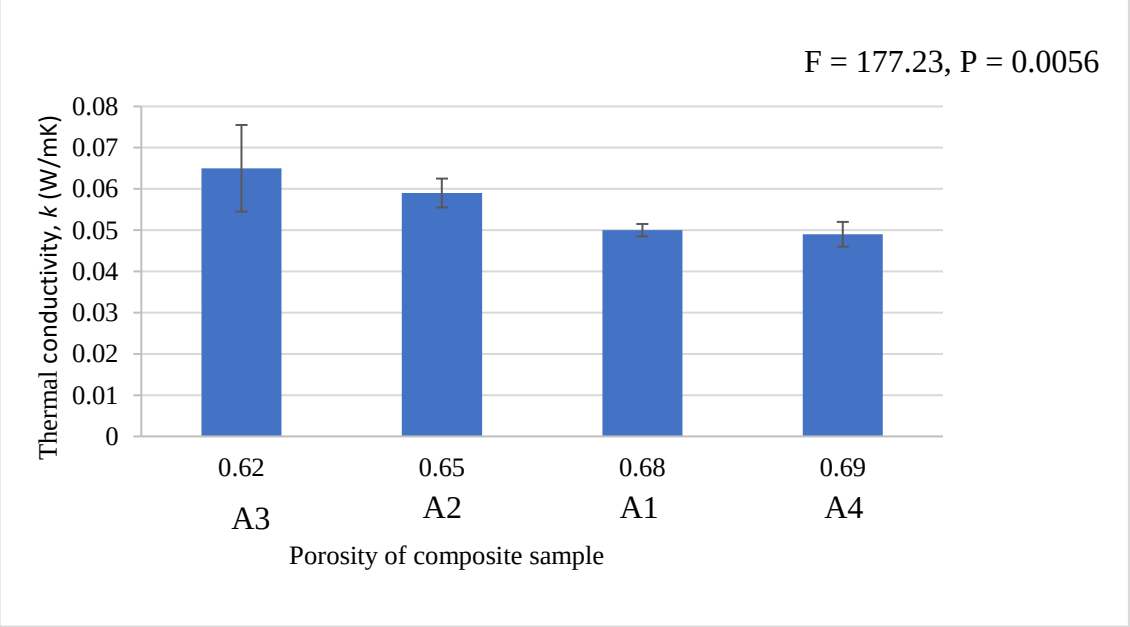

Figure 3.19. Relation of porosity with thermal conductivity of composite panels.

Influence of porosity on thermal conductivity has been shown in figure 3.19. It is found that porosity has significant effect on thermal conductivity (F = 177.23, P = 0.0056). Porosity is inversely related to thermal conductivity, i.e., with the increase in porosity, thermal conductivity decreases. Higher porosity means more void structure within composite panels. Most structure which is normally filled with air hampered thermal conduction. Air has very low thermal conductivity, 0.025 W/mK [46], which is lower than any type of solid material. Thus, with the increase of void volume within a structure, overall conductivity of the material decrease. Sample A4 has higher porosity and lower thermal conductivity.

Similar to porosity, density also has a significant impact on thermal conductivity (F = 69.17, P = 0.0142) (figure 3.20). However, contrary to porosity, thermal conductivity increases with the increase of density. Higher density means lower air void structure, and closer contact of solid components results in higher thermal conductivity.

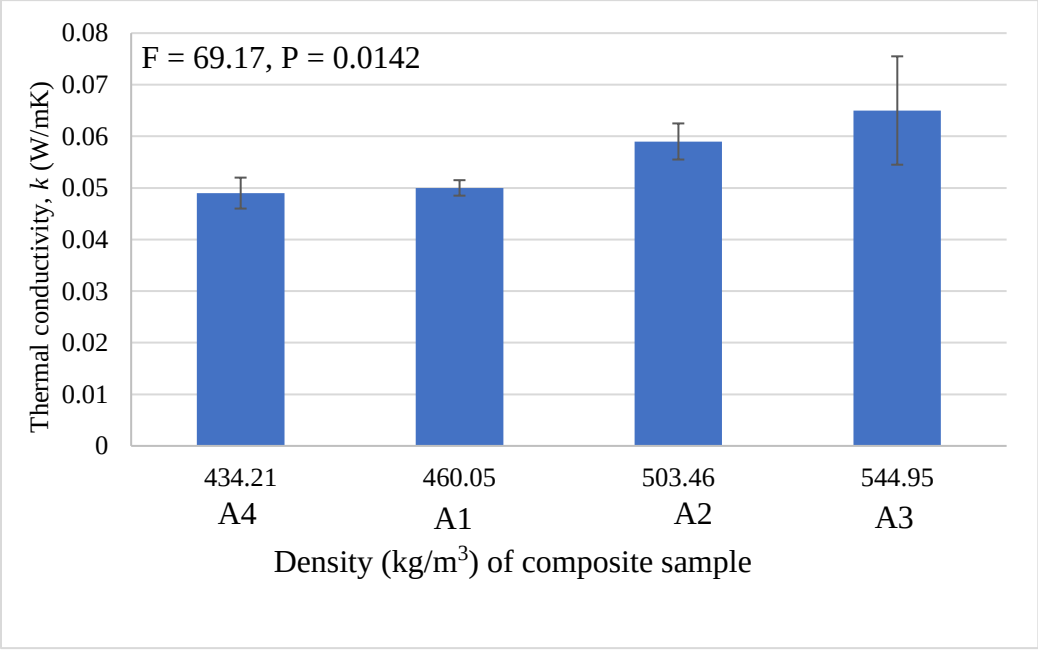

Figure 3.20. Relation of density with thermal conductivity of composite panels.

Similar to sound transmission loss, a regression analysis was also done to develop statistical model of thermal conductivity with the variation of density and porosity. Two models are combined in figure 3.21 to compare and predict the effect of density and porosity on thermal conductivity. The r^2 value of models is very high (close to 1), which indicates that almost all of the variation of thermal conductivity can be explained by the relation between thermal conductivity with density and porosity.

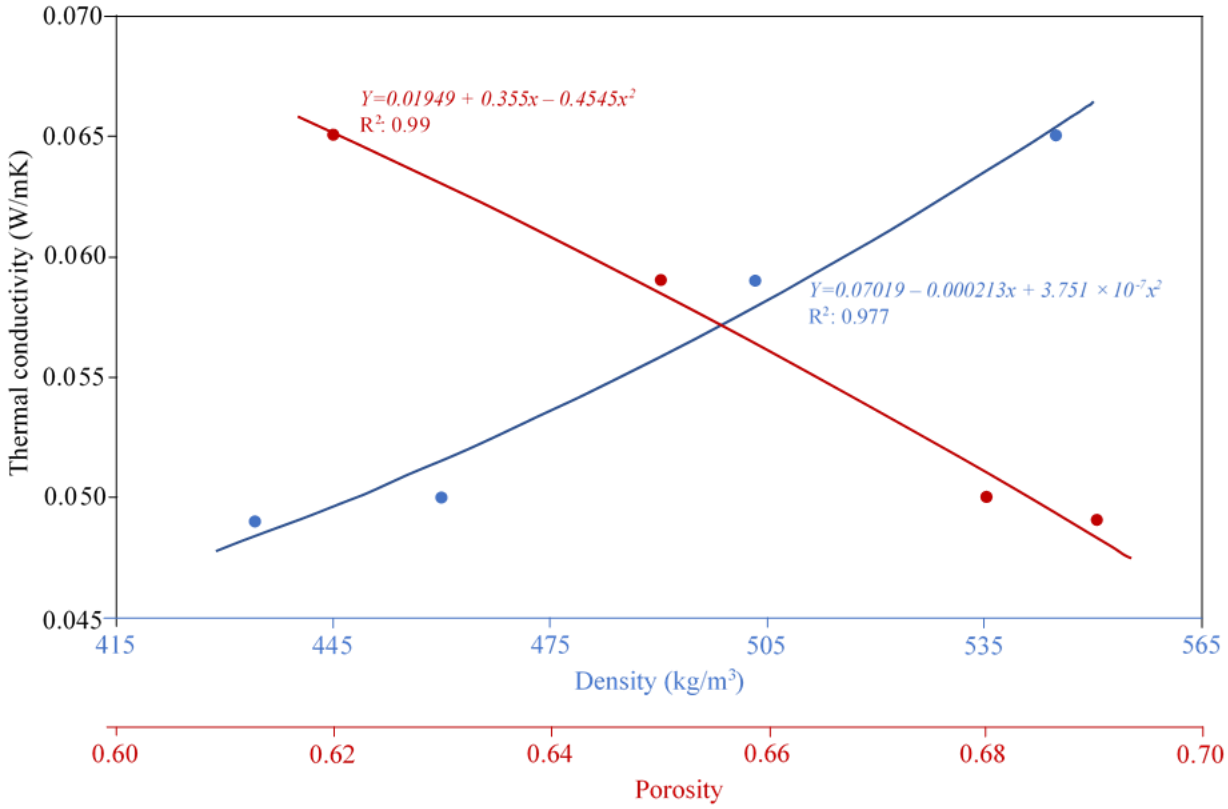

Figure 3.21. Statistical model of thermal conductivity with variation of density and porosity.

3.3.12. Comparison with commercially available thermal insulation materials

One of the commonly used thermal insulation materials is mineral wool. A comparison was made with commercially available mineral wool and produced insulation panels (table 3.10). It was found that the thermal conductivity of samples A1 and A4 are very much comparable with the thermal conductivity mineral wool. It was also found that the density of produced insulation

materials is very much higher than mineral. Thus, thermal insulation properties of produced insulation panels can be further reduced by increasing the porosity and decreasing density. This indicates that the recycled composite panels have great potential to be used as both thermal and acoustic insulating materials. Gypsum board which has good acoustic insulation properties, does not have good thermal insulation properties. Thermal conductivity of gypsum board is very high. But our produced insulation panels have both excellent thermal and acoustic insulation properties, which is a great advantage for commercialization.

Table 3.10. Comparison with commercially available insulation panels.

Materials	Density	Thermal conductivity (W/mK)	Relative thermal conductivity to air (0.025 ~ 1	Ref.
A1	460.05	0.050±0.002	2	--
A2	503.46	0.059±0.004	2.36	--
A3	544.95	0.065±0.011	2.6	--
A4	434.21	0.049±0.003	1.96	--
Gypsum board	--	0.28	11.2	[47]
Mineral wool	36	0.040–0.045	1.6 – 1.8	[48]

3.4. Summary

In this study, waste textiles were used to produce environmentally-friendly alternative thermal and acoustic insulation materials. Recycled denim and Sorona®/PLA binder fibers were blended at different ratios to produce four different composite panels. Several structural parameters were measured. It is found that the composite panels are microporous, and most of them are within the range of 10 – 25 micrometers. Similarly, most of the fiber diameters are situated within the range of 12 to 22 µm, and the distribution of diameters is unimodal, close to symmetrical. Produced

insulation materials also have good flame retardance properties that can be improved further by applying flame retardant finishes.

Samples produced from recycled denim and PLA blend (60% recycled denim and 40% PLA) show maximum transmission loss of over 23 dB at around 1200 to 1600 Hz. The effect of several structural parameters, including air permeability, thickness, and areal density, on sound transmission loss, was analyzed. Sound transmission loss increases with increase in thickness and areal density but decreases with the increase of air permeability. With the decrease of biodegradable binder fiber (Sorona®), the performance of sound absorption of composite panels have improved. Statistical models were developed and compared with actual measured values. It is observed that the measured value and predicted value are almost similar. From the regression model, it can be predicted that composite materials with around 1125 (g/m^2) areal density and 2.7 mm thickness give optimum acoustic insulation properties. A comparison of acoustic properties was checked with commercially used insulation material gypsum board, and it is noticed that composites panels produced from waste denim have better acoustic insulation properties.

Similar to acoustic insulation, all the composite panels have very good thermal insulation properties and very much suitable to be used as thermal insulation panels. Samples produced from recycled denim and PLA blend (60% recycled denim and 40% PLA) show the lowest thermal conductivity value of 0.049 W/mK. The effect of several structural parameters, including air permeability, density, and porosity, on thermal conductivity was investigated. Tested results showed that air permeability doesn't have significant effect on thermal conductivity, whereas porosity and density have significant influence on thermal conductivity. Thermal conductivity decreases with the increase of porosity and with the decrease of density. A comparison of thermal insulation properties was made with commercially used insulation material mineral wool, and it is

noticed that composites panels produced from waste denim have comparable thermal insulation properties with insulation properties of commercial mineral wool. Thermal insulation properties can be further increased by increasing porosity and decreasing density.

The environmental benefits of produced composite materials are also very high and are not only limited to the reduction of energy consumption and harmful effects of noise pollutions. These composite panels will help get rid of the adverse environmental effects due to landfilling of textile waste as well as also help the reduction of fiber production by extraction or agricultural methods. These materials will also help to reduce the production of presently used synthetic insulation panels. This study demonstrated that recycled textiles could have another life as insulation materials before being safely disposed of in composting environment, where they can break down into simple chemicals. However, additional research work, including life cycle assessment, is necessary to get complete idea about the environmental effect of these insulation materials.

3.5. References

[1] M. EL Wazna, A. Gounni, A. EL Bouari, M. EL Alami, and O. Cherkaoui, “Development, characterization and thermal performance of insulating nonwoven fabrics made from textile waste,” *J. Ind. Text.*, vol. 48, no. 7, pp. 1167–1183, 2019, doi: 10.1177/1528083718757526.

[2] S. Islam and G. Bhat, “Environmentally-friendly thermal and acoustic insulation materials from recycled textiles,” *J. Environ. Manage.*, vol. 251, p. 109536, 2019.

[3] J. Zach, A. Korjenic, V. Petránek, J. Hroudová, and T. Bednar, “Performance evaluation and research of alternative thermal insulations based on sheep wool,” *Energy Build.*, vol. 49, pp. 246–253, 2012.

[4] A. Patnaik, “Materials Used for Acoustic Textiles,” in *Acoustic Textiles*, R. Padhye and R. Nayak, Eds. Singapore: Springer, 2016, pp. 73–92.

[5] M. Zakriya, G. Ramakrishnan, N. Gobi, N. K. Palaniswamy, and J. Srinivasan, “Jute-reinforced non-woven composites as a thermal insulator and sound absorber–A review,” *J. Reinf. Plast. Compos.*, vol. 36, no. 3, pp. 206–213, 2017.

[6] H. S. Seddeq, N. M. Aly, A. Marwa, and M. Elshakankery, “Investigation on sound absorption properties for recycled fibrous materials,” *J. Ind. Text.*, vol. 4, no. 1, pp. 56–73, 2013, doi: 10.1177/1528083712446956.

[7] F. Asdrubali, F. D’Alessandro, and S. Schiavoni, “A review of unconventional sustainable building insulation materials,” *Sustain. Mater. Technol.*, vol. 4, pp. 1–17, 2015, doi: 10.1016/j.susmat.2015.05.002.

[8] P. Ricciardi, E. Belloni, and F. Cotana, “Innovative panels with recycled materials: thermal and acoustic performance and life cycle assessment,” *Appl. Energy*, vol. 134, pp. 150–162, 2014, doi: 10.1016/j.apenergy.2014.07.112.

[9] E. Castro-Aguirre, F. Iñiguez-Franco, H. Samsudin, X. Fang, and R. Auras, “Poly (lactic acid)—Mass production, processing, industrial applications, and end of life,” *Adv. Drug Deliv. Rev.*, vol. 107, pp. 333–366, 2016.

[10] L. T. Lim, R. Auras, and M. Rubino, “Processing technologies for poly (lactic acid),” *Prog. Polym. Sci.*, vol. 33, no. 8, pp. 820–852, 2008.

[11] E. T. H. Vink and S. Davies, “Life cycle inventory and impact assessment data for 2014 Ingeo™ polylactide production,” *Ind. Biotechnol.*, vol. 11, no. 3, pp. 167–180, 2015.

[12] J. V Kurian, “A new polymer platform for the future—Sorona® from corn derived 1, 3-propanediol,” *J. Polym. Environ.*, vol. 13, no. 2, pp. 159–167, 2005.

[13] A. E. Tiuc, H. Vermeşan, T. Gabor, and O. Vasile, “Improved sound absorption properties of polyurethane foam mixed with textile waste,” *Energy Procedia*, vol. 85, pp. 559–565, 2016, doi: 10.1016/j.egypro.2015.12.245.

[14] D. Trajković, S. Jordeva, E. Tomovska, and K. Zafirova, “Polyester apparel cutting waste as insulation material,” *J. Text. Inst.*, vol. 108, no. 7, pp. 1238–1245, 2017.

[15] R. Maderuelo-Sanz, A. V Nadal-Gisbert, J. E. Crespo-Amorós, and F. Parres-García, “A novel sound absorber with recycled fibers coming from end of life tires (ELTs),” *Appl. Acoust.*, vol. 73, no. 4, pp. 402–408, 2012.

[16] J. Ramis Soriano, J. Alba Fernández, R. M. del Rey Tormos, E. M. Escuder Silla, S. RICO, and V. JORGE, “Nuevos materiales absorbentes acústicos basados en fibra de kenaf,” *Constr. Mater.*, vol. 60, no. 299, pp. 133–143, 2010.

[17] S. Huda and Y. Yang, “Composites from ground chicken quill and polypropylene,” *Compos. Sci. Technol.*, vol. 68, no. 3–4, pp. 790–798, 2008.

[18] “Phoenix Fibers,” *Fiber Conversion*, 2015. http://www.phxfibers.com/fiber-conversion/ (accessed Apr. 14, 2019).

[19] “ISO 9073-2,” *Textiles -- Test methods for nonwovens -- Part 2: Determination of thickness*, 1995. https://www.iso.org/standard/16652.html.

[20] A. Majumdar, *Soft computing in textile engineering*. Cambridge: Woodhead Publishing, 2010.

[21] “ASTM D737,” *Standard Test Method for Air Permeability of Textile Fabrics*, 2018. https://www.astm.org/Standards/D737.htm.

[22] N. Mao, “Methods for characterisation of nonwoven structure, property, and performance,” in *Advances in Technical Nonwovens*, G. Kellie, Ed. Cambridge: Woodhead Publishing, 2016, pp. 155–211.

[23] S. Fatima and A. R. Mohanty, “Acoustical and fire-retardant properties of jute composite materials,” *Appl. Acoust.*, vol. 72, no. 2–3, pp. 108–114, 2011.

[24] S. B. Warner, *Fiber science*. Englewood Cliffs, NJ: Prentice-Hall, 1995.

[25] J. Bear, *Dynamics of fluids in porous media*. New York: Dover Publications, Inc., 2013.

[26] K. Attenborough, “Models for the acoustical properties of air-saturated granular media,” *Acta Acústica*, vol. 1, pp. 213–226, 1993.

[27] "ASTM F316-03," *Standard Test Methods for Pore Size Characteristics of Membrane Filters by Bubble Point and Mean Flow Pore Test*, 2019. https://www.astm.org/Standards/F316.htm.

[28] "ASTM D1230-17," *Standard Test Method for Flammability of Apparel Textiles*, 2017. https://www.astm.org/Standards/D1230.htm (accessed May 30, 2021).

[29] "ASTM D2495 – 07," *Standard Test Method for Moisture in Cotton by Oven-Drying*. ASTM International, West Conshohocken, PA, 2019, doi: 10.1520/D2495-07R19.

[30] S. S. Jung, Y. T. Kim, Y. B. Lee, S. Il Cho, and J. K. Lee, "Measurement of sound transmission loss by using impedance tubes," *J. Korean Phys. Soc.*, vol. 53, p. 596, 2008.

[31] G. Bhat and M. El Messiry, "Effect of microfiber layers on acoustical absorptive properties of nonwoven fabrics," *J. Ind. Text.*, vol. 50, no. 3, pp. 312–332, 2020, doi: 10.1177/1528083719830146.

[32] "ASTM E2611," *Standard Test Method for Normal Incidence Determination of Porous Material Acoustical Properties Based on the Transfer Matrix Method*, 2017. https://www.astm.org/Standards/E2611.htm.

[33] "ASTM F1868 - 17," *Standard Test Method for Thermal and Evaporative Resistance of Clothing Materials Using a Sweating Hot Plate*, 2017. https://www.astm.org/Standards/F1868.

[34] "Aeroblaze," *Flammability of Automotive Materials (FMVSS 302)*, 2021. https://www.aeroblazelab.com/tests/flammability-interior-materials-fmvss-302 (accessed May 30, 2021).

[35] N. K. Kim, N. Mao, R. Lin, D. Bhattacharyya, M. C. M. van Loosdrecht, and Y. Lin, "Flame retardant property of flax fabrics coated by extracellular polymeric substances recovered from both activated sludge and aerobic granular sludge," *Water Res.*, vol. 170, pp. 1–8, 2020, doi: 10.1016/j.watres.2019.115344.

[36] "STC," *Automotive Interior Materials Flammability Test*, 2018. https://www.dgstc.group/en/media/extendinfo/id/41 (accessed May 30, 2021).

[37] "ASTM C208 - 12," *Standard Specification for Cellulosic Fiber Insulating Board*. ASTM International, West Conshohocken, PA, 2017, doi: 10.1520/C0208-12R17E02.

[38] J. W. S. Hearle and W. E. Morton, *Physical properties of textile fibres*. Cambridge: Woodhead Publishing, 2008.

[39] R. Reixach, R. Del Rey, J. Alba, G. Arbat, F. X. Espinach, and P. Mutjé, “Acoustic properties of agroforestry waste orange pruning fibers reinforced polypropylene composites as an alternative to laminated gypsum boards,” *Constr. Build. Mater.*, vol. 77, pp. 124–129, 2015.

[40] U. Berardi and G. Iannace, “Acoustic characterization of natural fibers for sound absorption applications,” *Build. Environ.*, vol. 94, pp. 840–852, 2015.

[41] U. Berardi and G. Iannace, “Predicting the sound absorption of natural materials: Best-fit inverse laws for the acoustic impedance and the propagation constant,” *Appl. Acoust.*, vol. 115, pp. 131–138, 2017, doi: 10.1016/j.apacoust.2016.08.012.

[42] T. Koizumi, N. Tsujiuchi, and A. Adachi, “The development of sound absorbing materials using natural bamboo fibres,” in *High performance structures and materials IV.*, C. A. Brebbia & De Wilde, WP., Ed. Southampton: WIT Press, 2002, pp. 157–166.

[43] X. Liu, X. Tang, and Z. Deng, “Sound absorption properties for multi-layer of composite materials using nonwoven fabrics with kapok,” *J. Ind. Text.*, 2020, doi: 10.1177/1528083720904926.

[44] M. Küçük and Y. Korkmaz, “The effect of physical parameters on sound absorption properties of natural fiber mixed nonwoven composites,” *Text. Res. J.*, vol. 82, no. 20, pp. 2043–2053, 2012, doi: 10.1177/0040517512441987.

[45] H. Binici, M. Eken, M. Dolaz, O. Aksogan, and M. Kara, “An environmentally friendly thermal insulation material from sunflower stalk, textile waste and stubble fibres,” *Constr. Build. Mater.*, vol. 51, pp. 24-33., 2014.

[46] S. Wei, C. Yiqiang, Z. Yunsheng, and M. R. Jones, “Characterization and simulation of microstructure and thermal properties of foamed concrete,” *Constr. Build. Mater.*, vol. 47, pp. 1278–1291, 2013.

[47] K. G. Wakili and E. Hugi, “Four types of gypsum plaster boards and their thermophysical properties under fire condition,” *J. Fire Sci.*, vol. 27, no. 1, pp. 27–43, 2009, doi: 10.1177/0734904108094514.

[48] M. El Wazna, M. El Fatihi, A. El Bouari, and O. Cherkaoui, “Thermo physical characterization of sustainable insulation materials made from textile waste,” *J. Build. Eng.*, vol. 12, pp. 196–201, 2017.

CHAPTER 4

Application of the Central Composite Design to Understand the Effect of Processing Parameters on Thermal and Acoustic Insulation Properties of Nonwoven Composite Materials[2]

[2] Islam, S. and Bhat, G. To be submitted to *Journal of Industrial Textiles*.

Abstract

Thermal and acoustic insulation property of materials produced from recycled textiles using nonwoven techniques has depended on several factors, including thickness, density, air permeability, and porosity. Again these factors depend on several processing parameters like consolidating time and temperature. The goal of this research is to investigate the effect of two processing parameters, consolidating time and temperature (during thermal bonding of insulation panels), on thickness, density, air permeability, and porosity and subsequently on thermal and acoustic insulation properties of composite panels. Thirteen different composite panels were produced from recycled textiles (50% cotton and 50% nylon) and biodegradable PLA fibers using nonwoen techniques with varying consolidation time and temperature. A response surface methodology (central composite design) was utilized in order to understand the effect of consolidating time and temperature. It was determined that bonding time and temperature have strong influence on the structural properties of insulation materials, with the increase of bonding time and temperature thickness decrease whereas density increases. Air permeability initially slightly increases and then decreases. It is interesting to find out that thermal and acoustic insulation properties follow opposite trends with the increase of bonding time and temperature, acoustic insulation property increases, but thermal insulation property decreases. Results also indicate that produced insulation materials have very good thermal and acoustic insulation properties. The lowest obtained thermal conductivity was 0.0339 W/mK, and the highest obtained sound transmission loss was 18.46 dB at the frequency of 1600 Hz.

Keywords: Nonwoven composite, bonding time, bonding temperature, acoustic insulation, thermal insulation.

4.1. Introduction

Based on the result of chapter three, it can be concluded that some of the most important parameters that influence the insulation properties of composite panels are thickness, density, air permeability, and porosity. Thermal and acoustic insulation properties of composite panels, produced from waste textiles using nonwoven techniques, can be controlled by controlling the thickness, density, air permeability, and porosity of the composite panels. Thus, in order to obtain insulation materials with desired insulation properties, first, we need to control these properties. However, controlling these properties is not an easy task as several processing parameters have strong influence on the properties. Like porosity and permeability of needle punched thermally bonded nonwoven composites are influenced by fiber shape and distribution; type, size, penetration, and density of needles; and bonding time and temperature during thermal bonding [1]–[3]. Various studies have been conducted to investigate the effects of these processing parameters on the properties such as air permeability and porosity of nonwoven composite materials [4]–[10].

Rawal and Anandjiwala investigated the effect of feeding rate, needling stroke frequency, and depth of needle penetration on the permeability of polyester and flax-based nonwoven fabric [8]. Debnath and Madhusoothanan studied the influence of fiber blend ratio, needling density, thickness, and fabric weight on air permeability and thermal resistance of needle punched nonwoven fabrics [11]. Mohammadi et al. performed an experimental investigation of multilayered needle-punched nonwoven samples produced from ceramic and glass fibers to check the variation of air permeability with varying web layers and number of barbs in felting needles [4], [5].

Most of these earlier researches are based on the effect of needle punching parameters. There is a lack of research on the effect of processing parameters during thermal bonding. However,

bonding time and temperature have strong influence on the properties of final products. Again, previous researches mainly focused on air permeability, and did not give on emphasis on the effect of processing parameters on composite thickness, density, and porosity. But from the study discussed in the previous chapter, it was found that the composite thickness, density, and porosity have strong influence on thermal and acoustic insulation properties. Therefore, the main purpose of this study is to investigate the effect of bonding time and temperature on the properties of thickness, density, porosity, and air permeability and, subsequently, on the thermal and acoustic insulation properties of nonwoven composites.

Nonwoven fabrics are generally produced by randomly deposited fibers and binding them together by various methods, including mechanical, thermal, and chemical bonding [12]. In this study, both mechanical (needle punching) and thermal bonding were utilized to produce composite panels. Additional thermal bonding makes the structure more compact and increases the strength of composite panels as PLA fibers melt and bond together due to heating. However, due to melting and bonding of thermoplastic PLA fiber, several structural changes occurred, that include compactness, pore size, and pore shape [13], [14]. The melted thermoplastic PLA fibers fused together (after removing heat) resulting in change in morphology of composite panels especially at the surface. Structural changes that occur due to thermal bonding have strong influence on the structure and properties of composite materials, including thickness, density, porosity, and air permeability [15]–[18].

Thus, the goal of this study is to investigate the effect of two processing parameters, bonding time and temperature (during thermal bonding of insulation panels), on thickness, density, air permeability, and porosity, and subsequently on thermal and acoustic insulation properties. Thirteen different composite panels were produced from recycled textiles (50% cotton and 50%

nylon) and biodegradable PLA fibers using nonwoven techniques with varying bonding times and temperatures. A response surface methodology (central composite design) was utilized to analyze the tested data.

4.2. Materials and Methods

4.2.1. Materials

Thermal insulation panels were prepared by blending recycled textile fibers with thermoplastic PLA binder fibers at different ratios (table 4.1). Textile wastes from Bluewater Defense, a military apparel producer in Purto Rico, were shredded into loose fiber bundles by Cross Plains Trading Company, Chatsworth, GA. These recycled textiles consisted of 50% natural cotton fibers and 50% synthetic nylon fibers. PLA staple fibers (derived from corn starch as the source) were obtained from Fiber Innovation Technology, Inc., Johnson City, TN. The properties of used PLA fibers obtained from the manufacturer are listed in table 3.1 (chapter 3).

4.2.2. Preparation process

At first, collected waste textiles were cut into small pieces. After that, cut fabrics were passed through a fabric recycling machine similar to a card, where textile waste was opened into fiber bundles. Then these fiber bundles were passed through a laboratory carding machine to open the fibers and mixed with a thermoplastic binder PLA fiber 15% by weight. The carded web was lightly bonded by needle-punching. Carding and needle punching were done at Southeastern Nonwovens, Spartanburg, SC. Needled webs were cut into desired size and then consolidated using pressure (1200 lbs) and various temperatures using a hot press in our laboratory. The schematic of the sample preparation process is shown in figure 4.1. Several composite samples (table 4.1) were produced by varying the temperature and time of consolidation in the hot press.

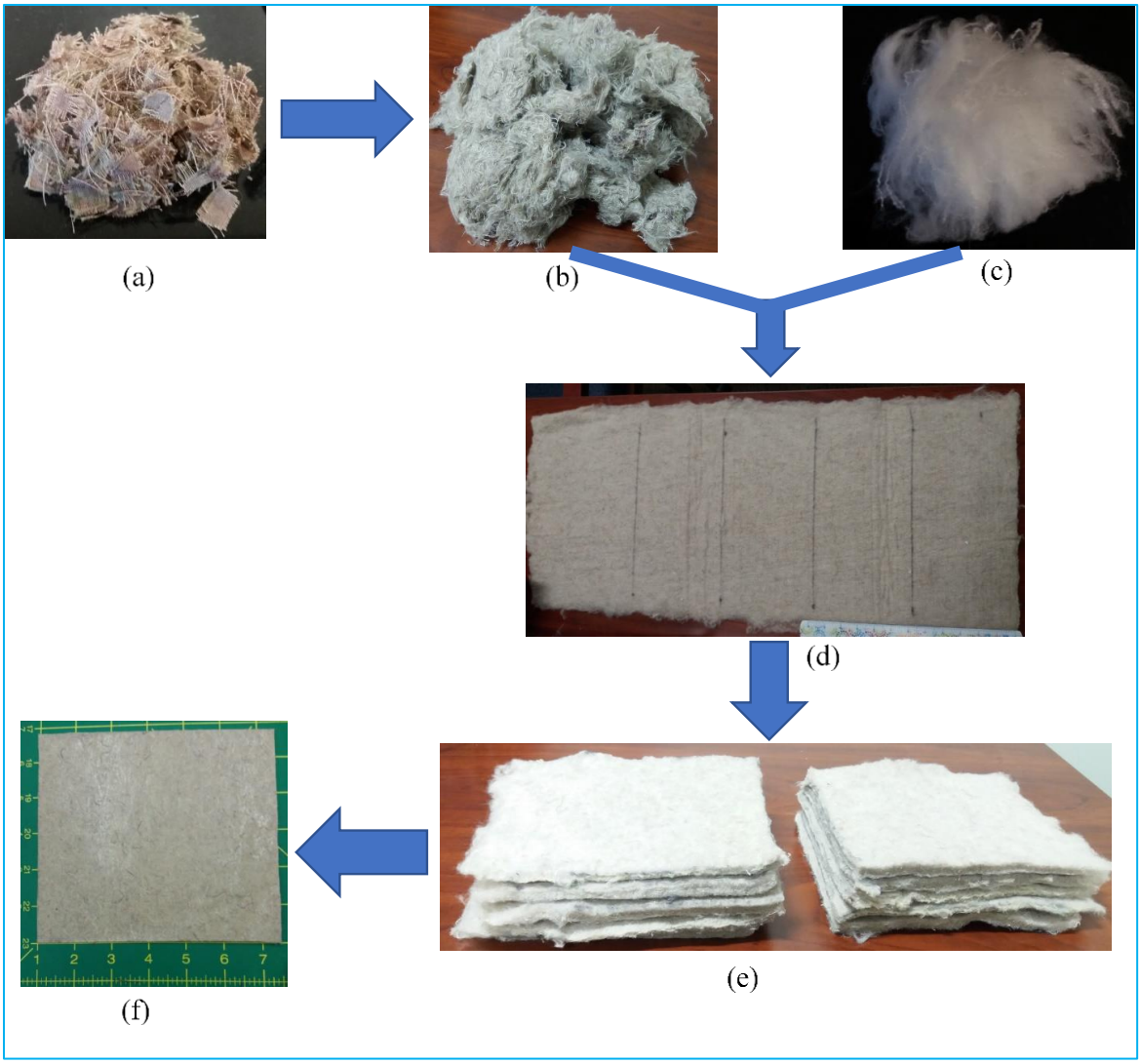

Figure 4.1. Composite sample preparation process. (a) Cut pieces of waste fabric (b) Carded waste fiber (c) PLA fiber (d) Needle-punched sample (e) sample is cut into desired size (f) hot-pressed composite sample.

Table 4.1. Different parameters of composite samples.

Sample no.	Sample Id.	Fiber type	Temperature (°C)	Time (S)
1	S1	42.5% Cotton/42.5% Nylon/15% PLA	150	90
2	S2	42.5% Cotton/42.5% Nylon/15% PLA	180	90
3	S3	42.5% Cotton/42.5% Nylon/15% PLA	144	180
4	S4	42.5% Cotton/42.5% Nylon/15% PLA	165	180
5	S5	42.5% Cotton/42.5% Nylon/15% PLA	165	180
6	S6	42.5% Cotton/42.5% Nylon/15% PLA	186	180
7	S7	42.5% Cotton/42.5% Nylon/15% PLA	150	270
8	S8	42.5% Cotton/42.5% Nylon/15% PLA	180	270
9	S9	42.5% Cotton/42.5% Nylon/15% PLA	165	307
10	S10	42.5% Cotton/42.5% Nylon/15% PLA	165	53
11	S11	42.5% Cotton/42.5% Nylon/15% PLA	165	180
12	S12	42.5% Cotton/42.5% Nylon/15% PLA	165	180
13	S13	42.5% Cotton/42.5% Nylon/15% PLA	165	180

4.2.3. Characterization

A series of testing and experiments were conducted in order to understand the effect of bonding time and temperature on thickness, density, air permeability, and porosity of nonwoven composite panels and subsequently on thermal and acoustic insulation properties. Before characterization, all the samples were conditioned for 48 hours in a standard testing atmosphere, i.e., (20 ± 2)°C temperature and (65 ± 2)% relative humidity.

4.2.3.1. Determination of thickness and density

Thickness of samples was determined in accordance with the standard testing method of ISO 9073-2 [19]. Thickness was measured using the progage thickness tester. Samples were weighed using an electronic balance, and area of the samples was measured. After that, areal density, s (g/m^2) was calculated by dividing weight over area. Bulk density, ρ (kg/m^3), was calculated from areal density and thickness by using the following formula.

$$\rho = \frac{s}{t} \tag{4.1}$$

where, s = areal density in kg/m^2 and t = thickness in m.

Multiple measurements were taken for each sample as per the standard, and average values of thickness, areal density, and bulk density were calculated.

4.2.3.2. Determination of air permeability

Air permeability is the rate of airflow passing perpendicularly through a known area of porous material under a certain air pressure difference [20]. Air permeability was measured using a Textest FX 3300 instrument following the standard method of ASTM D737 [21].

4.2.3.3. Determination of porosity

Porosity is the ratio of the voids to the total volume of materials [22]. Porosity (ϕ) of composite panels was calculated using the following relation [23].

$$\phi = 1 - \frac{\rho}{\rho'} \tag{4.2}$$

where, ρ' is the density of fiber and ρ is the density of composite panels. In this experiment, three different types of fibers, cotton, nylon, and PLA, were used. The average densities of cotton, nylon, and PLA used in the calculation were 1.52 g/cm^3 [24], 1.14 g/cm^3 [25], and 1.25 g/cm^{3,} respectively.

4.2.3.4. Structure of composite panels

An FEI Teneo field emission scanning electron microscope (FE-SEM) was used to analyze the surface of composite panels. Gold coating was done to each sample before capturing SEM pictures.

4.2.3.5. Determination of acoustic properties

Acoustic properties of a material can be determined by measuring several parameters, including transmission coefficient, transmission loss, and absorption coefficient. In this research,

transmission loss was measured using four-microphone impedance tube. The principle of measurement has been discussed in our previously published paper [26]. A data acquisition (DAQ) instrument was attached with four microphones and a computer. BK precision signal generator was connected to a speaker that delivered different frequency to the sample. Fast Fourier Transform (FFT) spectrum analyzer was used to analyze the signal and measure the sound in decibel at different microphone points. International standard ASTM E2611 – 17 [27] was followed as guidance to complete the test procedure. Transmission loss was calculated using equation 4.3.

$$\textit{Transmission loss, } TL = -20\log|\tau| \tag{4.3}$$

4.2.3.6. Determination of thermal properties

Thermal resistance, *R*-value, and heat flux (*Q*) of insulation panels were measured using sweating guarded hotplate following the standard ASTM-F18868-C [28]. According to this standard, thermal resistance was measured by total heat loss where plate & guard temperature was kept at 35℃, and ambient temperature was kept at 25℃. Thermal conductivity (*k*) was measured from heat flux, thickness, and temperature differences using following equation:

$$k = \frac{Q \times t}{\Delta T} \tag{4.4}$$

where *Q* is the heat flow (W/m^2), *t* is the thickness (m) of the specimen, and ΔT is the temperature difference (K) between hot and cold surfaces.

4.2.3.7. Statistical analysis

Statistical analysis (central composite design) was conducted to determine the effect of time and temperature on composite properties and to optimize the desired properties. Central composite design is one of the popular experimental designs of response surface methodology used for developing quadratic model of response variable.

4.3. Results and Discussions

4.3.1. Physical properties

Physical properties of composite samples, including air permeability, thickness, areal density, bulk density, and porosity, are shown in table 4.2. From data in table 4.2, it is obvious that there is a variation of thickness, density, air permeability, and porosity of composite panels with the variation of bonding time and temperature. Sample S10 has the highest thickness of 1.56 mm, which is about 1.5 times thicker than the lowest thickness (1.07 mm) of sample S6. Porosity of the composite panels is high and varies from 0.76 to 0.83. Air permeability and density of composite panels vary from 25.2 to 42.4 cfm and 327.6 to 377.6 kg/m^{3,} respectively, due to variation of bonding time and temperature.

Table 4.2. Properties of tested samples.

Sample	Avg-thickness (mm)	Avg. air permeability (cfm)	GSM (average)	Density sample (kg/m^3)	Porosity avg.
S1	1.53±0.36	36.7±2.5	340.5±6.1	222.7±4.0	0.83
S2	1.32±0.27	29.2±0.1	366.3±0.2	278.4±0.1	0.79
S3	1.43±0.12	37.8±1.2	327.6±0.1	228.6±0.1	0.83
S4	1.28±0.21	39.4±1.2	342.5±0.1	268.3±0.1	0.80
S6	1.07±0.15	39.1±0.2	339.6±0.1	317.4±0.1	0.76
S7	1.43±0.23	27.5±1.2	377.6±0.3	264.9±0.2	0.80
S8	1.16±0.20	25.2±1.1	371.8±0.0	320.5±0.0	0.76
S9	1.10±0.20	41.2±0.0	329.1±0.0	298.0±0.0	0.77
S10	1.56±0.28	33.8±0.1	368.5±0.1	236.5±0.1	0.82
S11	1.37±0.13	42.4±0.3	357.2±0.2	260.3±0.1	0.80
S12	1.27±0.17	30.3±0.0	360.2 ±0.1	282.9±0.1	0.79
S13	1.26±0.09	35.4±3.0	356.7±0.1	284.1±0.0	0.78

Mean value ± SD

4.3.2. Analysis of composite surface

SEM pictures allow us to analyze the morphology of the prepared composite panels. The convolutions of cotton fibers and round shape of PLA and nylon fibers are clearly visible in figure 4.2. It is apparent that the binder fibers have partially melted and fused together during bonding, which results in change in void structure. It is also observed that there are enough void spaces in the structure resulting in high porosity and air permeability.

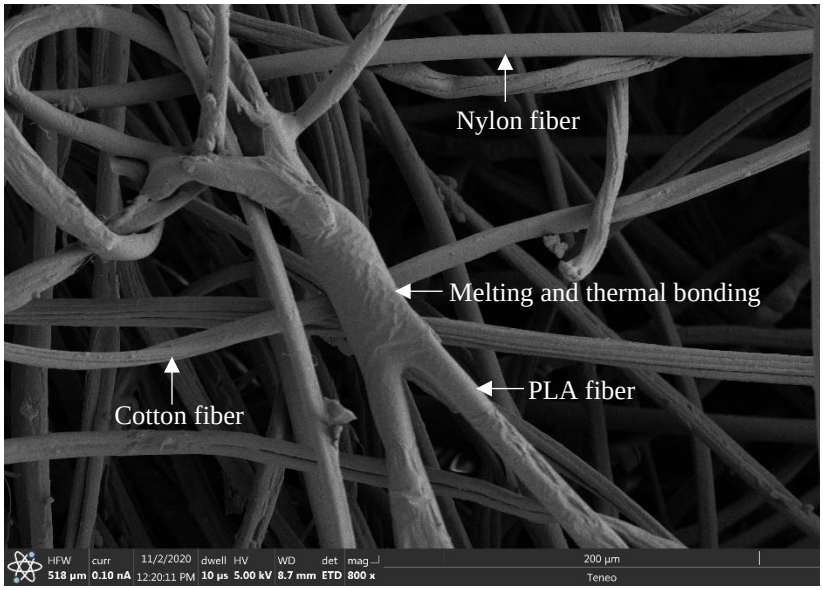

Figure 4.2. SEM image of prepared composite samples.

4.3.3. Effect of bonding time and temperature on thickness, air permeability, porosity, and density

Response surface analysis (central composite design) was conducted in order to understand the effect of bonding time and temperature on thickness (figure 4.3), air permeability (figure 4.4), density (figure 4.5), and porosity (figure 4.6). From the analysis, it can be concluded that composite sample thickness, air permeability, and density change with changes in processing time and temperature. With increase in time and temperature, thickness decreases, whereas density increases. Air permeability initially slightly increases then decreases.

From figure 4.3 to 4.6, green color of the response surface indicates lower thickness, air permeability, density, and porosity region, and red color indicates higher thickness, air permeability, density, and porosity region. The legend at the right upper side of each figure (4.3a to 4.6a) indicates the scale of color variation. A contour plot is shown (2D presentation of response surface) in figures 4.3b to 4.6b. The orange line of contour plot represents the regression line with specific value.

Thickness

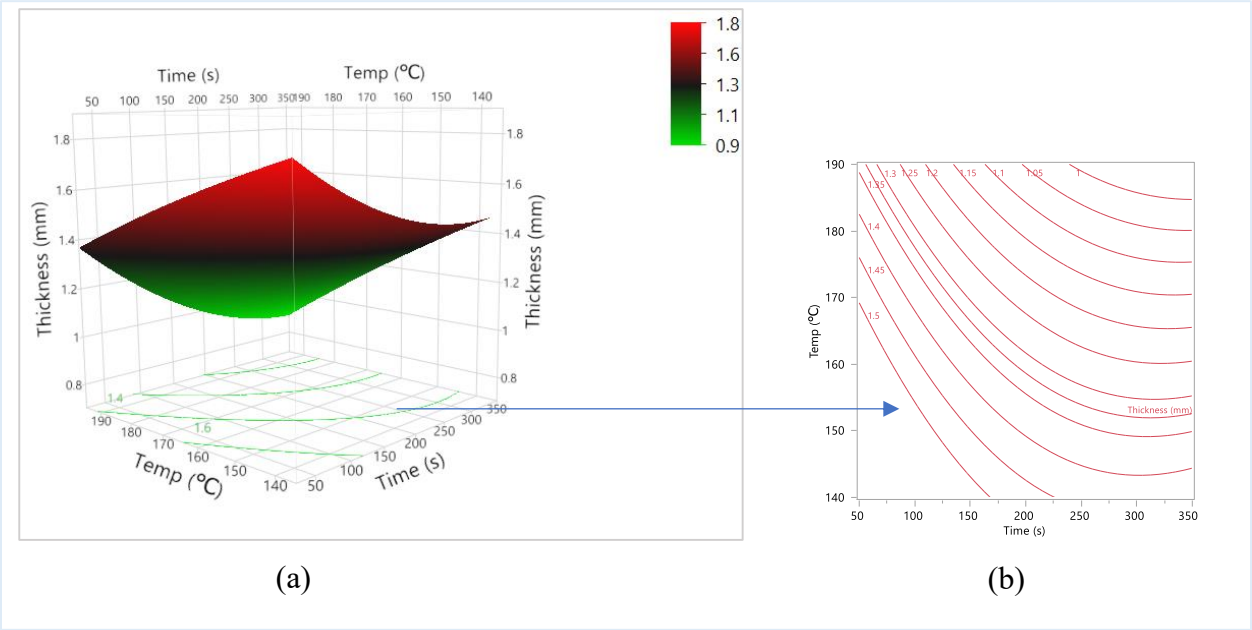

Figure 4.3. (a) Thickness of composites with the variation of time and temperature (b) Contour plot.

Data in figure 4.3 shows the relation of bonding time and temperature with the thickness of composite panel. It can be found that the thickness is high when bonding time and temperature are low and vice versa. With higher bonding time and temperature, higher amount of thermoplastic PLA fibers melt, and the cylindrical PLA fibers turn into a film-like structure upon removal of temperature resulting in reduction of thickness. Wang also found similar effect of shrinkage of fibers during thermal bonding resulting in the reduction in the size of the fabrics [29]. The orange

line of contour plot (figure 4.3b) is helpful in order to select specific bonding time and temperature to obtain composite panels with specific thickness. For example, if we select any point on the line of 1.5 (figure 4.3b) and mark a horizontal and vertical line to temperature and time axis, then we will get specific bonding temperature and time in order to obtain 1.5 mm thick composite panel.

Air permeability

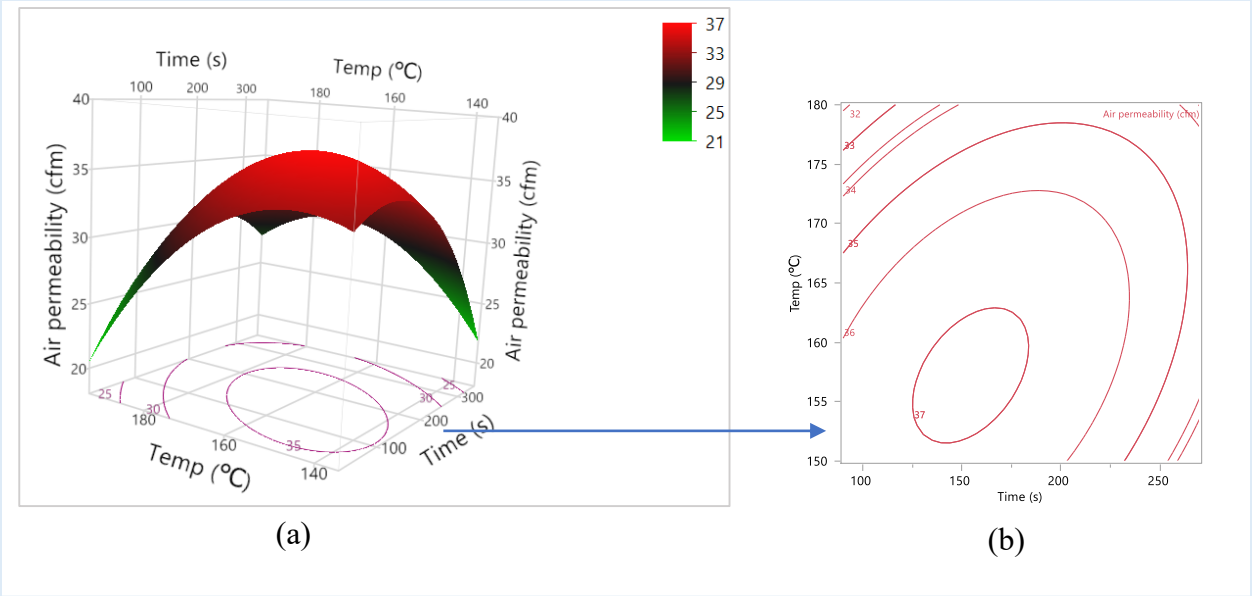

Figure 4.4. (a) Air permeability of composites with the variation of bonding time and temperature (b) Contour plot.

The relation of bonding time and temperature with the air permeability of composite panel are shown in Figure 4.4. With the increase of bonding time and temperature, air permeability initially increases, and then decreases again. At higher temperature and time, more PLA fibers melt and form film-like structure that blocks and reduce the porosity resulting in lower air permeability. Again, at higher temperature and time, thickness of composite panels decreases a lot that reduces the tortuous path of airflow direction result in higher air permeability. Due to these opposite two actions, air permeability initially increases and then decreases with the increase of bonding time and temperature. Higher air permeability (37 cfm) was obtained in the mid-region of 155 to 165°C

and 130 to 18s. The orange line of contour plot (figure 4.4b) is helpful in order to select specific bonding time and temperature to obtain composite panels with specific air permeability. For example, if we select any point on the line of 37 (figure 4.4b) and mark a horizontal and vertical line to temperature and time axis, then we will get specific bonding temperature and time in order to obtain composite panel with the air permeability of 37 cfm.

Density

The relation of bonding time and temperature with the density of composite panel is shown in Figure 4.5. The density is low when bonding time and temperature are low and vice versa. With higher bonding time and temperature, higher amount of thermoplastic PLA fibers melt that reduces thickness of composite panels, but mass per unit area remains same, resulting in higher density of composite panels. The orange line of contour plot (figure 4.5b) is helpful in order to select specific bonding time and temperature to obtain composite panels with specific density. For example, if we select any point on the line of 225 (figure 4.5b) and mark a horizontal and vertical line to temperature and time axis, then we will get specific bonding temperature and time in order to obtain composite panel with 225 kg/m^3 density.

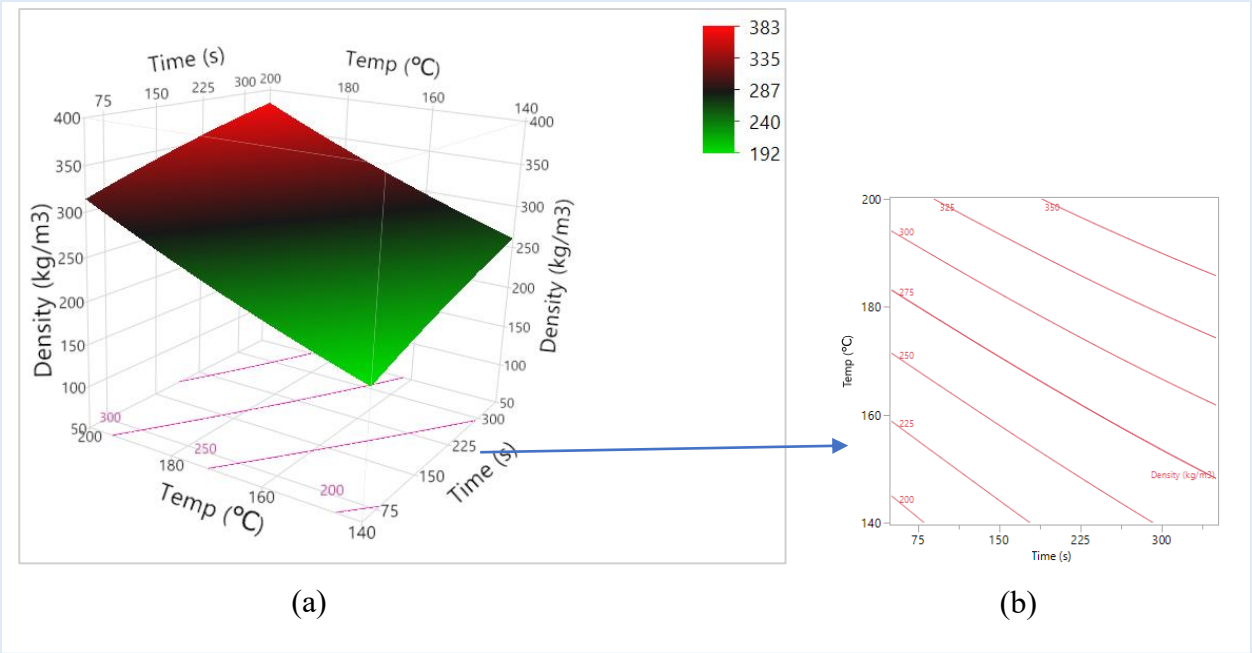

Figure 4.5. (a) Density of composites with the variation of bonding time and temperature (b) Contour plot.

Porosity

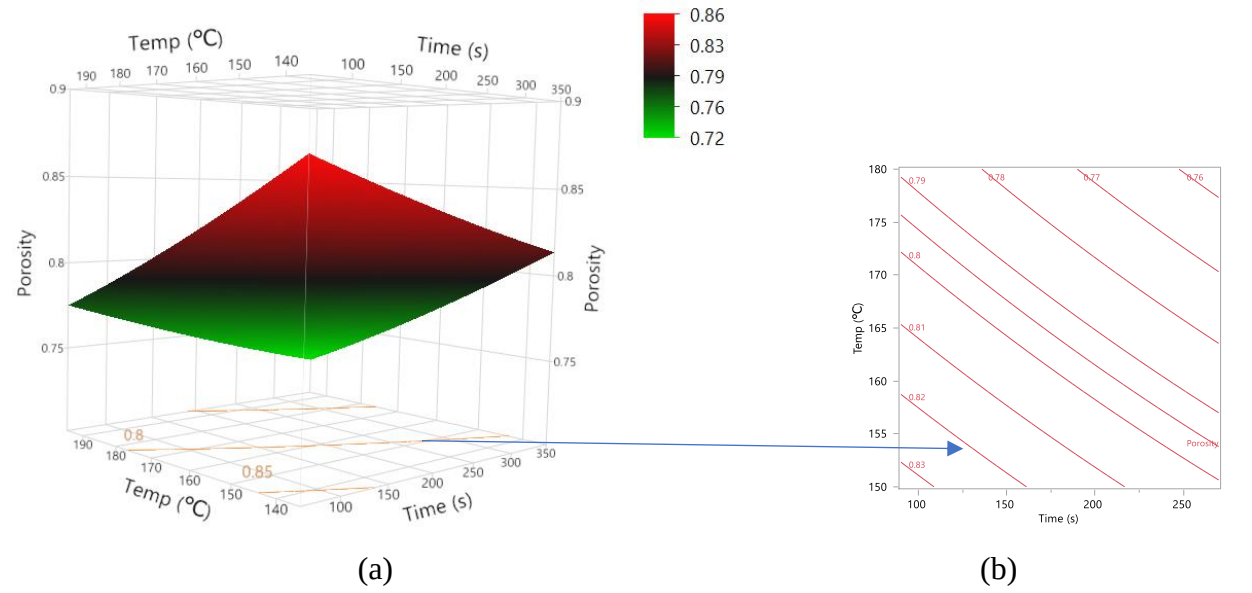

Figure 4.6. (a) Porosity of composites with the variation of bonding time and temperature (b) Contour plot.

The relation of bonding time and temperature with the porosity of composite panels are shown in Figure 4.6. The porosity is high when bonding time and temperature are low and vice versa. With higher bonding time and temperature, more amount of thermoplastic PLA fibers melt that reduce the pore size of composite panels, resulting in the reduction of porosity. Again, reduction of thickness in higher bonding time and temperature leads to further reduction in porosity. The orange line of contour plot (figure 4.6b) is helpful to select specific bonding time and temperature to obtain composite panels with specific porosity. For example, if we select any point on the line of 0.82 (figure 4.6b) and mark a horizontal and vertical line to temperature and time axes, then we will get specific bonding temperature and time in order to obtain composite panel with the porosity of 0.82.

4.3.4. Acoustical measurement

Sound transmission loss of produced composite panels at different frequencies is presented in table 4.3. It was found that all the composite panels have very good acoustic insulation properties with the normalized insulation property being higher than that of the insulation properties of commercially used gypsum boards [30]. Sample S8 shows maximum transmission loss of 18.46 dB at the frequency of 1600 Hz. Average lowest transmission loss (4.21 dB) was obtained from sample S3 which was produced with the bonding time and temperature of 180s and 144 ℃. On the other hand, average highest transmission loss (6.67 dB) was obtained from sample S8 which was produced with the bonding time and temperature of 270s and 180 ℃. Lower bonding time and temperature of S3 lead to lower melting and fusing of PLA filament, lower density, and higher air permeability, resulting in lower sound transmission loss. Although lower bonding time and temperature give higher thickness (higher thickness gives higher transmission loss) but overall

effects of lower density and higher air permeability are more prominent on transmission loss and combinedly give lower sound transmission loss of sample S3.

Table 4.3. Transmission loss in dB of composite panels at different frequencies.

	Transmission loss, *TL* (dB), at different frequencies											
Sample Id.	125 Hz	160 Hz	200 Hz	250 Hz	315 Hz	400 Hz	630 Hz	1000 Hz	1600 Hz	2000 Hz	2500 Hz	Average
S1	0.00	0.75	2.41	4.23	3.12	5.93	4.32	5.74	16.79	13.82	0.00	5.19
S2	0.00	0.00	3.26	5.03	4.10	4.32	5.99	6.51	17.88	15.38	0.33	5.71
S3	0.00	0.00	1.6	3.38	2.26	6.23	3.98	5.03	16.66	6.65	0.48	4.21
S4	0.00	0.00	2.76	4.72	3.66	5.12	5.29	5.57	17.08	9.17	0.98	4.94
S6	0.00	0.00	2.72	4.51	3.16	5,88	5.21	5.96	16.62	8.03	0.00	4.74
S7	0.00	0.10	3.41	5.22	3.81	5.08	6.21	6.64	18.39	8.63	0.00	5.23
S8	0.00	0.00	3.51	5.34	3.88	5.37	6.75	13.66	18.46	15.87	0.50	6.67
S9	0.00	0.00	2.66	4.80	4.81	3.61	4.72	11.05	16.35	8.54	.09	5.15
S10	0.00	0.00	3.17	4.50	2.84	5.40	5.30	11.61	17.48	8.58	0.00	5.35
S11	0.00	0.00	2.29	4.03	2.51	6.38	4.37	11.72	17.72	10.35	0.00	5.40
S13	0.00	0.00	2.72	4.41	2.53	5.56	5.70	11.74	17.92	6.74	0.69	5.27

4.3.5. Effect of bonding time and temperature on sound transmission loss

The relation of bonding time and temperature with the sound transmission loss (TL) of composite panels is shown in Figure 4.7. The sound transmission loss is high when bonding time and temperature are high. Higher bonding time and temperature lead to higher melting and fusing of PLA fibers, and the composite structure results in higher density and lower air permeability. Again, with the increase of density and decrease of air permeability, sound transmission loss increases. Thus, higher transmission loss was obtained at higher bonding time and temperature. Green color of response surface indicates lower TL region, and red color indicates higher TL region (figure 4.7a). The legend at the right upper side of figure 4.7a, indicate TL scale in dB in different color. A contour plot is shown (2D presentation of response surface) in figure 4.7b. The orange line of contour plot (figure 4.7b) is helpful in order to select specific bonding time and temperature to obtain composite panels with specific acoustic property. For example, if we select any point on

the line of 5.8 (figure 4.7b) and mark a horizontal and vertical line to temperature and time axis, in that case, we will get specific bonding temperature and time in order to obtain composite panels with average sound transmission loss of 5.8 dB.

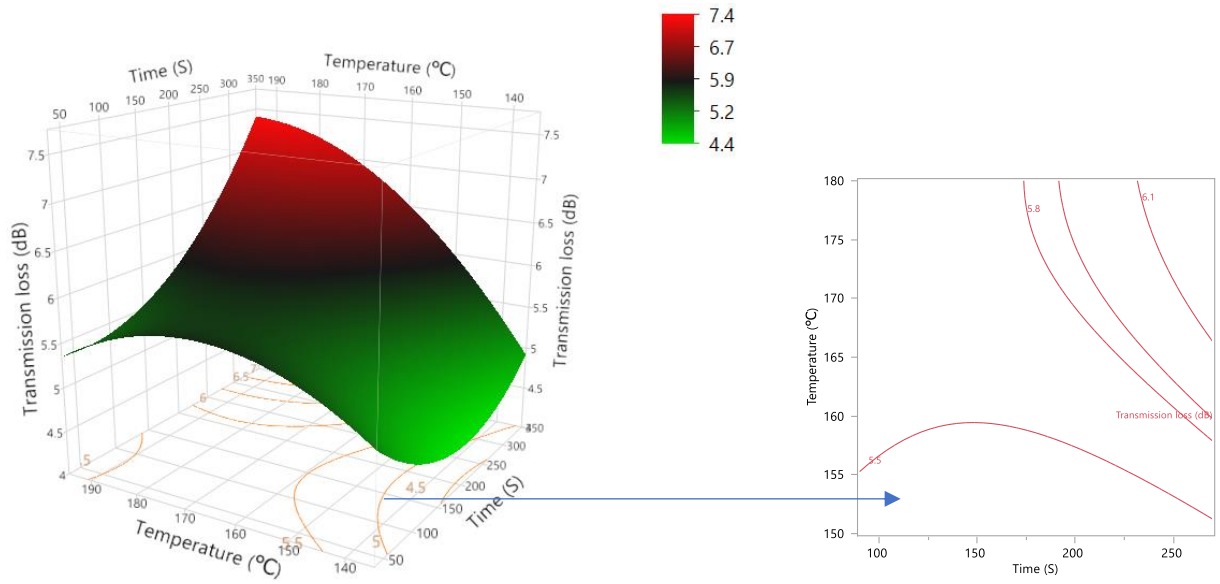

(a) (b)

Figure 4.7. (a) Sound transmission loss in dB with the variation of bonding time and temperature (b) Contour plot.

4.3.6. Thermal measurement

The thermal properties of all composite samples are shown in table 4.4, and figures 4.8 and 4.9. The results clearly show that all of the composite panels have very good thermal insulation properties. According to the literature, a material with a thermal conductivity lower than 0.07 W/mK can be regarded as a good thermal insulator [31]. As all the insulation panels (except samples S8 and S9) have thermal conductivity lower than 0.07 W/mK, materials produced here can be successfully used as thermal insulation in buildings. Among the insulation panels, the lowest thermal conductivity (0.0339 W/mK) was obtained for sample S10, and is very much lower than those of presently available synthetic thermal insulation materials of mineral wool which have thermal conductivity of 0.040–0.045 W/mK [32]. Sample S8 was produced with the bonding time

and temperature of 53s and 165 ℃. On the other hand, sample S8 has the lowest thermal insulation properties (TC of 0.105 W/mK) which was produced with the bonding time and temperature of 270s and 180 ℃. Lower bonding time and temperature of S10 lead to lower melting and fusing of PLA filament, lower density, and higher porosity, which result in lower TC and excellent thermal insulation properties. It is interesting to notice that sample S8 gives the highest acoustic insulation property but the lowest thermal insulation property.

Table 4.4. Thermal properties of produced tested samples.

Sample	Time (S)	Temperature (℃)	Thermal resistance (m^2K/W)	Thermal conductivity (W/mK)
S1	90	150	0.2885 ± 0.0095	0.0602 ±0.0053
S2	90	180	0.2890 ± 0.0152	0.0579 ± 0.0083
S3	180	144	0.3005 ±0.0103	0.0534 ± 0.0046
S4	180	165	0.2990 ±0.0144	0.0527 ±0.0064
S6	180	186	0.3103 ±0.0197	0.0466 ±0.0071
S7	270	150	0.3494 ±0.0170	0.0379 ±0.0038
S8	270	180	0.2385 ±0.0146	0.1053 ±0.0280
S9	307	165	0.2601 ±0.0128	0.0762 ±0.0125
S10	53	165	0.3734 ±0.0209	0.0339 ±0.0037
S11	180	165	0.3093 ±0.0140	0.0493 ±0.0054
S13	180	165	0.2918 ± 0.0329	0.0560 ±0.0180

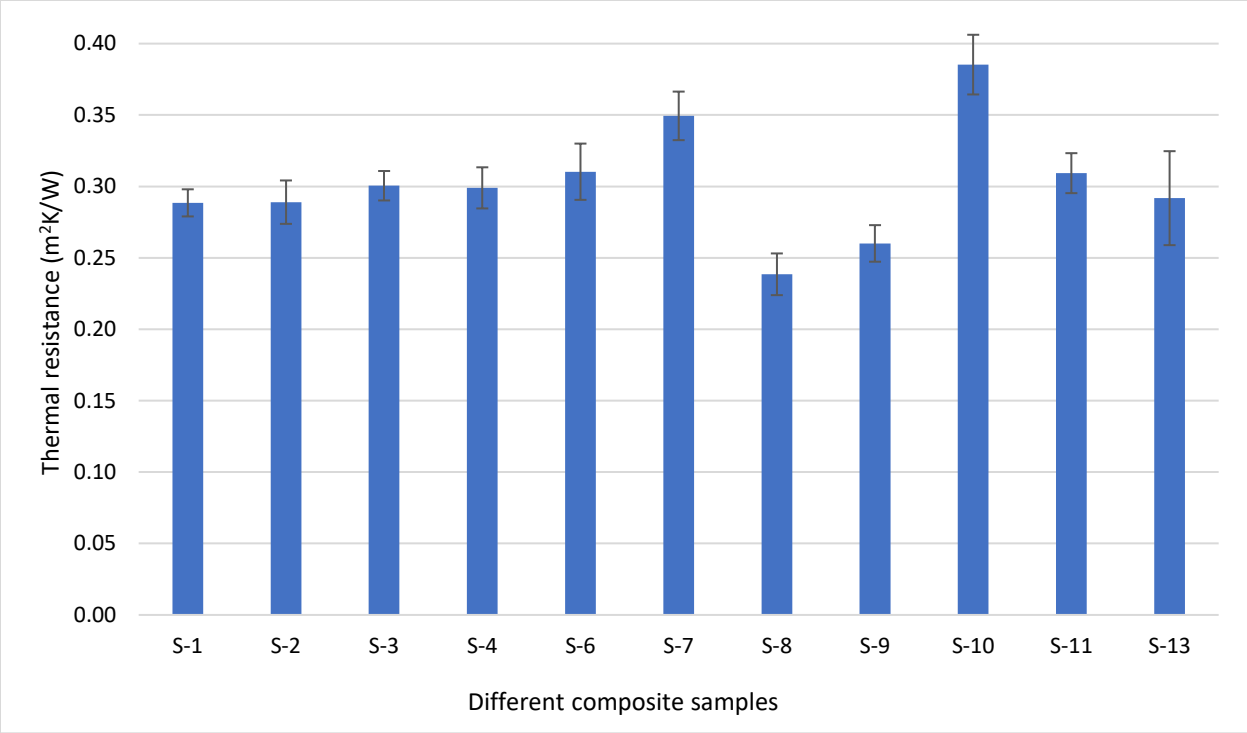

Figure 4.8. Thermal resistance (m^2K/W) of different composite samples.

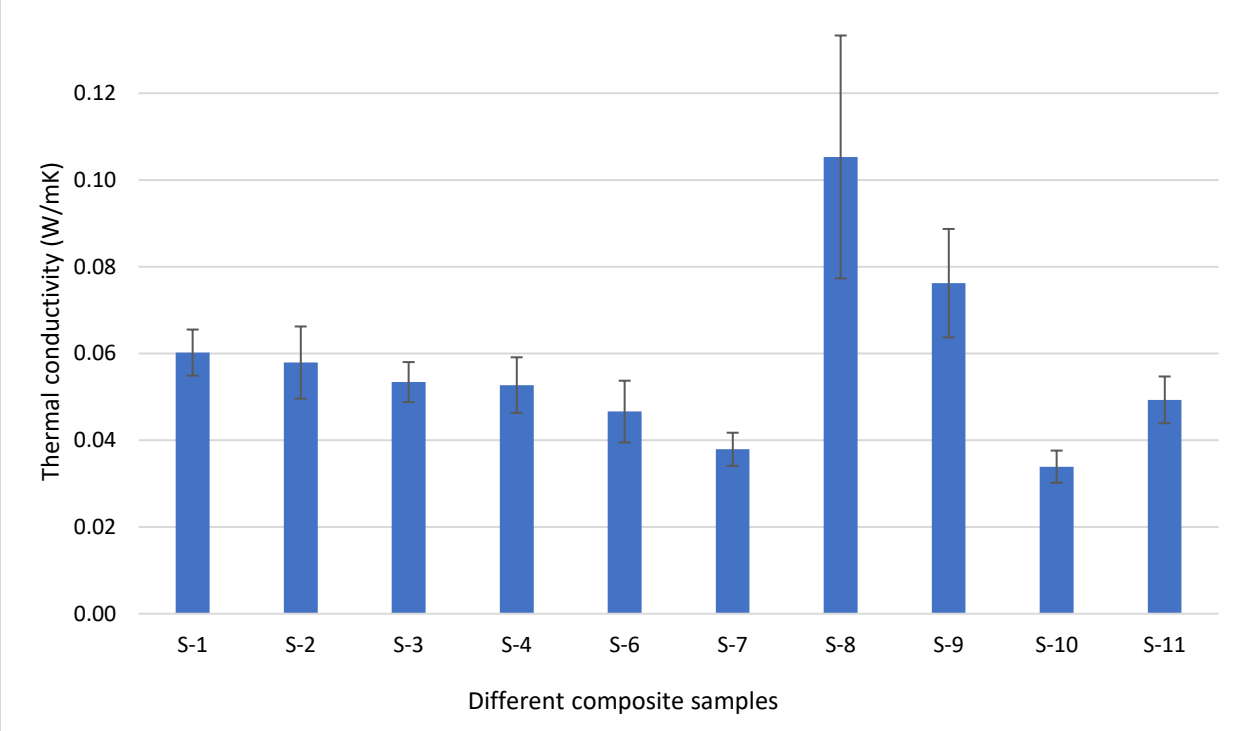

Figure 4.9. Thermal conductivity (W/mK) of different composite samples.

4.3.7. Effect of bonding time and temperature on thermal conductivity

The relation of bonding time and temperature with the thermal conductivity (TC) of composite panels is shown in Figure 4.10. TC is high when bonding time and temperature are high. Higher bonding time and temperature lead to higher melting and fusing of PLA filament and densify the composite structure, resulting in higher density and lower porosity. Again, with the increase of density and decrease of porosity, TC increase. Thus, higher TC was obtained at higher bonding time and temperature. Green color of response surface indicates lower TC region, and red color indicates higher TC region (figure 4.10a). The legend at the right upper side of figure 4.10a, indicate TC scale in W/mK at different color. A contour plot is shown (2D presentation of response surface) in figure 4.10b. The orange line of contour plot (figure 4.10b) can be used to select specific bonding time and temperature to obtain composite panels with specific thermal insulation property. For example, if we select any point on the line of 0.06 (figure 4.10b) and mark a horizontal and vertical line to temperature and time axis, then we will get specific bonding temperature and time in order to obtain composite panel with average TC of 0.06 W/mK.

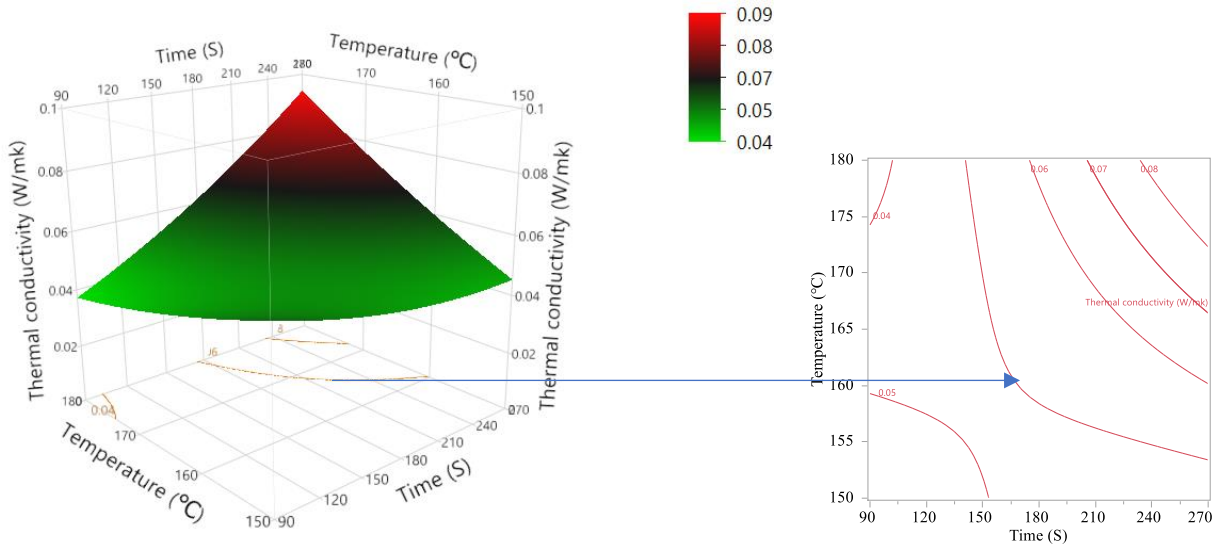

(a) (b)

Figure 4.10. (a) Thermal conductivity of composites with the variation of bonding time and temperature (b) Contour plot.

4.4. Summary

Thermal and acoustic insulation materials were produced from a blend of recycled textiles (cotton and nylon) and thermoplastic PLA fibers. Thirteen different insulation panels were produced by mixing waste textile and PLA fibers (42.5% cotton, 42.5% nylon, and 15% PLA) using nonwoven techniques. The preparation process of all of the composite panels is exactly same except the thermal bonding conditions. The thermal bonding time and temperature of different composites were varied in order to understand the effect of variation of bonding conditions on thickness, density, air permeability, and porosity, and subsequently on thermal and acoustic insulation properties. A response surface methodology (central composite design) was utilized to analyze the data and understand the influence of consolidating time and temperature on the properties of produced composite panels.

Results indicate that bonding time and temperature have a strong influence on the properties of insulation materials. With the increase of bonding time and temperature thickness decreases,

whereas density increases. Air permeability initially slightly increases and then decreases. It is interesting to find that thermal and acoustic insulation properties follow opposite trends. With the increase of bonding time and temperature, acoustic insulation properties increase, but thermal insulation properties decrease. The sample S8 has the highest acoustic insulation property (average TL of 6.67 dB), but it has the lowest thermal insulation property (average TC of 0.1053 W/mK). Thus, in order to use composite panels as both thermal and acoustic insulation materials, optimum bonding time and temperature should be selected (either medium time and temperature showed in table 4.1 (around 180s and 165℃) or lower time-higher temperature or higher time-lower temperature combinations.

Results also indicate that produced insulation materials have very good thermal insulation properties and meet the criteria thermal insulation property (except samples S8 and S9). The lowest thermal conductivity (0.0339 W/mK) was obtained for sample S10, and is very much lower than those of presently available synthetic thermal insulation materials of mineral wool which have thermal conductivity of 0.040–0.045 W/mK. Similarly, all the samples have very good acoustic insulation property, with the normalized insulation property being higher than that of the insulation properties of commercially used gypsum boards.

4.5. References

[1] S. Lukić and P. Jovanić, “Structural analysis of abrasive composite materials with nonwoven textile matrix,” *Mater. Lett.*, vol. 58, no. 3–4, pp. 439–443, 2004, doi: 10.1016/S0167-577X(03)00521-4.

[2] R. Vallabh, P. Banks-Lee, and A.-F. Seyam, “New approach for determining tortuosity in fibrous porous media,” *J. Eng. Fiber. Fabr.*, vol. 5, no. 3, pp. 7–15, 2010, doi: 10.1177/155892501000500302.

[3] E. Çinçik and E. Koç, “An analysis on air permeability of polyester/viscose blended needle-punched nonwovens,” *Text. Res. J.*, vol. 82, no. 5, pp. 430–442, 2012, doi: 10.1177/0040517511414977.

[4] M. Mohammadi, P. Banks-Lee, and P. Ghadimi, “Air permeability of multilayer needle punched nonwoven fabrics: Theoretical method,” *J. Ind. Text.*, vol. 32, no. 1, pp. 45–57, 2002, doi: 10.1106/152808302031065.

[5] M. Mohammadi, P. Banks-Lee, and P. Ghadimi, “Air permeability of multilayer needle punched nonwoven fabrics: Experimental method,” *J. Ind. Text.*, vol. 32, no. 2, pp. 139–150, 2002, doi: 10.1106/152808302031161.

[6] S. Y. Yeo, O. S. Kim, D. Y. Lim, S. W. Byun, and S. H. Jeong, “Effects of processing condition on the filtration performances of nonwovens for bag filter media,” *J. Mater. Sci.*, vol. 40, no. 20, pp. 5393–5398, 2005, doi: 10.1007/s10853-005-4337-x.

[7] A. Rawal, “A cross-plane permeability model for needle-punched nonwoven structures,” *J. Text. Inst.*, vol. 97, no. 6, pp. 527–532, 2006, doi: 10.1533/joti.2005.0219.

[8] A. Rawal and R. Anandjiwala, “Comparative study between needlepunched nonwoven geotextile structures made from flax and polyester fibres,” *Geotext. Geomembranes*, vol. 25, no. 1, pp. 61–65, 2007, doi: 10.1016/j.geotexmem.2006.08.001.

[9] R. D. Anandjiwala and L. Boguslavsky, “Development of needle-punched nonwoven fabrics from flax fibers for air filtration applications,” *Text. Res. J.*, vol. 78, no. 7, pp. 614–624, 2008, doi: 10.1177/0040517507081837.

[10] M. E. Yuksekkaya, M. Tercan, and G. Dogan, “An experimental investigation of nonwoven filter cloth with and without reinforcement of woven fabric,” *J. Text. Inst.*, vol. 101, no. 11, pp. 950–957, 2010, doi: 10.1080/00405000902986133.

[11] S. Debnath, “Thermal resistance and air permeability of jute-polypropylene blended needle-punched nonwoven,” *Indian J. Fibre Text. Res.*, vol. 36, pp. 122–131, 2011.

[12] A. Rawal and S. K. Agrahari, “Pore size characteristics of nonwoven structures under uniaxial tensile loading,” *J. Mater. Sci.*, vol. 46, no. 13, pp. 4487–4493, 2011, doi: 10.1007/s10853-011-5342-x.

[13] S. Ncube, L. Ndlovu, P. Sibanda, and Y. Tusiimire, “Airr permeabilty properties of thermal bonded nonwoven fabrics,” *Mater. Sci. An Indian J.*, vol. 12, no. 7, pp. 263–268, 2015, [Online]. Available: https://www.tsijournals.com/abstract/airr-permeabilty-properties-of-thermal-bonded-nonwoven-fabrics-4882.html.

[14] K. Guittian and Z. Zenghui, “How hot-air bonding production parameters affect bi-component fiber nonwovens,” *International Fiber Journal*, 2020. https://fiberjournal.com/how-hot-air-bonding-production-parameters-affect-bi-component-fiber-nonwovens/ (accessed Jun. 06, 2021).

[15] S. Chand, G. S. Bhat, J. E. Spruiell, and S. Malkan, “Structure and properties of polypropylene fibers during thermal bonding,” *Thermochim. Acta*, vol. 367, pp. 155–160, 2001, doi: 10.1016/S0040-6031(00)00672-9.

[16] S. Chand, G. S. Bhat, J. E. Spruiell, and S. Malkan, “Role of fiber morphology in thermal bonding,” *Int. Nonwovens J.*, vol. OS-11, no. 3, pp. 12–20, 2002, doi: 10.1177/1558925002OS-01100305.

[17] B. S. Gupta and D. K. Smith, “Nonwovens in absorbent materials,” in *Textile Science and Technology*, vol. 13, Elsevier, 2002, pp. 349–388.

[18] R. Jubera, A. Ridruejo, C. González, and J. LLorca, “Mechanical behavior and deformation micromechanisms of polypropylene nonwoven fabrics as a function of temperature and strain rate,” *Mech. Mater.*, vol. 74, pp. 14–25, 2014, doi: 10.1016/j.mechmat.2014.03.007.

[19] “ISO 9073-2,” *Textiles -- Test methods for nonwovens -- Part 2: Determination of thickness*, 1995. https://www.iso.org/standard/16652.html.

[20] A. Majumdar, *Soft computing in textile engineering*. Cambridge: Woodhead Publishing, 2010.

[21] “ASTM D737,” *Standard Test Method for Air Permeability of Textile Fabrics*, 2018. https://www.astm.org/Standards/D737.htm.

[22] N. Mao, “Methods for characterisation of nonwoven structure, property, and performance,” in *Advances in Technical Nonwovens*, G. Kellie, Ed. Cambridge: Woodhead Publishing, 2016, pp. 155–211.

[23] S. Fatima and A. R. Mohanty, “Acoustical and fire-retardant properties of jute composite materials,” *Appl. Acoust.*, vol. 72, no. 2–3, pp. 108–114, 2011.

[24] S. B. Warner, *Fiber science*. Englewood Cliffs, NJ: Prentice-Hall, 1995.

[25] H. Unal, F. Fındık, and A. Mimaroglu, "Mechanical behavior of nylon composites containing talc and kaolin," *J. Appl. Polym. Sci.*, vol. 88, no. 7, pp. 1694–1697, 2003, doi: 10.1002/app.11927.

[26] S. Islam, M. El Messiry, P. P. Sikdar, J. Seylar, and G. Bhat, "Microstructure and performance characteristics of acoustic insulation materials from post-consumer recycled denim fabrics," *J. Ind. Text.*, 2020, doi: doi.org/10.1177/1528083720940746.

[27] "ASTM E2611," *Standard Test Method for Normal Incidence Determination of Porous Material Acoustical Properties Based on the Transfer Matrix Method*, 2017. https://www.astm.org/Standards/E2611.htm.

[28] "ASTM F1868 - 17," *Standard Test Method for Thermal and Evaporative Resistance of Clothing Materials Using a Sweating Hot Plate*, 2017. https://www.astm.org/Standards/F1868.

[29] X. Hou, M. Acar, and V. V Silberschmidt, "2D finite element analysis of thermally bonded nonwoven materials: Continuous and discontinuous models," *Comput. Mater. Sci.*, vol. 46, no. 3, pp. 700–707, 2009, doi: 10.1016/j.commatsci.2009.07.007.

[30] R. Reixach, R. Del Rey, J. Alba, G. Arbat, F. X. Espinach, and P. Mutjé, "Acoustic properties of agroforestry waste orange pruning fibers reinforced polypropylene composites as an alternative to laminated gypsum boards," *Constr. Build. Mater.*, vol. 77, pp. 124–129, 2015.

[31] F. Asdrubali, F. D'Alessandro, and S. Schiavoni, "A review of unconventional sustainable building insulation materials," *Sustain. Mater. Technol.*, vol. 4, pp. 1–17, 2015, doi: 10.1016/j.susmat.2015.05.002.

[32] M. El Wazna, M. El Fatihi, A. El Bouari, and O. Cherkaoui, "Thermo physical characterization of sustainable insulation materials made from textile waste," *J. Build. Eng.*, vol. 12, pp. 196–201, 2017.

CHAPTER 5

Thermal and Acoustic Performance Evaluation of 3D-Printed PLA Materials[3]

[3] Islam, S. and Bhat, G. To be submitted to *International Journal of Heat and Mass Transfer*.

Abstract

Thermal and acoustic insulation properties depend on several structural parameters, including thickness, density, air permeability, and porosity. In order to produce materials with good insulation properties, there should be precise control on these structural parameters during manufacturing process, which is very difficult using conventional fabrication methods. Additive manufacturing or 3D printing technology can be utilized in this case, which has the ability to produce materials with precise and controlled shape and structure. Thus, the goal of this study was to design and produce insulation materials with controlled structure utilizing 3D printing technology using biodegradable PLA filament as the feedstock. The effect of structural parameters on insulation properties was also evaluated as it is assumed that precise structural parameters would show accurate relation compared to nonwoven composites, which are irregular by nature. A comprehensive evaluation was also conducted to check whether this new branch of technology is suitable to produce insulation materials. Testing results revealed that insulation materials produced from 3D printing technology have excellent thermal and acoustic insulation properties. Maximum sound transmission loss of about 48.27 dB was obtained at around 1600 Hz, and the lowest obtained thermal conductivity value was 0.037 W/mK. When compared with commercially available acoustic insulation material (gypsum board) and thermal insulation panel (mineral wool), produced 3D printed samples gave better insulation properties. This indicates that produced insulation materials have very good potential to be used with the concrete walls.

Keywords: 3D printing, PLA filaments, thermal insulation, acoustic insulation

5.1. Introduction

As discussed in chapters 1 and 2, one of the best approaches to reducing energy consumption and minimize the adverse effect of sound pollution is to use effective thermal and acoustic insulation materials in buildings [1]. In general, thermal insulation materials consist of a number of voids that entrap air within the structure [2], [3]. This entrapped air increases the insulation properties of materials as air has very low heat conduction or high thermal resistance. Similarly, with longer path and internal reflection of sound energy within the void structure, the sound energy is converted and dissipated into thermal and viscous heat [4].

Hence in this study, insulation materials were produced by carefully designing air voids within the structure using 3D printing techniques to compare them to the conventional building insulation materials of extruded polystyrene, mineral wool, and others which have adverse environmental effects. The adverse environmental effects of conventional insulation materials are discussed in detail in chapter 2 [1]. PLA filaments are used as it has good insulation property (thermal conductivity of PLA is 0.13 W/mK [5]) and less environmental adverse effects [4] (environmental benefit of PLA fibers are discussed in chapter three). 3D printing technology was used for fabrication as it provides good controllability with precise sizes, shapes, and structures, which have strong influence on insulation properties.

Additive manufacturing or 3D printing is a modern manufacturing method of real and three-dimensional objects using layer by layer or point by point processes [6], [7]. This manufacturing technique allows designers to produce materials with complex geometrical forms, shapes, and dimensions [6], [8]. It also provides opportunities for producing materials with high forming precision and strong controllability [6]. These excellent features of 3D printing provide opportunities for manufacturers to fabricate products efficiently for new application fields beyond

the conventional ones [9]. Nowadays, this technology has been successfully used in a wide variety of fields, including aerospace, medical, automotive, electronics, architecture, fashion, and domestic products [9]. Several researchers also utilized 3D printing techniques to produce porous materials in order to use them in a variety of applications, including water filtration, catalysis, biomedical scaffolds, and lightweight structural elements [10]–[17]. Changfeng et al. fabricated 3D printed PU foam which has similar resilience properties to that of bulk rubber [18]. Gama et al. produced 3D printed cork/polyurethane composite foams for thermal applications with enhanced mechanical properties [19]. However, producing thermal and acoustic insulation materials using 3D printer is still in its initial stage, although it has very good potential as materials with specific pore shape, size, permeability, and overall porosity can be produced using 3D printers. All these parameters strongly influence the thermal and acoustic insulation properties [19]–[23]. The secondary goal of this study was to investigate whether this new branch of 3D printing technology is applicable to produce insulation materials.

Again, producing insulation materials with both good acoustic and thermal insulation properties is difficult by conventional method as they follow opposite trends (chapter 4). In order to get good acoustic insulation, air permeability should be low, whereas, for good thermal insulation, porosity should be higher. This type of complex design can be relatively easily created using 3D printed technology.

Hence, the objectives of this study were to utilize 3D printing technology to design and fabricate insulation materials using PLA filaments. Several different insulation materials with varying density and porosity were produced, keeping the thickness and air permeability same. Then the effect of density and porosity on insulation properties were statistically analyzed to check whether the effect is similar to the effect of waste textiles because in waste textiles, we cannot

control all the factors simultaneously; like if we change density, air permeability will also change. Produced insulation materials were also compared with commercially available insulation materials.

5.2. Materials and Methods

5.2.1. Materials

Thermoplastic PLA filament (brand: Hatchbox) with a density of 1.27 g/cm^3, tensile strength of 46.76 MPa, and compressive strength of 17.92 MPa were obtained from Pomona, CA. The average thermal conductivity of PLA filament is 0.13 W/mK [5].

5.2.2. Methods

5.2.2.1. Design of 3D printed material

Porous structure is designed using Autodesk Tinkercad. Five different samples were designed with varying porosity. Samples are designed only by changing air void within the structure and keeping the rest of the parameters, including air permeability, thickness, length, and width same. The sample design of produced structure is shown in figure 5.1.

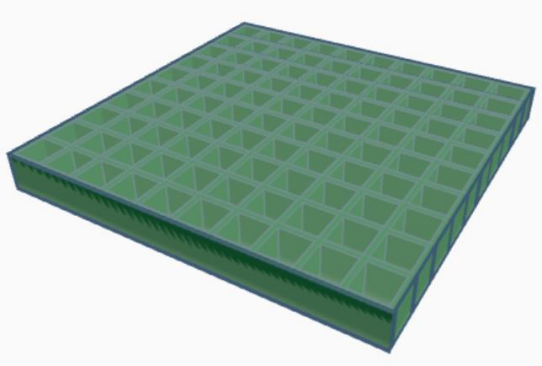

Figure 5.1. Design of 3D structure.

5.2.2.2 Production process

QIDI X-Plus 3D printer (QIDI Technology Co., Ltd., Zhejiang, China) was used to produce samples. At first, all printing parameters, including printing speed, layer width and height, and

infill density, were adjusted and sliced using Qidi print software. Then the sliced program was exported to the printer, and samples were produced using the filament. The printing parameters and produced samples are presented in table 5.1 and figure 5.2.

Table 5.1. 3D printing parameters.

Parameter	Value
Layer height	0.08 mm
Line width	0.3 mm
Infill density	100%
Infill pattern	Lines
Printing temperature	192 ℃
Build plate temperature	50 ℃
Printing speed	30 mm/s

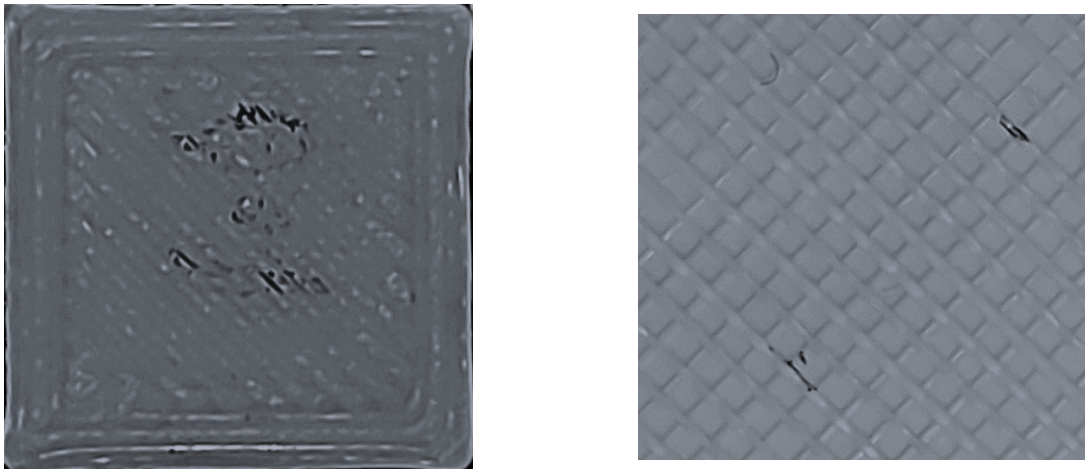

(a) (b)

Figure 5.2. Printed samples. (a) Surface of printed samples (b) Cross-section.

5.2.3. Characterization

A series of testing and experiments were conducted in order to evaluate the insulation performance of 3D-Printable PLA Materials. Before characterization, all the samples were conditioned for 48

hours in a standard testing atmosphere, i.e., (20 ± 2)℃ temperature and (65 ± 2)% relative humidity.

5.2.3.1. Determination of density

All the samples are designed with 4 mm in thickness. After printing, the thickness of samples is tested again to check whether there is any variation in thickness between actual samples and designed samples. After measuring thickness, density was calculated as per the process discussed in section 3.2.3.1 (chapter 3). After that actual and designed density was compared.

5.2.3.2. Determination of porosity

All the samples were designed with specific porosity. After printing, the porosity of samples was tested again to check for any variation in porosity between actual samples and designed samples. Porosity (ϕ) of composite panels was calculated by the following relation [24].

$$\phi = 1 - \frac{\rho}{\rho'} \tag{5.1}$$

where, ρ' is the density of PLA filaments and ρ is the density of porous samples. In this experiment, the average density of used PLA filaments is 1.27 g/cm^3.

5.2.3.3. Determination of average void distance

All the samples are designed with a specific void diameter. After printing, average pore diameter of samples is tested again to check whether there is any variation in pore diameter between actual samples and designed samples.

5.2.3.4. Surface morphology of composite panels

An FEI Teneo field emission scanning electron microscope (FE-SEM) was used to analyze the surface of composite panels. Gold coating was done to each sample before capturing SEM pictures.

5.2.3.5. Determination of thermal properties

Thermal resistance, *R*-value, and heat flux (*Q*) of insulation panels were measured using sweating guarded hotplate following the standard ASTM-F18868-C [25]. According to this standard, thermal resistance was measured by total heat loss where plate & guard temperature was kept at 35℃, and ambient temperature was kept at 25℃. Thermal conductivity (*k*) was measured from heat flux, thickness, and temperature differences using following equation:

$$k = \frac{Q \times t}{\Delta T} \tag{5.2}$$

where *Q* is the heat flow (W/m^2), *t* is the thickness (m) of the specimen, and ΔT is the temperature difference (K) between hot and cold surfaces.

5.2.3.6. Determination of acoustical properties

Acoustic properties of a material can be determined by measuring several parameters, including transmission coefficient, transmission loss, and absorption coefficient. In this research, transmission loss was measured using four-microphone impedance tube. The principle of measurement using an impedance tube has been discussed in our previously published paper [4]. A data acquisition (DAQ) instrument was attached with four microphones and a computer. BK precision signal generator was connected to a speaker that delivered different frequency to the sample. Fast Fourier Transform (FFT) spectrum analyzer was used to analyze the signal and measure the sound in decibel at different microphone points. International standard ASTM E2611 – 17 [26] was followed as guidance to complete the test procedure. Transmission loss was calculated using following equation.

$$\textit{Transmission loss, } TL = -20\log|\tau| \tag{5.3}$$

5.2.3.7. Statistical analysis and modeling of acoustic properties

Statistical analysis of different test results of the samples carried out. A statistical regression model of sound transmission coefficient and transmission loss was carried out using JMP software. Model is helpful to predict sound transmission loss at different frequencies. Comparison of measured and predicted sound transmission loss of composite panels at different frequencies was also carried out (using JMP software) to check whether there is any deviation between predicted value of sound transmission loss with measured value of sound transmission loss. Relation of transmission loss with respect to thickness, areal density, and air permeability are plotted.

A statistical regression model of thermal insulation was also carried out using JMP software. Relation of thermal insulation with respect to thickness, areal density, and air permeability was also plotted.

5.3. Results and Discussions

5.3.1. Physical properties

Physical properties of composite samples, including thickness, density, and porosity, are shown in table 5.2.

Table 5.2. Properties of tested samples.

Sample Id.	Thickness (mm)		Density (kg/m^3)		Porosity, ϕ	
	Designed	Actual	Designed	Actual	Designed	Actual
I-10	4	3.95	367.6	366.5	0.71	0.71
I-20	4	3.96	467.9	459.2	0.63	0.64
I-30	4	3.96	568.2	546.8	0.55	0.57
I-40	4	3.97	668.4	635.7	0.47	0.50
I-50	4	3.97	768.7	721.3	0.40	0.43

From data in table 5.2, it is obvious that the densities of samples ranged from 366.5 kg/m^3 to 721.3 kg/m^3, and porosities are in the range of 0.43 to 0.71. Density of sample I-50 is comparatively higher, and porosity is comparatively lower. As expected, samples designed with higher voids have lower density but higher porosity. There are some differences between actual printed samples and designed samples. The actual printed samples' height and density are a little bit lower than the designed one, whereas porosity is a little bit higher. The lower density and higher porosity may be due to the shape of the printed layer. The printed layers' shape is not completely rectangular; a little bit curved at the edge (figure 5.3) resulting in lower density and higher porosity. This is likely due to the flow of the material between deposition and cooling as the part is being built.

5.3.2. Analysis of composite surface

SEM pictures allow us to analyze the surface morphology of the prepared samples. From figure 5.3, it is clearly visible that the printed layer is not completely rectangular; instead, it is close to a cylindrical shape resulting in lower density and higher porosity. The surface of the layer is not completely uniform. A slight descends occurred all over the surface, which may result in lower height (3.95 mm) of printed samples. Average printed layer thickness is 0.32 mm, which is a little bit higher than the designed layer thickness of 0.3 mm.

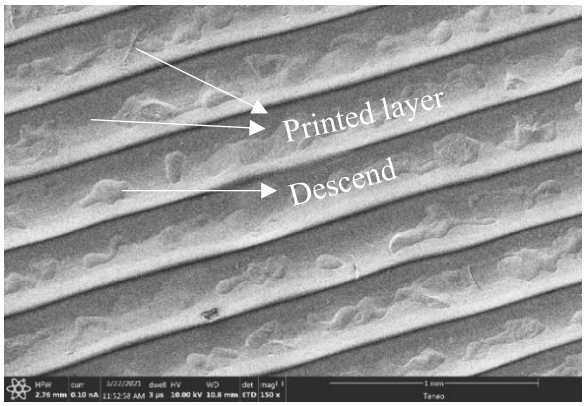

Figure 5.3. SEM image of printed sample.

5.3.3. Pore size

The pore size and volume are important parameters as they have influence on functional performance of insulation materials, including porosity and thermal insulation. Experimental data revealed that pore size of I-10, I-20, I-30, I-40, and I-50 are (2.71 ± 0.12) mm, (1.93 ± 0.04) mm, (1.21 ± 0.07) mm, (0.87 ± 0.08), and (0.52 ± 0.08) respectively.

5.3.4. Thermal measurement

The thermal insulation properties of printed PLA samples are shown in table 5.3. The thermal conductivity of printed samples ranges from 0.037 W/mK to 0.07 W/mK, which is much lower than that of the presently available building insulation materials. According to the literature, a material with a thermal conductivity value lower than 0.07 W/mK can be regarded as a good thermal insulator [27]. As all printed samples have thermal conductivity lower than 0.07 W/mK, thus, it can be said that the produced 3D printed samples have very good potential to be used as building insulation materials.

Table 5.3. Thermal insulation properties of printed samples.

Sample Id.	Thermal resistance (m^2K/W)	Heat flow (W/m^2)	Thermal conductivity (W/mK)
I-10	0.216	46.296	0.037
I-20	0.195	51.282	0.041
I-30	0.152	65.920	0.052
I-40	0.128	78.125	0.062
I-50	0.114	88.106	0.070

5.3.5. Effect of density and porosity on thermal conductivity

A statistical regression analysis (locally weighted scatterplot smoothing (figure 5.4) and quadratic fit line (figure 5.5)) was conducted in order to understand the influence of density and porosity on

thermal conductivity (TC). Similar to insulation materials from waste textiles, density and porosity have profound effect on thermal conductivity of 3D printed insulation materials. Thermal conductivity increases with increase in density. On the other hand, porosity is inversely related to thermal conductivity, i.e., with the increase in porosity, thermal conductivity decreases. An increase in porosity means more amount of air void. As the thermal conductivity of air (0.025 W/mK [28]), which is much lesser than the thermal conductivity of PLA filaments (0.13 W/mK [5]), higher porosity or air void structure leads to decrease in thermal conductivity.

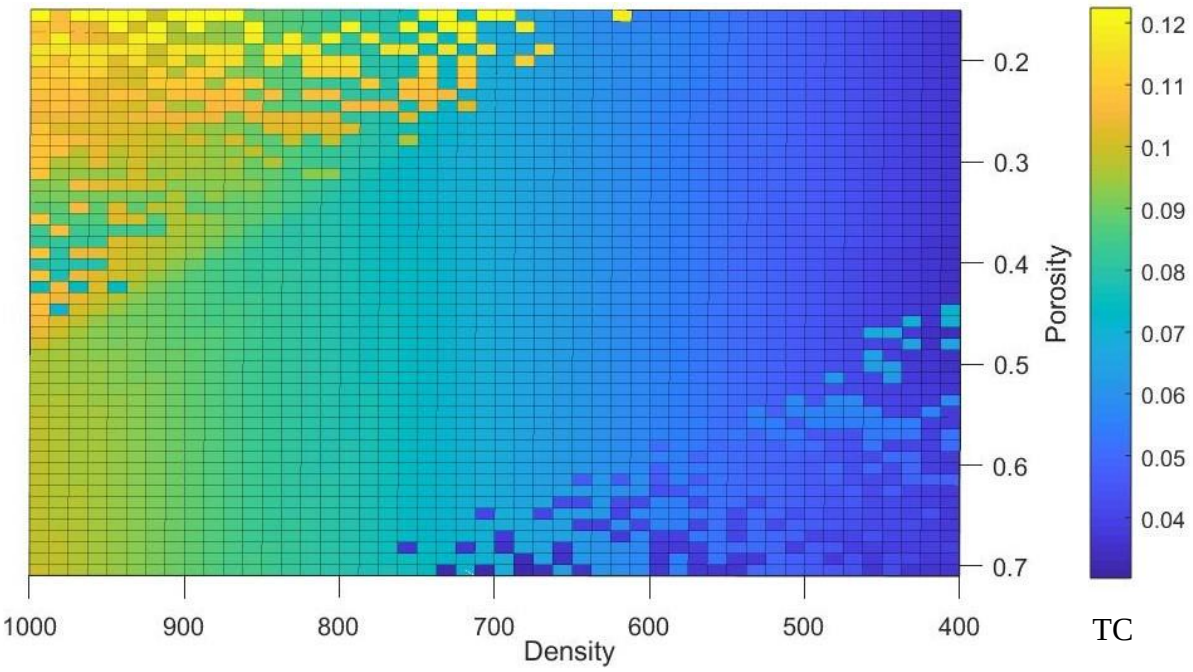

Figure 5.4. Locally weighted scatterplot smoothing of TC. Here x and y-axis denote density and porosity. Color represents TC. A legend of TC is shown on the right side.

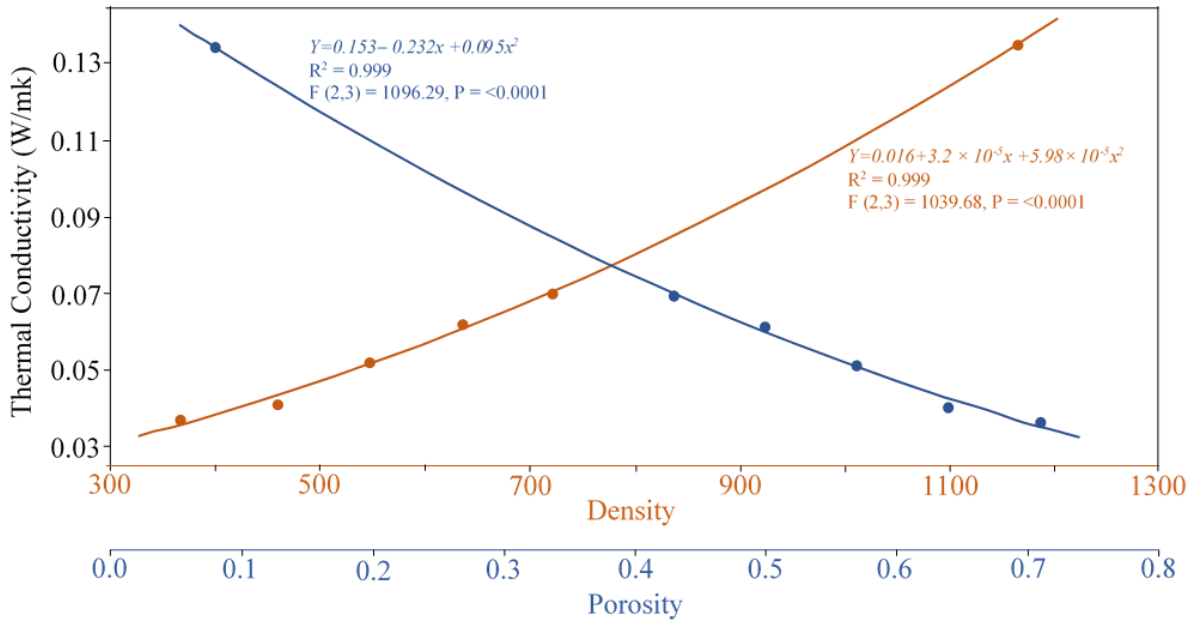

Figure 5.5. Quadratic fit line of TC. X-axes represent density & porosity, and y-axis represents thermal conductivity. Orange color is for density curve, and blue color is for porosity curve.

5.3.6. Comparison with commercially available thermal insulation materials

Some of the commonly used thermal insulation materials for buildings are Polyurethane foam, Glass wool, Stone wool, EPS, and XPS. A comparison was made among these insulation materials with produced 3D printed insulation materials (table 5.4). It was found that the thermal conductivity of samples I-10 and I-20 are very much comparable to the TC of those commercial materials. Further reduction in thermal conductivity is possible by increasing the porosity and careful architecture of pore shape. This indicates that the PLA (or any other suitable) 3D printed materials have great potential to be used as thermal insulation materials in building.

Table 5.4. Comparison of thermal conductivity of printed samples with commercially available insulation panels.

Materials	Density	Thermal conductivity (W/mK)	Relative thermal conductivity to air (0.025 ~ 1	Ref.
I-10	366.46	0.037	1.48	--
I-20	459.22	0.041	1.64	--
I-30	546.75	0.052	2.08	--
I-40	635.70	0.062	2.48	--
I-50	721.26	0.070	2.80	--
Polyurethane foam	30-80	0.02-0.027	0.8-1.08	[29]
Glass wool	92.5	0.040	1.6	[30]
Stone wool	30-180	0.033-0.045	1.32-1.8	[31]
Expanded polystyrene (EPS)	16-35	0.037-0.038	1.48-1.52	[29]
Extruded polystyrene (XPS)	26-45	0.030-0.032	1.2-1.28	[29]

5.3.7. Acoustical measurement

Transmission loss of sound while passing through the produced printed samples at different frequencies is presented in table 5.5.

Table 5.5. Transmission loss in dB of four composite panels at different frequencies.

	Transmission loss, *TL* (dB), at different frequencies											
Sample Id.	125 Hz	160 Hz	200 Hz	250 Hz	500 Hz	630 Hz	1000 Hz	1250 Hz	1600 Hz	2000 Hz	2500 Hz	Average
I-10	7.73	9.47	17.67	25.46	14.81	22.20	31.15	27.23	42.28	26.97	0.83	20.53
I-20	7.02	17.31	27.91	25.34	21.63	23.71	31.49	29.98	48.37	25.36	0.00	23.47
I-30	14.21	23.00	29.91	22.48	23.46	23.99	33.21	31.67	48.27	24.98	6.02	25.56
I-40	15.80	23.71	28.39	42.55	24.03	28.63	35.40	33.83	42.25	30.42	0.00	27.73
I-50	13.65	23.00	28.95	34.04	26.72	28.17	35.42	33.78	42.28	28.01	13.98	28.00

Transmission loss of sound produced from 3D printed samples shows similar trends to the TL of nonwoven composites from waste textiles. Transmission loss is low at low and high frequencies, and transmission loss is very high at the medium frequency range from 1000 to 2000 Hz. Sample I-5 exhibited comparatively higher transmission loss, whereas sample I-1 exhibited comparatively lower transmission loss. This is due to the difference in density as other two parameters, thickness and air permeability, are kept exactly same for all printed samples. A regression model of transmission loss (figure 5.6) was developed that may be helpful in predicting transmission loss at different frequencies.

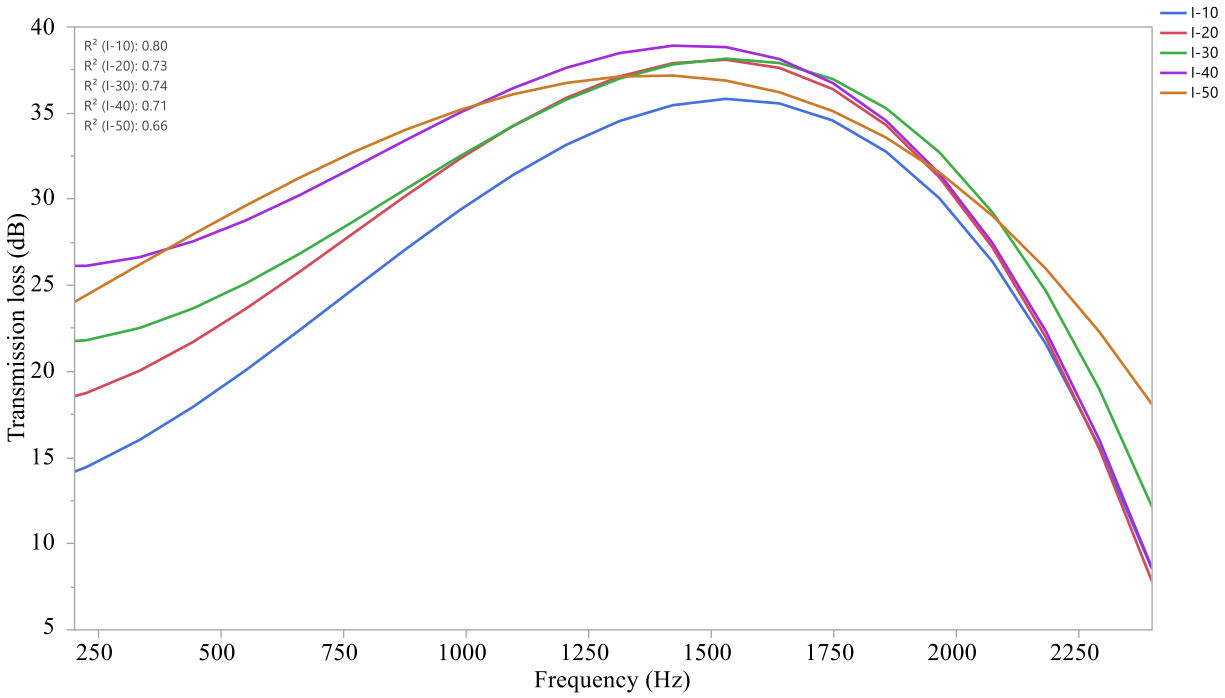

Figure 5.6. Statistical model of sound transmission loss (dB) of printed samples at different frequencies.

Model was also compared with the experimental data of printed samples (figure 5.7). It was observed that the experimental data of sound transmission loss is almost similar to the predicted value. There are some deviations at the lower frequency, but the deviation is very small.

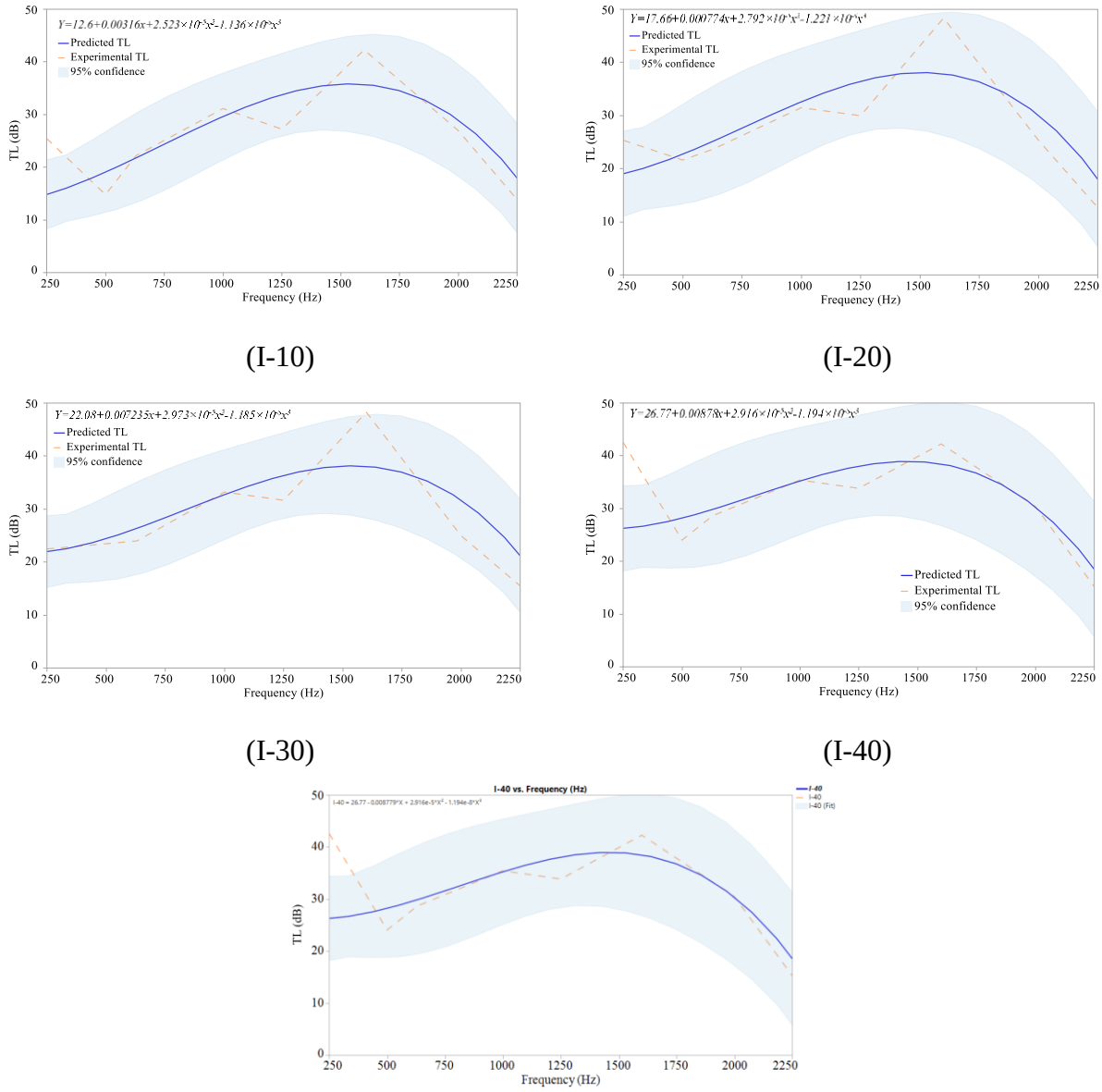

Figure 5.7. Comparison of experimental and predicted sound transmission loss (*TL*) in dB of printed samples at different frequencies.

Several other researchers also observed similar trends of lower acoustic insulation properties for porous materials at low frequencies and higher acoustic insulation properties at medium frequency range [32]. When sound waves enter into porous materials, air molecules within the pores vibrate that transform sound energy into thermal and viscous heat [33], [34]. At low frequencies, this energy is dissipated by the isothermal process (limited amount), but at high-

frequency range, energy is lost by the adiabatic process [35]. As a result, a low amount of sound is absorbed in low-frequency range, but absorption is higher at higher frequencies (resulting in low TL at low frequencies). That's why porous materials show good acoustic insulation properties at medium frequency range. On the other hand, energy of waves decreases with the increases of frequency. At very high frequency, sound energy is not strong enough to vibrate the air molecules. Therefore, transformation of sound energy to thermal and viscous heat is less and as a result transmission loss of sound is also less.

5.3.8. Effect of density and porosity on sound transmission loss

Effect of density and porosity on sound transmission loss in 3D printed samples were investigated using statistical regression analysis (locally weighted scatterplot smoothing (figure 5.8) and quadratic fit line (figure 5.9)). Similar to insulation materials from waste textiles, density and porosity have profound effect on transmission loss of 3D samples. It was observed that sound transmission loss increases with the increase of density and decrease of porosity. With the increase of porosity and decrease of density, less internal reflection of sound energy occurs within the porous structure, and as a result, less sound energy is converted and dissipated into thermal and viscous heat. That's why less transmission loss occurred. In this study, sample I-50 has comparatively low porosity and high density, thereby higher sound transmission loss (28 dB).

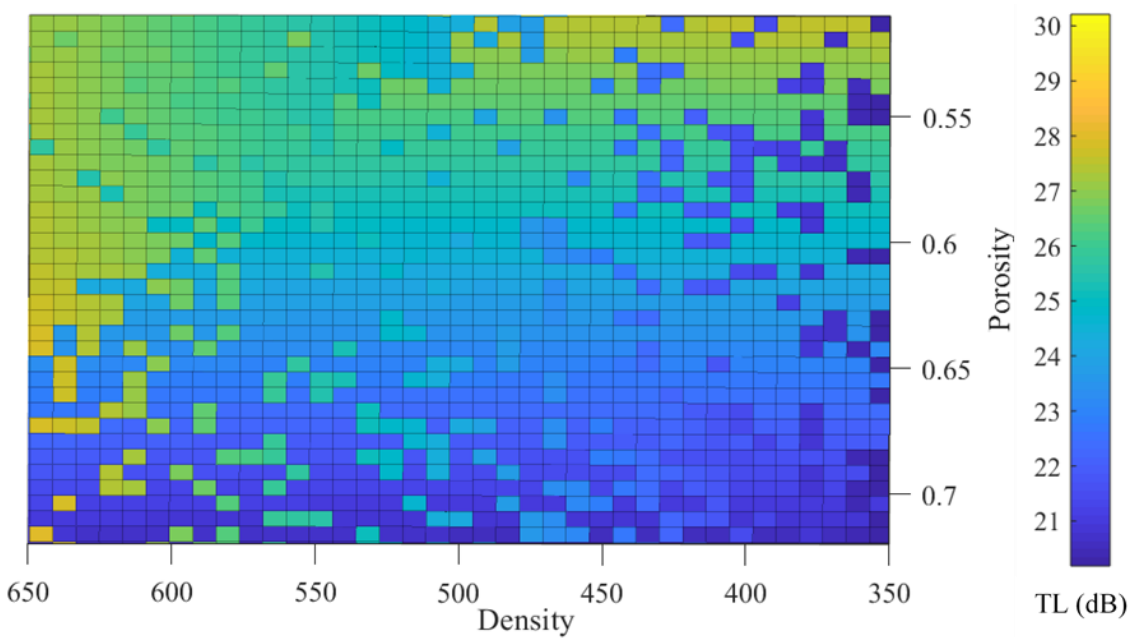

Figure 5.8. Locally weighted scatterplot smoothing of transmission (TL). Here x and y-axis denote density and porosity. Color represents TL value. A legend of TL is shown on the right side.

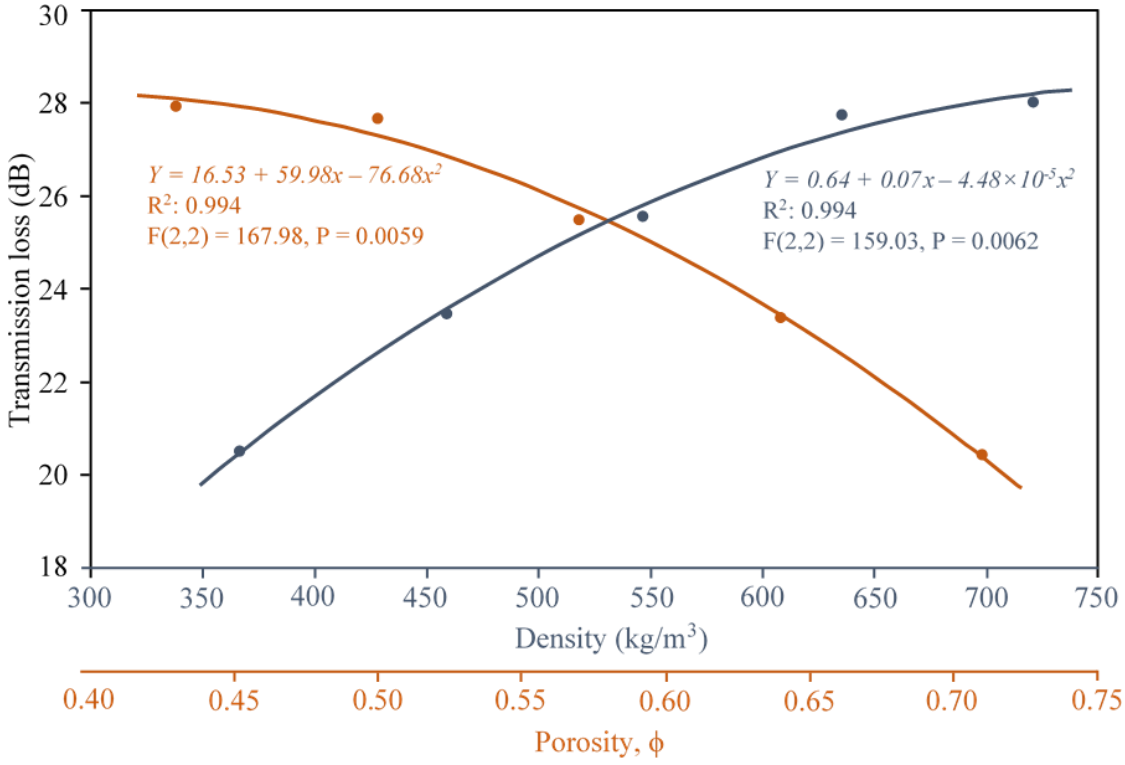

Figure 5.9. Quadratic fit line of TL. X-axes represent density & porosity, and y-axis represents transmission loss. Blue color is for density curve, and orange color is for porosity curve.

5.3.9. Comparison with commercially available acoustic insulation materials

Acoustic insulation properties of produced 3D printed insulation materials was compared with the insulation properties of commercially used gypsum board (table 5.6). The sound transmission loss of 15 mm thick gypsum board is 26.3 dB [32]. Thus, the normalized sound transmission loss of gypsum board per mm is 1.76 dB. The normalized sound transmission loss of printed samples I-10, I-20, I-30, I-40, and I-50 is higher than the normalized value of gypsum board (assuming the normalization holds good) by +295.5%, +336.9%, +367.1%, +397.2%, and +400.5%, respectively. This indicates that 3D printed samples have great potential to be used as acoustic insulating materials.

Table 5.6**.** Comparison of sound transmission loss with gypsum board.

Sample	Thickness (mm)	TL (dB)	Normalized TL (dB) per mm	Comparison with respect to gypsum
I-10	3.95	20.53	5.20	+295.5%
I-20	3.96	23.47	5.93	+336.9%
I-30	3.96	25.56	6.46	+367.1%
I-40	3.97	27.73	6.99	+397.2%
I-50	3.97	28.00	7.05	+400.5%
Gypsum	15.00	26.3	1.76	0.00%

5.4. Summary

In this study, PLA filaments have been used to develop insulation materials by 3D printing technology, which gives more precise control for design and development of advanced insulation materials. Tested results showed that 3D printed samples have very good insulation properties, The lowest obtained thermal conductivity is 0.037 W/mK for porosity of 0.71 and density of 366.46 kg/m^3 which is significantly lower than those of the commonly used thermal insulation materials, glass wool (0.04 W/mK). The highest obtained sound transmission loss is 28.0 dB

(average value from 125Hz to 2500 Hz) for porosity 0.43 and density 721.26 kg/m^3 which is significantly higher than the TL of gypsum board. This indicates the potential for using 3D printed PLA as building insulation materials and as a substitute for conventional insulation materials. It also has potential to replace the tiles or paints of building walls. However, there are some limitations of using PLA as thermal insulation materials as the melting point of PLA is relatively low. High-temperature insulation is not suitable for PLA, unless it is modified, or other alternate materials are used.

Investigation was also done to understand the microstructure of printed samples and the effect of density and porosity on insulation properties of printed samples. A detailed investigation was also conducted to understand the effect of structural parameters including thickness, density, air permeability, and porosity on the insulation properties nonwoven composite produced from waste textiles in chapter three. But the problem of nonwoven composite was that we could not control all the parameters simultaneously, like if we change density or thickness then air permeability will also change. Therefore, in 3D printed samples we have more ability to control, and allow us to produce printed samples by keeping same thickness and air permeability and changing density and porosity. Tested results in printed samples showed similar effect of structural parameters on insulation properties that we had observed in nonwoven composites, i.e., with the increase of density and decrease of porosity, acoustic insulation property increases but thermal insulation property decreases.

5.5. References

[1] S. Islam and G. Bhat, "Environmentally-friendly thermal and acoustic insulation materials from recycled textiles," *J. Environ. Manage.*, vol. 251, p. 109536, 2019.

[2] N. Narayanan and K. Ramamurthy, "Structure and properties of aerated concrete: a review," *Cem. Concr. Compos.*, vol. 22, no. 5, pp. 321–329, 2000, doi: 10.1016/S0958-9465(00)00016-0.

[3] A. M. Neville, *Properties of concrete*, vol. 4. Harlow, England: Pearson Education Limited, 1995.

[4] S. Islam, M. El Messiry, P. P. Sikdar, J. Seylar, and G. Bhat, "Microstructure and performance characteristics of acoustic insulation materials from post-consumer recycled denim fabrics," *J. Ind. Text.*, 2020, doi: doi.org/10.1177/1528083720940746.

[5] P. Keane, "Thermally Conductive Polymer Materials for 3D Printing," 2020. https://3dprinting.com/3d-printing-use-cases/thermally-conductive-polymer-materials/#:~:text=PLA has a thermal conductivity of about 0.13,%28m%2AK%29%2C depending on the alloy and other factors.

[6] X.-R. Li *et al.*, "Analysis of Morphology and Electrical Insulation of 3D Printing Parts," in *2018 IEEE International Conference on High Voltage Engineering and Application (ICHVE)*, 2018, pp. 1–4.

[7] B. Grabowska and J. Kasperski, "The Thermal Conductivity of 3D Printed Plastic Insulation Materials—The Effect of Optimizing the Regular Structure of Closures," *Materials (Basel).*, vol. 13, no. 19, pp. 1–15, 2020, doi: 10.3390/ma13194400.

[8] N. V Gama, A. Ferreira, and A. Barros-Timmons, "Polyurethane foams: Past, present, and future," *Materials (Basel).*, vol. 11, no. 10, pp. 1–35, 2018, doi: 10.3390/ma11101841.

[9] R. Noorani, *3D printing: technology, applications, and selection*. Boca Raton, FL: CRC Press, 2017.

[10] A. Vyatskikh, A. Kudo, S. Delalande, and J. R. Greer, "Additive manufacturing of polymer-derived titania for one-step solar water purification," *Mater. Today Commun.*, vol. 15, pp. 288–293, 2018, doi: 10.1016/j.mtcomm.2018.02.010.

[11] Y. Chen, H. Yao, and L. Wang, "Acoustic band gaps of three-dimensional periodic polymer cellular solids with cubic symmetry," *J. Appl. Phys.*, vol. 114, no. 4, pp. 43521(1–8), 2013, doi: 10.1063/1.4817168.

[12] Y. Chen, F. Qian, L. Zuo, F. Scarpa, and L. Wang, "Broadband and multiband vibration mitigation in lattice metamaterials with sinusoidally-shaped ligaments," *Extrem. Mech. Lett.*, vol. 17, pp. 24–32, 2017, doi: 10.1016/j.eml.2017.09.012.

[13] M. L. Lifson, M.-W. Kim, J. R. Greer, and B.-J. Kim, “Enabling simultaneous extreme ultra low-k in stiff, resilient, and thermally stable nano-architected materials,” *Nano Lett.*, vol. 17, no. 12, pp. 7737–7743, 2017, doi: 10.1021/acs.nanolett.7b03941.

[14] C. Minas, D. Carnelli, E. Tervoort, and A. R. Studart, “3D printing of emulsions and foams into hierarchical porous ceramics,” *Adv. Mater.*, vol. 28, no. 45, pp. 9993–9999, 2016, doi: 10.1002/adma.201603390.

[15] B. G. Compton and J. A. Lewis, “3D-printing of lightweight cellular composites,” *Adv. Mater.*, vol. 26, no. 34, pp. 5930–5935, 2014, doi: 10.1002/adma.201401804.

[16] A. K. Singh, B. Patil, N. Hoffmann, B. Saltonstall, M. Doddamani, and N. Gupta, “Additive manufacturing of syntactic foams: part 1: development, properties, and recycling potential of filaments,” *JOM*, vol. 70, no. 3, pp. 303–309, 2018, doi: 10.1007/s11837-017-2734-7.

[17] A. K. Singh, B. Saltonstall, B. Patil, N. Hoffmann, M. Doddamani, and N. Gupta, “Additive manufacturing of syntactic foams: Part 2: Specimen printing and mechanical property characterization,” *JOM*, vol. 70, no. 3, pp. 310–314, 2018, doi: 10.1007/s11837-017-2731-x.

[18] C. Ge, L. Priyadarshini, D. Cormier, L. Pan, and J. Tuber, “A preliminary study of cushion properties of a 3D printed thermoplastic polyurethane Kelvin foam,” *Packag. Technol. Sci.*, vol. 31, no. 5, pp. 361–368, 2018, doi: 10.1002/pts.2330.

[19] N. Gama, A. Ferreira, and A. Barros-Timmons, “3D printed cork/polyurethane composite foams,” *Mater. Des.*, vol. 179, pp. 1–9, 2019, doi: 10.1016/j.matdes.2019.107905.

[20] E. Gallucci, K. Scrivener, A. Groso, M. Stampanoni, and G. Margaritondo, “3D experimental investigation of the microstructure of cement pastes using synchrotron X-ray microtomography (μCT),” *Cem. Concr. Res.*, vol. 37, no. 3, pp. 360–368, 2007, doi: 10.1016/j.cemconres.2006.10.012.

[21] R. C. K. Wong and K. T. Chau, “Estimation of air void and aggregate spatial distributions in concrete under uniaxial compression using computer tomography scanning,” *Cem. Concr. Res.*, vol. 35, no. 8, pp. 1566–1576, 2005, doi: 10.1016/j.cemconres.2004.08.016.

[22] S.-Y. Chung, T.-S. Han, T. S. Yun, and K. S. Youm, “Evaluation of the anisotropy of the void distribution and the stiffness of lightweight aggregates using CT imaging,” *Constr. Build. Mater.*, vol. 48, pp. 998–1008, 2013, doi: 10.1016/j.conbuildmat.2013.07.082.

[23] C. Zhang, J. Li, Z. Hu, F. Zhu, and Y. Huang, “Correlation between the acoustic and porous cell morphology of polyurethane foam: Effect of interconnected porosity,” *Mater. Des.*, vol. 41, pp. 319–325, 2012, doi: 10.1016/j.matdes.2012.04.031.

[24] S. Fatima and A. R. Mohanty, “Acoustical and fire-retardant properties of jute composite materials,” *Appl. Acoust.*, vol. 72, no. 2–3, pp. 108–114, 2011.

[25] “ASTM F1868 - 17,” *Standard Test Method for Thermal and Evaporative Resistance of Clothing Materials Using a Sweating Hot Plate*, 2017. https://www.astm.org/Standards/F1868.

[26] “ASTM E2611,” *Standard Test Method for Normal Incidence Determination of Porous Material Acoustical Properties Based on the Transfer Matrix Method*, 2017. https://www.astm.org/Standards/E2611.htm.

[27] F. Asdrubali, F. D’Alessandro, and S. Schiavoni, “A review of unconventional sustainable building insulation materials,” *Sustain. Mater. Technol.*, vol. 4, pp. 1–17, 2015, doi: 10.1016/j.susmat.2015.05.002.

[28] S. Wei, C. Yiqiang, Z. Yunsheng, and M. R. Jones, “Characterization and simulation of microstructure and thermal properties of foamed concrete,” *Constr. Build. Mater.*, vol. 47, pp. 1278–1291, 2013.

[29] M. S. Al-Homoud, “Performance characteristics and practical applications of common building thermal insulation materials,” *Build. Environ.*, vol. 40, no. 3, pp. 353–366, 2005.

[30] R. Pennacchio *et al.*, “Fitness: Sheep-wool and hemp sustainable insulation panels,” vol. 111, pp. 287–297, 2017.

[31] A. M. Papadopoulos and E. Giama, “Environmental performance evaluation of thermal insulation materials and its impact on the building,” *Build. Environ.*, vol. 42, no. 5, pp. 2178–2187, 2007, doi: 10.1016/j.buildenv.2006.04.012.

[32] R. Reixach, R. Del Rey, J. Alba, G. Arbat, F. X. Espinach, and P. Mutjé, “Acoustic properties of agroforestry waste orange pruning fibers reinforced polypropylene composites as an alternative to laminated gypsum boards,” *Constr. Build. Mater.*, vol. 77, pp. 124–129, 2015.

[33] U. Berardi and G. Iannace, “Acoustic characterization of natural fibers for sound absorption applications,” *Build. Environ.*, vol. 94, pp. 840–852, 2015.

[34] G. Bhat and M. El Messiry, “Effect of microfiber layers on acoustical absorptive properties of nonwoven fabrics,” *J. Ind. Text.*, vol. 50, no. 3, pp. 312–332, 2020, doi: 10.1177/1528083719830146.

[35] U. Berardi and G. Iannace, “Predicting the sound absorption of natural materials: Best-fit inverse laws for the acoustic impedance and the propagation constant,” *Appl. Acoust.*, vol. 115, pp. 131–138, 2017, doi: 10.1016/j.apacoust.2016.08.012.

CHAPTER 6

Predictive Models for Thermal Insulation Properties of Porous Composite Materials[4]

[4] Islam, S. and Bhat, G. To be submitted to *International Journal of Heat and Mass Transfer*.

Abstract

An effective model for thermal insulation can provide opportunity to design insulation materials with specific insulation properties and contribute to the insulation industry by decreasing costs and saving time on laboratory testing. Although previously several research have been conducted to develop theoretical and experimental models for predicting thermal insulation properties of composite materials, there is a lack of appropriate models for predicting effective thermal conductivity of porous materials. Hence the primary goal of this study was to develop an analytical model for predicting thermal insulation properties of porous materials. This study also investigated the applicability of existing models (series, parallel, ME1, ME2, and EMT) for predicting thermal insulation properties of such materials. The experimental result showed that among the five basic models, EMT model gives comparatively better prediction. However, none of the existing models give satisfactory results for predicting thermal insulation properties of porous materials. Hence, a model combining ME1 and ME2 models and including the effect of radiation in order to get better prediction of thermal properties of porous composite materials has been proposed. Predictability of the proposed model was verified using experimental data, and was also compared with other existing models. Results showed that the proposed model provides better prediction for porous insulation materials.

Keywords: Porous materials, thermal conductivity, modeling, comparison of models

6.1. Introduction

Historically direct measurement was the ideal method of obtaining accurate insulation properties of materials, but this is a complicated job that required time, special equipment, and accurate sample size, which is not always feasible [1]. Thus, the use of a predictive model may often be the best way of estimating insulation properties.

For some materials, data of thermal conductivities can be found in the literature [2], [3]. But, the databases are available only for some limited materials, which are mainly for pure single components like aluminum, nylon, polyester, and cotton. Hence, a predictive method for measuring thermal insulation property is essential due to the limitations of available data and feasibility of direct measurements.

Currently available predictive methods for measuring thermal insulation properties in the literature are developed mostly by simple empirical correlations of temperature and/or composition [4]. The applicability of these empirical correlations is limited to composite materials as the properties of composite vary a lot with the variation of individual components. In case of porous composite materials, the task is more complex, as thermal properties of porous materials not only rely on the properties of the solid component and porosity, but also the overall structure of the materials [5], [6]. A rigorous numerical simulation using the finite difference method, the finite element method, or other numerical techniques can be utilized in this case when the microstructure of porous composites is known [7]–[9]. However, analytical models are more suitable than numerical models as analytical models are rapid with low cost of calculation, and provide sufficient accuracy even when microstructure is uncertain [10].

Most of the available models for determining thermal insulation properties are based on five basic structural models, which are Series [11], Parallel [11], Maxwell–Eucken (ME) 1 and 2 [12],

and Effective medium theory (EMT) [13]. These models are based on mathematical formulas that are derived from several known physical laws like mass and energy balances, reaction kinetics, and thermodynamics [4]. However, reliability of these models is limited as these models are developed based on certain physical structures of materials and are not applicable if the structure of the materials changes [4], [5]. The series and parallel models assume that the layers of materials are aligned in series and parallel to heat flow [14]. The ME models are developed by considering structures where one phase is dispersed in another continuous phase. The EMT model assumes completely random distributions of all components [14]. Thus, these five basic models are suitable for predefined physical structures, but not fully appropriate for other than those defined structures [10]. Porous composites have complicated physical structures which don't match any predefined structure of five basic models [6]. Up to now, there is no single model that can predict thermal insulation properties of all types of porous composite materials [14]. Apart from predefined structure, there is another fundamental limitation of five basic models. These models only assume heat flow by conduction and ignore the heat flow by convection and radiation. This assumption may be appropriate for complete solid structure, but for porous materials, heat flow occurs not only by conduction but also by convection and radiation. Therefore, estimating thermal insulation properties using five basic models is questionable. Hence, the main purpose of this study was to develop an effective model to predict thermal insulation properties of porous materials.

This study also investigated several existing models to check the applicability of these models for porous insulation materials. A comparison was done between the experimental data and estimated data from models in order to check differences, and to understand whether these differences are within the allowable limit. Considering the limitation of existing models, a modified thermal analysis model was proposed combining ME1 and ME2 and including the effect

of radiative heat transfer process in order to predict thermal properties of porous composite materials more efficiently. After that, feasibility of the proposed model was verified using experimental data, and was compared with other existing models.

6.2. Thermal Conductivity Models

Heat transfers as a form of energy from a high-temperature region to a low-temperature region. In general, heat transfer occurs by three mechanisms: conduction, convection, and radiation [15]. In conduction method, heat transfers from one substance to adjoining substances by direct contact without intermixing or flow of any material [16]. When rapidly moving or vibrating atoms and molecules come in contact with other atoms and molecules, then heat transfers from molecules with higher energy (temperature) to the molecules with lower energy (temperature) [17], [18]. Heat transfer by conduction can be quantified by Fourier's law (equation 6.1).

$$Q = -k.A\frac{dT}{dx} \tag{6.1}$$

where, Q = rate of heat flow (W), k = material conductivity (W/mK), A = area normal to direction of heat flows (m^2), dT/dx = temperature gradient in the direction of heat flow(K/m).

Conduction is the most significant means of heat transfer in a solid material where atoms and molecules stay in contact. In liquids and gases, molecules are normally staying apart resulting in lower probability of molecules colliding and passing of energy by conduction [15]. Heat transfer in liquids and gases mainly occurs by convection process where energy is transferred from high temperature to low-temperature regions due to the movements of fluids (liquids, gases). The third mechanism of heat transfer is thermal radiation, where energy transfers from hot body to a cooler body in the form of electromagnetic waves [15]. Heat can transfer in this process even without an intervening medium [19].

In general, heat transfer is constant in isotropic materials. For composite materials, heat transfer depends on the structure and properties of each of the constituent materials [20]. In the case of porous materials, heat transfer depends on solid phase and pore size, and shape of the materials [20]. If there is an absence of air voids within a solid structure, then heat transmission mainly occurs by conduction process. With porous materials, heat transfer takes place through the air void by convection and radiation process as well [21]. Thus, determining heat transmission through porous composite structures is a complex task as all the heat transfer mechanisms and structures of each component need to be considered during calculation.

In the case of materials with air void structure, Skochdopole experimentally presented that heat transfer by convection does not exist for void cell diameters smaller than 4 mm [22]. As most of the porous composite materials, especially those which are produced from textile fibers, have pore diameter in micrometer range thus, heat transfer by convection can be negligible. Similarly, heat transfer by radiation at room temperature is also very low, which can also be negligible. Therefore, heat transfer at room temperature mainly occurs by conduction. Heat transfer in materials only by conduction is mathematically analogous to the electrical conductivity, permittivity, and magnetic permeability of a material [23]. Thus, similar to electric conductivity, five basic structural models, including the Series, Parallel, Maxwell–Eucken (two forms), and EMT models, can be utilized to estimate the heat transfer of two-component materials [14].

6.2.1. Series model

The series model is developed by considering that the composite material consists of homogeneous components which are in contact with each other. Each component is placed perpendicular to the direction of heat flow, as shown in figure 6.1(a) [24], [25].

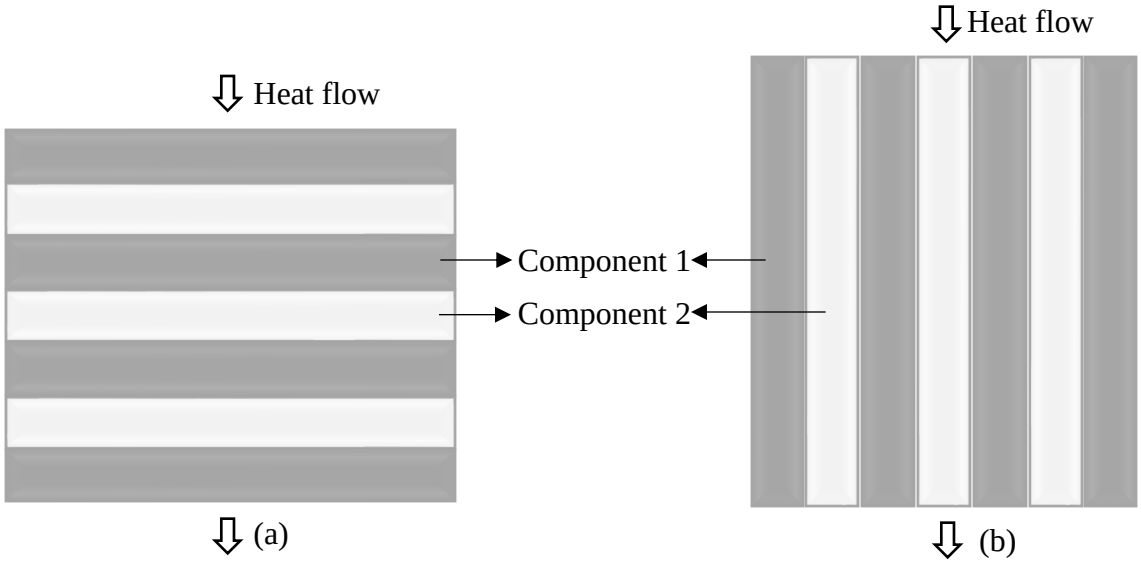

Figure 6.1. Schematic illustrations of the (a) series model (b) parallel model.

The effective thermal conductivity of composite materials can be estimated using the series model applying equation 6.2 [26].

$$k_e = \frac{1}{\frac{v_1}{k_1} + \frac{v_2}{k_2}} \tag{6.2}$$

where, k_e is the effective thermal conductivity, k and v are thermal conductivity and volume fraction of components 1 and 2, respectively.

6.2.2. Parallel model

Similar to the series model, parallel model is developed by assuming that the composite materials consist of homogeneous components which are in contact with each other. But here, each component is placed in parallel to heat flow, as shown in figure 6.1(b) [27].

Effective thermal conductivity of the composite material can be estimated using parallel model applying equation 6.3 [26].

$$k_e = v_1 k_1 + v_2 k_2 \tag{6.3}$$

where, k_e is the effective thermal conductivity, k and v are thermal conductivity and volume fraction of components 1 and 2, respectively.

6.2.3. Maxwell-based ETC model

The first analytical expressions for effective conductivity of heterogenic medium were discussed by Maxwell [23], [28]. The Maxwell model was initially developed to estimate electric conductivity by considering a structure where one phase (spherical in shape) is dispersed in an infinite medium, considering that there is no interaction (or negligible interaction) between two spheres [29], [30]. The schematics of such materials are shown in figure 6.2.

Eucken modified maxwell's model in order to measure thermal conductivity and termed as Maxwell-Eucken (ME) model, which allows composite structure with more than one dispersed phase [23], [31]. Similar to the Maxwell model, the ME model also assumes that the dispersed particles are isolated, and there is no interaction among them during heat conduction [26].

There are two forms of ME model, which are referred to as ME 1 and ME 2. For example, if a composite material consists of two components (component 1 with thermal conductivity of k_1 (marked as grey-black color in figure 6.2), and component 2 with thermal conductivity of k_2 (marked as grey-white color in figure 6.2), then these two components can arrange in the composite structure in one of the following two ways.

In one case, component 1 may form a continuous path, and component 2 may form a dispersed phase (figure 6.2a). This arrangement can be denoted as the ME 1 model.

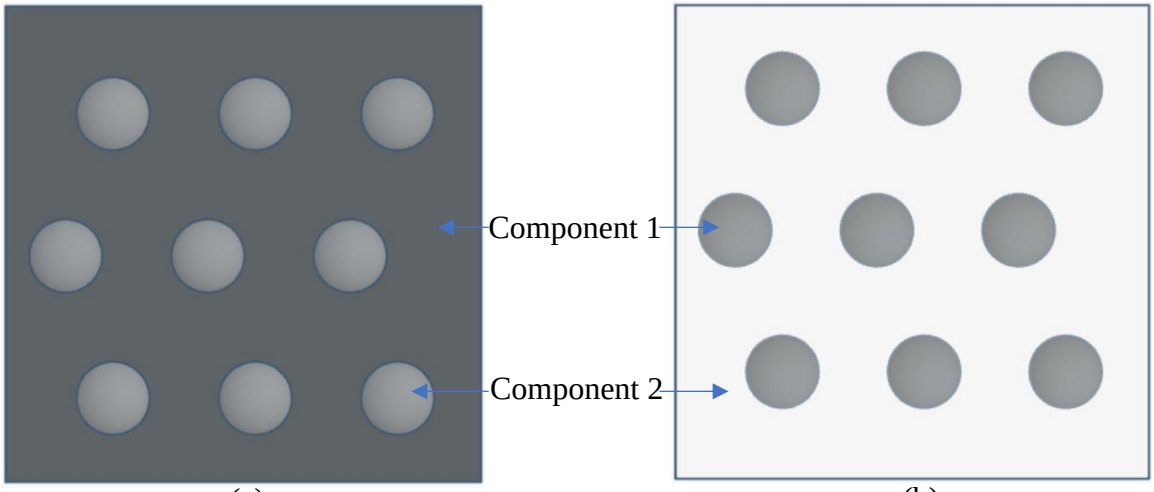

Figure 6.2. Schematic illustrations of the (a) Maxwell-Eucken 1 (b) Maxwell-Eucken 2.

The effective thermal conductivity (k_e) of ME 1 model can be obtained using the following equation [32], [33].

$$k_e = \frac{k_1 v_1 + k_2 v_2 \dfrac{3k_1}{2k_1 + k_2}}{v_1 + v_2 \dfrac{3k_1}{2k_1 + k_2}} \tag{6.4}$$

In the second case, component 2 may form a continuous path, and component 1 may form a dispersed phase (figure 6.2b). This arrangement is denoted as ME 2 model.

The effective thermal conductivity (k_e) of ME 2 model can be obtained using the following equation [32], [33].

$$k_e = \frac{k_2 v_2 + k_1 v_1 \dfrac{3k_2}{2k_2 + k_1}}{v_2 + v_1 \dfrac{3k_2}{2k_2 + k_1}} \tag{6.5}$$

Several researchers further improved ME model to include various effects [23]. Hamilton modified the ME model that provides opportunity to use this model for non-spherical dispersed phase in the continuous medium (equation 6.6) [1], [34].

$$k_e = k_1 \frac{(n-1)k_1 + k_2 - (n-1)(k_1 - k_2)v_2}{(n-1)k_1 + k_2 + (k_1 - k_2)v_2} \tag{6.6}$$

where, n is the shape factor, n =2 for cylindrical shaped dispersed phase (equation 6.7) and n =3 for spherical shaped dispersed phase (equation 6.8 and 6.9).

$$k_e = k_1 \frac{k_1 + k_2 - (k_1 - k_2)v_2}{k_1 + k_2 + (k_1 - k_2)v_2} \tag{6.7}$$

For spherical dispersed phase, Hamilton modification of ME 1 and ME 2 model can be written as equations 6.8 and 6.9, respectively.

ME1 model for spherical shape based on Hamilton modification:

$$k_e = k_1 \frac{2k_1 + k_2 - 2(k_1 - k_2)v_2}{2k_1 + k_2 + (k_1 - k_2)v_2} \text{ (component 1 continuous)} \tag{6.8}$$

ME2 model for spherical shape based on Hamilton modification:

$$k_e = k_2 \frac{2k_2 + k_1 - 2(k_2 - k_1)v_1}{2k_2 + k_1 + (k_2 - k_1)v_1} \text{ (component 2 continuous)} \tag{6.9}$$

6.2.4. Effective medium theory (EMT) model

Landauer initially developed effective medium theory (EMT) for obtaining the electrical conductivity of alloys [13]. Using similarity between heat conduction and electrical conduction, this model is also used for predicting thermal conductivity of composite materials [35]. The model is developed based on the assumption that the distribution of different phases within the composite structure is completely random (figure 6.3) [25].

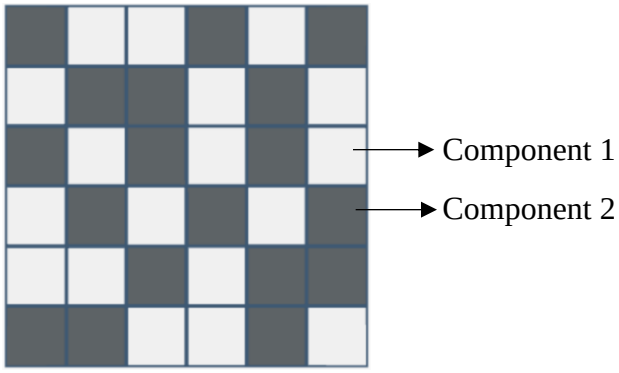

Figure 6.3. Schematic illustrations of the effective medium theory.

The effective thermal conductivity of a two-phase composite material can be calculated by EMT model using following equation [5].

$$v_1 \frac{k_1 - k_e}{k_1 + 2k_e} + v_2 \frac{k_2 - k_e}{k_2 + 2k_e} = 0 \qquad (6.10)$$

where, *k* and *v* are thermal conductivity and volume fraction, and subscripts of e, 1, and 2 represent the composite materials, components 1 and 2, respectively.

6.3. Model Development

The five basic models that were discussed in the previous sections to estimate thermal conductivity have limitations and proved to be inadequate for several composite structures [25]. Those models were initially developed for estimating electric conductivity, later used to predict thermal conductivity, assuming that heat is transferred only by conducting and neglecting the heat transfer by convection and radiation. Again, the structure of porous composite materials does not fully match any of the five basic models.

Thus, we propose a new model by modifying the existing model, ME, in order to suit the structure of porous composite materials. If component 1 (grey-black color of figure 6.2) of the ME model becomes solid phase and component 2 (grey-white color of figure 6.2) of ME model

becomes gaseous phase, then this model can be utilized for porous structure using the following formula.

Maxwell–Eucken 1

$$k_e = k_s \frac{2k_s + k_a - 2(k_s - k_a)\varphi}{2k_s + k_a + (k_s - k_a)\varphi} \tag{6.11}$$

Here, solid phase is continuous. k_s is the thermal conductivity of solid phase, k_a is the thermal conductivity of gas (air), and ϕ is the porosity.

Maxwell–Eucken 2

$$k_e = k_a \frac{2k_a + k_s - 2(k_a - k_s)\varphi}{2k_a + k_s + (k_a - k_s)\varphi} \tag{6.12}$$

Here, gas (air) phase is continuous.

These two models can be further modified in order to make them suitable for porous composite structures that have more than one solid phase. In that case, thermal conductivity of solid phase (k_s) will be the weighted harmonic mean of the thermal conductivity of several individual solid components of those materials (equation 6.13).

$$k_s = \frac{\sum_{i=1}^{n} v_i}{\sum_{i=1}^{n} \frac{v_i}{k_i}} \tag{6.13}$$

Here, v is the volume fraction of solid components, k is the thermal conductivity, and i = 1,2,3,…….n.

As total volume fraction of all solid components is one unit, the equation 6.13, can be written as,

$$k_s = \frac{1}{\sum_{i=1}^{n} \frac{v_i}{k_i}} \tag{6.14}$$

For example, if a composite structure consists of two solid components with the volume fraction of component 1 is 0.4 and volume fraction of component 2 is (1 – 0.4) or 0.6, then weighted harmonic mean thermal conductivity of solid phase can be estimated using the following formula (equation 6.15).

$$k_s = \frac{1}{\frac{0.4}{k_x} + \frac{0.6}{k_y}} \tag{6.15}$$

Here, k_x and k_y are the thermal conductivities of solid components 1 and 2, respectively.

However, the structure of a porous composite material is not completely similar to ME1, where the solid phase forms a continuous path and gas-phase remains as a sphere, or ME2, where solid spheres remain discontinuous in gaseous phase. That's why we proposed the following model by a combination of ME1 and ME2 (equation 6.16).

$$k = \frac{k_{ME1} \times k_{ME2}}{\left(f \times k_{ME1}\right) + \left(\left(1 - f\right) \times k_{ME2}\right)} \tag{6.16}$$

Here, k = thermal conductivity of porous composite samples, k_{ME2} is the thermal conductivity in ME2, k_{ME1} is the thermal conductivity in ME1, and f is the fraction of continuous gas path, which is very much similar to porosity, and $(1 - f)$ is the fraction of continuous solid path.

This model can effectively represent both ME1 and ME2 structures. Like, if $f = 0$ or fraction of continuous gas path is zero, then $k = k_{ME1}$ and if $f = 1$, then $k = k_{ME2}$.

Now, f and $1 - f$ can be rewritten as follows:

$$\frac{f}{1-f} \approx \frac{V_V}{V_S} \; or \; \frac{V_v}{V_T - V_V} \; or \; \frac{\frac{V_v}{V_T}}{\frac{V_T - V_V}{V_T}} \; or \; \frac{\phi}{1-\phi} \tag{6.17}$$

Here, V_v, V_S, and V_T are Void volume, solid volume, and total volume respectively.

Hence, equation 6.16 can be rewritten as,

$$k = \frac{k_{ME1} \times k_{ME2}}{\left(\phi \times k_{ME1}\right) + \left(\left(1-\phi\right) \times k_{ME2}\right)} \tag{6.18}$$

This model can be utilized in all types of porous composite materials with different shapes of structure as continuous gas or solid path of ME model is replaced by porosity.

The above model is developed based on two basic models, ME 1 and ME 2. One of the main assumptions of ME 1 and ME 2 model is that heat flow is only by conduction and convection and radiation heat flow processes are absent. This assumption is mostly appropriate for solid materials. But in case of porous materials along with conduction, heat also flows by convection (when pore diameter is more than 4 mm) and there is contribution from radiation process as well [22].

In reality, with most of the composite materials, especially fibrous composite materials, pore diameters are in micrometer range. Thus, we can exclude convection heat transfer process. But heat transfer by radiation is not completely negligible for porous materials. Although heat transfer by radiation at room temperature is very low, we need to consider this process in order to develop an appropriate model.

Wei et al. investigated the importance of inclusion of radiation process during heat transfer. Experimental results showed that at 293 K temperature, radiation contributes about 6% of heat transfer for highly porous materials [36]. The contribution of radiation heat transfer for porous materials can be calculated using equation 6.19 [37], [38].

$$k_{rad} = \frac{2}{3} \times 4d\phi\sigma T^3 \tag{6.19}$$

where, d is the average pore diameter, ϕ is the porosity, T is the mean temperature in kelvin, and σ is Stefan–Boltzmann constant (5.67×10^{-8} W/m^2 K^4).

Therefore, considering heat transfer by both conduction and radiation, the model becomes,

$$k_e = \frac{k_{ME1} \times k_{ME2}}{\left(\phi \times k_{ME1}\right) + \left(\left(1-\phi\right) \times k_{ME2}\right)} + \frac{8d\varphi\sigma T^3}{3} \tag{6.20}$$

Equation 6.20 is our proposed final model for predicting thermal insulation properties of porous composite materials.

6.4. Experimental Design

In this study, two different porous composite materials, nonwoven insulation from waste textiles (discussed in chapter 3) and 3D printed insulation from PLA filaments (discussed in chapter 7), were used to test the applicability of models.

6.4.1. Determination of thermal properties

Thermal resistance, *R*-value, and heat flux (*Q*) of two different insulation materials (nonwoven insulation from waste textiles and 3D printed insulation from PLA filaments) were measured experimentally using sweating guarded hotplate following the standard ASTM-F18868-C [39]. According to this standard, thermal resistance was measured by total heat loss where plate & guard temperature was kept at 35°C, and ambient temperature was kept at 25°C. Thermal conductivity (*k*) was measured from heat flux, thickness, and temperature differences using following equation:

$$k = \frac{Q \times t}{\Delta T} \tag{6.21}$$

where *Q* is the heat flow (W/m^2), *t* is the thickness (m) of the specimen, and ΔT is the temperature difference (K) between hot and cold surfaces.

Along with experimental measurement, thermal conductivity of waste textiles and 3D printed samples were estimated using five basic models (series, parallel, ME 1, ME 2, and EMT) and model proposed in this experiment. For estimating thermal conductivity of 3D printed samples, the solid phase (PLA filament) thermal conductivity is used as k_S = 0.13 W/mK [40], and gaseous phase (air) thermal conductivity is used as k_a = 0.025 W/mK [36], based on literature. Similarly,

for estimating thermal conductivity of nonwoven composite panels, the solid phase cotton, Sorona®, and PLA fibers' thermal conductivity are used as k_{S1} = 0.243 W/mK [41], k_{S2} = 0.2 W/mK [42], and k_{S3} = 0.13 W/mK [40] respectively and gaseous phase (air) thermal conductivity is used as k_a = 0.025 W/mK [36], based on literature. In order to calculate thermal property using this model, it is also necessary to determine the porosity and pore size of composite materials. Porosity (ϕ) of composite panels was calculated by the following relation [43].

$$\phi = 1 - \frac{\rho}{\rho'} \tag{6.22}$$

For nonwoven composite isulation, ρ' is the density of cotton, Sorona®, and PLA fibers ρ is the density of composite panels. For 3D printed samples, ρ' is the density of PLA filaments and ρ is the density of printed samples. The average densities of cotton, Sorona®, and PLA fibers used for calculation were 1.52 g/cm^3 [44], 1.32 g/cm^3, and 1.25 g/cm^{3,} respectively; and the average density of used PLA filaments were 1.27 g/cm^3. Pore diameter of nonwoven composite panels were determined using porous materials Inc. (PMI), model no. CFP-100AEX following the standard test method ASTM F316-03 [45]. On the other hand, 3D printed samples were designed with a specific pore diameter. After printing, average pore diameter of samples is tested again to check whether there is any variation in pore diameter between actual samples and designed samples.

6.4.2. Comparisons of Model Predictions with experimental data and five basic models

The proposed model was compared to the experimental data with three different processes, calculating difference, percentage differences, and mean absolute discrepancies (AD_M) of experimental and predicted data. The AD_M between the data and the models was calculated using the following equations [1].

$$AD_M = \frac{\sum_n \sqrt{\left(k_{\exp eriment} - k_{predicted}\right)^2}}{n_d} \quad (6.23)$$

Here, n_d is number of data points.

The experimental data were also compared with five basic models to check which model most appropriately estimates thermal insulation properties of porous materials. The proposed model was also compared with five basic models.

6.5. Results and Discussions

6.5.1. Experimental thermal conductivity

The experimental thermal conductivity (TC) measured by sweating guarded hot plate are shown in table 6.1 (nonwoven composite produced from waste textiles) and table 6.2 (3D printed insulation from PLA).

6.5.2. Thermal conductivity calculating by model

The predicted thermal conductivity (TC) values of all nonwoven composite panels and 3D printed insulation panels using the proposed model and five basic models are shown in table 6.1 and table 6.2, respectively.

6.5.3. Comparison of proposed model with experimental data

The comparison of TC values obtained by experiment and prediction using proposed model is shown in table 6.1 (nonwoven composite produced from waste textiles) and table 6.2 (3D printed sample from PLA). Results indicate that for both nonwoven composites and 3D printed samples, predicted TC values have a reasonable agreement with experimental TC values. The differences between model and experimental data were also calculated. It is evident that the estimated TC values agree very well with experimental data with a maximum difference of 0.004 (for nonwoven composites) and 0.006 (for 3D printed sample). This difference is much less than some other

recently developed TC models [46]. Therefore, it can be concluded that the developed model is very helpful and reliable for the prediction of thermal conductivity.

Table 6.1. Comparison of TC values obtained from experiment and predicted by proposed model (nonwoven composite).

Sample Id.	Density (kg/m^3)	Porosity	Pore size (mm)	Solid phase (k_S)			Gaseous phase, air (k_a)	Predicted TC, k (W/mK)	Experimental TC, k (W/mK)	Differences
				Cotton (k_{S1})	Sorona® (k_{S2})	PLA (k_{S3})				
A1	460.05	0.68	0.163	0.243	0.200		0.025	0.054	0.050	0.004
A2	503.46	0.65	0.168	0.243	0.200		0.025	0.058	0.059	0.001
A3	544.95	0.62	0.162	0.243	0.200		0.025	0.063	0.065	0.002
A4	434.21	0.69	0.174	0.243		0.130	0.025	0.049	0.049	0.000

Table 6.2. Comparison of TC values obtained from experiment and predicted by proposed model (3D printed samples).

Sample Id.	Density (kg/m^3)	Porosity	Solid phase, PLA (k_S)	Gaseous phase, air (k_a)	Predicted TC, k (W/mK)	Experimental TC, k (W/mK)	Differences
I-10	366.46	0.71	0.13	0.025	0.042	0.037	0.005
I-20	459.22	0.64	0.13	0.025	0.047	0.041	0.006
I-30	546.75	0.57	0.13	0.025	0.052	0.052	0.001
I-40	635.70	0.50	0.13	0.025	0.058	0.062	0.004
I-50	721.26	0.43	0.13	0.025	0.065	0.070	0.005

6.5.4. Comparison of proposed model with five basic models

Comparison was also made among five basic models (series, parallel, ME1, ME2, and EMT), proposed model, and experimental data. It was found that the TC values from experimental data were mostly similar to the developed model compared to those of five basic models in case of both nonwoven composite panels (figure 6.4) and 3D printed samples (figure 6.5). The mean absolute discrepancies between experimental data and models are presented in table 6.3 (composite panels)

and table 6.4 (3D printed samples). The mean absolute discrepancies between experimental data and models are 0.0011 for composite panels and 0.0021 for 3D printed samples. These discrepancies are much lower than the discrepancies between experimental data and five basic models. Thus, it can be said that the proposed model has ability to predict thermal properties of porous materials more efficiently compared to the five basic models. The average percentage differences between proposed models are 3.0% for composite panels and 8.4% for printed samples. In both cases, the percentage difference is less than ±10% which indicates that the accuracy of model is sufficient to be used in industrial sectors [1].

For both composite panels and 3D printed samples, among five basic models, it was found that ME 2 and EMT models are comparatively closer to the experimental data, i.e., provided comparatively better prediction of thermal conductivity. This is because structural assumptions of both EMT and ME 2 models are closer to porous composite materials. Thus, if anyone wants to apply five basic models for predicting thermal properties of porous materials, EMT and ME2 will give better predictions.

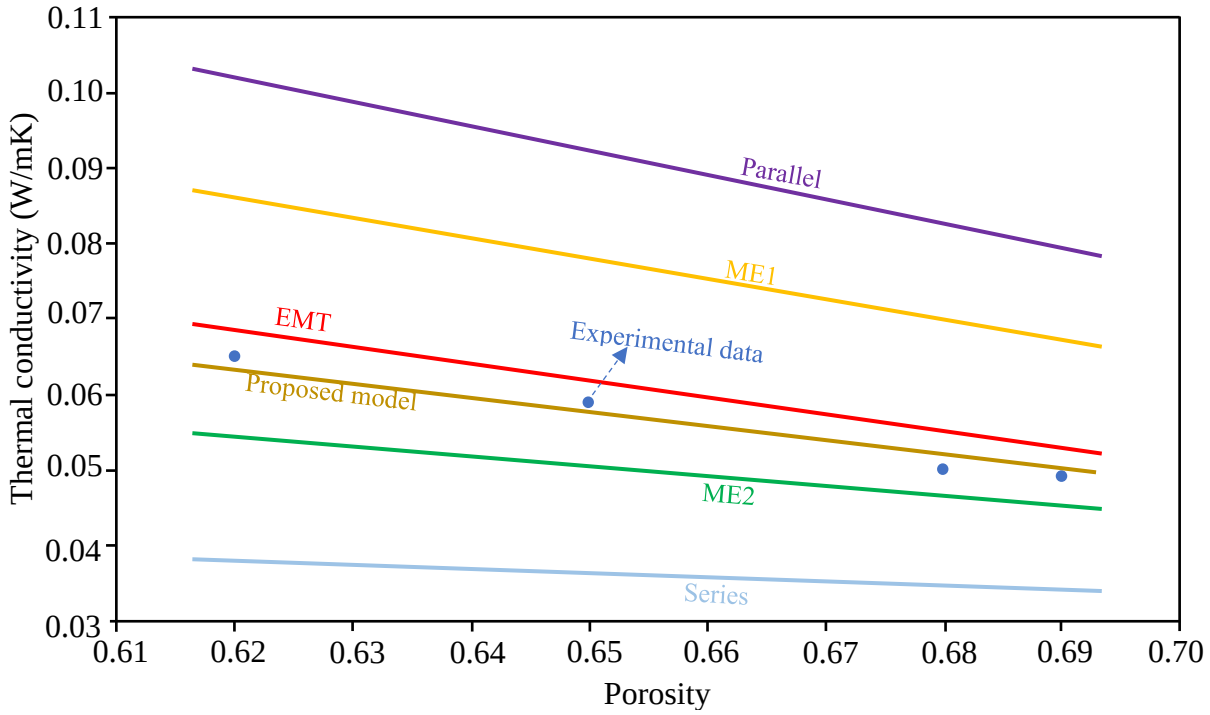

Figure 6.4. Comparison among five basic models, proposed model, and experimental data (nonwoven composite).

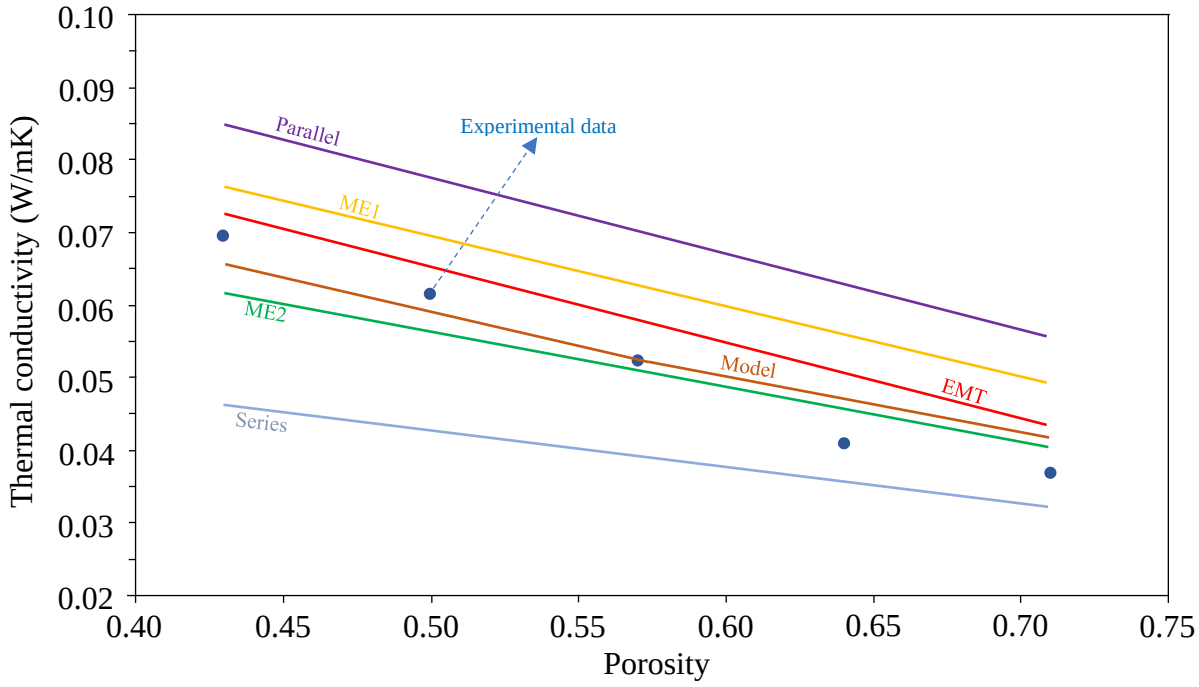

Figure 6.5. Comparison among five basic models, proposed model, and experimental data (printed sample).

Table 6.3. Difference between experimental data and models (nonwoven composite).

Model	Mean absolute discrepancies	Average percentage difference
Series	0.0104	56.3%
Parallel	0.0167	36.9%
ME 1	0.0098	25.5%
ME 2	0.0038	13.8%
EMT	0.0020	5.9%
Developed model	0.0011	3.0%

Table 6.4. Difference between experimental data and models (printed samples).

Model	Mean absolute discrepancies	Average percentage difference
Series	0.0070	33.0%
Parallel	0.0080	26.3%
ME 1	0.0048	17.3%
ME 2	0.0023	9.2%
EMT	0.0024	9.2%
Developed model	0.0021	8.4%

Although the developed model prediction is very close to experimental data, still, there are some discrepancies. The discrepancies may arise from several sources. During calculation using the model, TC of cotton, Sorona®, and PLA was considered as 0.243 W/mK, 0,2 W/mK. And 0.13 W/mK, respectively. All of these are average values, and slight deviation may occur within materials. TC value of air is considered 0.025 W/mK, which may also vary with the variation of temperature. Previous research showed that TC of gas could vary up to 5% [47]. Discrepancy may also arise from the measurement of porosity and pore size. All these factors contribute to some discrepancies. Discrepancy may also arise from experimental data as the accuracy of thermal conductivity measurement is not 100%.

6.6. Summary

In this study, a new model was proposed to measure the thermal insulation properties of porous materials. This study also investigated five basic thermal conductivity models in order to understand which models are most suitable to predict the insulation properties of porous materials. It was observed that among the five basic models, only EMT and ME2 models provide reasonable predictions for porous materials. The discrepancies between experimental and predicted data of other models are very high, like for nonwoven composite panels, discrepancy is as high as 56.3% in series model. The proposed model more efficiently estimates the thermal insulation properties of porous materials compared to five basic models. From comparative analysis, it was found that the estimated thermal conductivity value agrees well with the experimental data with a discrepancy of about 0.0011 (nonwoven composite panels) and 0.0021 (3D printed samples). The average percentage difference between model and experimental data is less than 8.5% for both nonwoven composite and 3D printed samples. In general, if the difference between model predictions and experimental measurements are within ±10%, it is considered that the accuracy is sufficient for industrial purposes [1]. Thus, it can be concluded that the proposed model is suitable for predicting thermal insulation properties of porous materials. However, additional experimental study is encouraged to further verify the model.

6.7. References

[1] J. K. Carson, "Prediction of the thermal conductivity of porous foods: a thesis submitted in partial fulfilment of the requirements for the degree of Doctor of Philosophy in Food Engineering, Massey University, Palmerston North, New Zealand, 2002," Massey University, 2002.

[2] "Thermtest Instrument," *Materials thermal properties database*, 2021. https://thermtest.com/materials-database (accessed Jun. 07, 2021).

[3] "NCFS," *Thermal properties: databases online interfaces*, 2021. https://ncfs.ucf.edu/burn_db/Thermal_Properties/material_thermal.html (accessed Jun. 07, 2021).

[4] J. K. Carson, "Review of effective thermal conductivity models for foods," *Int. J. Refrig.*, vol. 29, no. 6, pp. 958–967, 2006, doi: 10.1016/j.ijrefrig.2006.03.016.

[5] L. Gong, Y. Wang, X. Cheng, R. Zhang, and H. Zhang, "A novel effective medium theory for modelling the thermal conductivity of porous materials," *Int. J. Heat Mass Transf.*, vol. 68, pp. 295–298, 2014, doi: 10.1016/j.ijheatmasstransfer.2013.09.043.

[6] L. Miettinen, P. Kekäläinen, T. Turpeinen, J. Hyväluoma, J. Merikoski, and J. Timonen, "Dependence of thermal conductivity on structural parameters in porous samples," *AIP Adv.*, vol. 2, no. 1, pp. 1–15, 2012, doi: 10.1063/1.3676435.

[7] R. Bolot, G. Antou, G. Montavon, and C. Coddet, "A two-dimensional heat transfer model for thermal barrier coating average thermal conductivity computation," *Numer. Heat Transf. Part A Appl.*, vol. 47, no. 9, pp. 875–898, 2005, doi: 10.1080/10407780590921953.

[8] R. P. A. Rocha and M. A. E. Cruz, "Computation of the effective conductivity of unidirectional fibrous composites with an interfacial thermal resistance," *Numer. Heat Transf. Part A Appl.*, vol. 39, no. 2, pp. 179–203, 2001, doi: 10.1080/10407780118981.

[9] E. Divo, A. Kassab, and F. Rodriguez, "Characterization of space dependent thermal conductivity with a BEM-based genetic algorithm," *Numer. Heat Transf. Part A Appl.*, vol. 37, no. 8, pp. 845–875, 2000, doi: 10.1080/10407780050045865.

[10] J. Wang, J. K. Carson, M. F. North, and D. J. Cleland, "A new structural model of effective thermal conductivity for heterogeneous materials with co-continuous phases," *Int. J. Heat Mass Transf.*, vol. 51, no. 9–10, pp. 2389–2397, 2008, doi: 10.1016/j.ijheatmasstransfer.2007.08.028.

[11] A. G. Leach, "The thermal conductivity of foams. I. Models for heat conduction," *J. Phys. D. Appl. Phys.*, vol. 26, no. 5, pp. 733–739, 1993, doi: 10.1088/0022-3727/26/5/003.

[12] Z. Hashin and S. Shtrikman, “A variational approach to the theory of the effective magnetic permeability of multiphase materials,” *J. Appl. Phys.*, vol. 33, no. 10, pp. 3125–3131, 1962, doi: 10.1063/1.1728579.

[13] R. Landauer, “The electrical resistance of binary metallic mixtures,” *J. Appl. Phys.*, vol. 23, no. 7, pp. 779–784, 1952, doi: 10.1063/1.1702301.

[14] J. Wang, J. K. Carson, M. F. North, and D. J. Cleland, “A new approach to modelling the effective thermal conductivity of heterogeneous materials,” *Int. J. Heat Mass Transf.*, vol. 49, no. 17–18, pp. 3075–3083, 2006, doi: 10.1016/j.ijheatmasstransfer.2006.02.007.

[15] D. Kuvandykova, *A model for predicting thermal properties of asphalt mixtures from their constituents*. University of New Brunswick (Canada), 2010.

[16] O. Levenspiel, “The three mechanisms of heat transfer: conduction, convection, and radiation,” in *Engineering Flow and Heat Exchange*, O. Levenspiel, Ed. New York: Springer, 2014, pp. 179–210.

[17] B. J. Dempsey and M. R. Thompson, “A heat transfer model for evaluating frost action and temperature-related effects in multilayered pavement systems,” *Highw. Res. Rec.*, no. 342, pp. 39–56, 1970, [Online]. Available: https://trid.trb.org/view/102331.

[18] D. F. Adkins and G. P. Merkley, “Mathematical model of temperature changes in concrete pavements,” *J. Transp. Eng.*, vol. 116, no. 3, pp. 349–358, 1990, doi: 10.1061/(ASCE)0733-947X(1990)116:3(349).

[19] T. L. Bergman, F. P. Incropera, D. P. DeWitt, and A. S. Lavine, *Fundamentals of heat and mass transfer*. Hoboken, NJ: John Wiley & Sons, 2011.

[20] M. Bohorquez de Silva, “Study of microstructure effect on the thermal properties of Yttria-stabilized-Zirconia thermal barrier coatings made by atmospheric plasma spray and pressing machine,” Louisiana State University, 2010.

[21] C. Deng *et al.*, “Insulation effect of air cavity in sand mold using 3D printing technology,” *China Foundry*, vol. 15, no. 1, pp. 37–43, 2018, doi: 10.1007/s41230-018-7243-y.

[22] R. E. Skochdopole, “The thermal conductivity of foamed plastics,” *Chem. Eng. Prog.*, vol. 57, no. 10, pp. 55–59, 1961.

[23] K. Pietrak and T. S. Wisniewski, “A review of models for effective thermal conductivity of composite materials,” *J. Power Technol.*, vol. 95, no. 1, pp. 14–24, 2015, [Online]. Available: https://papers.itc.pw.edu.pl/index.php/JPT/article/view/463.

[24] G. Xu, “Direct measurement of through-plane thermal conductivity of partially saturated fuel cell diffusion media,” University of Tennessee, Knoxville, 2013.

[25] D. P. Hochstein, “Thermal Conductivity of Fiber-Reinforced Lightweight Cement Composites,” Columbia University, 2013.

[26] J. K. Carson, S. J. Lovatt, D. J. Tanner, and A. C. Cleland, “Thermal conductivity bounds for isotropic, porous materials,” *Int. J. Heat Mass Transf.*, vol. 48, no. 11, pp. 2150–2158, 2005, doi: 10.1016/j.ijheatmasstransfer.2004.12.032.

[27] E. Sadeghi, M. Bahrami, and N. Djilali, “Analytic determination of the effective thermal conductivity of PEM fuel cell gas diffusion layers,” *J. Power Sources*, vol. 179, no. 1, pp. 200–208, 2008, doi: 10.1016/j.jpowsour.2007.12.058.

[28] J. C. Maxwell, *A treatise on electricity and magnetism*, vol. 1. Oxford, UK: Oxford University Press, 1904.

[29] L. N. McCartney and A. Kelly, “Maxwell’s far-field methodology applied to the prediction of properties of multi-phase isotropic particulate composites,” *Proc. R. Soc. A Math. Phys. Eng. Sci.*, vol. 464, no. 2090, pp. 423–446, 2008, doi: 10.1098/rspa.2007.0071.

[30] R. B. Bird, W. E. Stewart, and E. N. Lightfoot, *Transport phenomena*, vol. 1. Hoboken, NJ: John Wiley & Sons, 2006.

[31] A. Eucken, “W armeleitf ahigkeit keramischer feuerfester Stoffe-Berechnung aus der W armeleitf ahigkeit der Bestandteile,” *Forsch. auf dem Gebiet des Ingenieurwesens*, vol. 3, p. 16, 1932.

[32] J. C. Maxwell, *A Treatise on Electricity and Magnetism*. New York, NY: Dover Publications Inc., 1954.

[33] A. Eucken, “Allgemeine gesetzmäßigkeiten für das wärmeleitvermögen verschiedener stoffarten und aggregatzustände,” *Forsch. auf dem Gebiet des Ingenieurwesens A*, vol. 11, no. 1, pp. 6–20, 1940, doi: 10.1007/BF02584103.

[34] R. L. Hamilton and O. K. Crosser, “Thermal conductivity of heterogeneous two-component systems,” *Ind. Eng. Chem. Fundam.*, vol. 1, no. 3, pp. 187–191, 1962, doi: 10.1021/i160003a005.

[35] D.-H. Shin, H.-K. Cho, N.-I. Tak, and G.-C. Park, “Evaluation of Effective thermal conductivity models on the prismatic fuel block of a Very High Temperature Reactor by CFD analysis,” 2014. https://inis.iaea.org/collection/NCLCollectionStore/_Public/48/076/48076893.pdf (accessed Apr. 01, 2021).

[36] S. Wei, C. Yiqiang, Z. Yunsheng, and M. R. Jones, “Characterization and simulation of microstructure and thermal properties of foamed concrete,” *Constr. Build. Mater.*, vol. 47, pp. 1278–1291, 2013.

[37] J. Yuan, “Intumescent coating performance on steel structures under realistic fire conditions.” The University of Manchester, 2009.

[38] C. Di Blasi and C. Branca, “Mathematical model for the nonsteady decomposition of intumescent coatings,” *AIChE J.*, vol. 47, no. 10, pp. 2359–2370, 2001, doi: 10.1002/aic.690471020.

[39] “ASTM F1868 - 17,” *Standard Test Method for Thermal and Evaporative Resistance of Clothing Materials Using a Sweating Hot Plate*, 2017. https://www.astm.org/Standards/F1868.

[40] P. Keane, “Thermally Conductive Polymer Materials for 3D Printing,” 2020. https://3dprinting.com/3d-printing-use-cases/thermally-conductive-polymer-materials/#:~:text=PLA has a thermal conductivity of about 0.13,%28m%2AK%29%2C depending on the alloy and other factors.

[41] J. W. S. Hearle and W. E. Morton, *Physical properties of textile fibres*. Cambridge: Woodhead Publishing, 2008.

[42] “DuPont,” *DuPontTM Sorona® 3301 NC010 renewable sourcedTM thermoplastic polymer*. https://www.gc.co.th/upload/datasheet/sorona_3301_nc_010.pdf (accessed Jun. 07, 2021).

[43] S. Fatima and A. R. Mohanty, “Acoustical and fire-retardant properties of jute composite materials,” *Appl. Acoust.*, vol. 72, no. 2–3, pp. 108–114, 2011.

[44] S. B. Warner, *Fiber science*. Englewood Cliffs, NJ: Prentice-Hall, 1995.

[45] “ASTM F316-03,” *Standard Test Methods for Pore Size Characteristics of Membrane Filters by Bubble Point and Mean Flow Pore Test*, 2019. https://www.astm.org/Standards/F316.htm.

[46] B. Grabowska and J. Kasperski, “The Thermal Conductivity of 3D Printed Plastic Insulation Materials—The Effect of Optimizing the Regular Structure of Closures,” *Materials (Basel).*, vol. 13, no. 19, pp. 1–15, 2020, doi: 10.3390/ma13194400.

[47] Y. S. Touloukian, P. E. Liley, and S. C. Saxena, “Thermophysical properties of matter-the tprc data series. volume 3. thermal conductivity-nonmetallic liquids and gases,” Thermophysical and electronic properties information analysis center, 1970. [Online]. Available: https://apps.dtic.mil/sti/citations/ADA951937.

CHAPTER 7

Life Cycle Assessment of Thermal Insulation Materials Produced from Recycled Textiles[5]

[5] Islam, S., Bhat, G., and Mani, S. To be submitted to *Resources, Conservation & Recycling*.

Abstract

This study aims to produce environment-friendly thermal insulation materials from recycled textiles, to evaluate the environmental impact of produced insulation materials using life cycle assessment (LCA) method, and finally compare the environmental impact of competing insulation materials. In this study, three different insulation panels were produced using textile wastes at different percentages, temperatures, and pressure conditions. They are composed of 100% recycled cotton (N1), 90% recycled cotton/10% PLA (N2), and 42.5% recycled cotton/42.5% recycled nylon/15% PLA (N3). A cradle to gate LCA study was conducted to assess the key environmental impacts based on the ISO 14040/44 guidelines. The N1 and N2 insulation materials had lower environmental impacts than that of N3 insulation panel. However, all three insulation panels had comparable environmental impacts with that of commercially available insulation materials (stone wool, recycled PET bottle, and flax). LCA results showed that insulation panels N1 and N2 have eleven and three times (respectively) lower global warming potential than stone wool and sixteen and four times (respectively) lower global warming potential than flax-based insulation panels. Opportunities exist to further reduce the environmental impacts of waste textile insulation panels by process intensification and using recycled PLA fibers.

Keywords: Thermal insulation, textile wastes, recycling, nonwoven, greenhouse gas emissions.

7.1. Introduction

LCA is a comprehensive method to systematically assess the environmental impacts (such as global warming, acidification, ozone depletion, etc.) throughout the whole life cycle of a product [1]. It is a set of activities that estimates environmental impacts starting from extraction of raw materials, then several manufacturing stages, intended use, and finally ends with the disposition of that materials. LCA methodology can also be used to assess the environmental impacts at different manufacturing stages of products to identify which stage has larger environmental impacts. These activities give opportunity to highlight potential stages that can be modified to reduce environmental impacts instead of replacing the entire production process [2]. LCA can also be applied to compare several products with similar functions or technology and identify which product or technology has the least environmental impacts.

Thus, the overall objectives of this study were to manufacture sustainable thermal insulation materials from recycled textiles using nonwoven fabrication techniques, to carry out the cradle to gate LCA to assess the environmental impacts of produced insulation materials, and compared with commercial insulation materials (natural flax, recycled PET bottle, and synthetic stone wool) and to conduct the sensitivity analysis of key input parameters influencing the final environmental impacts to improve the overall environmental performances.

7.2. Preparation and Analysis of Thermal Insulation Materials

7.2.1. Preparation

Thermal insulation panels were prepared by blending waste textile fibers with thermoplastic binder polylactic acid (PLA) fibers at different ratios (table 7.1). Textile waste from Bluewater Defense, a military apparel producer in Purto Rico, were shredded into loose fiber/yarn bundles by Cross

Plains Trading Company, Chatsworth, GA. PLA staple fibers (synthesized from corn starch) were obtained from Fiber Innovation Technology, Inc., Johnson City, TN.

Waste textiles are converted into small fabric strips (around 5cm × 2 cm) using a shredding machine. These cut fabrics were passed through a special fabric recycling carding machine, also called garnett, to open into fibers, and then blended with PLA fibers. A carded web of fiber blends was produced at the end of this process. Three different samples were produced, which were denoted as N1, N2, and N3 (table 7.1). The production process of insulation materials is shown in figure 7.1. For all three insulation materials, recycling of waste textiles and forming nonwoven fiber webs were completely similar. However, the web bonding process was different. For insulation panel N1, mechanical bonding was done by needle punching. For insulation panel N2 and N3, after mechanical bonding, thermal bonding was also done in order to increase mechanical properties. For thermal bonding, low melting thermoplastic binder fiber, PLA, was blended with recycled fibers during nonwoven fiber web formation. When heat (165 ℃) is applied, PLA fiber melts partially to cause necessary adhesion between fibers. In N3 insulation panels, high pressure (800 lbs) was also applied at the time of heating that consolidates the fiber web and further increases the strength and stability of insulation panels.

Table 7.1. Different parameters of composite samples.

Sample Id.	Fiber type	Temperature (℃)	Time (m)	Pressure (kPa)
N1	100% recycled cotton fibers (control)	No	No	No
N2	90% recycled cotton fibers/10% PLA	165	10	No
N3	42.5% recycled cotton fibers/42.5% recycled nylon fibers/15% PLA	165	3	800 lbs

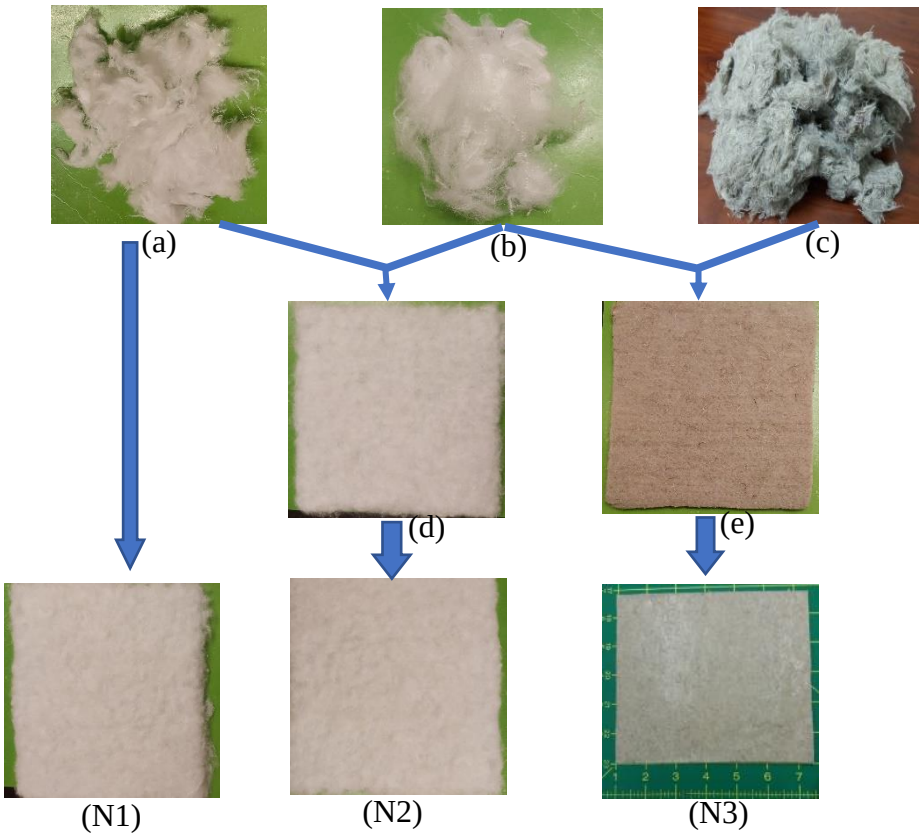

Figure 7.1. Composite sample preparation process: (a) Carded waste fibers (100% cotton), (b) PLA fibers, (c) Carded waste fibers (50% cotton/50% nylon), (d) Needle punched sample (90% cotton/10% PLA), (e) Needle-punched sample (42.5% cotton/42.5% nylon/15% PLA), (N1) Needle-punched thermal insulation panels (100% cotton), (N2) Insulation panel after heat setting (90% cotton/10% PLA), (N3) Insulation panels after heat and press.

7.2.2. Characterization of insulation panels

At first, the insulation panels were conditioned for 48 hours in a standard testing environment, i.e., $(20\pm2)^0$C temperature and (65±2)% relative humidity. After conditioning, thickness (t), area (A), weight (w), areal density (s), and bulk density (ρ) were measured. For calculating areal density (s), insulation panels were weighed using an electronic balance, and area of the samples was measured. Then areal density, s (g/m^2), was calculated by dividing weight over area. Bulk density, ρ (kg/m^3) was calculated by dividing areal density (s) over thickness (t).

Multiple measurements (five) were taken for each sample as per the standard, and average values of thickness, areal density, and bulk density were calculated.

Thermal resistance, *R*-value, and heat flux (*Q*) of insulation panels were measured using sweating guarded hotplate based on the standard ASTM-F18868-C [3]. The thermal resistance was measured by total heat loss where plate & guard temperature was kept at 35℃, and ambient temperature was kept at 25℃. Thermal conductivity (*k*) was measured from heat flux, thickness, area, and temperature differences.

The thickness of insulation panels was adjusted to get thermal resistance value of 1 m^2 K/W, which is helpful to compare these insulation materials with similar types of other insulation materials. The related properties of insulation materials to get 1 m^2 K/W are given in table 7.2.

7.3. LCA Methodology

LCA is a process that is used to analyze, quantify, and evaluate the environmental aspects and the potential impacts associated with a product, process, or activity [4]. According to ISO 14044 standard, LCA methodology consists of four main steps, which are goal and scope definition, inventory assessment, impact assessment, and interpretation of results.

In this study, a cradle to gate LCA method was applied as per the standard of ISO 14040 [5] and 14044 [6] to produce thermal insulation materials from waste textiles. The detailed sub-process includes collection of waste textiles, fabric shredding, the extraction of PLA fibers from raw materials, fiber web formation, needle punching, and heat setting. The reference thermal insulation materials considered for comparison purposes were natural flax fiber, recycled PET fiber from plastic bottle, stone wool (combination of virgin and waste stone wool). The environmental impact data for flax fiber, recycled PET, and stone wool was collected from available literature.

7.3.1. Goal and Scope

The insulation materials produced from textile wastes are expected to be used as building thermal insulation materials. The purpose of the LCA study was to evaluate environmental impacts of produced materials, analyze the environmental impacts at different stage of production process and find out which stages need to be modified for reducing environmental impacts, compare with similar other insulation materials, and finally to check whether the waste textile based insulation materials have significantly lower environmental impacts than that of other available insulation materials such as flax fibers, recycled PET fibers from plastic bottle, and stone wool.

The scope of the LCA study defines the functional unit, system boundaries, and interested impact categories of thermal insulation panels from textile wastes [4], [7], [8]. In this study, we assumed that the waste textiles that would otherwise be dumped in the landfills will be utilized for producing thermal insulation panels.

7.3.1.1. Functional unit

According to the ISO 14040 standard, the functional unit (*f.u.*) is the reference unit through which product system performance is quantified [9], [10]. As similar to other LCA studies of thermal insulation materials, *f.u.* of this study was defined as the mass (kg) of thermal insulation panel required to provide the thermal resistance (*R-value*) of 1 m^2 K/W (equation 7.1).

$$f.u. = Rk\rho A \quad (7.1)$$

where, R is the thermal resistance of 1 (m^2 K/W), k is thermal conductivity measured as W/mK, ρ is the density of insulation products in kg/m^3 and A is the area of 1 m^2.

According to the above definition of *f.u.*, the amount of insulation materials (kg) required to meet the thermal resistance of 1 m^2 K/W are shown in table 7.2.

Table 7.2. Functional unit (kg) required to provide a thermal resistance of 1 (m^2 K)/W (R = 1).

Sample Id	Thickness (mm)	Bulk density (kg/m^3)	Thermal conductivity (W/mK)	Weight per *f.u.* (kg)
N1	9	24.8	0.027	0.67
N2	8	27.9	0.028	0.80
N3	9	190.8	0.036	6.92

Most of the thermal insulation materials have service life of 35 to 50 years or average lifetime of the buildings [11]. The insulation materials produced from cellulosic fibers have lifetime of 50 years [11]. As used textile wastes are mostly cotton with cellulosic fibers, the service life would be around 50 years.

7.3.1.2. System boundary

Figure 7.2 shows the system boundaries to produce three thermal insulation panels from waste textiles. As this is a cradle-to-gate LCA, so the use and disposal phases are positioned outside of the system boundaries. The use phase and disposal phase were not included to compare as impacts are similar for all insulation materials [12]. Irrespective of the type of materials, an insulation material can save more than 100 times impacts to production and disposal during its service life [12].

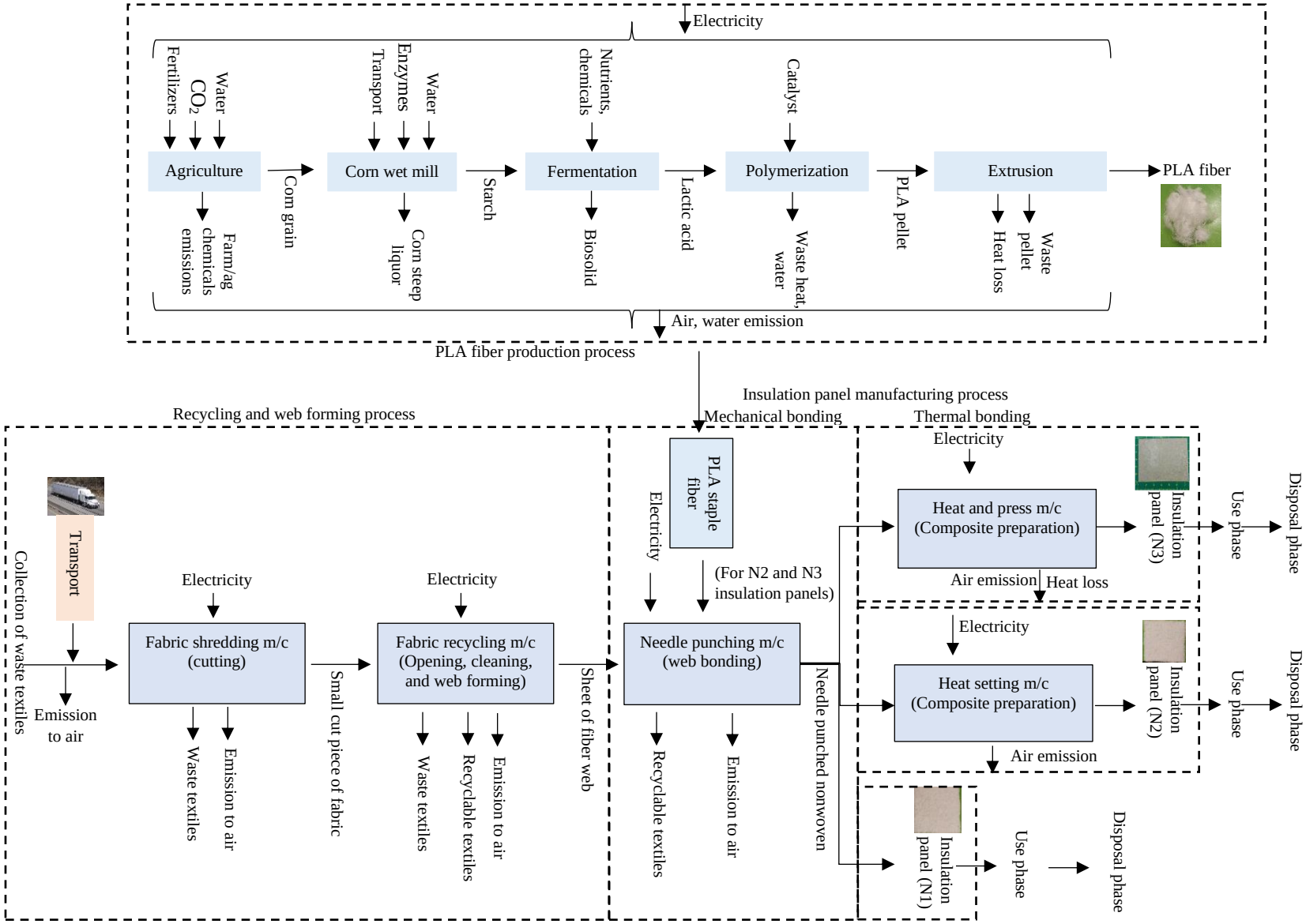

Figure 7.2. System boundary for production of thermal insulation panels from waste textiles.

7.3.2. Inventory assessment

7.3.2.1. Inventory data

The inventory analysis is the second step of LCA, where all required data on input and output of energy, material, and emissions are gathered and quantified [13]. We assumed that the manufacturing of waste textile based thermal insulation plan would be located in the Continental U.S. and all energy and material resources would be acquired from U.S. sources. The emissions data for electricity consumption was acquired from U.S. electricity production mix.

Inventory data of this study was either estimated or obtained based on large scale production system. The mass distribution and thermal performances of the insulation panels were obtained from laboratory experiments. The energy consumption and the capacity of each unit operation for large-scale production were obtained from literature sources. The complete inventory data starting from waste textile collections, shredding, recycling, mechanical bonding, and thermal bonding are shown in table 7.3.

The first process for producing thermal insulation materials is to collect waste textiles and transport them to the production sites. The average in-state transport distance in the USA from waste collection to production site is about 250 km [14]. The next process is fabric shredding. Industrially used fabric shredding machines can shred on average 1000 kg fabric per hour with 13.2 kW electric power [15]. The average process loss or rejection amount during shredding process of waste textiles is about 3% [16]. Thus, at the end of this process, 3% of solid waste had been produced.

After shredding, cut fabrics were passed through a carding machine to open and clean the fibers. In this process, waste textiles are converted into fibers. For N2 and N3 insulation panels, thermoplastic PLA fibers (as a binder for thermal bonding) were blended with recycled fibers. A

carded fiber web was produced at the end of this process. Industrially used textile waste fabric recycling machine has an average production capacity of 275 kg per hour with 51.7 kW electric power [17]. The process loss for fiber opening, cleaning, and web forming is about 14% to 16% [18], which consists of dirt and short fibers. Thus, at the end of the recycling process, some recyclable fibers that may be fed back into the system, and some solid wastes are produced.

The produced fiber web can were mechanically bonded using needle punching machine. Industrially used nonwoven needle punching machine can have an average production capacity of 800 kg fabric per hour with 17 kW power use [19]. Insulation material N1 was prepared and ready for use after needle punching.

In order to increase the bonding strength, samples N2 and N3 have been further bonded thermally. When heat is applied, low melting temperature thermoplastic PLA fiber melts and bonds other fibers together. For sample N2, heat is applied for melting PLA. Industrially used furnace has capacity to give heat-set (Heat treatment condition: T = 165 ^{o}C for 10 min) of 92 kg per hour with 6 kW electric power use [20]. For N3 insulation panels, high pressure was also applied at the time of heating that consolidates the fiber web and increases strength and stability of insulation panels. In this process, Geo Knight 12" x 14" JetPress machine was used for applying both heat and pressure. The instrument can produce 7.8 kg per hour (Heat treatment condition: T = 165 ^{o}C, 3 min) with 1.2 kW power rating. Heat loss occurs during this process, which was estimated to about 23.86 kJ per kg of insulation panels. We also assumed that the entire production process generates no or limited fugitive emissions, but generates both heat losses and solid wastes and accounted for each process.

Table 7.3. The inventory data for producing 1000 *f.u.* of insulation panels from waste textiles.

Process	Element	Input			Output			Waste/loss		
		Value for 1000 f.u.			Value for 1000 f.u.			Value for 1000 f.u.		
		N1	N2	N3	N1	N2	N3	N1	N2	N3
Waste textile collection	Cotton waste textiles (kg)	810	864.3	7100						
	Transport (tkm)	202.3	216.07	1775						
	Waste textiles at production site (kg)				810	864.3	7100			
Fabric shredding	Waste textiles (kg)	810	864.3	7100						
	Electricity (kWh)	10.7	11.41	93.74						
	Small cut piece of fabric (kg)				785.50	839.2	6895			
	Waste (solid) (kg)							24.5	25.2	206
Fiber web formation	Small cut piece of fabric (kg)	785.50	839.2	6895						
	Electricity (kWh)	147.70	157.75	1296						
	PLA fiber (kg)	----	80.4	1050						
	Fiber web (kg)				677.5	803.8	6992			
	Recyclable solid waste (kg)							86.5	92.6	760.8
	Waste (Solid) (kg)							21.5	23.2	190.2
Needle punching	Fiber web (kg)	677.5	803.8	6992						
	Electricity (kWh)	14.25	17.08	148.6						
	Mechanically bonded insulation panels (kg)				670.5	795.8	6923			
	Recyclable solid waste (kg)							7.5	8.0	69
Heat setting/ Heat & press	Mechanically bonded insulation panels (kg)	---	795.8	6923						
	Electricity (kWh)	---	51.84	1065						
	Thermally bonded insulation panels (kg)				---	795.8	6923			
	Heat loss (air) (MJ)							---	---	49.85

PLA fibers used in this study was obtained from renewable corn sources provided by Fiber Innovation Technology, Inc., Johnson City, TN, USA. A thorough LCA data of PLA from corn sources was obtained from the literature [21]–[23]. Inventory data for corn production was obtained from US Life Cycle Inventory Database [24] and available literature [22]. Inventory data for the production of PLA pellet from corn grain was obtained from Landis, A. E. [23]. The next

step is to convert PLA pellet into PLA fiber. Industrially used polyester staple fiber production machine has capacity to produce on average 1100 kg per hour using electricity 1200 kW [25]. It was also estimated that during production PLA staple fibers from PLA pellets about 1202.6 kJ heat had been lost and 7.89 g of solid waste had been produced [26]. The complete inventory data for the production of 1000 kg PLA fibers has been presented in supplementary table 7.1.

7.3.2.2. Inventory database

The mass and energy data obtained for the production system was converted to emission data using US life cycle inventory (US LCI) database. US electricity mix of the year 2020 (supplementary table 7.2) is considered for analysis of all energy or electricity consumption.

7.3.3. Impact assessment method

The next step of LCA study is impact assessment, where environmental, ecological and human impacts are quantified based on the life cycle inventory emission data for the product using TRACI 2 V. 3.03 assessment method. Nine different impact categories are selected (supplementary table 7.3) for impact assessment. Among these 9 different impact categories, global warming (GW) occurs by greenhouse gases (carbon dioxide, methane, nitrous oxide, fluorinated gases, etc.), and in this LCA study, GW is reported in kg equivalent of CO_2. Acidification (Ad), a process where water and soil become acidic, occurs due to the emission of sulfur dioxide and nitrogen oxides in air during burning of fossil fuel, and due to the release of ammonia during agricultural activities. In this LCA study, moles of equivalent H^+ has been used for reporting Ad. Carcinogenics (Cr), non carcinogenics (NC) are reported in kg equivalent of benzene and toluene respectively. NC impact are mostly coming from power generation and transportation. Respiratory effect (RE) is reported in Kg equivalent of PM2.5, which means particles with a diameter less than 2.5 μm. Eutrophication (Eu), reported in kg of equivalent N, occurs when water is overly enriched with

minerals and nutrients like nitrogen or phosphorus resulting in excessive growth of algae, blockage of sunlight, and oxygen depletion in water body [27]. Ozone depletion (OD), reduction in the amount of ozone in the stratosphere that increases UV radiation on earth's surface, is reported by kg equivalent of CFC-11. OD causes hazardous effect on plant and human health. Ecotoxicity (Ec), toxic effect caused by pollution that harms ecosystems, has been reported by Kg equivalent of 2,4-D, which is a type of herbicide. Finally, the smog formation (Sm), reported by Kg equivalent of NOx, occurs due to the reactions of NOx, volatile organic compounds (VOCs), other pollutants, and sunlight, which have adverse effects on human health and vegetation [28].

The entire thermal insulation manufacturing process generates limited wastes with no co-product production. Hence, the overall impact has only been distributed only to the main products, thermal insulation panels.

7.3.4. Sensitivity analysis approach

The impact assessment of this study was conducted based on average input data during production of thermal insulation panels from waste textiles. Hence, a sensitivity analysis was performed in order to understand the effect of variations in key input parameters on the environmental impacts. The key input parameters chosen for sensitivity analysis were transportation distance, amount of PLA fiber, and electricity consumption. In this study, each input parameter was varied to ± 20% from the average value. This means that impact assessment will be conducted by increasing the input data value by 20% and decreasing the input data value by 20% for each selected parameter.

7.3.5. Reference thermal insulation panels

The LCA data of produced thermal insulation materials from waste textiles was compared with three different insulation panels obtained from the literatures. The details of all insulation materials are presented in table 7.4. Stone wool is currently used as a commercial insulation panel, which is

a synthetic material. Flax based insulation is obtained from natural sources, and the third one is produced from post-consumer PET bottles representing recycled products.

Table 7.4. A list of reference insulation materials with the functional unit (in kg) necessary to provide a thermal resistance of 1 m^2K/W (R= 1).

Materials	Density (kg/m^3)	Thermal resistance (m^2 K/W)	Weight per f.u. (kg)	Thickness (mm)	Ref.
Recycled PET bottles	30	1	1.065	35.5	[26]
Stone wool (combination of virgin and recycled materials)	32	1	1.184	37	[12]
Flax	30	1	1.26	42	[12]

7.4. Results and Discussions

7.4.1. Impact assessment

The cradle to gate LCA results of selective environmental impacts and their normalized relative percentage of insulation panels N1, N2, and N3 are shown in table 7.5, 7.6, and 7.7 and figure 7.3, 7.4, and 7.5 respectively. From the data, it is clear that the overall environmental impacts of all selected categories to produce insulation panels-N1 and N2 is very low. However, insulation panel N3 has comparatively higher environmental impacts.

For N1 insulation panel (table 7.5 and figure 7.3), it was found that the fiber web formation process has the highest environmental impacts, as this process requires the most energy in terms of electricity compared to other processes. After the fiber web formation process, collection of waste textiles have high environmental effect, especially in the categories of ecotoxicity and smog as diesel is used for transportation. Shredding process has the highest environmental effect in the category of ozone depletion as huge amount of waste is produced during this process.

Table 7.5. Impact assessment to produce 1 *f.u.* (0.67 kg) thermal insulation panels (N1) from waste textiles (100% recycled cotton).

Impact category	Unit	Waste textiles collections	Shredding	Fiber web formation	Needle punching	Thermal insulation panels (N1)
GW	Kg CO_2 eq	0.0189	0.0262	0.0995	0.0082	0.1527
Ad	H^+ moles eq	0.0062	0.0032	0.0371	0.0035	0.0500
Cr	Kg benzen eq	6.14×10^{-6}	3.96×10^{-6}	4.73×10^{-5}	4.50×10^{-6}	6.19×10^{-5}
NC	Kg toluen eq	0.1294	0.0257	0.3266	0.0314	0.5147
RE	Kg PM2.5 eq	7.15×10^{-6}	1.19×10^{-5}	1.49×10^{-4}	1.43×10^{-5}	1.83×10^{-4}
Eu	Kg N eq	5.96×10^{-6}	5.94×10^{-6}	1.29×10^{-5}	8.61×10^{-7}	2.57×10^{-5}
OD	Kg CFC-11 eq	7.08×10^{-13}	7.50×10^{-11}	6.90×10^{-11}	1.40×10^{-12}	1.46×10^{-10}
Ec	Kg 2,4-D eq	0.0036	4.80×10^{-3}	0.0062	0.0006	0.0109
Sm	g NOx eq	1.29×10^{-3}	2.39×10^{-5}	1.7×10^{-3}	1.51×10^{-5}	3.34×10^{-4}

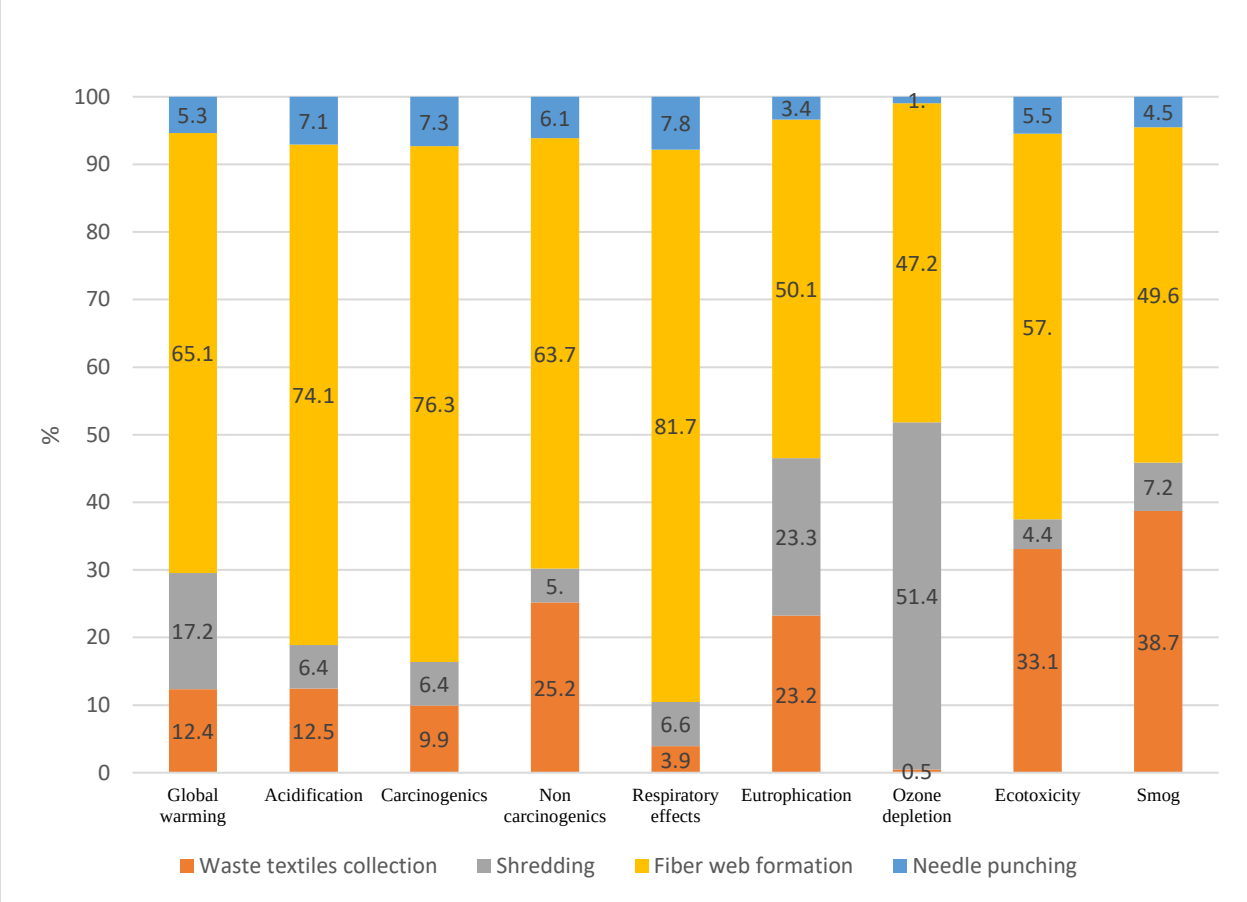

Figure 7.3. Relative comparison of environmental impacts analysis of different processes to produce thermal insulation panel -N1 (normalized to 100%).

The major environmental impacts of insulation N1 are almost related to energy consumption, which is required for operating machinery during production. About 64.7% of GWP is associated with the electricity mix (supplementary figure 7.1). As expected, electricity from bituminous coal and natural gas contributes 26.3% and 36% respectively of total global warming, as 20.80% and 44.32% of electricity in the US comes from coal plants and natural gas respectively. On the other hand, electricity from wind, water, and solar plants do not have any significant contribution to global warming. Hence, by reducing coal power plants and increasing renewable power plants, global warming potential could be further reduced.

For N2 insulation panel (table 7.6 and figure 7.4), it was found that the major contribution to the environmental categories comes from PLA fiber productions (about 67% for GWP). Although PLA fiber is produced from natural corn source, which is renewable, but use of fertilizer and energy during corn production, chemical to convert corn to PLA pellets, and energy to convert PLA pellets to PLA fibers, combinedly have huge environmental effect. Apart from PLA fiber production, fiber web formation process also has high environmental effect. Shredding process has the highest environmental effect in the category of ozone depletion as huge amount of waste is produced during this process.

Table 7.6. Impact assessment to produce 1 *f.u.* (0.80 kg) thermal insulation panels (N2) from waste textiles (90% cotton/ 10% PLA).

Impact category	Unit	Waste textiles collections	Shredding	PLA fiber	Fiber web formation	Needle punching	Heat setting	Thermal insulation panels (N2)
GW	Kg CO_2 eq	0.0201	0.0274	0.3922	0.1062	0.0098	0.0298	0.5840
Ad	H^+ moles eq	0.0066	0.0034	0.0693	0.0395	0.0042	0.0129	0.1363
Cr	Kg benzen eq	6.55×10^{-6}	7.07×10^{-6}	3.15×10^{-5}	5.04×10^{-5}	5.41×10^{-6}	1.64×10^{-5}	1.14×10^{-4}
NC	Kg toluen eq	0.1383	0.0275	0.2261	0.3492	0.0375	0.1142	0.8931
RE	Kg PM2.5 eq	7.61×10^{-6}	1.28×10^{-5}	1.37×10^{-4}	1.59×10^{-4}	1.72×10^{-5}	5.21×10^{-5}	3.87×10^{-4}
Eu	Kg N eq	6.36×10^{-6}	6.21×10^{-6}	5.30×10^{-4}	1.37×10^{-5}	1.03×10^{-6}	3.12×10^{-6}	5.58×10^{-4}
OD	Kg CFC-11 eq	7.56×10^{-13}	7.73×10^{-11}	9.62×10^{-12}	7.39×10^{-11}	1.67×10^{-12}	5.07×10^{-12}	1.69×10^{-10}
Ec	Kg 2,4-D eq	0.0038	5.07×10^{-4}	0.0044	0.0066	7.13×10^{-4}	0.0022	0.0183
Sm	g NOx eq	1.32×10^{-4}	2.51×10^{-5}	0.0097	1.80×10^{-4}	1.81×10^{-5}	5.50×10^{-5}	0.0100

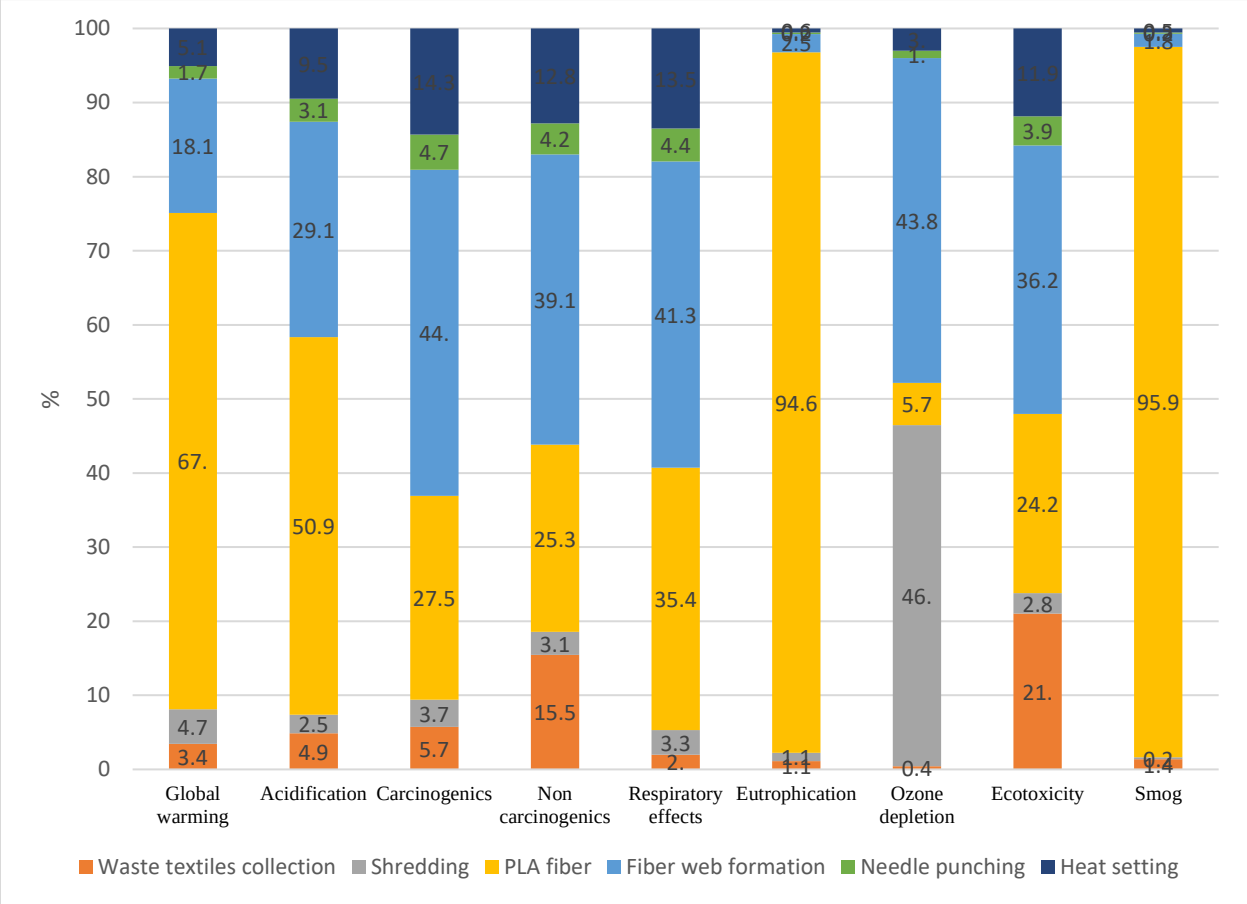

Figure 7.4. Relative comparison of environmental impacts analysis of different processes to produce thermal insulation panel -N2 (normalized to 100%).

In contrast to insulation panels N1 and N2, the overall environmental impacts of insulation panel N3 are very high (table 7.7 and figure 7.5). The comparative environmental impacts of N3 insulation material at different stages are very much similar to that of N2 panels, i.e., PLA fibers contribute (about 72.3% GWP) most of the environmental impacts followed by fiber web formation and shredding. This is even higher than the contribution of PLA in N2, as the percentage of PLA fibers is higher (15% PLA in N3, compared to 10% in N2).

Table 7.7. Impact assessment to produce 1 *f.u.* (6.92 kg) thermal insulation panels (N3) from waste textiles (42.5% cotton/ 42.5% Nylon/ 15% PLA).

Impact category	Unit	Waste textiles collections	Shredding	PLA fiber	Fiber web formation	Needle punching	Heat and press	Thermal insulation panels (N3)
GW	Kg CO_2 eq	0.1656	0.2309	5.1267	0.8728	0.0851	0.6100	7.0873
Ad	H^+ moles eq	0.0548	0.0282	0.9063	0.3253	0.03689	0.2643	1.6121
Cr	Kg benzen eq	5.39×10^{-5}	3.49×10^{-5}	4.11×10^{-4}	4.14×10^{-4}	4.71×10^{-5}	3.37×10^{-4}	0.0013
NC	Kg toluen eq	1.1372	0.2266	2.9627	2.8756	0.3282	2.3528	9.8758
RE	Kg PM2.5 eq	6.27×10^{-5}	1.05×10^{-4}	0.0018	0.0013	1.50×10^{-4}	0.0011	0.0045
Eu	Kg N eq	5.23×10^{-5}	5.24×10^{-5}	0.0069	1.13×10^{-4}	8.98×10^{-6}	6.43×10^{-5}	0.0072
OD	Kg CFC-11 eq	6.22×10^{-12}	6.58×10^{-10}	1.26×10^{-10}	6.07×10^{-10}	1.45×10^{-11}	1.04×10^{-10}	1.51×10^{-09}
Ec	Kg 2,4-D eq	0.0315	0.0042	0.0578	0.0545	0.0062	0.0446	0.1990
Sm	g NOx eq	0.0011	2.10×10^{-4}	0.1262	0.0015	1.57×10^{-4}	0.0011	0.1303

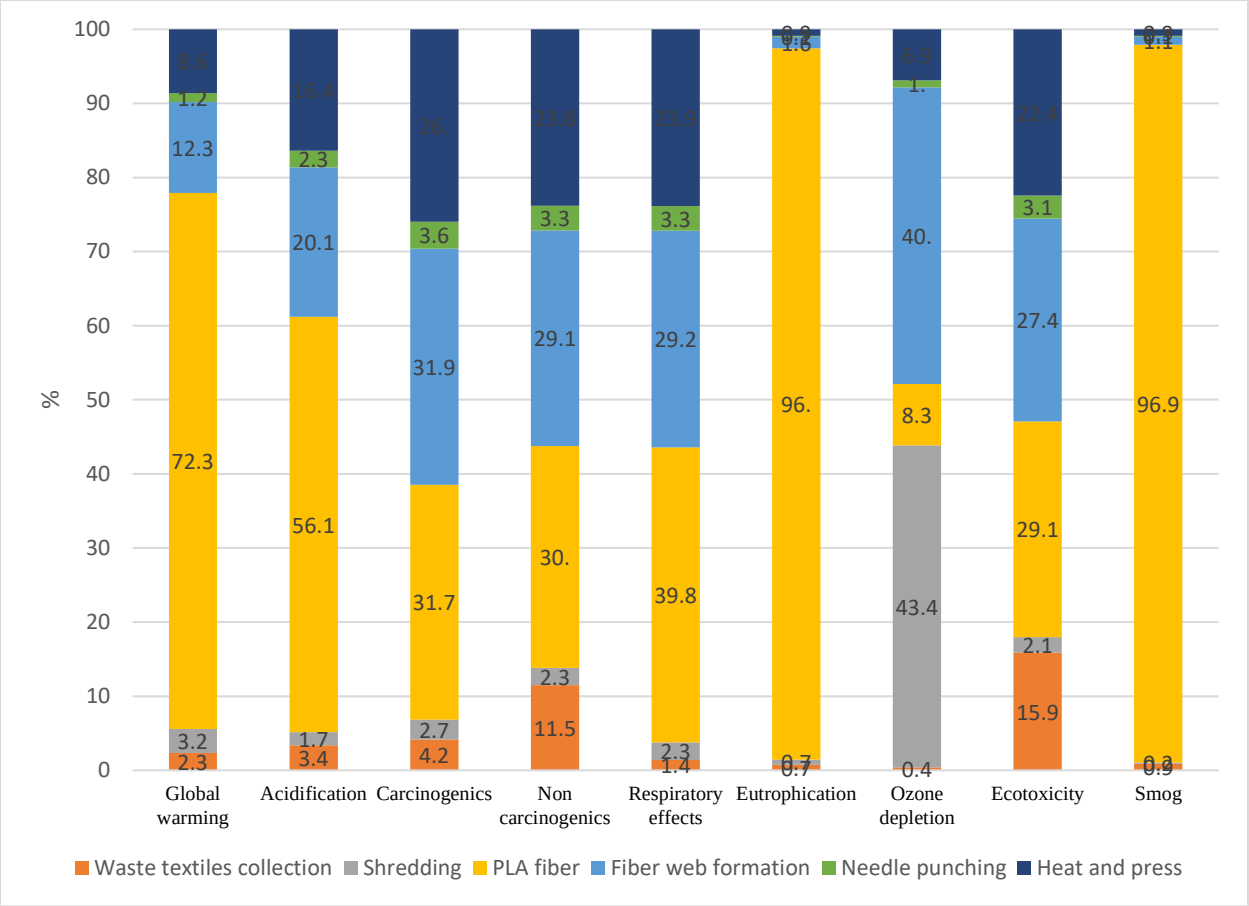

Figure 7.5. Relative comparison of environmental impacts analysis of different processes to produce thermal insulation panel - N3 (normalized to 100%).

From comparative impact analysis of thermal insulation panels (figure 7.6), it was found that in all types of selected impact categories, insulation panel N3 has much higher impacts than N1 and N2. In case of GWP, N3 has >40 times higher than N1 and >10 times higher than N2 insulation panel.

In comparison to N1 and N2 insulation panel, N1 has lower environmental impacts in all impact categories. In case of GWP, N1 has 3.8 times lower impact compared to N2. As it is already discussed, use of PLA fibers with sample N2 contributes to high environmental impacts.

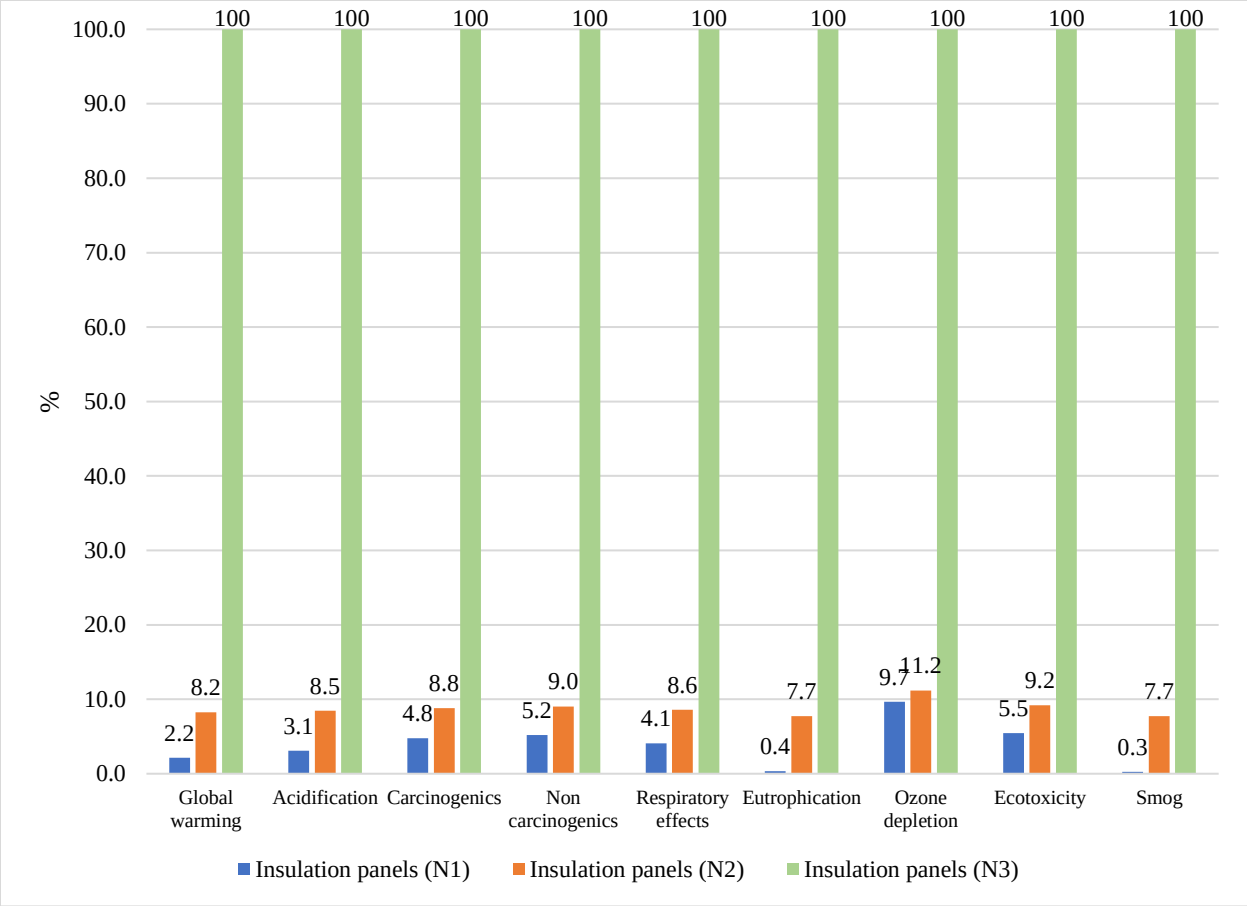

Figure 7.6. Relative comparison of impact assessment of insulation panels N1, N2, and N3 after normalizing highest impacts of each category to 100%.

The higher environmental impacts of N3 are very much expected as 6.92 kg materials are required to produce 1 *f.u.* insulation panels, which is more than 8 times higher in weight compared to N1 and N2. Insulation panel N3 was prepared applying high pressure for consolidation, which increases density; as a result, more weight of insulation material is required for one *f.u.* Thus, high amount of waste textiles and PLA fibers are required, which result in high environmental impacts. In order to reduce the environmental impacts, production process has to be slightly modified. Preparation process of N3 has to be similar to the preparation process of N2, i.e., avoiding the process of applying high pressure after heat setting as high pressure increases the density and thermal conductivity resulting in very high amount of materials in kg per *f.u.*

PLA fibers have also higher contribution on the environmental impacts of insulation panel N2 and N3. By using natural fertilizer and developing eco-friendly technology for conversion of corn to PLA fiber, overall environmental impacts could be minimized. More research is necessary to increase the production of PLA pellet and fiber by reducing chemicals and energy. Using recycled thermoplastic fibers instead of virgin PLA could improve the overall impacts a lot.

Among 9 different impact categories (supplementary table 7.3), the major source of global warming, acidification, and ecotoxicity comes from the emission of fossil fuels that have been used as energy sources and for production of the US electricity mix, especially with coal power plants. Among these three impacts, the effect of ecotoxicity is very low. Acidification also comes from the production of corn.

The carcinogenic effect of producing thermal insulation is very less (almost negligible amounts), and most of this comes from power generation and transportation. Noncarcinogenics, mostly coming from power generation and transportation are reported in kg of equivalent toluene.

Besides carcinogenic and noncarcinogenic health risks, there are some respiratory effects during the production of insulation materials. Respiratory effect mainly comes from dust produced during recycling, burning fuel, and chemical reactions during PLA formation.

The eutrophication effect of sample N1 is negligible, but samples N2 and N3 have some eutrophication effect, which mainly comes from PLA fiber due to using fertilizer during corn production.

Negligible amount of ozone depletion effects and smog formation occur during production of insulation materials. Impact of ozone depletion mainly comes from waste produced during the shredding process. When waste degrades, methane gas is produced that can lead to ozone depletion. Whereas smog formation mainly occurs during PLA pellet formation and transportation.

7.4.2. Sensitivity analysis

Changing of final environmental impacts of insulation materials with the change of 20% key input parameters (transportation distance, amount of PLA fiber, and electricity consumption) have been presented in the figure 7.7 and figure 7.8. The effect of changing each parameter on the final results has been investigated individually while keeping the other parameters at the base-case value.

In case of Insulation panel N1(figure 7.7), the variation (± 20%) of electricity has highest impacts on respiratory effect, whereas variation (± 20 %) of transport distance has highest impacts on smog. It was also revealed that about (± 12.97%) and (± 2.43%) changes in global warming could have occurred on the final impact with variation (± 20%) of electricity consumption and transport distance, respectively.

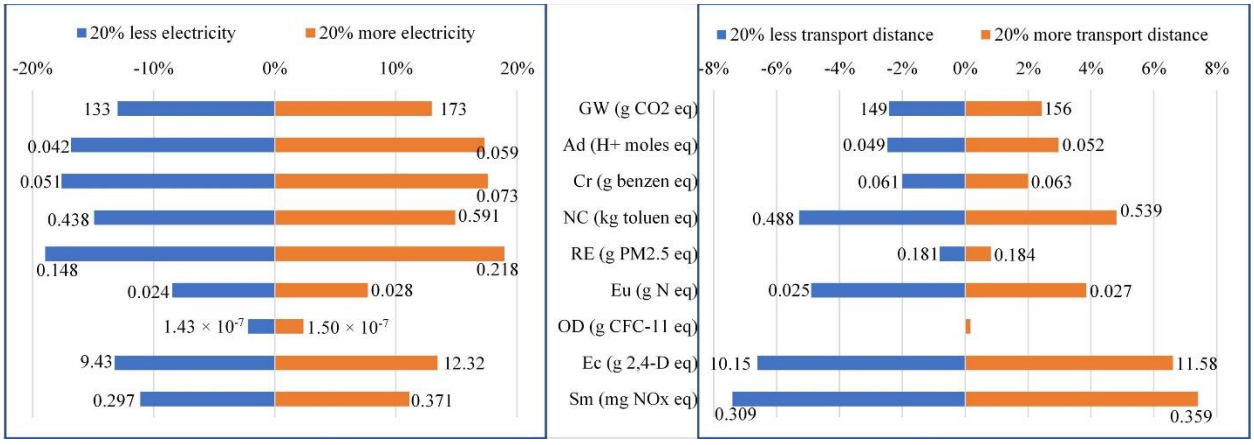

Figure 7.7. Sensitivity analysis of selected environmental impacts for 20% less and 20% more electricity consumption and transport distance during the production of thermal insulation panels N1 (solid color represent percentage changes and actual value is written at the end).

In case of Insulation panel N2 (figure 7.8), the variation (± 20 %) of electricity has the highest impact on carcinogenic, whereas variation (± 20%) of PLA has the highest impact on smog and eutrophication. It was also revealed that change in global warming is very high on the final impact of insulation panel N2. However, the increase and decrease of impacts are not consistent. The 20% increase in the consumption of electricity increase the emission of global warming by 6.86%

(0.624 kg CO_2 eq), while 20% decrease in the consumption of electricity reduced the net emission of global warming by 6.37% (0.547 kg CO_2 eq). Similarly, 20 % increase in the production of PLA fiber lowered the emission of global warming by 9.31% (0.53 kg CO_2 eq) while 20% decrease in the production of PLA fiber improved the net emission of global warming by 14.71% (0.70 kg CO_2 eq).

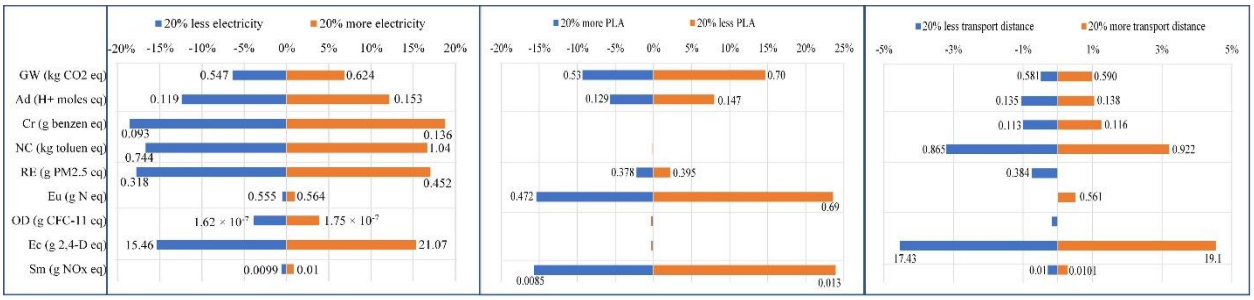

Figure 7.8. Sensitivity analysis of selected environmental impacts for 20% less and 20% more electricity consumption, amount of PLA fiber, and transport distance during the production of thermal insulation panels N2 (solid color represent percentage changes and actual value is written at the end).

In case of Insulation panel N3, the variation of final environmental impacts with the variation of (± 20 %) of input parameters (transportation distance, amount of PLA fiber, and electricity consumption) (supplementary figure 7.4, 7.5, and 7.6) are almost similar to that of insulation panel N2.

7.4.3 Comparison with several other insulation panels

The comparative environmental impacts per *f.u.* of different thermal insulation materials have been reported in table 7.8.

Table 7.8. Comparative impact assessment for the production of 1 *f.u.* of different insulation materials.

Impact category	Unit	Insulation panel-N1	Insulation panel-N2	Insulation panel-N3	Recycled PET	Flax	Stone wool
GW	Kg CO_2 eq	0.1527	0.5840	7.0873	1.8	2.43	1.69
Ad	H^+ moles eq	0.0500	0.1363	1.6121	0.33	0.941	0.659
Cr	Kg benzen eq	6.19×10^{-5}	1.14×10^{-4}	0.0013	5.49×10^{-6}	0.0217	0.00939
NC	Kg toluen eq	0.5147	0.8931	9.8758	0.116	699	305
RE	Kg PM2.5 eq	1.83×10^{-4}	3.87×10^{-4}	0.0045	1.54×10^{-3}	5.63×10^{-4}	1.28×10^{-4}
Eu	Kg N eq	2.57×10^{-5}	5.58×10^{-4}	0.0072	5.33×10^{-6}	1.53×10^{-3}	7.74×10^{-4}
OD	Kg CFC-11 eq	1.46×10^{-10}	1.69×10^{-10}	1.51×10^{-9}	2.05×10^{-7}	2.28×10^{-9}	1.82×10^{-10}
Ec	Kg 2,4-D eq	0.0109	0.0183	0.1990	0.00322	4.98	2.11
Sm	g NOx eq	3.34×10^{-4}	10.0×10^{-3}	0.1303	3.07×10^{-3}	9.17×10^{-3}	4.88×10^{-3}

From the comparative data, it is evident that the insulation panel N3 has comparatively higher environmental impacts. Thus, in the following LCA analysis, the result of insulation panel N3 has been avoided.

The normalized impact values of other five insulation materials are presented in figure 7.9, where the maximum value of each impact category is referred to as 100% relative scale. The impacts of five insulation materials are also ranked from 1 to 5 in table 7.9, where 1 means comparatively best and 5 means comparative worst environmental impacts. All five insulation materials have very low environmental impacts as the insulation materials are produced from recycled PET bottles, natural flax, and commercially used stone wool, which are produced by combination of natural minerals and recycled post-production waste materials. Among these, insulation materials produced from 100% recycled cotton (N1) has the overall lowest environmental impacts and could be considered the best environmental-friendly material. The global warming and acidification impact of insulation panel N1 is about eleven times lower than stone wool and sixteen times lower than natural flax. Ozone depletion impact is completely

negligible for all insulation materials (table 7.8). Compared to flax and stone wool, impacts of N1 and N2 are completely negligible in the category of carcinogenic, noncarcinogenic, and ecotoxicity. There is a comparatively higher impact of N1 and N2 on the category of respiratory effects compared to stone wool. However, its total value (1.83×10^{-4} Kg PM2.5 eq for N1 and 3.87×10^{-4} Kg PM2.5 eq for N2) is very low. The respiratory effect may come from dust produced during recycling, burning fuel during electricity production from coal and gas. N2 insulation panel has also comparatively higher impact on the category of smog formation which mainly occurs during PLA pellet formation.

Surprisingly, among five insulation materials, flax has the most adverse environmental effect, even higher than synthetic stone wool, although flax is considered a renewable natural material. This is due to the use of artificial fertilizers during cultivation of flax. During the production of fertilizers, N_2O is emitted, which contributes to high global warming and acidification. On the other hand, stone wool has relatively lower environmental impact after N1 and N2. Melting of stone wool requires very high temperature, and high energy or fossil fuel is required, but interestingly its environmental impacts are not so high. This may be due to the use of recycled materials along with virgin stone wool. In addition to that, as stone wool is a commercialized product, its production process is highly developed for many years with maximum production efficiency, which contributes to overall low environmental impacts.

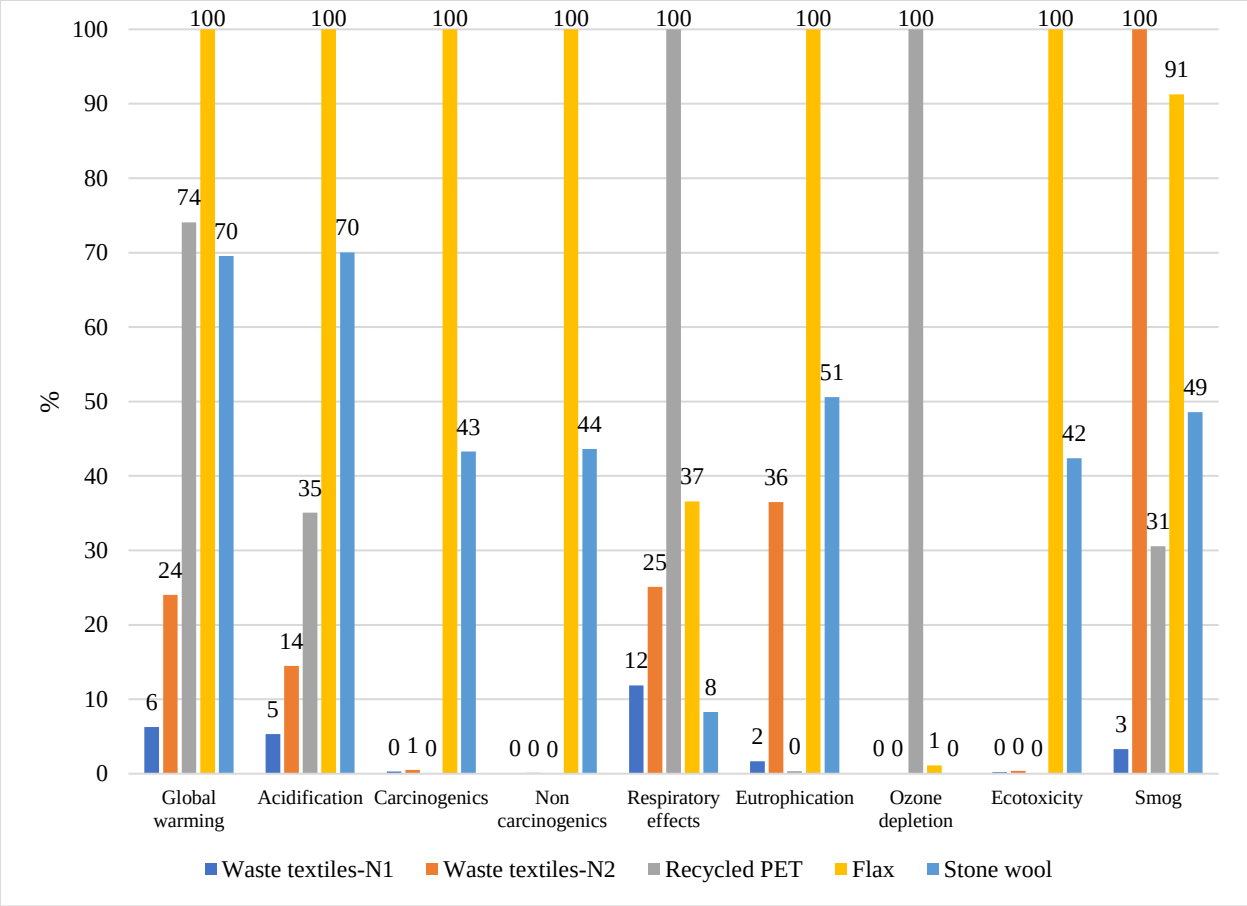

Figure 7.9. Normalized impact factors for 1 *f.u.* of different insulating materials.

Table 7.9. Ranking of the five insulation panels with respect to selected environmental impacts (1 = best, 5 = worst).

Impact category	Unit	Waste textiles-N1	Waste textiles-N2	Recycled PET bottle	Flax	Stone wool
Global warming	Kg CO_2 eq	1	2	4	5	3
Acidification	H^+ moles eq	1	2	3	5	4
Carcinogenics	Kg benzen eq	2	3	1	5	4
Non carcinogenics	Kg toluen eq	2	3	1	5	4
Respiratory effects	Kg PM2.5 eq	2	3	5	4	1
Eutrophication	Kg N eq	2	3	1	5	4
Ozone depletion	Kg CFC-11 eq	1	2	5	4	3
Ecotoxicity	Kg 2,4-D eq	2	3	1	5	4
Smog	g NOx eq	1	5	2	4	3

Insulation materials produced from textile wastes, either from natural or recycled sources, are still in initial developmental stages. The processing techniques often lack optimization compared to the production process of conventional synthetic materials [29]. Hence, further research for optimization in production process, and developing appropriate technology will improve the sustainability of insulation materials from recycled or natural sources.

7.5. Summary

In this study, sustainable thermal insulation materials were produced from recycled textiles. Three different insulation materials, N1, N2, and N3, were produced by varying composition, temperature, and pressure. A cradle to gate LCA analysis was conducted to estimate the environmental impacts of produced thermal insulation materials.

Results showed that the produced materials have very good thermal insulation properties. LCA study revealed that N1 and N2 insulation panels have very low environmental impacts of all the selected categories, and therefore could be considered as eco-friendly products.

Insulation panel N1 has comparatively lower environmental impacts, most of which come from the US electricity mix (64.7%). In USA, still, 20.8% and 44.32% of electricity come from coal and natural gas (supplementary table 7.2) resulting in higher impacts from electricity mix. Environmental impacts will be much less when coal and gas-based electricity are replaced by solar or wind-based electricity. Compared to N1, insulation panel N2 has slightly higher (3.8 times higher global warming) environmental impacts, most of which (67%) comes from PLA fibers. Although PLA comes from natural corn, fertilizer and energy used during corn cultivation and chemicals used during conversion of corn to PLA adversely affect the environment.

Despite much of environmental effects come from PLA fibers in N2 and N3, still its' environmental impacts are much less than glue which had been previously used as a binder for

producing insulation panels [30]. Replacing virgin PLA fibers with recycled PLA or other low melting thermoplastic recycled fibers will further reduce environmental impacts. In case of using recycled PLA fiber instead of virgin one, the environmental effect of global warming would reduce by 67% for N2 and 72% for N3. Another way to further reduce the environmental effects is to minimize the amount of solid waste produced in several processes.

In contrast to N1 and N2, insulation panel N3 has higher environmental impacts in all categories. Heat and pressure during manufacturing cause high density and higher thermal conductivity of N3 resulting in higher weight (kg) and environmental impacts per *f.u.* Environmental impacts of N3 can be reduced a lot by slightly modifying the manufacturing process, i.e., avoiding high pressure after heat setting which will reduce density and thermal conductivity.

Sensitivity analysis also revealed that the US electricity mix and PLA fibers are the most important input parameters that influence the overall environmental impacts. LCA results of produced insulation materials from waste textiles were also compared with three other insulation materials (stone wool, recycled PET bottle, and flax). Among these, N1 has overall very low environmental impacts. The global warming potential (GWP) of recycled PET bottle, flax and stone wool is more than ten times higher than that of the GWP of N1.

The LCA study exposed a clear insight into the environmental impacts of several stages of production process, which may be helpful to optimize or modify the processes and produce an eco-friendlier thermal insulation material. However, there are some limitations related to the present study, as well. This study is a cradle to gate analysis. In future, cradle to grave analysis will be more interesting. Checking of use phase and disposal will give additional environmental insight. It will be interesting to see from future studies how much environmental benefits can be obtained

throughout the entire use phase of such thermal insulation materials. Future research can also focus on the cost and social aspects of life cycle sustainability.

7.6. References

[1] A. D. La Rosa *et al.*, "Environmental impacts and thermal insulation performance of innovative composite solutions for building applications," *Constr. Build. Mater.*, vol. 55, pp. 406–414, 2014, doi: 10.1016/j.conbuildmat.2014.01.054.

[2] I. Z. Bribián, A. V. Capilla, and A. A. Usón, "Life cycle assessment of building materials: Comparative analysis of energy and environmental impacts and evaluation of the eco-efficiency improvement potential," *Build. Environ.*, vol. 46, no. 5, pp. 1133–1140, 2011, doi: 10.1016/j.buildenv.2010.12.002.

[3] "ASTM F1868 - 17," *Standard Test Method for Thermal and Evaporative Resistance of Clothing Materials Using a Sweating Hot Plate*, 2017. https://www.astm.org/Standards/F1868.

[4] R. Azari, "Integrated energy and environmental life cycle assessment of office building envelopes," *Energy Build.*, vol. 82, pp. 156–162, 2014, doi: 10.1016/j.enbuild.2014.06.041.

[5] "ISO 14040," *Environmental management — Life cycle assessment — Principles and framework*, 2006. https://www.iso.org/standard/37456.html.

[6] "ISO 14044," *Environmental management -- Life cycle assessment -- Requirements and guidelines*, 2006. https://www.iso.org/standard/38498.html.

[7] N. K. Llantoy Huamán, "Comparative Life Cycle Assessment of insulation materials for the building sector," 2019. https://repositori.udl.cat/bitstream/handle/10459.1/67970/nllantoyh.pdf?sequence=1.

[8] G. Rebitzer *et al.*, "Life cycle assessment: Part 1: Framework, goal and scope definition, inventory analysis, and applications," *Environ. Int.*, vol. 30, no. 5, pp. 701–720, 2004, doi: 10.1016/j.envint.2003.11.005.

[9] F. Ardente, M. Beccali, M. Cellura, and M. Mistretta, "Building energy performance: a LCA case study of kenaf-fibres insulation board," *Energy Build.*, vol. 40, no. 1, pp. 1–10, 2008, doi: 10.1016/j.enbuild.2006.12.009.

[10] K. Menoufi, A. Castell, L. Navarro, G. Pérez, D. Boer, and L. F. Cabeza, "Evaluation of the environmental impact of experimental cubicles using Life Cycle Assessment: A highlight on the manufacturing phase," *Appl. Energy*, vol. 92, pp. 534–544, 2012, doi: 10.1016/j.apenergy.2011.11.020.

[11] J. Kono, Y. Goto, Y. Ostermeyer, R. Frischknecht, and H. Wallbaum, "Factors for eco-efficiency improvement of thermal insulation materials," in *Key Engineering Materials*, 2016, vol. 678, pp. 1–13, doi: 10.4028/www.scientific.net/KEM.678.1.

[12] A. C. Schmidt, A. A. Jensen, A. U. Clausen, O. Kamstrup, and D. Postlethwaite, “A comparative life cycle assessment of building insulation products made of stone wool, paper wool and flax,” *Int. J. Life Cycle Assess.*, vol. 9, no. 1, pp. 53–66, 2004, doi: 10.1007/BF02978536.

[13] R. D. Schlanbusch, B. P. Jelle, L. I. C. Sandberg, S. M. Fufa, and T. Gao, “Integration of life cycle assessment in the design of hollow silica nanospheres for thermal insulation applications,” *Build. Environ.*, vol. 80, pp. 115–124, 2014, doi: 10.1016/j.buildenv.2014.05.010.

[14] B. Kuczenski and R. Geyer, “PET bottle reverse logistics—environmental performance of California’s CRV program,” *Int. J. Life Cycle Assess.*, vol. 18, no. 2, pp. 456–471, 2013, doi: 10.1007/s11367-012-0495-7.

[15] “Joful Industry,” *Old Clothes Waste Textile Shredder Machine*, 2020. http://www.industrialwasteshredder.com/sale-10461514-old-clothes-waste-textile-shredder-machine-scrap-fiber-textile-waste-cutting-machine.html.

[16] M. Wendin, “LCA on Recycling Cotton,” 2016. .

[17] “Qingdao Shinejary Textile Machinery Co., Ltd.,” *Textile fabric waste recycling machine for spinning*, 2020. https://shinejary.en.alibaba.com/productgrouplist-816189902/Recying_machine.html?spm=a2700.icbuShop.88.45.200532f8BCrtko.

[18] L. Frazer, “New spin on an old fiber,” *Environ. Health Perspect.*, vol. 112, no. 13, pp. 754–757, 2004, doi: 10.1289/ehp.112-a754.

[19] “Changshu Chenyang Nonwoven Machinery Co., Ltd.,” *High Quality Nonwoven Needle Punching Felt Machine*, 2020. https://cs-chenyang.en.alibaba.com/productgrouplist-806809212/Needle_Punch_solution.html?spm=a2700.icbuShop.88.26.2804f3beFApE02.

[20] “TPS,” *Industrial thermal book*, 2017. https://www.thermalproductsolutions.com/data/uploads/contentblock/Brochures/4213 TPS Industrial Thermal Book.pdf.

[21] E. T. H. Vink, K. R. Rabago, D. A. Glassner, and P. R. Gruber, “Applications of life cycle assessment to NatureWorks™ polylactide (PLA) production,” *Polym. Degrad. Stab.*, vol. 80, no. 3, pp. 403–419, 2003, doi: 10.1016/S0141-3910(02)00372-5.

[22] C. W. Murphy and A. Kendall, “Life cycle inventory development for corn and stover production systems under different allocation methods,” *Biomass and Bioenergy*, vol. 58, pp. 67–75, 2013, doi: 10.1016/j.biombioe.2013.08.008.

[23] A. E. Landis, “The environmental impacts of biobased production,” University of Illinois at Chicago, 2007.

[24] "NREL," *U.S. Life Cycle Inventory Database*, 2012. https://www.nrel.gov/lci/.

[25] "Cissco Machinery Co., Ltd.," *High Efficiency Polyester Staple Fibre Producing Machine*, 2020. https://www.alibaba.com/product-detail/High-Efficiency-Polyester-Staple-Fibre-Producing_1653737133.html?spm=a2700.7724857.normalList.25.2ebc6fc3b8ol3r&bypass=true.

[26] F. Intini and S. Kühtz, "Recycling in buildings: an LCA case study of a thermal insulation panel made of polyester fiber, recycled from post-consumer PET bottles," *Int. J. Life Cycle Assess.*, vol. 16, no. 4, pp. 306–315, 2011.

[27] P. Eyerer, M. Weller, and C. Hübner, *Polymers Opportunities and Risks II Sustainability, Product Design and Processing*. New York: Springer, 2010.

[28] C. Bayer, M. Gamble, R. Gentry, and S. Joshi, *AIA guide to building life cycle assessment in practice*. Washington, DC: The American Institute of Architects, 2010.

[29] R. Vidal, P. Martínez, and D. Garraín, "Life cycle assessment of composite materials made of recycled thermoplastics combined with rice husks and cotton linters," *Int. J. Life Cycle Assess.*, vol. 14, no. 1, pp. 73–82, 2009, doi: 10.1007/s11367-008-0043-7.

[30] P. Ricciardi, E. Belloni, and F. Cotana, "Innovative panels with recycled materials: thermal and acoustic performance and life cycle assessment," *Appl. Energy*, vol. 134, pp. 150–162, 2014, doi: 10.1016/j.apenergy.2014.07.112.

[31] P. Zummo, "American public power association," *America's Electricity Generating Capacity*, 2020. https://www.publicpower.org/resource/americas-electricity-generating-capacity.

Supplementary Document

Supplementary table 7.1: Input parameters for 1000 kg PLA fiber production.

	Value	Unit	Ref.
Corn production			[22], [24]
- Nitrogen (as N)	6.68	kg	
- Phosphorous (as P2O5)	3.72	kg	
- Potassium (as K2O)	4.90	kg	
- Electricity (US)	8.85	kWh	
PLA pellet production			[23]
- Transport	202.94	tkm	
- enzymes (α-amylase)	10.24	kg	
- Lacto baccili	11.49	Culture volume%	
- D-glucose	115.63	kg/L	
- Water	34.8	kL	
- yeast extract	5.04	kg/L	
- Tween®80	0.50	kg/L	
- K_2HPO_4	1.00	kg/L	
- $MgSO_4$	100.8	g/L	
- $MnSO_4$	25.2	g/L	
- ammonium citrate	3.02	kg/L	
- $CaCO_3$	76.61	kg/L	
- H_2SO_4	85.68	kg/L	
- Alamine 336	705.60	wt%	
- methyl isobutyl ketone	131.04	wt%	
- keroses	201.60	wt%	
- Irganox	2.52	wt%	
- Electricity (polymerization)	6249.60	MJ	
- Electricity (waste water treatment)	1108.80	kWh	
- Fossil fuels	13557.60	MJ	
PLA fiber production			[25]
- Electricity mix	1098.72	kWh	

Supplementary table 7.2. USA electricity mix (2020) [31].

Fuel type	Capacity (MW)	Share %
Natural gas	533,742.80	44.32
Coal	250,436.47	20.80
Nuclear	106,330.64	8.83
Wind	103,775.38	8.62
Hydro	100.799.42	8.37
Solar	41,888.08	3.46
Distillate fuel oil	22,476.86	1.87
Residual fuel oil	15,261.80	1.27
Others	29.625.63	2.46

Supplementary table 7.3. Selected environmental impact categories.

Impact category	Benchmark unit
Global warming (GW)	Kg CO_2 eq
Acidification (Ad)	H^+ moles eq
Carcinogenics (Cr)	Kg benzen eq
Non carcinogenics (NC)	Kg toluen eq
Respiratory effects (RE)	Kg PM2.5 eq
Eutrophication (Eu)	Kg N eq
Ozone depletion (OD)	Kg CFC-11 eq
Ecotoxicity (Ec)	Kg 2,4-D eq
Smog formation (Sm)	g NOx eq

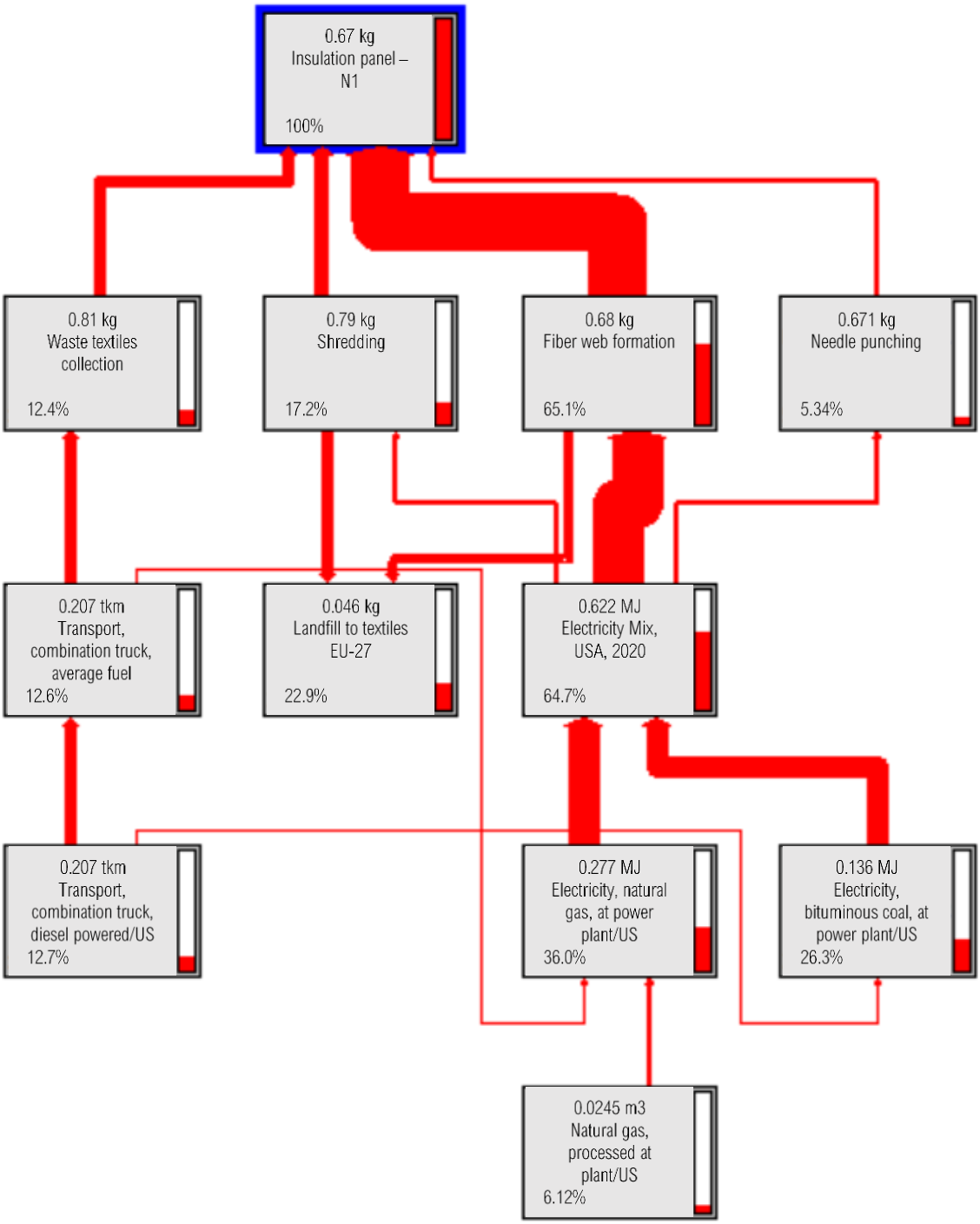

Supplementary figure 7.1. Network of the involved processes and the relating global warming potential percentage evaluated for 1 *f.u.* (0.67 kg) of thermal insulation panel -N1.

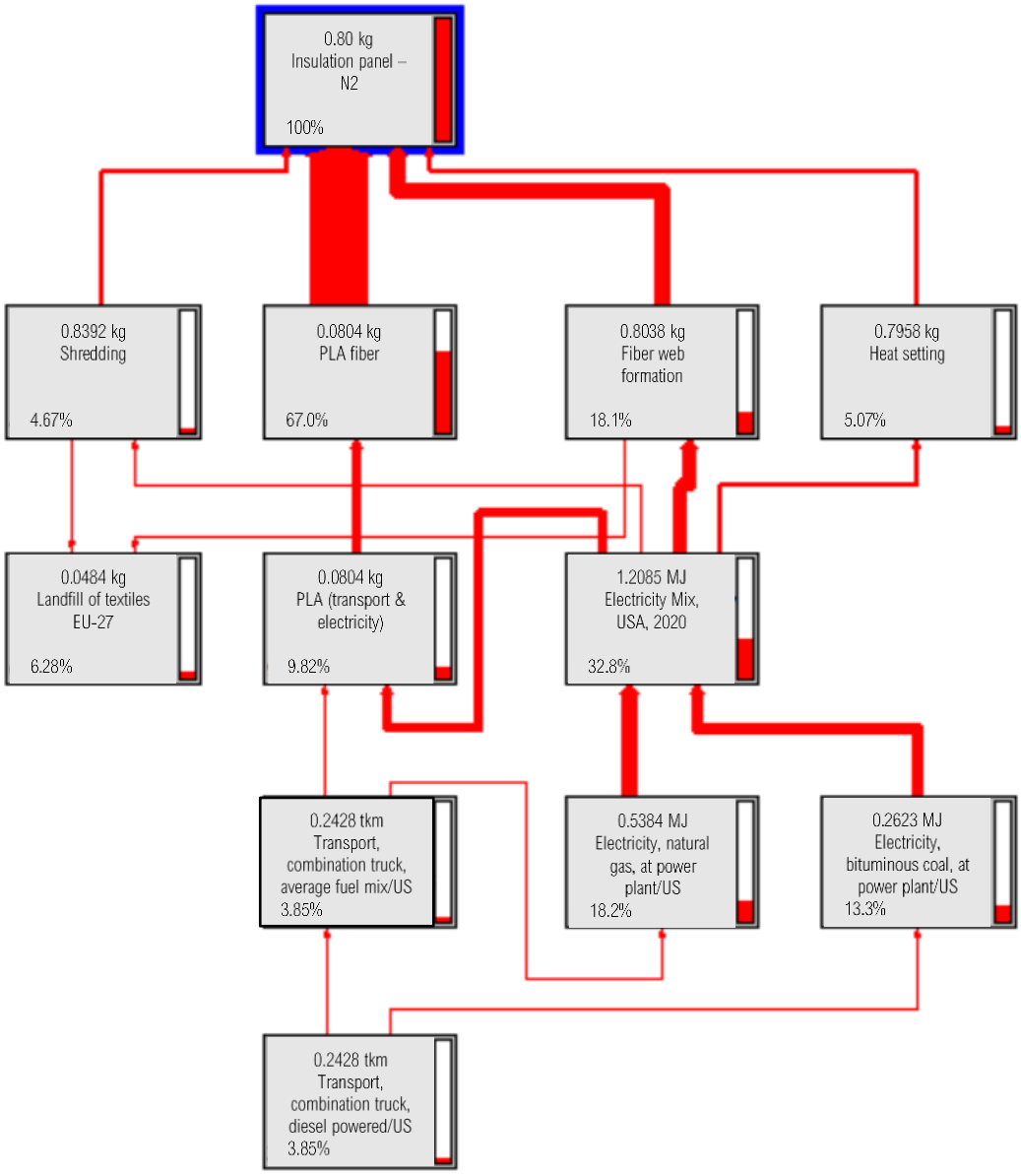

Supplementary figure 7.2. Network of the involved processes and the relating global warming potential percentage, evaluated for 1 *f.u.* (0.80 kg) of thermal insulation panel -N2.

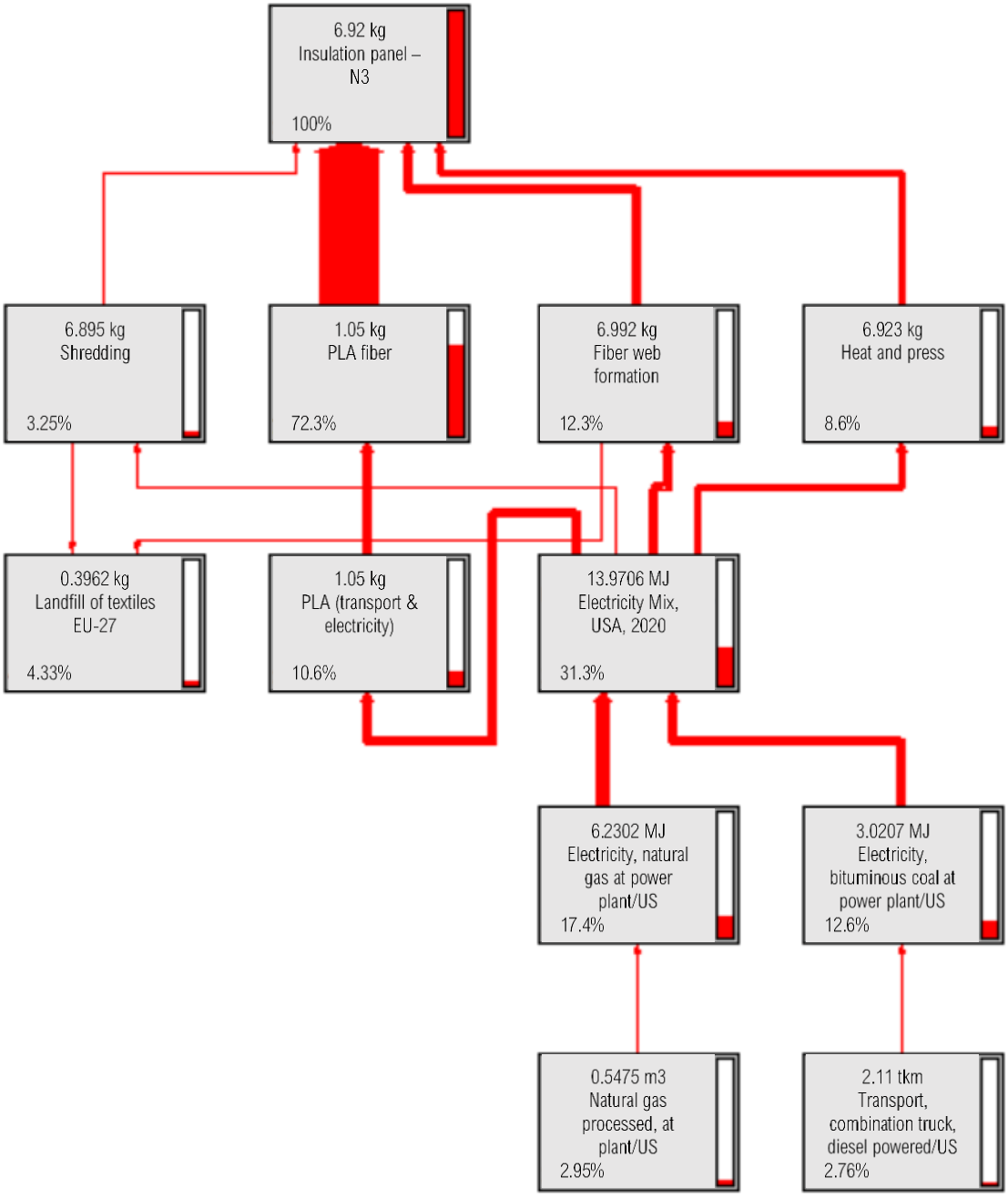

Supplementary figure 7.3. Network of the involved processes and the relating global warming potential percentage, evaluated for 1 *f.u.* (6.92 kg) of thermal insulation panel -N3.

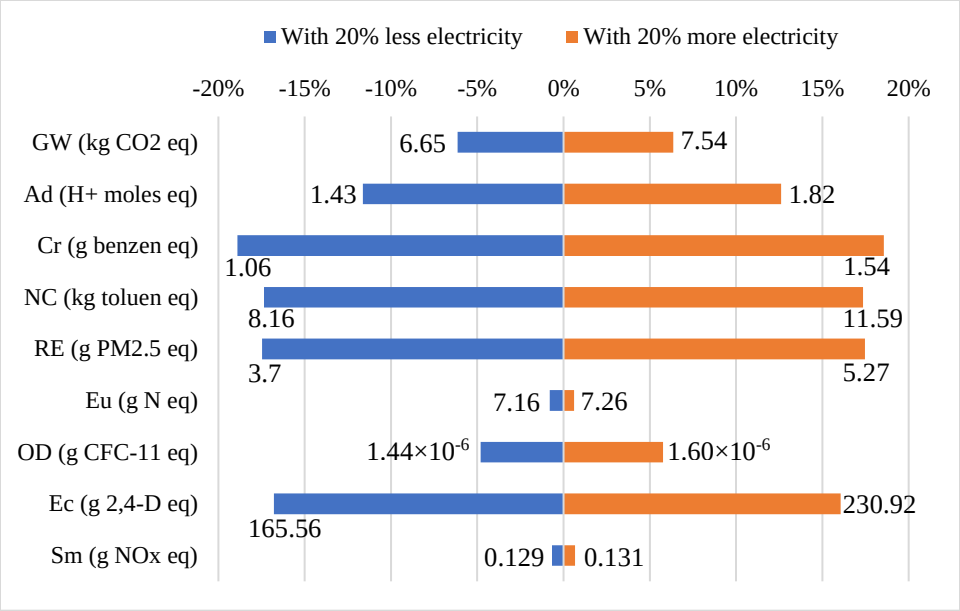

Supplementary figure 7.4. Sensitivity analysis of selected environmental impacts for 20% less and 20% more electricity consumption during the production of thermal insulation panels N3 (solid color represent percentage changes and actual value is written at the end).

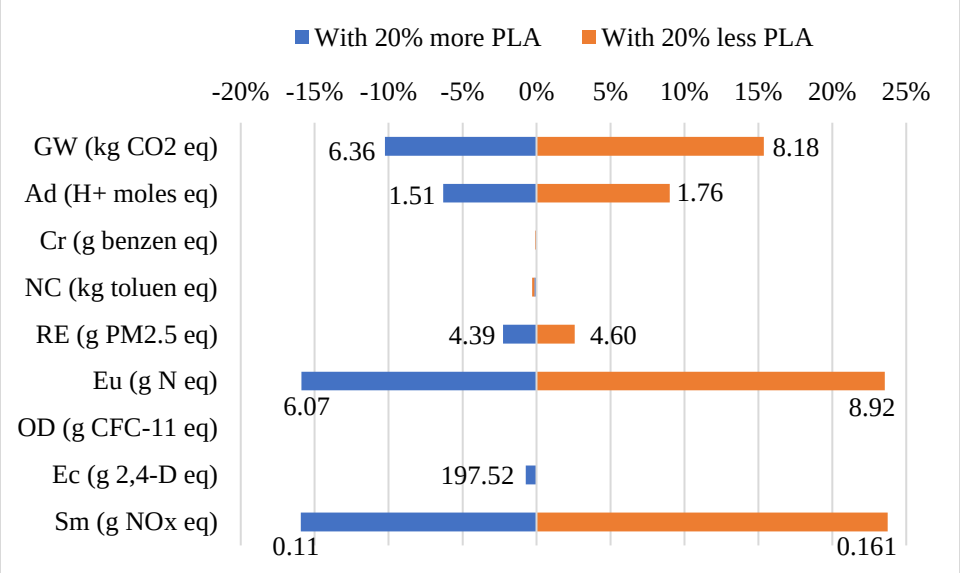

Supplementary figure 7.5. Sensitivity analysis of selected environmental impacts for 20% more and 20% less PLA fiber production for the thermal insulation panels N3 (solid color represent percentage changes and actual value is written at the end).

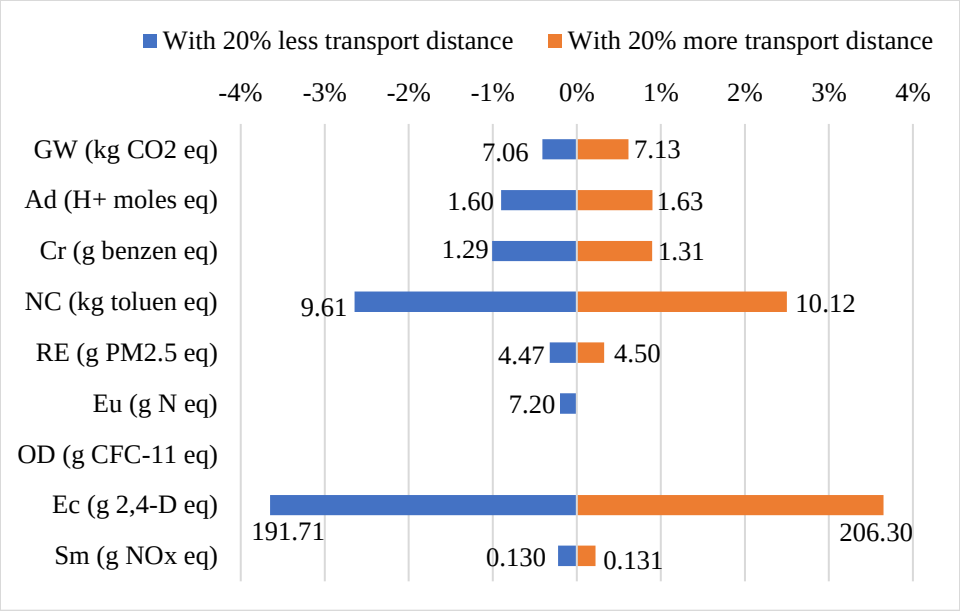

Supplementary figure 7.6. Sensitivity analysis of selected environmental impacts for 20% less and 20% more transport distance during the production of thermal insulation panels N3 (solid color represent percentage changes and actual value is written at the end).

CHAPTER 8

Conclusions and Recommendations

8.1. Overall Summary

In this study, a thorough investigation was conducted to understand the potential of recycled textiles to be used as environmentally friendly insulation materials. Study was also conducted to understand the process-structure-property relationship of insulation materials.

Recycled denim and Sorona®/PLA binder fibers were used to produce environmentally-friendly alternative thermal and acoustic insulation materials (chapter three). The results showed that produced insulation materials have very good insulation properties with maximum transmission loss of about 24 dB at around 1000 Hz and minimum thermal conductivity value of 0.049 W/mK. When compared with commercially available insulation materials, the produced insulation materials have very good thermal insulation properties and meet the criteria of thermal insulation property of 0.07 W/mK [1]. Obtained thermal conductivity is very much comparable to those of the presently available synthetic thermal insulation material of mineral wool, which has thermal conductivity of 0.040–0.045 W/mK [2]. Similarly, all the samples have very good acoustic insulation property, with normalized insulation property being higher than that of the commercially used gypsum board [3]. The effect of several structural parameters, including air permeability, thickness, density, and porosity, on insulation properties was analyzed. The sound transmission loss increases with increase in thickness and areal density but decreases with the increase of air permeability, whereas thermal conductivity decreases with the increase of porosity and with the decrease of density. This observation is consistent based on the mechanism of sound transmission.

The determined relationship allows one to produce the required structure in the insulation to achieve desired results.

Further study was conducted to understand the effect of processing parameters on the structural parameters (thickness, density, air permeability, and porosity) and subsequently on the thermal and acoustic insulation properties of products from recycled textiles (chapter four). A response surface methodology (central composite design) approach showed that bonding time and temperature have strong influence on the structure of insulation materials. With the increase of bonding time and temperature thickness decreases, whereas density increases, air permeability initially slightly increases and then decreases, and acoustic insulation property increases, but thermal insulation property decreases. The acoustic and thermal insulation properties showed opposite trends. For example, sample S8 has the highest acoustic insulation property (average TL of 6.67 dB), but it has the lowest thermal insulation property (average TC of 0.1053 W/mK).

Insulation materials were also produced utilizing 3D printing, which has the ability to produce materials with precise and controlled shape and structure (chapter five). The effect of structural parameters on insulation properties was evaluated as it is assumed that the structures produced with individual and better control over parameters would show more reliable relation compared to nonwoven composites, which are irregular by nature. Results showed a similar effect of structural parameters on insulation properties that we had observed with nonwoven composites, i.e., with the increase of density and decrease of porosity, acoustic insulation property increases, but thermal insulation property decreases. A comprehensive evaluation was also conducted to check whether additive manufacturing, the emerging technology is suitable to produce insulation materials. Test results revealed that insulation materials produced from 3D printing technology have better thermal and acoustic insulation properties than commercially available synthetic insulation

materials (gypsum board and mineral wool), with the lowest thermal conductivity of 0.037 W/mK and highest average sound transmission loss is 28.0 dB. This indicates the potential for using 3D printed insulation materials as a substitute for conventional insulation materials, especially when they are produced using the right feedstock.

Also, an analytical model was proposed by combining and modifying the Maxwell-Eucken model to predict thermal insulation properties of porous materials. The experimental data from a systematic study showed that for both types of insulation materials (nonwoven composites from waste textiles and 3D printed samples from PLA), experimental data agrees with the predicted data with a percentage difference of less than 8.5%, which indicates that the accuracy of the model for prediction is sufficient enough to be used for industrial purposes [4]. Investigation of five basic thermal conductivity models showed that among the five basic models, only EMT and ME2 models provided some reasonable predictions for porous materials.

Environmental effects of insulation materials from recycled textiles were evaluated using life cycle assessment (LCA) method and compared with several other insulation materials (chapter seven). Three different insulation panels. N1 (100% recycled cotton), N2 (90% recycled cotton/10% PLA), and N3 (42.5% recycled cotton/42.5% recycled nylon/15% PLA) were produced using textile waste at different compositions, temperatures, and pressures. A cradle-to-gate LCA study was conducted based on ISO 14040/44. The result of impact assessment showed that produced insulation materials (N1, N2) have overall very low environmental impacts compared to stone wool, recycled PET, and natural flax. The environmental impact of produced insulation panels from waste textiles can be reduced further by process intensification and using alternates such as recycled PLA fibers. The LCA study exposed a clear insight into the environmental impacts of

several stages of production process, which may be helpful to optimize or modify the processes and produce an eco-friendlier thermal insulation material.

8.2. Recommendations for Future Work

In this study, environmentally-friendly insulation materials were successfully produced, and their structure-property relations were thoroughly investigated. However, there are still some limitations. For successful commercialization additional information regarding insulation materials is required and following future studies are recommended to improve the understanding and help the technology become a commercial reality.

1. Flammability test revealed that produced insulation materials have good flame retardance properties. But there is a scope for improving flame retardance properties. It will be interesting if a biodegradable and environmental-friendly chitosan and alginate coating on composite panels can be effective as a flame retardant finish. Other affordable and environmentally safe finishes may be investigated as well.

2. Moisture test revealed that at both standard atmosphere and high humid atmosphere, the MC value is less than the acceptable MC value of building insulation materials. Again, produced insulation materials are recommended for use with walls as a sandwich structure, where effect of moisture is minimum. Still, it is recommended that the effect of moisture on insulation properties, biological decomposition (including degradation by bacteria, mildew, and fungi), and application of sustainable finishes to reduce the effect of moisture may be investigated.

3. The service life of insulation materials at different atmospheric conditions, as well as the effect of some other important factors, including cleaning process, resistance against pest, dust, fungi, and bacteria are recommended studies in future research.

4. One of the important factors that influences commercialization is the cost and performance benefit of the product. A thorough cost-performance evaluation should be done in future research.

5. An analytical model was proposed to predict thermal conductivity of porous insulation materials, which gives better prediction compared to existing thermal conductivity models. However, more experimental study is encouraged with other combination of materials and processing conditions to determine the broader applicability of the model.

6. A study was conducted to check the applicability of PLA for producing insulation materials using 3D printing technology. However, insulation materials produced from PLA are only suitable for use in room temperature conditions, and not suitable for use in high-temperature conditions. Future research may focus on improving the temperature resistance using some chemical treatment and/or use of high temperature resistant biodegradable thermoplastic materials.

7. LCA study revealed that produced insulation materials have less adverse environmental effects. However, there are some scopes to further reduce the environmental impacts. Most of the environmental impacts of produced insulation materials come from the US electricity mix (64.7% GWP for N1) and PLA fibers (67% GWP for N2). Future research on use of recycled PLA or other low melting thermoplastic fibers as a binder is recommended. Also, in future, cradle to grave analysis should be conducted as that will provide more environmental insight. Future research can also focus on the cost and social aspects of life cycle sustainability.

8.3. References

[1] F. Asdrubali, F. D'Alessandro, and S. Schiavoni, "A review of unconventional sustainable building insulation materials," *Sustain. Mater. Technol.*, vol. 4, pp. 1–17, 2015, doi: 10.1016/j.susmat.2015.05.002.

[2] M. El Wazna, M. El Fatihi, A. El Bouari, and O. Cherkaoui, "Thermo physical characterization of sustainable insulation materials made from textile waste," *J. Build. Eng.*, vol. 12, pp. 196–201, 2017.

[3] R. Reixach, R. Del Rey, J. Alba, G. Arbat, F. X. Espinach, and P. Mutjé, "Acoustic properties of agroforestry waste orange pruning fibers reinforced polypropylene composites as an alternative to laminated gypsum boards," *Constr. Build. Mater.*, vol. 77, pp. 124–129, 2015.

[4] J. K. Carson, "Prediction of the thermal conductivity of porous foods: a thesis submitted in partial fulfilment of the requirements for the degree of Doctor of Philosophy in Food Engineering, Massey University, Palmerston North, New Zealand, 2002," Massey University, 2002.

Publications:

Journal articles

1. Islam, S., & Bhat, G. (2019). Environmentally-friendly thermal and acoustic insulation materials from recycled textiles. Journal of environmental management, 251, 109536. https://doi.org/10.1016/j.jenvman.2019.109536

2. Islam, S., El Messiry, M., Sikdar, P. P., Seylar, J., & Bhat, G. (2020). Microstructure and performance characteristics of acoustic insulation materials from post-consumer recycled denim fabrics. Journal of Industrial Textiles, https://doi.org/10.1177/1528083720940746

3. Islam, S., & Bhat, G. (2021). Progress and challenges in self-healing composite materials. Materials Advances. https://doi.org/10.1039/D0MA00873G

4. Sikdar, P., Bhat, G., Hinchliff, D., Islam, S., Condon, B. (2021). Microstructure and physical properties of composite nonwovens produced by incorporating cotton fibers in elastic spunbond and meltblown webs for medical textiles. Journal of Industrial Textiles, https://doi.org/10.1177/15280837211004287

Book chapter

1. Bhat, G., Malkan, S., Islam, S. (2021). Polymer-laid web formation. In S. Russel (Eds), Handbook of nonwovens, New York, NY: CRC Press.

Conference proceeding

1. Islam, S., & Lyu, J. (2020). A Mixed Pedagogical Approach to Promote Undergraduate Students' Active Learning in the Retail Planning and Buying Course. In International Textile and Apparel Association Annual Conference Proceedings, 77 (1), 1-3. https://doi.org/10.31274/itaa.11820

Conference presentation

1. Islam, S., Seylar, J., Sikdar, P.P., El Messiry, M., Bhat, G. (2019, February). Environmentally-Friendly Acoustic Insulation Materials from Post-Consumer Recycled Fabrics. Paper presented at the Techtextil North America, Raleigh, NC.

2. Islam, S., Seylar, J., Sikdar, P.P., El Messiry, M., Bhat, G. (2019, May). Development of Value-added Products from Recycled Mixed Fibers and Fabrics. Paper presented at the Center for Bioplastics and Biocomposites, Athens, GA.

3. Islam, S., Seylar, J., El Messiry, M., Bhat, G. (2019, October). Processing, Structure and Properties of Sustainable Insulation Materials from Textile Waste. Paper presented at the International Symposium on Materials from Renewables, Athens, GA.

4. Uddin, M., Saremi, R., Islam, S., Sharma, S. (2019, october). Application of Core (PLA) - sheath (PHB) nanofibrous yarn as implantable medical textiles. International Symposium on Materials from Renewables, Athens, GA, USA

5. Islam, S., Bhat, G. (2020, May). Processing and Properties of Nonwoven-Based Composites from Recycled Textile Waste. Techtextil North America, Atlanta, GA, USA, Cancel due to COVID.

6. Islam, S., Lyu, J. (2020, november). A Mixed Pedagogical Approach to Promote Undergraduate Students' Active Learning in the Retail Planning and Buying Course. International Textile and Apparel Association. Denver, CO, USA.

Working papers

1. Islam, S., Bhat, G., & Mani, S. (In progress). Life cycle assessment of thermal insulation materials produced from waste textiles. Resources, Conservation & Recycling.

2. Islam, S., & Bhat, G. (In progress). Thermal performance evaluation and modeling of 3D-printable PLA materials. International Journal of Heat and Mass Transfer.

3. Islam, S., & Bhat, G. (In progress). Effect of processing parameters on thermal and acoustic insulation properties produced from recycled textiles. Journal of Industrial Textiles

4. Islam, S., Azari, H., & Bhat, G. (In progress). Reinforcement of polypropylene fiber with graphene nanocomposite. The Journal of Textile Institute.

5. Islam, S., & Bhat, G. (In progress). Application of self-healing composite materials. Composites Part A.

6. Islam, S., & Lyu, J. (In progress). Effective teaching for undergraduate retail math class - insights from a mixed pedagogical approach. International Journal of Fashion Design, Technology and Education.